1-1-2017

Reliability Based Design Optimization Of Load And Rating Models For Bridge Structures In Michigan

Vahid Kamjoo
Wayne State University,

RELIABILITY BASED DESIGN OPTIMIZATION OF LOAD AND RATING MODELS FOR BRIDGE STRUCTURES IN MICHIGAN

by

VAHID KAMJOO

DISSERTATION

Submitted to the Graduate School

of Wayne State University,

Detroit, Michigan

in partial fulfillment of the requirements

for the degree of

DOCTOR OF PHILOSOPHY

2017

MAJOR: CIVIL ENGINEERING (Structural)

Approved By:

_____

Advisor Date

_____

_____

_____

DEDICATION

To my wife and my parents, for their limitless love and support

ACKNOWLEDGMENTS

I take immense pleasure in thanking Dr. Christopher D. Eamon, Associate Professor at the Department of Civil and Environmental Engineering at Wayne State University, for his guidance, support and professional academic supervision, which assisted me in completing this Ph.D. dissertation.

I am grateful to Dr. Christopher D. Eamon, Dr. Hwai-Chung Wu, Dr. Mumtaz Usmen, from the Department of Civil and Environmental Engineering at Wayne State University, and Dr. Kazuhiko Shinki, from the Department of Mathematics at the Wayne State University, for their time and effort serving as my Dissertation Committee Members.

PREFACE
DEVELOPING RELIABILITY BASED DESIGN OPTIMIZATION TO CALCULATE LOAD FACTOR

The main research objectives of this study are to determine the most accurate and consistent method for predicting live load factor for design and rating of MDOT bridge, determine the reliability index of load factor for different bridge types, develop Reliability Based Design Optimization to calculate the optimized load factor.

Keywords: Reliability Based Design Optimization; Design and Rating models; WIM data

TABLE OF CONTENTS

LIST OF TABLES

LIST OF FIGURES

CHAPTER 1: INTRODUCTION

1.1 Statement of The Problem

The load models developed for Load and Resistance Factor Design (LRFD) (AASHTO LRFD 2010) and Load and Resistance Factor Rating (LRFR) (AASHTO MBE 2011) are based on a generic, small sample of truck traffic. Although some adjustments are specified for average daily truck traffic (ADTT), these models are otherwise assumed to apply to all bridges. However, these data were used to determine bridge design loads to be used across all states. This is problematic as many states have vehicular traffic loads that differ significantly from those used to develop the AASHTO LRFD live load. An example of one such state is Michigan. Although the Michigan Department of Transportation (MDOT) has modified both the design as well as the rating process to better correspond to Michigan loads (Curtis and Till 2008), these modifications are similarly based on a generic and greatly limited data set. Of particular concern is heavy vehicle side-by-side frequency, which was taken as a constant value across structures for development of design loads (1/15 for the LRFD code). For development of LRFR evaluation and rating loads, side-by-side heavy truck probability was taken as 1/15 for an ADTT (Average Daily Truck Traffic) of 5000 (1/30 for the modified rating loads used by MDOT); as 1/100 for an ADTT of 1000, and as 1/1000 for an ADTT of 100 (Moses 2001). The assumptions used for heavy truck side-by-side frequency has a significant effect on the expected load on bridge girders. Applying this generic load model to Michigan bridges, which may have significantly different traffic profiles than those used to develop the LRFD/LRFR load models, may result in inconsistencies in safety level for design as well as evaluation. Moreover, as the LRFD/LRFR side-by-side multiple presence assumptions are generally thought to be overly-conservative (Curtis and Till 2008; Moses 2001; Ghosn 2008), use of the resulting design and evaluation loads leads to some Michigan bridges being over-designed

as well as under-rated, potentially wasting design and construction resources and unnecessarily restricting truck traffic.

1.2 Background

In 1994, the 1st Edition of the AASHTO LRFD Bridge Design Specifications was published, with the intent to provide a consistent level of reliability to bridge structures by using the probabilistically calibrated LRFD format. Later, the Manual for Bridge Evaluation (MBE) was published by AASHTO in 2008, replacing the 1998 Manual for Condition Evaluation of Bridges (based on Load Factor Rating, LFR) and the 2003 Manual for Condition Evaluation and Load and Resistance Factor Rating (LRFR) of Highway Bridges. In 2007, FHWA required that bridge structures be designed with LRFD as opposed to the Load Factor Design (LFD) approach previously used by MDOT. Moreover, in 2010, FHWA required that structures designed by LRFD were to be rated with LRFR, as in the MBE. The result of moving to LRFD/LRFR from LFD/LFR was significant for MDOT. Most bridges previously designed by LFD and rated by LFR could carry all Michigan legal loads and Class A permit overloads. However, if structures were designed and rated according to the unmodified LRFD and LRFR approaches, many bridges would be unable to carry some Michigan legal loads as well as permit overloads (Curtis and Till 2008).

The differences between using LRFD/LRFR and LFD/LFR are primarily a result of the revised LRFD/LRFR load models. Due to the limited amount of traffic data available at the time, the LRFD load model was developed from a 2-week sample of truck weights measured in Ontario in 1975. Moreover, several assumptions were made to allow for data extrapolation to the 75-year expected mean maximum load used to calibrate the design load. Of particular importance is the presence of side-by-side trucks in adjacent lanes, which has significant impact on load effects. For the LRFD calibration, it was assumed that every 1/15 ‘heavy’ truck was side-by-side with another,

where a 'heavy' truck was taken as the top 20% of the truck population. Moreover, it was assumed that 1/30 side-by-side truck events occur with fully correlated (i.e. identical) truck weights. These assumptions resulted in a model which stipulated that, for every 3rd random truck passage, it is side-by-side with another truck, and for every 1/450 heavy truck crossing, it is side-by-side with an equally heavy truck. Simulations from this model determined that the case of two side-by-side, fully-correlated trucks governed the maximum load effect. In this case, each truck was 85% of the maximum 75-year single lane truck, which were equivalent to 1.0-1.2 times the equivalent HL-93 load, depending on bridge span. This maximum governing load was assumed normally distributed with coefficient of variation from 0.14 to 0.18, depending on span length. This model led to the development of the HL-93 load with live load factor of 1.75 (without impact) and associated multi-lane and ADTT adjustment factors, to meet the minimum target reliability level for LRFD design of β=3.5. Note that bridges with spans greater than 200 ft were not considered (Nowak 1999).

For bridge evaluation with LRFR, for ADTT $\geq$ 5000, the LRFD truck traffic model with side-by-side probability of 1/15 for heavy trucks was maintained for consistency, although this was known to be an extremely conservative value (Moses 2001; Ghosn 2008; Sivakumar 2007). For the 2 and 5-year return periods originally used to develop the LRFR load models, use of the LRFD traffic load assumptions resulted in a mean maximum load event to be the multiple presence of two side-by-side 120 kip (for a 2-year return period) or 130 kip (for a 5-year return period) trucks, of 3S2 equivalent truck configurations. This governing live load was assumed to be lognormally distributed with a coefficient of variation of 0.18. To maintain the target evaluation reliability levels of β=3.5 for inventory ratings and β=2.5 for operating ratings using LRFR with this model, the resulting legal load factor was 1.8 for truck weights up to 100 kips (for ADTT $\geq$

5000). To maintain the target reliability for permit trucks, the live load factor was linearly interpolated between 1.8 and 1.3 for truck gross vehicle weights (GVWs) between 100 and 15.

The conservativeness of multiple presence assumptions in LRFD/LRFR can be practically seen in the work of Ghosn, who studied Weigh-in-Motion (WIM) data from multiple states and generally found that the reliability levels associated with two-lane load effects, as designed/rated, are significantly higher than the one-lane load effects. In California, for example, the LRFD load factor would require a reduction from 1.75 to 1.2 for the two-lanes loaded case to maintain a consistent reliability level with the one-lane loaded case (Ghosn 2008).

A previous study considering Michigan traffic loads (Eamon et. Al. 2014) found that there is a significant variation in the required live load factor from one bridge to another to produce uniform levels of reliability. As the pattern of required load factors is relatively complex, an ideal approach to minimize the load factor variation for all bridge designs is the use of an optimization procedure. There are various optimization techniques that can be used to solve engineering problems, such as classical methods and heuristics. Some of classical methods include sequential quadratic programming (SQP) and calculus-based gradient techniques. SQP is an iterative method that can be used to solve a nonlinear optimization problem. This method is used in problems for which the objective function and constraints are continuously differentiable (Soler et. al. 2013). Calculus-based gradient techniques require the construction or approximation of derivative information. This method can only hope to find local optima (Goldberg and Kuo, 1987). Some heuristics methods include particle swarm optimization (PSO) (Kennedy 2011) and artificial bee colony optimization (Karaboga and Basturk 2007).

In design optimization, stochastic uncertainty associated with load intensity, material properties, geometric dimensions, etc. is represented by random variables and propagated by

mathematical models that quantify variability in responses that depend on such random variables. Probability theory is most commonly used to model stochastic uncertainty in design optimization. This combination of probabilistic modeling and mathematical design optimization framework leads to reliability-based design optimization (RBDO). There are multiple ways of formulating and solving an RBDO problem (Enevoldsen and Sorensen 1994; Frangopol 1995; Tu et al. 1999; Rais-Rohani and Xie 2005; Kharmanda and Olhoff 2007; Aoues and Chanteaueuf 2010, etc). Different approaches for the evaluation of probabilistic constraints have been developed (Enevoldsen and Sorensen 1994; Tu et al. 1999). More recently, Du and Chen (2004) proposed the replacement of each probabilistic constraint with an equivalent deterministic constraint and the decoupling of reliability analysis and design optimization in each design cycle, whereas Qu and Haftka (2004) suggested the use of a probability safety factor in the modeling of each probabilistic constraint.

Previous research has applied design optimization on specific structures, such as to minimize weight or maximize performance criteria such as strength or stiffness. The propose of this study is to use design optimization to in a new way: to develop an optimal load model that can be used to design and load rate a variety of different bridge structures. This would allow any structure that uses the developed model to be optimally designed or rated, without the need for applying further, computationally intensive optimization techniques to each structure individually. The goal of the optimization is to determine an idealized live load (truck model) that produces the lowest discrepancies in reliability among the different bridge structures, while under the constraints that no bridge designed or rated using the model falls below the minimum required reliability level.

1.3 Objective and Scope

The goal of this study is to develop and optimal live load model (in the form of idealized trucks) that can be used for both design and rating. The specific research objectives are to:

- Clean, sort, and analyze a large quantity of weight in motion (WIM) truck traffic data collected from Michigan roadways.
- From a detailed analysis of the WIM data, statistically quantify the load effects, in terms of moments and shears, generated by the recorded truck traffic, extrapolated to the appropriate return periods for design and evaluation (rating).

Based on the load effect statistics, develop corresponding probabilistic load models and incorporate these models into a reliability model for bridges.

- Develop a procedure to apply reliability based design optimization (RBDO) to develop design and rating load models in order to minimize variation in bridge reliability.
- Propose recommendations for vehicular live loads to be used for bridge design and evaluation, such that bridges can meet uniform target reliability levels and avoid unnecessary traffic restrictions.

CHAPTER 2: LITERATUR REVIEW

For bridge design using the AASHTO LRFD Bridge Design Specifications (2010), due to the limited amount of traffic data available at the time, the LRFD load model was developed from a 2-week sample of truck weights measured in Ontario in 1975. Moreover, several assumptions were made to allow extrapolation of the data to the 75-year expected mean maximum load used to calibrate the design load. For multiple presence of side-by-side trucks in adjacent lanes, it was assumed that every 1/15 'heavy' truck was side-by-side with another, where a 'heavy' truck was taken as the top 20% of the truck population. It was also assumed that 1/30 side-by-side truck events occur with fully correlated (i.e. identical) truck weights. These assumptions resulted in a model which stipulated that, for every 3rd. random truck passage, it is side-by-side with another truck, and for every 1/450 heavy truck crossings, it is side-by-side with an equally heavy truck. Simulations from this model determined that the case of two side-by-side, fully-correlated trucks governed maximum load effect. The governing trucks were each 85% of the maximum 75-year single lane truck, which were equivalent to 1.0-1.2 times the equivalent HL-93 load, depending on bridge span. This maximum governing load was assumed normally distributed with coefficient of variation from 0.14 to 0.18, depending on span length. In addition to vehicular live load, the statistics for other random variables (RVs) necessary for reliability assessment were established for the AASHTO LRFD Code development. These include bridge component dead loads and girder moment and shear resistances. These RVs, as well as the corresponding reliability models and associated limit states have been identified and quantified for steel, concrete, and prestressed concrete bridge girders in NCHRP 368 (Nowak 1999), as used for the calibration of the LRFD code. Using these statistics for reliability assessment led to the development of the HL-93 load with live load factor of 1.75 (without impact) and associated multi-lane and ADTT adjustment

factors, to meet the minimum target reliability level for LRFD design of β=3.5. Bridges with spans greater than 200 ft were not considered.

The Manual for Bridge Evaluation (MBE) was published by AASHTO in 2008, replacing the 1998 Manual for Condition Evaluation of Bridges (based on Load Factor Rating, LFR) and the 2003 Manual for Condition Evaluation and Load and Resistance Factor Rating (LRFR) of Highway Bridges. In the original publication of the MBE, for bridge evaluation with LRFR, for AADT ≥ 5000, the LRFD truck traffic model with side-by-side probability of 1/15 for heavy trucks was maintained for consistency, although this was known to be an extremely conservative value (Ghosn 2008; Sivakumar et al. 2007). It was also taken as 1/100 for an ADTT of 1000, and as 1/1000 for an ADTT of 100. For the 2 and 5-year return periods used to develop the LRFR load models, use of the LRFD traffic load assumptions resulted in a mean maximum load event to be the multiple presence of two side-by-side 120 kip (for a 2-year return period) or 130 kip (for a 5-year return period) trucks, of 3S2 equivalent truck configurations. This governing live load was assumed to be lognormally distributed with a coefficient of variation of 0.18. To maintain the target evaluation reliability levels of β=3.5 for inventory ratings and β=2.5 for operating ratings using LRFR with this model, the resulting legal load factor was 1.8 for truck weights up to 100 kips (for ADTT ≥ 5000). To maintain the target reliability for permit trucks, the live load factor was linearly interpolated between 1.8 and 1.3 for truck gross vehicle weights (GVW)s between 100 and 150 kips.

The MBE was later revised in 2011 (Sivakumar and Ghosn 2011) using WIM data from six states (New York, Mississippi, Indiana, Florida, California, and Texas). Four vehicle scenarios on a bridge were considered: a permit vehicle alone; two routine permit vehicles side-by-side; a routine permit vehicle alongside a random vehicle; and a special permit alongside a random

vehicle. Based on a 5-year return period, the revisions recalibrated the LRFR live load factors to result in a target reliability level of β=2.5 for permit loads, with a minimum level of β=1.5. Using the LRFR rating procedures, permit live load factors varied from 1.4 to 1.15 using two- lane load distribution factors, depending on ADTT and the load effect (gross vehicle weight divided by truck axle length).

2.1 MDOT REPORTS AND STANDARDS

MDOT released several research reports that involve load model development from WIM data, including RC-1413 (Van de Lindt and Fu 2002), which estimates the reliability of MDOT bridges using Michigan WIM data; RC-1466 (Fu and Van de Lindt 2006), which calibrated the live load factor for design using LRFD based on WIM data; and R-1511 (Curtis and Till 2008), which developed modified load and rating models for LRFD/LRFR based on NCHRP 454 (Moses 2001) and earlier reports.

From the information in these reports, best summarized in R-1511, MDOT determined that if structures were designed and rated according to the unmodified LRFD and LRFR approaches, many bridges would be unable to carry some Michigan legal loads as well as permit overloads (which were previously allowed under the Manual for Condition Evaluation of Bridges). Under the LFR approach, MDOT overload vehicles were assumed to have no multiple presence with other similar heavy trucks on a bridge, but using the LRFR system in the MBE, multiple presence is assumed, and this subject the overload vehicles to the multi-lane GDFs and load factors associated with legal-heavy vehicles, causing the lower bridge ratings under the LRFR approach.

As a result, MDOT modified both the design as well as the rating process to better correspond to Michigan loads, although these modifications are based on a generic and greatly limited data set. The modifications were designed to avoid the restrictive results of LRFD/LRFR

on Michigan traffic, and involved changing LRFR load factors for legal as well as overload vehicles, based on WIM data from Metro Detroit area bridges as well as other sources. This resulted in the LRFR- mod provisions, which present a series of adjusted load factors to be used for bridge evaluation. However, the LRFR-mod rating factors were based on limited, generic (although from Michigan) multiple presence data, where a multiple presence probability of 1/30 was used to develop the LRFR-mod load factor for AADT $\geq$ 5000. This adjustment did not completely solve the problem of new bridges being under-rated for traffic loads that were previously allowed, so MDOT additionally changed the base LRFD design load to the HL-93-mod load, which considers an additional single 60-kip axle load as well as an increased load factor of 1.2 over the LRFD loads. With these modifications in rating and design, the ratios of Michigan legal loads and overload moments to design moments were returned to values less than 1.0 for spans less than 200 ft. (longer spans were not investigated).

The MDOT Bridge Analysis Guide (2009) documents 28 common legal vehicle configurations, while the legal loads greater than 100 kips are classified as legal-heavy vehicles. For purposes of this report, routine permits as described as vehicles that exceed the legal loads but produce load effects (i.e. moment and shear) that fall below the requirements for a special permit; i.e. the lowest overload classification (C). Vehicles that exceed the Class C limit are special permit vehicles and may be issued a single passage permit over specific structures.

2.2 CURRENT MDOT PRACTICE

Based on some of this previous research, to avoid the restrictive results of LRFD/LRFR on Michigan traffic described above, MDOT modified the LRFR load factors for legal as well as overload vehicles, based on WIM data from Metro Detroit area bridges as well as other sources, resulting in the LRFR-mod provisions, which present a series of adjusted load factors to be used

for bridge evaluation. This did not completely solve the problem of new bridges being under-rated for traffic loads that were previously allowed, so MDOT additionally changed the base LRFD design load to the HL-93-mod load, which considers an additional single 60 kip axle load as well as an increased load factor of 1.2 over the LRFD loads. With these modifications in rating and design, the ratios of Michigan legal loads and overload moments to design moments were returned to values less than 1.0 for spans less than 200 ft (longer spans were not investigated) (Curtis and Till 2008).

As noted, a critical issue involving use of the LRFD and LRFR design and evaluation loads is the assumption used for multiple presence of side-by-side trucks, as this has a large impact on load effect. For example, under the LFR approach, MDOT overload vehicles were assumed to have no multiple presence with other similar heavy trucks on a bridge, but using the LRFR system in the Manual For Bridge Evaluation (MBE) (AASHTO 2011), multiple presence is assumed, and this subjects the overload vehicles to the multi-lane girder distribution factors (GDFs) and load factors associated with legal-heavy vehicles, causing the lower bridge ratings under the LRFR approach. Although this issue was accounted for in general by using the LRFR-mod rating load factors and HL-93-mod loads, the LRFR-mod rating factors were based on limited, generic (although from Michigan) multiple presence data. This recognition opens an opportunity to further refine the LRFR-mod as well as the HL-93-mod rating and design loads to more precisely account for multiple presence using the recently available, high-frequency time stamp WIM data for Michigan roadways. The use of this data provides a basis to recalibrate the design and rating methods and may result in a more uniform level of reliability across structures, more realistic criteria for posting restrictions and granting permits, as well as a more consistent expenditure of design and maintenance resources.

2.3 NCHRP REPORTS

NCHRP Report 368 (Nowak 1999) describes the development of the LRFD load model discussed above, while NCHRP Reports 454 (Moses 2001) and 20-07(285) (Sivakuman and Ghosn 2011) describe the development of the LRFR load models. In NCHRP 454, it was found that the characterizing multiple presence (multiple trucks crossing the bridge simultaneously) probability for load modeling is difficult, as multiple presence is affected by traffic volume, speed, road grade, weather, traffic obstacles, truck grouping, as well as other parameters. Moreover, load effects from multiple presence are strongly interlinked with truck headway distance (i.e. distance between trucks), which is also a function of various road and traffic conditions. The LRFR live load factor is given in NCHRP Report 454 (Moses 2001), as:

$$\gamma_L = 1.8\frac{W_T}{240}\times\frac{72}{W} \tag{1.1}$$

Where W = gross weight of vehicle and WT = expected maximum total weight of rating and alongside vehicles, calculated as: WT + RT + AT. In the latter expression, RT = rating truck and is computed for legal loads as: $R_T = W^*_T + t_{ADTT}\times\sigma_{3S2}$ or for permit load as: $R_T = P + t_{ADTT}\times\sigma^*_{along}$ Here, W^*_T = mean value of the top 20% of legal trucks taken from the 3S2 population; σ_{3s2} = standard deviation of the top 20% of legal trucks; P = weight of permit truck; and σ^*_{along}= standard deviation of the top 20% of the alongside trucks. The alongside truck, A_T, is compute as: $A_T = W^*_{along} + t_{ADTT}\times\sigma^*_{along}$. In this equation, W^*_{along}= mean of the top 20% of alongside trucks.

In the above expressions, t_{ADTT} = fractile value corresponding to the number of side-by-side events, N. The number of side-by-side crossings is computed as:

$$N(legal) = (ADTT) \times (365 \frac{days}{year}) \times (evaluation \ \ period) \times (P_{s/s}) \times (\% \ \ of \ \ record) \quad (1.2)$$

$$N(permit) = (N_P) \times (365 \frac{days}{year}) \times (evaluation \ \ period) \times (P_{s/s}) \quad (1.3)$$

Where NP = number of observed single trip permits (STPs) in the WIM data extrapolated over the evaluation period and Ps/s = probability of side-by-side concurrence. LRFD and LRFR calibrations assumed a 1/15 (6.7%) probability of side-by-side events for truck passages. This assumption was based on visual observations and is conservative for most sites.

In an effort to refine load models for special hauling vehicles, NCHRP 575 (Sivakumar et al. 2007) developed a multiple presence model with additional complexity. Different multiple presence statistics were calculated for variations in bridge span as well as adjacent lane truck headway distances, where headway distance separations up to 60 ft were considered to indicate multiple presence, depending on bridge span. Moreover, side-by-side presence was taken as a function of truck headway distance in adjacent lanes (same direction of travel) and bridge span. It was found that, depending on span and vehicle configuration, significant load effect from multiple presence could occur within headway distances of 10 to 60 ft. More precisely, it was found that for spans less than 100 ft, headway distance under 40 ft produced significant side-by- side multiple presence moments, while for longer spans, headway distances up to 60 ft should be considered. Using this model, multiple presence was calculated from WIM data from 18 states, including Michigan (on US-23) and Ohio (on I-75). It was found that multiple presence probabilities ranged from 1.4- 3.35%. These are much lower multiple-presence probabilities than assumed in LRFD and LRFR, with the maximum side-by-side probabilities of 3.35% occurring at a three-lane site with ADTT > 5,000 and 1.37% for a two-lane site with ADTT > 2,500.

NCHRP 683 further developed the multiple presence model, considering various traffic configuration possibilities including multiple side-by-side trucks in adjacent lanes, and developed multiple presence statistics from WIM data for different ADTT and bridge spans. It was suggested that multiple presence loads could be generated by developing single-lane truck weight probability densities, then combining the multi-lane effects by convolution, as suggested by Croce and Salvatore (Croce and Salvatore 2001), as well as Monte Carlo Simulation (MCS), while maximum load effects for longer time periods were estimated by statistical extrapolation. Limitations of the model include an assumption that the GVW distribution is identical in adjacent lanes and that there is no correlation between truck weights. For the development of statistical load models used for reliability analysis, the upper tail of the distribution, where the heaviest vehicles are described, is most critical. However, it was noted that WIM data is particularly subjected to various collection errors in this region, caused by vehicle dynamics, tire configurations, and other factors.

NCHRP 683 further developed a general framework for data filtering, many of which are based on the FHWA Traffic Monitoring Guide (2001). Here four main subtasks are described: data filtering; review of eliminated data for verification; implementation of QC checks; and assessing the statistical adequacy of the data.

The purpose of the data filtering step is to flag collected results that appear to be unreliable or that may indicate an unrealistic vehicle. For example, axle weights and spacing that are unreasonably small or large; unreasonably high or low speeds (low-speed trucks are difficult to separate); and discrepancies in GVW and sum of axle weights. NCHRP 683 as well as other research efforts (O'Brien and Enright 2011; Pelphrey and Higgins 2006; Tabatabai et al. 2009) provide similar recommendations for a filtering process. The data recommended for flagging generally include: speeds below 10 or above 100 mph; truck length above 120 ft (or as

appropriate); total number of axles below 3 or above 13 (or as appropriate); first axle spacing below 5 ft; any axle spacing below 3.4 ft.; sum of axle spacing above total truck length; individual axle above 70 kips (or as appropriate); steer axle above 25 kips or below 6 kips; any axle below 2 kips; GVW below 12 kips or above 280 kips; sum of the axle weights is different from GVW beyond 5-10%.

For the data review step, a sample of the data eliminated is inspected and reviewed, and compared to expected truck configurations to ensure that the filtering procedure is working properly and realistic trucks are not unintentionally eliminated. If available, it is recommended that historical permit or nearby weigh station data will also be used to verify that the collected WIM data are reasonable.

Multiple QC checks are then used to verify data accuracy. In general, these checks include comparing truck percentages by type and GVWs found in the WIM data to historical values or manual counts, and comparing measured axle weights and configurations to reasonably expected values. The first check is to compare vehicle type percentages to expected values at the site if available. The following checks are suggested by NCHRP 683 for the common 5-axle (Class 9 or 3S2) semi-trailer truck data collected: compare the number and proportion of trucks over 100 kips to expected values; compare the mean drive axle weight to the mean values found in NCHRP Report 495 (Fu et al. 2003); compute the mean value for steering axle weight, which is typically between 9 kips and 11 kips; and check mean spacing between drive tandem axles, and compare to expected values. Finally, a histogram of GVW can be developed. The usual distribution is bi-modal, with one peak corresponding to an unloaded vehicle and the second for a loaded vehicle. These peaks can be compared to expected values (typically 30 kips unloaded and from 72 and 80 kips loaded).

Assessing the statistical adequacy of the data involves inspection of the confidence interval of the upper tail of WIM data. Because only a small sample of the entire truck population is collected from WIM data, using this limited data to model the entire population is associated with uncertainty. Of particular concern is the uncertainty associated with the upper tail (heaviest) of the truck weights. This uncertainty is statistically quantifiable with confidence interval evaluation (Ang and Tang 2007). NCHRP 683 recommends that the 95% confidence interval of the upper 5% of truck weights from the WIM data is considered. That is, what range of uncertainty is associated with critical distribution parameters such as mean value and standard deviation, to a 95% level of confidence. Here, the distribution type that best-fits, per standard goodness-of-fit tests, such as Kolmogorov-Smirnov, Chi-square, or Anderson Darling (Ang and Tang 2007), for example, the upper 5% of the Michigan WIM data is determined. Then, the appropriate confidence interval is constructed for mean value and standard deviation. Thus, the range of values representing uncertainty in the mean and standard deviation can be quantified, to a 95% confidence level. An unacceptably wide confidence interval indicates that an inadequate number of data were collected. In this case, additional data collection from these sites is recommended, or to remove the affected sites from the project database.

In NCHRP 683, several different truck placement possibilities that may cause variations in load effect were considered. Here, multiple presence statistics were generated for two "side-by-side" trucks (defined as two trucks in adjacent lanes overlapping by one-half of a truck length or more); two "staggered" trucks (two trucks with an overlap less than one-half of a truck length but a gap between them less than the bridge span); and for "multiple" trucks, where more than one truck side-by-side appears in both lanes.

Convolution was also suggested as a method to generate multiple presence effects, as described in NCHRP 683 and elsewhere (Croce and Salvatore 2001). Here, the single-lane load effect histograms are numerically integrated with the convolution equation, which provides the probability density function (PDF) of two events (i.e. two trucks side-by-side), (fxs), which is given by: $f_{xs}(X_s) = \int_{-\infty}^{+\infty} f_{x2}(X_s - x_1) f_{x1}(x_1) dx_1$, where f_{x1} and f_{x2} are the PDFs of truck load effects x_1, x_2 for lanes 1 and 2. Then, from the resulting PDF, the needed statistical parameters describing two-lane load effects can be directly calculated. However, it was found by (O'Brien and Enright 2011) that since the convolution process assumes independence between truck weights in each lane, which is not necessarily correct, it can lead to misrepresentation of maximum load effects.

NCHRP 495 (Fu et al. 2003) describes a process to evaluate the effect of changing allowable truck weights on the cost of maintaining highway bridges, due to the increased damage caused by increased truck loads. In order to estimate the damage on bridge structures, a process to obtain truck weight and frequency distributions was developed, considering the data obtained from state weight stations.

2.4 MULTIPLE PRESENCE MODELING

The definition of multiple presence is not straightforward, as even holding various other factors such as ADTT and site location constant, the load effect caused by multiple presence varies greatly depending on truck headway distance in adjacent lanes, in the same lane, bridge span, and truck weight correlations as well. Some approaches ignore these complexities and model multiple presence by placing two trucks exactly side-by-side on the analysis bridge, and provide an associated occurrence probability, such as in every 1/15 or 1/30 heavy truck passages, for example, potentially based on WIM data (Moses 2001; AASHTO 2003). These multiple presence

probabilities are directly calculated from the WIM data for various important scenarios such as a 'side-by-side', 'staggered', or 'multiple' truck scenario, for various span lengths. In this model, the precise definitions (truck headway distances and overlaps considered) used to characterize multiple presence statistics are determined based on those required to produce a significant increase in load effect over that of a single lane truck load, such as suggested by NCHRP 575 (Sivakumar et al. 2007) and others such as (Fu and You 2009; O'Brien and Enright 2011). Fu and You (2009) used this approach and considered multiple presence to occur if an adjacent truck increased the single-lane truck moment by 20% or more. Based on an analysis of WIM data from New York, they found multiple presence probabilities from 0.4 - 3.5%, as a function of ADTT and bridge span. However, this approach generally will not produce the most accurate multiple presence load effects, as typically, all relevant load information simply cannot be captured using this method, as significant variations in load effect are neglected (Sivakumar et al. 2011; O'Brien and Enright 2011).

Another approach is to directly determine multiple-lane load effects from Monte Carlo simulations of different traffic configurations statistically quantified from the WIM data, as suggested in (O'Brien and Enright 2011; Kwon et al. 2010). This approach is potentially most accurate, but is also most difficult to use and generalize to multiple locations, as a value for multiple presence probability is not directly calculated. This approach also requires a high-resolution timestamp in the WIM data of at least 1/100 second to properly capture the needed traffic patterns. For this simulation model, various truck parameters available from the WIM data are modeled as random variables (RVs), such as truck weights, speeds, and inter-vehicle gaps within and between lanes. These RVs are characterized by fitting the parameters to best-fit analytical probability distributions. In addition to the individual RV parameters, their inter-

relationships are also statistically characterized, which is done from high resolution WIM data by developing the correlation matrix between the RVs for linear relationships, or empirical copulas for more complex non-linear relationships (O'Brien and Enright 2011; Tabatabai et al. 2009).

Croce and Salvatore (2001) presented a more general theoretical stochastic traffic model to account for vehicular interactions. Their proposed model was based on a modified equilibrium renewal process of vehicle arrivals on a bridge, and formulates the problem of traffic actions in terms of the general theory of stochastic processes. An analytical expression for the cumulative distribution functions (CDF)s of the maximum load effect over a given time interval was developed under general assumptions. The resulting CDFs allowed studying multilane traffic effects, as well as the combined effects of traffic and other load actions, while accounting for arbitrary variations in traffic flow.

Later, Obrian and Caprani (2005) studied short to medium span, 2-lane bridges with opposing traffic for events involving more than two trucks simultaneously on the bridge. They statistically modeled vehicle headway distances measured from five days of WIM data collected from the two outermost lanes of a motorway near Auxerre, France. In the simulations, it was found that critical traffic load events are strongly dependent on the assumptions used for the headway distance (the time or distance between the front axle of a leading truck and the front axle of a following vehicle) and gap (the time or distance between the rear axle of the front truck and the front axle of the following truck) between successive trucks. Specifically, it was determined that mean load effect could be altered by 20% to 30% for reasonable gap choices. Headway distances were found to be a function of traffic flow, where headways of less than 1.5 seconds were insensitive to flow and could be fit well to quadratically increasing cumulative distribution functions, while headways from 1.5 to 4.0 seconds were strongly influenced by flow. Inter-truck

headway is influenced by truck driver behavior as well as the number of cars between trucks. They also determined that medium and long span bridge loads are strongly influenced by traffic congestion, where the gaps between vehicles become small and there is no significant dynamic interaction. For short span bridges, however, free-flowing traffic involving a small number of vehicles with dynamic interaction becomes more critical.

One of the most recent and sophisticated multiple presence models is given by O'Brien and Enright (O'Brien and Enright 2011), who carefully studied WIM data from European sites and found subtle but important correlations between vehicle weights, speeds and headway distances. They found that neglecting these correlations as in previous efforts could lead to errors close to 10% in maximum load effect. To properly model the multiple presence effect on a two-lane bridge, it was proposed that the truck traffic model includes three headway, or gap, distributions: in-lane gaps for each lane as well as an inter-lane gap. Moreover, inter-relationships exist between gap distance, vehicle weights, and speeds. To determine maximum lifetime load effect statistics from this model, a smoothed bootstrap simulation approach was used, which re-samples traffic scenarios based on the WIM data and uses kernel functions to introduce additional variation. They concluded that the model produced a better fit to the data than those neglecting the multi-lane correlations.

Some researchers also used PC simulation packages to model the dynamic response of heavy vehicles (Kordani et al. 2014a; Molan and Abdi 2014; Kordani et al. 2014b). Simulation modeling can be defined as another method for the studies related to dynamic effect of vehicles on highway structures; however, calibration should be considered as an important parameter and a precise modeling of driver behavior is required to increase the accuracy of outcomes.

2.5 COLLECTING AND ANALYZING WIM DATA

There are various methods for collecting and analyzing different forms of data in the literature (see (Aguwa, Olya and Monplaisir 2017; Hair, Anderson, Babin and Black 2010; Gelman, Carlin, Stern and Rubin 2014)). The Texas Department of Transportation (TxDOT) developed a procedure to determine equivalent single axle loads (ESALs) from WIM-collected traffic volume and classification data (Lee, C.E. and Souny-Slitine 1998). The system was also used to monitor weekly and monthly data trends such as the proportion of various vehicle classes and lane use. The system analyzed traffic data on-site by the WIM system computer and an Excel spreadsheet for vehicle classification and calculation of ESALs. The method used traffic volume and vehicle class data rather than axle load data directly, but found that the cumulative ESALs at a site depend on the traffic volume and axle loads.

Raz et al. (2004) proposed a data mining approach for automatically detecting anomalies in WIM data. The procedure was useful for automatically detecting unlikely and erroneously classified vehicles, and could identify hardware or software problems in WIM systems.

Monsere et al. (2008) studied methods for collecting, sorting, filtering, and archiving WIM data to permit development of long-term continuous records of high quality. The study used the WIM data archive to monitor WIM sensor health, develop loads for asphalt design and models for bridge rating and deck design. In addition, freight movement was monitored to develop volume, weight, safety, and time demands on highways. Data were analyzed and filtered to handle anomalous results. Axle load spectra and time of occurrence models was developed, and Monte Carlo techniques were used to generate load histories for pavement damage estimates. Moreover, side-by-side vehicular events were quantified using the precise time stamps available in the WIM

data. The long-term record was used to extrapolate the best possible statistical tail for single lane loading cases on bridges.

Pelphery et al. (2008) described a series suggestions for collecting and analyzing WIM data that includes filtering, sorting, quality control, as well as how to use the data in a load factor calibration process. The data were cleaned and filtered to remove records with formatting mistakes, spurious data, and other errors identified by the following criteria: a record does not follow the general format pattern; GVW less than 2 kips or greater than 280 kips; GVW differs from the sum of axle weights by more than 7%; an individual axle is greater than 50 kips; the speed is less than 10 mph or greater than 99 mph; truck length is greater than 200 ft; the sum of the axle spacing lengths are less than 7 ft or greater than the truck length; the first axle spacing is less than 5 ft or any axle spacing is less than 3.4 ft; and the number of axles is greater than 13. Note the similarities to these recommendations and those made by NCHRP 683. A conventional and modified sorting method for the WIM data were then developed and compared. The conventional method sorts vehicles based on their GVW, axle group weights, and truck length. This method accounts for the axle weights and spacing in assigning each vehicle to an appropriate weight table. The method tends to assign more vehicles to higher weight tables than the modified sort. The modified methods sort vehicles based only on their GVW and rear-to- steer axle length, and it does not account for axle groupings. This method assigns more vehicles to lower weight tables than the conventional sort. However, it produces higher coefficients of variation and hence higher live load factors, as compared to the conventional sort, as is thus more conservative overall than the conventional method. In the study, the conventional sort method was used to calculate live load factors, as this was believed to better represent the traffic regulatory and enforcement procedures used.

Additionally, only the top 20% of the truck weight data from each category was considered, as projected from the upper tail of the weight histogram.

2.6 DEVELOPMENT OF TIME-ADJUSTED LOAD EFFECT STATISTICS

From WIM data, load statistics can be directly calculated only for the period of time over which the data were collected. However, it is necessary to statistically quantify the maximum load effects caused by side-by-side events for the time period used for design or evaluation. For design, this time is taken as a 75-year return period according to LRFD (2014). Note that the life time of bridges may vary depending on load, maintenance and weather conditions (Eamon et. al 2014). For evaluation under LRFR, a 2 or 5-year return period is generally used (O'rien and Enright 2010). Various statistical projection techniques have been developed to extrapolate from WIM time periods to design and evaluation time periods.

One approach is to use extreme value theory to project the resulting side-by-side load effect (valid for the time period in which WIM data was collected) to the desired 5 (or 2) year and 75-year time periods. Probabilistically, it is known that the distribution of the largest values of events approaches Extreme Type distributions as the number of load events becomes large. For example, if the upper tail of the WIM load data best fits a normal distribution, the largest values approach an Extreme Type I (Gumbel) distribution; if the upper WIM data best fit a lognormal distribution, the largest values approach a Type II (Frechet) distribution, etc. (Ang and Tang 2007). Once the appropriate distribution is identified, statistics for the mean maximum load effect can be determined for any time period of projection using known distribution relationships. For example, as shown in (Ang and Tang 2007; Sivakumar et al. 2011), if a Type I distribution were considered, the 5-year mean maximum load (for side-by-side trucks) can be determined from: $\overline{x_k} + (\frac{\sqrt{6}}{\pi}) * \sigma_k * \ln\left(\frac{N}{k}\right)$, where $\overline{x_k}$ and σ_k are the mean and standard deviation computed from k side-by-side events

for the time longer period of time (i.e. N = k*5 if k was measured over 1 year and the desire is to project to a 5 year maximum). Similar relationships are available for the other distribution types as well.

Another projection technique is the plotting approach, where the cumulative distribution function (CDF) of the n WIM data, given by $F_x(x) = \frac{x_i}{1+n}$, is plotted on probability paper representing a certain trial distribution type. This is done by scaling the y-axis of the data appropriately such that a straight line will result on the plot if the actual CDF exactly represents the trial distribution. Then, the upper tail of the CDF is extended to load effects representing longer periods of time, by one of various possible extrapolation techniques. This approach was used in MDOT Report RC-1466 (Fu and Van de Lindt 2006) on actual Michigan WIM data, where several distribution types and extrapolation techniques were considered, including linear and nonlinear (polynomial) regression, applied to both the tail end and the entire CDF of the data, on normal, lognormal, and extreme type probability papers. It was found that the best fit could be obtained by representing the data with an Extreme Type I (Gumbel) distribution. However, when used to extrapolate to longer time periods, this approach provided inconsistent results with the projection process used to calibrate the LRFD code, resulting in much higher predicted load effects. Using the obtained results would have required either lowering the target reliability index for Michigan bridges, or an increase in bridge design capacity to meet the target LRFD index (Fu and Van de Lindt 2006).

To avoid this problem, RC-1466 recommended the projection process used for the LRFD code calibration, in which the CDF for the projected data (to 75 years) was developed by raising the CDF of the existing data to the nth power, where n is the ratio of the projected time to the equivalent time over which the WIM data were monitored (Nowak 1999; Fu and Van de Lindt

2006): $F_t(x) = F_{wim}(x)^n$, where $F_t(x)$ is the CDF of the time of interest (e.g. 5 or 75 years) and $F_{wim}(x)$ is the CDF of the WIM data. The benefit of this method is that it allows consistency with LRFD projection, such that Michigan target reliability index need not be adjusted.

To enhance the accuracy of the projection results for any of these techniques (extreme value theory, plotting approach, or LRFD approach), Monte Carlo Simulation has been employed (O'Brien and Enright 2010; Sivakumar et al. 2011; Gindy and Nassif 2006). In this approach, additional load effect data is simulated, although it was found that it is generally not possible to generate the large number of data required to directly calculate statistics for maximum evaluation or design loads with sufficient confidence, due to the computational effort required (Sivakumar et al. 2011; O'Brien and Enright 2011). However, MCS can be used to extend the data pool for a limited time beyond which the data were collected, potentially increasing the accuracy of the projection when extrapolated to longer periods of time. This process been used successfully by a variety of researchers (O'Brien and Caparani 2005, O'Brien and Enright 2010, 2011; Groce and Salvatore 2001), and is suggested in NCHRP 683 as well (Sivakumar et al. 2011).

2.7 LOAD MODEL DEVELOPMENT FOR BRIDGE DESIGN AND RATING

Early work includes that by Ghosn and Moses (1986), who, as a precursor to Nowak (1999) used reliability analysis with data from large scale field measurements of actual truck loadings and bridge responses. The data were used to project to maximum expected live loads in the lifetime of the structure and to calculate a safety index. A target safety index was extracted from these values and a new design procedure was proposed to achieve this target index to provide uniform reliability for the spans considered. The target safety index was derived from average AASHTO performance, and it was suggested that the approach could be extended to allow rating of existing bridges where load conditions were monitored by WIM systems.

Ghosn (2000) considered a reliability-based procedure to determine the optimal allowable loads on highway bridges considering static and dynamic effects and the effect of increasing the legal load limit on bridge safety. The procedure used to select the most appropriate allowable truck weight was developed as follows: choose suitable safety criteria; select an acceptable reliability level; choose a range of typical bridges (designed with different code criteria, span lengths, configurations, material types, and capacity levels); statistically describe the safety margins of these typical bridges (including the likelihood of overloads and simultaneous truck occurrence); calibrate a new allowable truck load; check the effect of the proposed truck loads on the existing network of bridges, and; verify that the number of bridge deficiencies under the new regulation will be acceptable in terms of the additional costs required to maintain the existing bridge network. In this process, the maximum permissible live load moment would be determined by trial and error to satisfy the target safety index for all of the bridge types considered. The allowable truck loads that would produce the permissible live load envelope is then to be determined.

Rather than relying upon WIM, Fu and Hag-Elsafi (2000) suggested that live load model development could be based on granted overload permit data. They presented a method to develop live load models based on the permit data, developed associated models for assessing reliability, and proposed permit-load factors for overload checking.

Miai and Chan (2002) developed a new approach for load model development based on a 'repeatable' methodology for short span bridges to obtain extreme daily moments and shears in simply supported bridges and compared the results to the traditional normal probability paper approach used to form the AASHTO LRFD load model. The method involved the following steps: calculate extreme daily bending moments and shear forces based on the WIM data; analyze the data statistically for load model parameters (axle weights, gross vehicle weights and axle spacing);

divide the traffic into two types: loose and dense traffic status; use the Equivalent Base Length for modeling bridge live load models. In the procedure, Monte Carlo simulation was used to simulate the complex interactions of random parameters governing truck loads. Axle spacings were divided into internal and tandem spacings. It was found that axle spacing was best modeled with a lognormal distribution, while axle weights as well as GVW best followed an inverse normal distribution. For 'loose' traffic density, the maximum value of axle weight and GVW for bridge design was found to follow an Extreme Type I distribution, and a Weibull distribution for 'dense' traffic.

Ghosn et al. (2008) describes how site-specific truck weight and traffic data collected using WIM data can be used to obtain estimates of the maximum live load for a 75-year design life for new bridges as well as the two-year return period for capacity evaluation of an existing bridge. It was determined that data from the upper tails of WIM data histograms from several sites match normal probability distributions, a finding allowing the application of extreme value theory to obtain the statistics of maximum load effect. It was also found that average bridge reliability varies considerably from state to state, and that the reliability levels associated with two-lane load effects, as designed/rated, are significantly higher than the one-lane load effects. This occurs because of the lower number of side-by-side events as well as the lower load effect produced by two-lane events when compared to the conservative multiple presence model used to calibrate the AASHTO LRFD Code. The conservativeness of the LRFD multiple presence assumptions are demonstrated by Ghosn (2008), who considered load data found in California, and determined that the LRFD load factor would require a reduction from 1.75 to 1.2 for the two- lanes loaded case to maintain a consistent reliability level with the one-lane loaded case.

O'Brian et al. (2010) predicted lifetime maximum truck load by using Monte Carlo simulation to simulate traffic representative of measured vehicle data for a given bridge. Such parameters as gross vehicle weight, number of axles, axle spacing, distribution of GVW between axles, and inter-vehicle spacing were included as parameters in the model. The study used WIM systems at two European sites and considered three different methods of modeling GVW, based on histograms of the weight data: parametric fitting, which produced a moderately good fit for most of the GVW range, but significantly underestimated the probabilities in the critical upper tail; nonparametric fitting, which produced a reasonable fit for the range of commonly observed GVWs, but presented problems in the upper region of the histogram where observations are few and there are gaps with no measured data, and GVWs heavier than the maximum measured value cannot be simulated; and semi-parametric fitting, which had the best accuracy in the critical tail region, and was the ultimately recommended approach.

For development of the Eurocode traffic live load model, load effects were estimated by extrapolating from WIM data as well as Monte Carlo simulation. However, each lane was simulated independently (Bruls et al. 1996; O'Connor et al. 2001), limiting the multiple presence model accuracy, similar to the NCHRP 683 model.

In addition to his work on the LRFD Code calibration, Nowak (Nowak et al. 2010) recently considered load models for long-span bridges, and developed a corresponding traffic simulation model for this case. It was found that the maximum load scenario is a traffic jam in which trucks tend to line up in one lane. He noted, however, that trucks are usually separated by lighter vehicles, and in this typical situation, a single overloaded truck did not have a significant effect on total load effect.

Ghosn et al. (2011), used the simplified adjustment procedure suggested in the MBE to develop a load and resistance factor rating method for permit and legal loading for NYSDOT from WIM data. ODOT calibrated live load factors used for design from WIM data (Pelphery et al. 2006), and Wisconsin DOT statistically modeled maximum load effects from WIM data by fitting multi-modal distributions to axle loads and spacings, then using MCS with empirical copulas to model the axle load and spacing relationships (Taatabai et al. 2009).

Missouri DOT recently completed a recalibration of load factors for bridge design and rating, based on local WIM data (Kwon et. al. 2010). Assumptions in the traffic model were that: minimum headway distance is 0.5 s; the time between trucks could be modeled with a shifted exponential distribution; and that 70% of trucks were in the right lane. Maximum load effects were then assumed to follow a Gumbel distribution, and extreme value theory was used for projection to the design maximum load. Similar to previous methods used to characterize multiple presence, the loads in adjacent traffic lanes were treated as independent.

2.8 RELIABILITY ANALYSIS METHODS

For structural reliability problems with well-behaved limit state functions (i.e. generally with mild or no nonlinearities and random variable types close to normal), most probable point of failure (MPP) search or reliability index-based methods are often the first choice for reliability analysis, as they can typically achieve accurate results with much less computational effort than simulation methods such as Monte Carlo simulation (MCS) or one of the various variance reduction techniques (VRTs). The widely-used reliability-index based methods include the first- and second-order reliability methods (FORM, SORM) (Rackwitz and Fiessler 1978; Breitung 1984), with many variants presented in the literature (Chen and Lind 1983; Wu and Wirsching 1987; Fiessler et al. 1979; Hohenbichler et al. 1987; Tvedt 1990; Der Kiureghian et al. 1987;

Ayyub and Haldar 1984, among many others). VRTs such as importance sampling (Rubinstein 1981; Engelund and Rackwitz 1993) and adaptive importance sampling (Wu 1992; Karamchandani et al. 1989), also make use of the MPP concept, and can similarly lead to significant reductions in computational effort over MCS. For ill-behaved or difficult to capture responses, however, such as those which may be discontinuous, highly nonlinear, or that contain multiple 'local' reliability indices on the limit state boundary, the most probable point (MPP) search algorithms may fail or produce unstable or erroneous results. In such cases, one must rely upon a greatly reduced selection of techniques, primarily those from the simulation family that do not rely upon an MPP search such as MCS and its advanced variants (Au and Beck 2001; Au et al. 2007; Eamon and Charumas 2011) or stratified sampling methods (Iman and Conover 1980). An alternative common approach is approximating the true limit state function with a response surface (RS), of which many examples exist (Bucher et al. 1990; Gomes et al. 2004; Cheng et al. 2009, etc.) Point integration or point estimation techniques would also be possible, although results may be highly unreliable (Eamon et al. 2005).

The drawback of most sampling techniques is the effort required, particularly for high-reliability problems involving a computationally expensive, implicit limit state function. Similarly, for complex responses (highly nonlinear or discontinuous), it is may be difficult to develop a sufficiently accurate response surface for reliability analysis without expending considerable computational effort.

For the reliability analysis of bridge structures, various bridge characteristics may affect results, such as span length, material type, girder spacing, traffic characteristics, and number of lanes. Generally, the first order MPP methods such as FORM have been found to be sufficiently

accurate for calibration efforts (Nowak 1999). Minimum target reliability indices were set as β=3.5 for design and β=2.5 for operating evaluation (Nowak 1999; Moses 2001).

2.9 RELIABILITY BASED DESIGN OPTIMIZATION

In design optimization, stochastic uncertainty associated with load intensity, material properties, geometric dimensions, etc. is represented by random variables and propagated by mathematical models that quantify variability in responses that depend on such random variables. Probability theory is most commonly used to model stochastic uncertainty in design optimization. This combination of probabilistic modeling and mathematical design optimization framework leads to reliability-based design optimization (RBDO).

Recently, RBDO has been used as an appropriate approach for structural optimization under uncertainty. Deterministic structural optimization problem in RBDO is modified by a non-deterministic one subject to a combined set of deterministic and reliability-based design constraints, with a set of designs as well as random variables (Eamon and Rais-Rohani 2009).

There are multiple ways of formulating and solving an RBDO problem (Enevoldsen and Sorensen 1994; Frangopol 1995; Tu et al. 1999; Rais-Rohani and Xie 2005; Kharmanda and Olhoff 2007; Aoues and Chanteaueuf 2010, etc). In its generic form, an RBDO problem seeks to minimize an objective function $f(\boldsymbol{X},\boldsymbol{Y})$, subject to a series of probabilistic constraints in the form $P_{f_i} = P\left[G_i(\boldsymbol{X},\boldsymbol{Y}) \le 0\right] \le P_{a_i}$; $i = 1, N_p$, side constraints on design variables $Y_k^l \le Y_k \le Y_k^u; k = 1, NDV$ with $\boldsymbol{X} = \{X_1, X_2, ..., X_n\}^T$ as vector of random variables. It is common to treat the mean values of random variables μ_X as the design variables. In this approach, the objective function can be written as $f(\boldsymbol{X},\boldsymbol{Y}) = a_1\mu_f(\boldsymbol{X},\boldsymbol{Y}) + a_2\tilde{\sigma}_f(\boldsymbol{X},\boldsymbol{Y})$, where μ_f and $\tilde{\sigma}_f$ represent the mean and standard deviation values of $f(\boldsymbol{X},\boldsymbol{Y})$, respectively, with coefficients a_1

and a_2 denoting scalar weighting factors that can be used to balance the requirements for efficiency and robustness in design (Rao 1992). Different approaches for the evaluation of probabilistic constraints have been developed (Enevoldsen and Sorensen 1994; Tu et al. 1999). More recently, Du and Chen (2004) proposed the replacement of each probabilistic constraint with an equivalent deterministic constraint and the decoupling of reliability analysis and design optimization in each design cycle, whereas Qu and Haftka (2004) suggested the use of a probability safety factor in modeling of each probabilistic constraint.

Various types of optimization algorithms are available. Some of these include Sequential Quadratic Programming (SQP) (Nocedal and Wright 2006), cross entropy methods (Fazlollahtabar and Olya 2013), Calculus-based gradient techniques (Goldberg and Kuo 1987), stochastic dynamic programming (Olya, Fazlollahtabar, and Mahdavi 2013; Olya 2014a; Molan and Abdi 2014), probabilistic dynamic programming with various density functions (Olya, 2014b; Olya & Fazlollahtabar, 2014) and normal density function (Olya, Shirazi, & Fazlollahtabar, 2013), Particle Swarm Optimization (PSO) (Kennedy 2011), Artificial bee colony optimization (Karaboga and Basturk 2007) and genetic algorithms. In some cases, genetic algorithms (GA) have been found to be more reliable for solving multi-objective optimization problems than other common optimization methods (Koumar et. al. 2017). Sakamoto and Oda (1993), combined a genetic algorithm and an optimality criteria method to optimize the layout and cross-sectional area of the trusses by minimizing the weight design of truss structures subjected to displacement constraint. Corso et. al. (2015), used a GA method for RBDO of thin copper films deposited on flat surfaces of polypropylene polymer. GA has also been used to solve a variety of structural problems. For example, Koumara et. al. (2017), used a GA to minimize the mass and compactness of scissor structures by considering shape and cross-sectional area as design variables and stress, buckling,

and deformation criteria as constraints. Kaveh and Shojaee (2003) applied the GA to minimize the weight of foldable structures. Garambois et. al. (2016), used a multi objective GA optimization to minimize the mass and Von Mises stress in the plate structure by considering thickness parameters under a dynamic load.

CHAPTER 3: ANALYSIS OF WIM DATA

3.1 WIM SITES

There are over 100 WIM stations in the State monitored by MDOT, as described in Appendix A (Table A1). Of these, the data from 37 were considered for possible use in this study, which represent stations for which high speed time stamp data of at least 100 Hz were collected for approximately two years. A data collection rate of this frequency is necessary to accurately record the positions of following and side-by-side vehicles. The stations considered in this study are given in Table 3.1. For the most part, these stations are on major routes (State and Interstate roadways) with relatively large traffic volumes. The data from Station 4249 were not used, as this station was reported to have a failing sensor that provided unreliable results for the period of time for which the data used in this study were collected. The data used in this study were collected from January 2011 to September 2012. Across all sites considered, there were approximately 92 million total vehicles recorded for processing (after the automatic small vehicle WIM filtering criteria were applied, as discussed below).

For the reliability calibration, a selection of representative sites were chosen in four ADTT categories, as shown below. Note that mid and low traffic volume categories have a small number of sites, because MDOT's data collection was limited to a few of these types of sites. All selected sites are shown in Figures 3.1-3.4.

Table 3.1. WIM Stations Used for Reliability Calibration.

Site	Location	ADTT	Site	Location	ADTT
High ADTT (≥ 5000)			Mid ADTT (~2500)		
9209	I-275	4850	5059	I-196	2520
7029	I-94	4930	6369	I-69	2650
8869	I-69	4980	6469	I-94	2640
9189	I-275	5120	Low ADTT (~1000)		
7269	I-69	5290	4049	I-75	850
8839	I-94	6340	5289	US-31	1050
7169	I-94	6480	6429	I-75	1340
7219	I-94	8440	5099	I-96	1350
7159	I-94	9900	8029	US-127	1560
9699	I-75	11100	Very Low ADTT (~400)		
			1199	M-95 (UP)	400
			2029	US-2 (UP)	420

Figure 3.1. WIM Sites With ADTT ≥5000.

Figure 3.2. WIM Sites With ADTT ~2500.

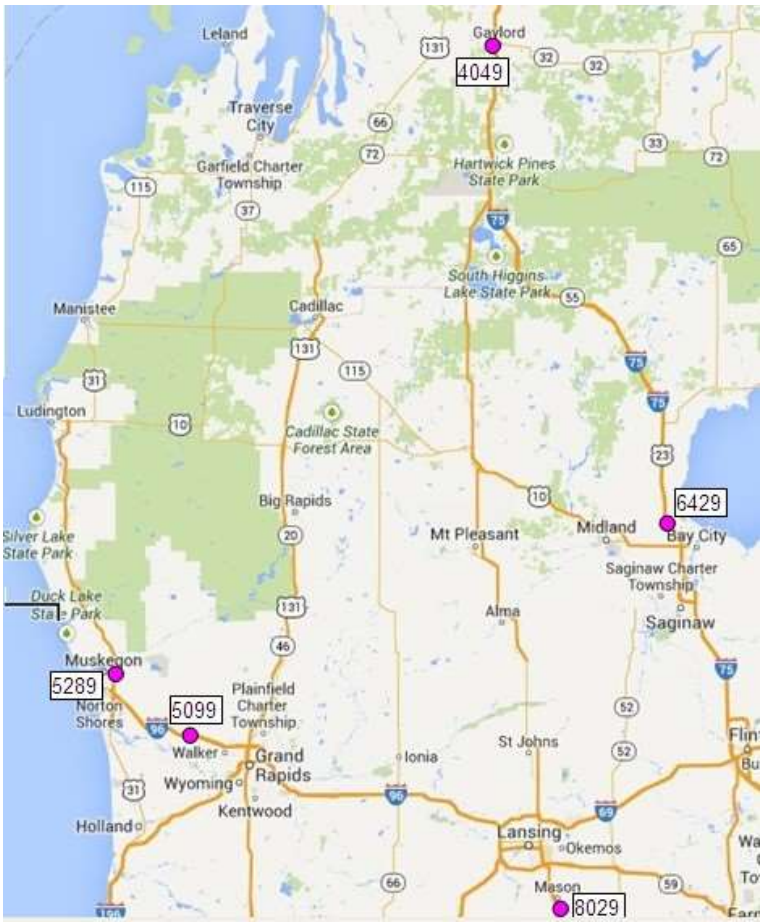

Figure 3.3. WIM Sites With ADTT ~1000.

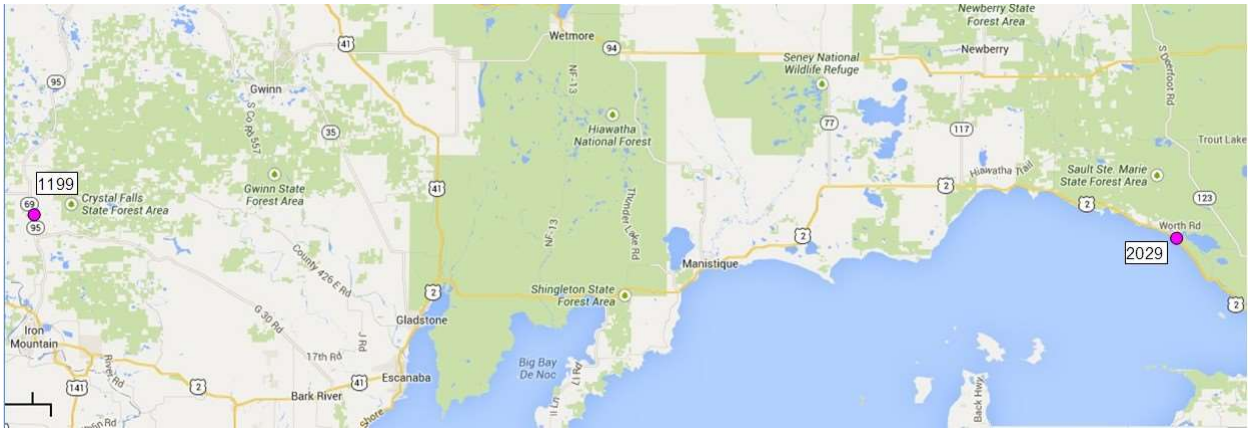

Figure 3.4. WIM Sites With ADTT ~400.

3.2 DATA FILTERING

3.2.1 Filtering Criteria

Each WIM station employs an automatic filtering system that removes the majority of non-critical traffic from the database. These lightweight vehicles include motorcycles, cars, and light trucks (vehicle classes 1-3). These vehicles are summarized in Table 3.2, below.

Table 3.2. Small Vehicles Filtering Criteria.

			Axle Spacing (ft)				
Class	Vehicle	Axles	1st	2nd	3rd	4th	Weight (k)
1	Motorcycle	2	0.1-6				0.1-3
2	Car	2	6-10.1				1-8
3	Truck	2	10.1-16				1-9
2	Car, 1-Axle Trailer	3	6-10.1	6-30			1-12
3	Truck, 1-Axle Trailer	3	10.1-16	6-30			1-15
2	Car, 2-Axle Trailer	4	6-10.1	6-30	1-12		1-12
3	Truck, 2-Axle Trailer	4	10.1-16	6-30	1-12		1-15
3	Truck, 3-Axle Trailer	5	10.1-16	6-30	1-12	1-12	1-15

After extensive discussions with the research advisory panel, additional data filtering criteria were employed to eliminate unrealistic vehicles from the database. Each criterion in Table 3.2 was determined by panel members, in conjunction with the recommendations of the WIM data

collection expert, to avoid vehicle configurations recorded by the WIM equipment which were deemed to likely represent false vehicles. These additional criteria are summarized in Table 3.3. Note it was found that the overall vehicle statistics are not particularly sensitive to reasonable modifications in the filtering criteria.

Table 3.3. WIM Data Filtering Criteria.

Criteria Type	Criteria for Elimination
Vehicle Class	Classes 1-3 (automatic elimination; see Table 3.2).
Gross Vehicle Weight	GVW < 12 kips (no upper limit).
	GVW differs from axle weight sum by more than 10%.
Axle Weight	First axle > 25 kips or < 6 kips.
	Any axle > 70 kips or < 2 kips.
Vehicle Length	Length < 5 ft.
	Length > 200 ft.
Axle Spacing	First axle spacing < 5 ft.
	Any axle spacing < 3.4 ft.
Speed	Speed < 20 or > 100 MPH for GVW vehicles < 200 kips.
	Speed < 20 or > 85 MPH for GVW vehicles > 200 kips.
Number of Axles	Number of axles < 2 or > 13*.

*The WIM equipment does not store axle weight and configuration data beyond 13 axles.

A summary of WIM data statistics is given in Appendix B. Using the criteria in Table 3.3, approximately 30% of the total vehicles were eliminated. Table B1 of the Appendix shows the proportion of eliminated data per WIM station. Most stations had about 30-40% of vehicles eliminated, with a range of about 17-66%. Station 4249 had the highest proportion of eliminated data (66%), while station 7189 had the lowest (17%). This elimination rate falls within the range of results reported in NCHRP 683 from data collected in California, Florida, Indiana, Mississippi, and Texas, for which the elimination rate varied from about 19-74%, with a mean rate of elimination of about 36%, depending on the WIM station considered.

Note that station 7169 (on I94 just east of I69) is associated with the large majority of heavy vehicles in the WIM data. It contains approximately 7.9% of all trucks over 150 kips, and approximately 94% of vehicles above 280 kips GVW.

Table B2 illustrates the effect of the filtering criteria on heavy weight vehicles. As shown in the table, only a relatively small number of vehicles are present that are very heavy after filtering, with 177 vehicles over 280 kips, and 52,554 vehicles present over 150 kips, with the heaviest vehicle having GVW (gross vehicle weight) of 543 kips. Tables B3 and B4 gives the statistics for vehicles that were excluded due to the different criteria in Table 3.3. As shown, most were excluded to axle weight (either too high or too low) and spacing violations. Table B5 presents a summary of the heaviest vehicles excluded. As shown in the table, the number of heavy weight vehicles excluded represents a small proportion of the entire excluded data. A summary of the WIM data collected by state region is given in Table B6.

Histograms of the WIM data are given in Figures B1-B31, which show statistics for various categories of the data, including all; correct (filtered); incorrect (excluded); by different vehicle weight and configuration categories; and by station location. Figures B32- B37 present plots relating vehicle length, gross vehicle weight (GVW), and number of axles.

3.2.2 Comparison to Permit Data

The projection method used in this study to determine the statistical parameters for the maximum load effect for the time periods of interest (i.e. 5 years for rating and 75 years for design) are based on the top 5% of the load effects, as described in detail later. Thus, an accurate profile of the heavy vehicles in the WIM data becomes most important. For additional verification of the reasonableness of the heavy vehicle data collected, a comparison was made to the available special permit records.

For this effort, a selection of single-passage (special) permit data collected by MDOT was made available for this study. The data were collected from 6/1/11-7/22/11 and from 1/1/13-7/1/13. Linearly extrapolating the 8 months of available permit data to the 22 months (the time period of

WIM data used) revealed an expected 146 vehicles over 280 kips GVW and 20,643 vehicles over 150 kips GVW. There is no expectation of seeing the same number of heavy vehicles in the special permit record as in the WIM data, as routes and particular WIM stations crossed are unknown, so a single vehicle in the permit record could pass over multiple or no WIM stations, and there also may be many legal as well as some illegal heavy vehicles in the WIM data not captured in the permit data. Moreover, the period of time for which the permit data was made available does not cover the entire time for which the WIM data were collected, and thus the expected number of heavy permit vehicles in the permit record was linearly projected to the same period of time covered by the WIM data, as described above. However, given these significant counting accuracy limitations, it appears that the number of heavy vehicles in the permit record reasonably corresponds to the number of heavy vehicles found in the filtered WIM data (i.e. 177 vehicles over 280 kips and 52,554 vehicles over 150 kips in the WIM data compared to 146 vehicles over 280k and 20,643 vehicles over 150 kips in the projected permit data).

For sake of comparison, an additional analysis was conducted to determine the effect on the WIM data statistics if the number of heavy vehicles in the WIM data were reduced to match those in the permit record. That is, the number of heaviest vehicles in WIM data were reduced to match the single-passage projected permit data. This comparison is summarized in Table B7, which compares the original and reduced data set statistics. As shown in the table, there are nearly identical results for most data sets, illustrating that the critical statistical parameters are not particularly sensitive to the precise number of heavy vehicles included. Therefore, the WIM filtering criteria were deemed acceptable for heavy vehicles.

3.2.3 Legal and Non-Legal Vehicles

In this study, vehicles are classified as legal if they meet the GVW, as well as axle weight and spacing limitations described in MDOT Document T1, *Maximum Legal Truck Loadings and Dimensions* (MDOT 2011). A vehicle is also classified as legal if it matches (within a 3% tolerance) any of the 28 Michigan Legal Vehicle configurations as described in the MDOT Bridge Analysis Guide (BAG) (MDOT 2005), with any of the axle spacing configurations along with axle weights that do not exceed the listed limits. Vehicles that meet these requirements but otherwise might be illegal due to width, height, cargo type, or other such restrictions are not included, as these cannot be identified in the WIM data. It was found that approximately 95% of trucks (not including small vehicles in categories 1-3 in Table 3.2 were found to be legal, as shown in Table B8. Table B9 classifies legal and non-legal vehicles into various categories of GVW/vehicle length. As expected, the number and percentage of legal as well as non-legal vehicles generally decreases as GVW/length increases, with peak GWV/length for legal vehicles below 80 kips between 0.5-1.0 kip/ft; for legal vehicles above 80 kips between 1.0-2.0 kips/ft; and for non-legal vehicles both below and above 80 kips between 1.0-2.0 kips/ft, with a large proportion of non-legal vehicles above 80 kips also between 1.0-2.0 kips/ft. Here, vehicle length is measured between the first and last axles.

3.2.4 Data Quality Checks

To confirm the reasonableness of the WIM data, several checks were implemented as recommended in NCHRP 683. Among these, the following numerical comparisons for 5-axle (Class 9 or 3S2) semi-trailer truck data were considered on a site-by-site basis:

- Drive tandem axle spacing: The mean distance between the drive axles is compared to a standard value of 4.3 ft (Fu et al. 2003). The computed mean value among all sites has a spacing

of 4.6 ft, which appears to be reasonably close. The range of means from site to site is from 4.5-4.9 ft, with a low coefficient of variation (COV) of 0.033.

- Drive axle weight: The mean drive (2^{nd}) axle weight is compared to the mean values found in NCHRP Report 505, which was taken as a maximum of 13 kips. The mean drive axle found from all sites was 11.4 kips with a range of means of 10.5 – 11.6 kips, with a low COV of 0.034.
- Steering axle weight: The typical range for steering axle weight was reported to be 9 - 11 kips (NCHRP 683). The mean drive axle found from all sites was 10.8 kips with a range of means of 10.4 – 11.0 kips, with a low COV of 0.026.
- GVW histogram: The histogram is expected to have a bimodal shape with peaks near 30 and 72-80 kips, representing unloaded and loaded trucks (NCHRP 683). The site histograms were found to have a similar bimodal shape with peaks close to the comparison values.
- Data Confidence Intervals: The typically large volume of site data available resulted in the mean and standard deviation of the load effect data used for projection to be estimated with reasonably high confidence. For example, consider the 100' simple span moment load effects of site 7029 which were used to project to 5 and 75-year load events. This site has a typical number of load effects. A 99% confidence interval for the mean load effect from the upper 5% of the data used for projection falls within 924.4 and 925.8. The worst cases considered result from low ADTT sites with relatively few load effects. One such site is 1199, which for simple span shear, has a 99% confidence interval of the mean of 55.8 to 56.3. Similar results were obtained for standard deviation. Therefore, the volume of data is deemed adequate to develop accurate load effect projections.

A summary of these numerical checks are given in Table B10, while (all vehicle) GVW histograms and 5-axle vehicle GVW histograms of the sites used in the calibration process are

given in Figures B38-B68. Based on these comparisons, the WIM data collected appear reasonable.

CHAPTER 4: MULTIPLE PRESENCE FREQUENCIES

4.1 General side-by-side probabilities

Multiple presence probabilities are calculated for two reasons; 1) to serve as an additional check on the quality and consistency of the WIM data; and 2) for use in reliability analysis of side-by-side cases. That latter is considered when there are insufficient instances of multiple presence in the WIM data such that multiple vehicle load effects can be directly calculated and projected accurately. Direct use of the WIM data is in general most accurate, as actual vehicle weights, relative placements, and frequencies of occurrence are accounted for to generate load effects with no or minimal simplification. In contrast, the use of side-by-side probability calculations involves various unavoidable approximations which may lead to inaccuracies. Therefore, discrete side-by-side probability calculations were used only when necessary. In this study, it was found that sufficient data were available to directly use the WIM data to develop multiple presence load effects for all cases except those involving special permit vehicles. This is described in Chapter 6.

Various multiple presence frequencies were calculated from the WIM data, for various combinations of:

a) Vehicle scenario (single, following, side-by-side, staggered, multiple);

b) Different side-by-side definitions (2);

c) Different side-by-side headway distances (10-100');

d) ADTT (<1000, 1000-2500, 2500-5000, >5000);

e) Vehicle types (2);

f) Bridge spans (20' – 200').

The following definitions are used for multiple presence modeling (NCHRP 683):

Gap: the distance between the last axle of the first truck and the first axle of the following truck.

Headway: the distance between front axles of side-by-side trucks.

Single: the case where only one truck is present on the bridge.

Following: the case where two or more trucks are in the same lane, with a gap less than the bridge span length.

Side-by-Side: when two trucks appear simultaneously in adjacent lanes. Various definitions are possible, either based on a headway distance or a truck overlap. In this research, side-by-side events were calculated based on various different maximum headway distances from 10 to 160 ft, as well as defining headway as 0.5*(length of truck in lane 1). A side-by-side event was ultimately taken as trucks in adjacent lanes within a 60' headway. This is consistent with that used in previous calibrations (Sivakumar et al. 2011).

Staggered: the case where trucks in adjacent lanes are present with an overlap of less than one-half the truck length of the first truck and a gap less than the span length.

Multiple: the simultaneous presence of trucks in adjacent lanes as well as in the same lane (i.e. a combination of following, side-by-side, and/or staggered.)

4.2 Side-by-side probability of special permit vehicles

As there are insufficient load effect events that involve trucks alongside special permit vehicles to develop adequate load projections, the associated side-by-side probabilities must be determined for the reliability analysis. It was found that the probability of a special permit truck alongside any other truck (with headway distance within 60') was 2.8% for high (>5000 ADTT) sites (note this is nearly identical to the value previously computed for Michigan, as shown in Table 4.1). This reasonably falls between the side-by-side probabilities calculated for ADTT

>5000 sites for any trucks between 40' and 80' headways, which were found to be 1.62% and 3.04%, respectively (see Tables C1-C16). Although this value could be developed for different ADTT levels, vehicle GWV categories, and other refinements for vehicles alongside special permits, it was determined that no further analysis was required. The reason for this is discussed in Chapter 6.

Moreover, based on a pooled analysis of data from all sites, the probability of two special permit trucks side-by-side was calculated to be approximately zero. This is not unexpected; due to the expected very low probability of this case, this condition was not considered in NCHRP 285.

4.3 Effect of Traffic Direction

The effect of traffic direction (i.e. vehicles traveling in the same direction or vehicles traveling in opposing directions) on side-by-side probability for the general truck population was explored. Results for four representative sites (with ADTT > 5000) are shown in Tables C17-C20 in the Appendix. In general, it was found that traffic direction does not have consistent nor significant effect on side-by-side probability. Within the headway distance considered (i.e. between 40 and 80 in the tables), there is only a slightly higher occurrence of side-by-side events for opposing directions as compared to same direction traffic. However, this difference is not large enough to significantly affect reliability calculations.

CHAPTER 5: VEHICLE LOAD EFFECTS

5.1 Load Effects from WIM Data

Vehicle load effects were calculated for span lengths of 20, 50, 80, 100 and 200 ft. Considered effects were maximum simple span moments and shears, for both single lane and two-lane load effects. This was done by incrementing actual vehicle configurations and spatial placements (i.e. the actual side-by-side locations and following distances) recorded from the WIM data (as well as the special permit record) across the considered span lengths and recording maximum load effect values. Due to the large volume of data considered, to maintain computational feasibility, the speeds of multiple presence vehicles were taken to be identical, such that their positions relative to one another do not change over the span length.

A selection of these results are presented in Table C1, which summarizes load effects; while Figures C1-C18 provide histograms of some of these load effects for various spans and load effects for one and two lane effects. A comparison of load effect as a function of bridge span and HL93 load effect is given in Figures C19-C20 in Appendix C. It can be seen that the maximum loads found in the WIM data are substantially higher than the HL93 (nominal) design load, nearly reaching 4 times the HL93 value for moment and 3.5 times the HL93 value for shear.

Table C2 compares single lane, single vehicle load effects to single lane, following vehicle (i.e. the effect of multiple vehicles in the same lane) load effects. It can be seen that following effects are insignificant at spans of 50’ or less, but become very significant at longer spans.

CHAPTER 6: RELIABILITY MODELS

The goal of this study is to find optimize trucks for design and rating. To meet this goal, live load factors for design and rating need to be determined to meet intended target and minimum reliability levels. To be consistent with the current LRFD and LRFR procedures, this study follows the general framework established in NCHRP Reports 368, 683 and 20-07(285). This chapter concerns the reliability-based design and rating load factor calculation for the Strength I (Design and Rating) limit states. The specific procedures used in this study are detailed below.

6.1 Reliability Based Design Procedure

In this study, Strength I limit state is considered. For Design, Strength I refers to strength-based limit states that involve the normal use of the bridge (not including wind effects). Maximum load effects are based on a 75-year design lifetime. In theory, all vehicular loads on the bridge are used to generate statistics for Strength I live load effects. The process is described below:

6.1.1 One Lane Effects

1. A selection of representative WIM sites is used to develop load effects. Individual site data must be kept separate, such that site-to-site variation in the results can be computed. However, mean results from the pool of sites are used to generate load effect statistics. This process is described in the Data Projection section below. The sites specifically considered for reliability model are given in Table 3.1 (see Chapter 3).

2. For each site, the vehicle load effects (moments and shears) are determined, as described in Chapter 5, where actual following vehicle (i.e. vehicle trains) load effects are included.

3. A data projection technique based on an Extreme Type I distribution fit, as described below, is used to estimate the mean and the coefficient of variation (COV, or V) of the maximum load effect, $\overline{L}_{\max}$ and $V_{\max}$, respectively, at 75 years.

4. $\overline{L}_{max}$ is determined as a load effect on a selection of hypothetical bridge girders. First, a selection of typical bridges is compiled such that dead load effects and girder distribution factors (DF)s can be calculated. The selection of bridges considered in this study is given in near the end of this Chapter. $\overline{L}_{max}$ for 1-lane moment on a girder ($\overline{L}_{max1M}$) is given by:

$$\overline{L}_{max1M} = \overline{L}_{max} * IM * DF_1/1.2 \quad (6.1)$$

Where

DF_1 = the 1-lane DF, as given in AASHTO LRFD. Note that it is divided by 1.2 to remove the multiple presence factor, which is directly accounted for in $\overline{L}_{max}$.

For most steel, prestressed concrete, and reinforced concrete girder bridges supporting a concrete deck, the AASHTO LRFD 1-lane DF for moment is taken as:

$$DF_1 = 0.06 + \left(\frac{S}{14}\right)^{0.4}\left(\frac{S}{L}\right)^{0.3}\left(\frac{K_g}{12Lt_s^3}\right)^{0.1} \quad (6.2)$$

Where

$K_g = n(I+Ae_g^2)$; A is the beam cross-sectional area; e the distance between the centroids of the beam and deck; I is for beam, and; n = modular ratio of beam and deck.

For shear, for most girder bridges,

$$DF_1 = 0.36 + \left(\frac{S}{25}\right) \quad (6.3)$$

Expressions in AASHTO LRFD for the other types of structures considered.

IM = the impact factor, taken as a mean value of 1.13 for one lane loaded with heavy vehicles, (Sivakumar et al. 2011).

5. Continue to step 6 below.

6.1.2 Two Lane Effects

1. A selection of representative WIM sites is used to develop load effects. Individual site data must be kept separate, such that site-to-site variation in the results can be computed. However, mean results from the pool of sites are used to generate load effect statistics. The same sites considered for the 1-lane effects are considered for 2-lane load effects.

2. For each site, the 2-lane vehicle load effects (moments and shears) are determined, as described in Chapter 5, where actual following vehicle (i.e. vehicle trains) load effects are included in each lane. Here, a complication arises in that there is no DF equation in AASHTO that allows for side-by-side vehicles of different weights and configurations. An analysis technique such as FEA or grillage modeling would be ideal in this case. However, the time involved to construct detailed numerical models for each of the many different bridge configurations considered is not feasible. Therefore, an approximate method is used, as suggested by Moses (2001) and implemented by Sivakumar et al. (2011a,b). Here, the total 2-lane moment effect (M_{12}) is given by:

$$M_{12} = M_1 * DF_1 + M_2(DF_2 - DF_1) \quad (6.4)$$

Where

M_1 = the moment due to the vehicle(s) in lane 1.

DF_1 = the AASHTO LRFD single lane DF (after dividing out the 1.2 multiple presence factor).

M_2 = the moment due to the vehicle(s) in lane 2 (while in the recorded spatial position on the span relative to the lane 1 vehicle(s); see Chapter 5).

DF_2 = the AASHTO LRFD 2-lane DF, which for most steel and prestressed concrete bridges supporting a concrete deck, is given as:

$$DF_2 = 0.075 + \left(\frac{S}{9.5}\right)^{0.6}\left(\frac{S}{L}\right)^{0.2}\left(\frac{K_g}{12Lt_s^3}\right)^{0.1} \quad (6.5)$$

For shear, the same process is followed above using equation 6.4, but 1 and 2-lane moment DFs are replaced with shear DFs. For example, for most steel and prestressed concrete bridges supporting a concrete deck, the 2-lane shear DF is given as:

$$DF_2 = 0.2 + \left(\frac{S}{12}\right) - \left(\frac{S}{35}\right)^{2.0} \quad (6.6)$$

This is done for each of the 2-lane load effects from the site considered.

3. The same data projection technique used for 1-lane load effects is also used for 2-lane effects. The projection is used to estimate the mean and COV of the maximum load effect, $\overline{L}_{\max}$ and $V_{\max}$, respectively, at 75 years, from the data set of the 2-lane load effects found in step 2, above.

4. $\overline{L}_{\max}$ is determined as a load effect on the selection of hypothetical bridge girders. The same structures used for the 1-lane load effects are used here as well. $\overline{L}_{\max}$ for 2-lane moments on a girder ($\overline{L}_{\max 2M}$) is given by:

$$\overline{L}_{\max 2M} = \overline{L}_{\max} * \text{IM} \quad (6.7)$$

Here, the DF is already embedded in the data, in Steps 2 and 3. IM is taken as a mean value of 1.10 for two lanes loaded with heavy traffic, as used in the MBE calibration (Sivakumar et al. 2011).

5. Continue to step 6 below.

6.1.3 For Both 1 and 2-Lane Effects (separately)

6. There are various uncertainties that must be accounted for in the live load model. These are as follows:

a) Uncertainty in the future data projection (V_{proj}). This is V_{max}, as found from the projection technique, as in Step 3 above (determined as $V_{proj} = V_{max} = \sigma_{L\,max} / \overline{L}_{max}$, where $\sigma_{L\,max}$ and $\overline{L}_{max}$ are found from the projection; see below).

b) Uncertainty in mean maximum load effects among different sites (V_{site}). Here, V_{site} can be computed directly as the COV of $\overline{L}_{max}$ values found from the different sites, for 1- and 2 lane load effects, for the particular load effect case considered. Note that different values in V_{site} will occur depending on bridge span and configuration.

c) Uncertainty in $\overline{L}_{max}$ based on the WIM data at a particular site (V_{data}). There is no direct way to assess this uncertainty. However, Sivakumar et al. (2011) suggests that it be estimated based on a standard deviation taken equal to the value of data at the 95% upper and lower confidence intervals (assessed by using a proportion confidence interval based on an estimated 50-interval CDF), where it is assumed that these values fall within 1.96 standard deviations of the mean. Thus, the standard deviation to use for V_{data} , σ_{Vdata} , is given by:

$$\sigma_{Vdata} = |(d_{95}) - \bar{x}| / 1.96 \qquad (6.8)$$

Where

(d_{95}) = the upper 95% upper or lower confidence interval value for $\overline{L}_{max}$. $\bar{x}$ = the mean; i.e. $\overline{L}_{max}$.

COV (V_{data}) can then be computed as usual (i.e. = $\sigma_{Vdata} / \bar{x}$). V_{data} is reported to be approximately 2% for 1-lane effects and 3% for 2-lane effects, for 1 year of WIM data (Sivakumar 2011). In this study, it was found that V_{data} was below 2% for all cases investigated. Therefore, the 2% and 3% values above are conservatively used. Note that, for most cases, total COV of live load is dominated by other sources of variation, and it was found that altering V_{data} from 0-3% has no significant effect on the total live load COV (see below).

d) Uncertainty in impact factor (V_{IM}). V_{IM} is taken as 9% for 1-lane effects and 5.5% for 2-lane effects (Sivakumar et al. 2011).

e) Uncertainty in load distribution (V_{DF}). Based on a series of field tests comparing actual load distribution effects to the AASHTO LRFD DF formula, V_{DF} is given in Table 6.1 below (Sivakumar et al. 2011). Bias factor λ refers to the mean value divided by the AASHTO LRFD value. Note that the bias factors presented in the table are not used for design calibration (i.e. λ=1.0).

Table 6.1. Statistical Parameters for DF.

Bridge Type		Moment		Shear	
		1 Lane	2 Lane	1 Lane	2 Lane
Composite Steel	λ	0.78	0.90	0.72	0.82
	COV	0.11	0.14	0.14	0.18
Reinforced Concrete	λ	0.79	0.93	0.76	0.88
	COV	0.16	0.15	0.12	0.18
Prestressed Concrete	λ	0.78	0.90	0.77	0.88
	COV	0.12	0.13	0.11	0.16

For each of the case combinations above (i.e. for a particular WIM data site, bridge configuration, and 1 or 2-lane load effect), the final COV of mean maximum load effect, Vmax L, is then determined. For a product function of random variables such as eq. 6.1 or 6.7 (and assuming the uncertainties from the data projection, site, and data are similarly represented in product form), it can be shown that if RVs are uncorrelated and COV is not too large, the COV of the function can be reasonably determined by ignoring the second order relationships as:

$$V_{max\ L} = (V_{proj}^2 + V_{site}^2 + V_{data}^2 + V_{IM}^2 + V_{DF}^2)^{1/2} \quad (6.9)$$

7. Reliability for the selection of bridges is then calculated. The general limit state function is:

$$g = R - (D_p + D_s + D_W) - LL \quad (6.10)$$

Random variables considered are girder resistance (R), dead load from prefabricated (Dp), site-cast (Ds), and wearing surface (Dw) components, and vehicular live load (LL). Statistics are taken from Nowak (1999) to be consistent with the AASHTO LRFD and MBE calibrations, and are given in Table 6.2.

Table 6.2. Random Variable Statistics.

Random Variable		Bias Factor	COV
Resistance RVs	R		
Prestressed Concrete, Moment		1.05	0.075
Prestressed Concrete, Shear		1.15	0.14
Reinforced Concrete, Moment		1.14	0.13
Reinforced Concrete, Shear*		1.20	0.155
Steel, Moment		1.12	0.10
Steel, Shear		1.14	0.105
Load RVs			
Vehicle Live Load	LL	from L_{max}; see above	
DL, Prefabricated	D_p	1.03	0.08
DL, Site-Cast	D_s	1.05	0.10
DL, Wearing Surface	D_w	mean 3.5”	0.25

*Assumes shear stirrups present

Although it is not precisely correct, in previous AASHTO design and rating calibrations, for reliability analysis, girder resistance is taken as a lognormal random variable while the sum of load effects is assumed normal.

Statistics for LL are calculated as described above. Mean R is calculated from $\overline{R}= Rn\lambda r$. Here, R_n is the nominal resistance, generally given by AASHTO LRFD. However, MDOT bridges are currently designed based on a revised load model, HL93mod. HL93mod is the AASHTO HL93 design load, but replaces the 25 k design tandem with a single 60 k axle, and adds an additional factor of 1.2 to the total live load (including impact). The HL93 design truck has a front axle of 8 k and two rear axles of 32 k, where the first axle spacing is 14’ and the second axle spacing is varied from 14-30’ to maximize load effect. The lane load is a uniform load applied along with the

design truck, equal to 0.64 k/ft. The distance between truck axles is taken as 14'. Resistance Rn is calculated as:

$$Rn = (1/\varphi)\ (1.25DC + 1.5DW + \gamma_L(DF2)\ (HL93mod)) \quad (6.11)$$

Where

γ_L = live load factor, to be determined.

HL93mod = 1.2*(lane load + max (HS20, 60k axle) * IM).

DC = component dead load.

DW = wearing surface dead load.

IM = impact factor, taken as 1.33 times the nominal vehicle design load (design truck or axle, but not lane load).

DF2 = AASHTO 2-lane girder distribution factor, as given in Section 4 of the AASHTO LRFD Code.

Φ = resistance factor, specific to the material and failure mode, as specified in AASHTO LRFD. For steel members, φ = 1.0 for moment and shear effects; for prestressed concrete members (assuming tension controlled), φ = 1.0 for moment and 0.9 for shear effects.

Due to the large number of reliability calculations required, the reliability analysis is conducted with the closed form, simplified First Order, Second Moment (FOSM) procedure, such that the required LF can be solved for directly. This method assumes all RVs are normal, which is conservative when resistance is lognormal, as assumed for bridge member resistance. To account for this, an adjustment factor was applied such that the reliability index computed by FOSM better approximates the exact value, as determined by direct Monte Carlo Simulation (MCS). The adjustment factor is applied directly to reliability index and for a typical case, was found to range from a maximum of 1.07 when the desired β=3.5 (i.e. the FOSM solution provides β=3.27 when

the true index is 3.5); 1.04 when the desired β=2.5, and 1.0 when the desired β=1.5. Results were spot-checked with MCS and were found to have excellent agreement to the exact value. Note that these adjustment factors are particular to the specific reliability problems considered in this study and cannot be applied to FOSM in general.

8. The live load factor γ_L is adjusted to achieve reliability results closest to the LRFD design target of β=3.5. For the LRFD Code, the load factor was chosen such that the minimum reliability index achieved for all designs was 3.5, which is the process used here.

6.2 Reliability Based Rating Procedure

This section concerns live load factor calculation for Legal Load Rating. For the purposes of load factor determination, a legal load is taken as that which can pass unrestricted over any (non-posted) MDOT bridge. Legal load factors are considered for the set of 28 Michigan Legal trucks given in the Bridge Analysis Guide.

In this study, for rating procedure, Strength I is used. Strength I refers to strength-based limit states that involve the normal use of the bridge. Maximum load effects are based on a 5-year return period. As with the Strength I Design calculation, the Strength I rating procedure will use the same data pool of all WIM vehicles. For the Strength I rating calculation, a target reliability index for rating is specified as 2.5, with a minimum limit of 1.5 for any case. A rating factor of 1.0 implies that if a bridge is designed to the legal load (rather than the design load), the reliability index for the structure will match the target (rating) level. Practically, the procedure is done by determining the hypothetical nominal capacity of the bridge using the legal loads in place of the design load, along with the corresponding AASHTO (LRFR or LFR, as appropriate) rating procedures. Once nominal capacity is determined (as a function of the unknown required live load factor), the rating factor is set at 1.0 and the live load factor is adjusted such that the target

reliability index is met. The procedure is similar to that outlined in the Strength I Design calculation, and is as follows:

6.2.1 One Lane Effects

1. A selection of representative WIM sites is used to develop load effects. Individual site data must be kept separate, such that site-to-site variation in the results can be computed. However, mean results from the pool of sites are used to generate load effect statistics. The same sites used for Strength I design are used for rating procedure.

2. For each site, the vehicle load effects (moments and shears) are determined, as described in Chapter 5, where actual following vehicle (i.e. vehicle trains) load effects are included.

3. A data projection technique based on an Extreme Type I distribution fit, as described below, is used to estimate the mean and the coefficient of variation (COV, or V) of the maximum load effect, $\overline{L}_{\max}$ and Vmax, respectively, at 5 years (as compared to 75 years for design).

4. $\overline{L}_{\max}$ is determined as a load effect on a selection of hypothetical bridge girders. First, a selection of typical bridges is compiled such that dead load effects and girder distribution factors (DF)s can be calculated. The selection of bridges used for rating is the same as that used for design.

The process for computing $\overline{L}_{\max}$ for 1-lane load effects on a girder ($\overline{L}_{\max 1M}$) is identical to that used for design calibration, and is given by eq. 6.1, above.

5. Continue to step 6 below.

6.2.2 Two Lane Effects

1. A selection of representative WIM sites is used to develop load effects. Individual site data must be kept separate, such that site-to-site variation in the results can be computed. However,

mean results from the pool of sites are used to generate load effect statistics. The same sites considered for the 1-lane effects are considered for 2-lane load effects.

2. For each site, the 2-lane vehicle load effects (moments and shears) are determined. This process is identical to that used for design calibration, and is given by eq. 6.4, above.

3. The same data projection technique used for 1-lane load effects is also used for 2-lane effects. The projection is used to estimate the mean and COV of the maximum load effect, $\overline{L}_{\max}$ and Vmax, respectively, at 5 years, from the data set of the 2-lane load effects found in step 2, above.

4. $\overline{L}_{\max}$ is determined as a load effect on the selection of hypothetical bridge girders. The same structures used for the 1-lane load effects are used here as well. This process is identical to that used for design calibration, where $\overline{L}_{\max}$ for 2-lane moments on a girder ($\overline{L}_{\max 2M}$) is given by eq. 6.7, above.

5. Continue to step 6 below.

6.2.3 For Both One and Two Lane Effects (separately):

6. The same live load uncertainties accounted for in design calibration must be accounted for in rating calibration. These are uncertainties in the future data projection (V_{proj}); the mean maximum load effects among different sites (V_{site}); in $\overline{L}_{\max}$ based on the WIM data at a particular site (V_{data}); impact factor (V_{IM}); and load distribution (V_{DF}). These are identical to those used in design calculation. However, for uncertainty in load distribution, the bias factors (as well as COVs) in Table 6.1 are used for rating. Note that for the design procedure, the bias factors were not used, as the original LRFD target of 3.5 was set without these bias factors. However, for rating, the bias factors were considered in the MBE process, and thus are used here.

For each of the case combinations above (i.e. for a particular WIM data site, bridge configuration, and 1 or 2-lane load effect), the final COV of mean maximum load effect, Vmax L, is then determined with eq. 6.9. This value will be identical to that used for design procedure.

7. Reliability for the selection of bridges is then calculated. The limit state function is given by eq. 6.10. Random variables considered are the same as those used in design section: girder resistance (R), dead load from prefabricated (Dp), site-cast (Ds), and wearing surface (Dw) components, and vehicular live load (LL). Statistics are given in Table 6.2. For reliability analysis, girder resistance is taken as a lognormal random variable while the sum of load effects is assumed normal. Mean R is calculated from $\overline{R}$= Rnλr. For rating, Rn is determined not from the design live load model, but by the load effect using the set of MDOT Legal Loads (MI legal truck) with the appropriate AASHTO code rating procedure when the rating factor is set to 1.0.

For LRFR calibration, Rn is determined by:

$$Rn = (1/\phi)\ (1.25DC + 1.5DW + \gamma_L\ (DF2)\ (MI\ legal\ truck + IM)) \qquad (6.12)$$

Parameters are defined with eq. 6.11, above.

For LFR calibration, Rn is determined by:

$$Rn = (1/\phi)\ (1.3D + \gamma_L\ (DF2s)\ (1/2)\ (MI\ legal\ truck + I)) \qquad (6.13)$$

Where

γ_L = live load factor, to be determined.

DF2s = two lane distribution factor specified in the AASHTO Standard (i.e. S/5.5 for most steel and prestressed concrete girder bridges applications, where S = girder spacing).

Appropriate expressions given in AASHTO Standard are used for the other cases considered in this research.

I = AASHTO Standard impact factor, taken as (50/(L+125), ≤ 0.30).

ϕ = resistance factor, which is the same as the corresponding LRFD resistance factor for all considered structures, except for reinforced concrete members in shear, where $\phi = 0.85$.

Note that the heaviest category of legal load is used that is available for that truck type (i.e. from normal, designated, or special designated).

For LRFR legal load rating, a 2-lane DF is used. For simple spans, only the truck is considered for load effects

8. The live load factor γ_L is adjusted to achieve reliability results closest to the target β for rating of 2.5, with a minimum β of 1.5 (rather than a target of 3.5 as with Design). In the MBE, the load factor was chosen such that the average of all cases considered met the target index of 2.5, and all cases met the minimum value of 1.5. This is the process used here.

6.3 Bridge Structures Considered

The following bridge characteristics were considered for load factor calibration:

1. Girder Type:
    a. Prestressed concrete I-girders
    b. Steel girders
2. Span Type:
    a. Simple Span
3. Span Lengths (ft):
    a. 20, 50, 80, 100, 200
4. Girder Spacing (as applicable, ft):
    a. 6, 8, 10, 12
5. Load Effect:
    a. Simple moments

b. Simple shears

Bridges are assumed to support a reinforced concrete deck and have a wearing surface and additional typical non-structural items relevant for dead load calculation. The dead load of these components is based on values used in the AASHTO LRFD as well as NCHRP reports 683 and 285. Dead load effects used in this study are given in Tables D1-D4 in Appendix D.

As per MDOT practice, for design, prestressed concrete bridges are assumed to act continuous for live load only. For rating, these structures are assumed to act as simply supported.

For girder distribution for moment, the term $\left(\frac{K_g}{12Lt_s^3}\right)^{0.1}$ in eq. 6.5 was found to have a minor effect on results for typical ranges of girder stiffness, and is taken as 1.0 as per the AASHTO LRFD and MBE calibrations.

6.4 Data Projection

The load effects calculated from the WIM data (see Chapter 5) were based on truck traffic collected over a 22-month period. For rating and design, however, load effects are to be based on 5 and 75 year periods, respectively. Thus, a data projection method is used to estimate load effect statistics for longer periods of time. This projection does not account for any possible changes in vehicle weights nor uncertainties in potential future vehicles. Rather, the projection only estimates what maximum load effect statistics would be found for the desired return period (i.e. 75 years for Strength I Design and 5 years for rating), by probabilistically extrapolating from the existing number of load effects calculated from the available WIM data pool.

If the tail end of the data is reasonably normally distributed, it can be shown that an Extreme Type I distribution can be used to extrapolate to future extreme load events with the following procedure (Ang and Tang 2007):

1. The cumulative distribution function (CDF; $F_x(x)$) of the load effects i: $F_x(x) = (i/1+n)$, is developed, where n is the total number of data and x is the load effect. Here, the data are a set of moments or shears calculated from the WIM data for a particular site.

2. The inverse standard normal CDF of each computed CDF value is taken: $F_x(x) = \Phi^{-1}(F_x(x))$.

3. As recommended by NCHRP 683, the upper 5% of these values is plotted as a function of load effect x. As the data are essentially plotted on a normal probability axis, a generally linear trend indicates that the data approach a normal distribution.

4. A linear regression line is constructed that best fits this data. The slope (m) and intercept (n) of the line are determined.

5. It can be shown that the mean value of the best-fit normal distribution is given as: $\bar{x} = -n/m$; with standard deviation $\sigma = \left((1-n)/m\right) - \bar{x}$.

6. Load effect statistics are extrapolated to longer periods of time by first computing N, the number of expected events in the extrapolated return period. It can be calculated as $N = n_w*(Y/t_w)$, where Y is the length of the new return period (years; for example, for 75 years, Y=75), n_w is the number of events in the WIM data (in step 1) to be used for extrapolation, and t_w is the number of years of WIM data considered. Alternatively, N can be calculated from $N = n_d*365*Y$, where n_d is number of events per day from the WIM data (i.e. number of load effects / days of WIM data considered).

7. The load effect statistics (mean maximum and standard deviation) for the new return period can be computed as follows:

$$\bar{L}_{\max} = \mu_N + \frac{0.5772157}{\alpha_N} \qquad (6.20)$$

$$\sigma_{L\max} = \frac{\pi}{\sqrt{6}\alpha_N} \tag{6.21}$$

Where

$$\mu_N = \bar{x} + \sigma\left(\sqrt{2\ln(N)} - \frac{\ln(\ln(N)) + \ln(4\pi)}{2\sqrt{2\ln(N)}}\right) \tag{6.22}$$

$$\alpha_N = \frac{\sqrt{2\ln(N)}}{\sigma} \tag{6.23}$$

A selection of results is given in Appendix E, Tables E1-E5. In the tables, the following conventions are used:

SITE: WIM site number.

Pool: the vehicle pool; either all vehicles ("a").

Lane: either single lane or two-lane load effects. "fol" refers to the single lane load effect, caused by single as well as following vehicle effects, if present. Note that fol effects are not reduced by DF within the load projection itself; this is done later in the analysis (see above). In contrast, as described earlier, two lane load effects must be combined together before the load projection is conducted. Thus, these numbers will appear similar in magnitude to fol effects in the Tables, rather than twice the fol values. The combination depends on the 1-lane and 2-lane DFs, as described earlier, and is thus bridge-case specific. In the Lane column, the specific bridge case is described; "xxG" refers to a girder bridge with girder spacing of "xx" ft.

Load: refers to the load effect; either simple moment (Ms), simple shear (Vs).

Span: bridge span (ft).

Year: the year of projection is either 5 (for rating) or 75 (for design).

Girder: this designation only applies for 2-lane effects. It refers to the specific bridge type for which DFs were used to generate the combined 2-lane load effect; either "PCRCx" for a bridge

girder type of steel or prestressed, for which the analysis DF formula is the same (i.e. AASHTO LRFD expression). “x” in this case refers to the girder spacing.

mLmax: $\overline{L}_{\max}$, found from the data projection.

Vproj: COV of $\overline{L}_{\max}$; i.e. $\sigma_{L\max} / \overline{L}_{\max}$.

This value generally fell within 0.02-0.05, a rather small source of load variation. Similar results were found by Sivakumar et al. (2011).

R^2: coefficient of determination, used to measure the goodness of fit. A value of 1.0 indicates a perfect linear fit. It was found that the majority of the data were well-fit by the regression line in step 4, with nearly all coefficients of determination (R2) above 0.95, and the majority in the range of 0.98 and above. This was true for all vehicles as well as permit vehicle pools.

Example projections are shown in Figures 6.1-6.4, below, which are for simple moments at site 7029.

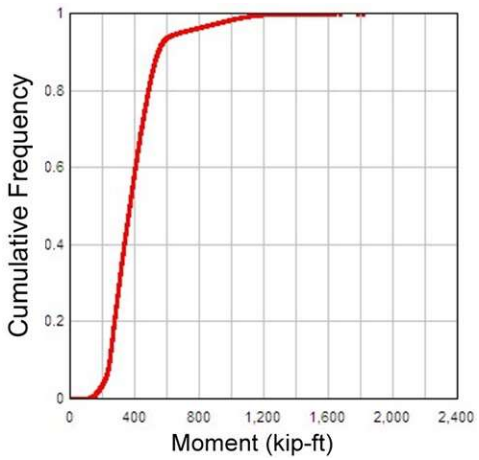

Figure 6.1. CDF of Top 5% of All Vehicles, Single Lane Simple Span Moments.

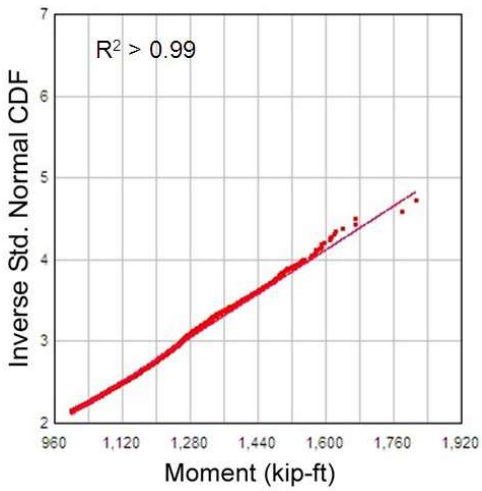

Figure 6.2. Normal Fit to 75 Year Projection, Singe Lane, Normal Probability Plot.

Note: Distribution factor included in plot

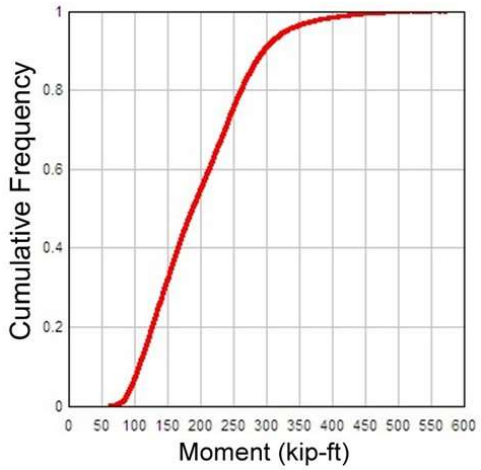

Figure 6.3. CDF of Top 5% of All Vehicles, Two Lane, Normal Probability Plot.

Note: Distribution factor included in plot

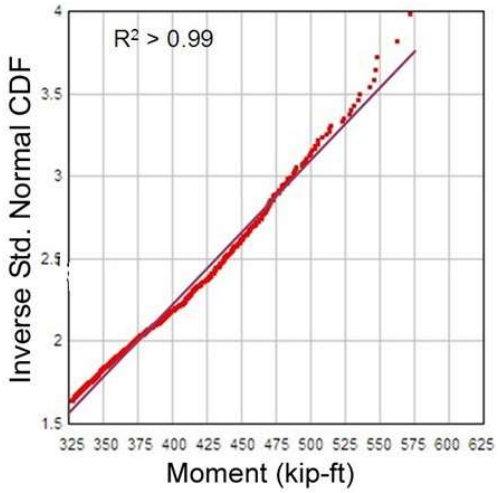

Figure 6.4. Normal Fit to 75 Year Projection, Two Lane, Normal Probability Plot.

As expected, it was found that the 75 year projections exceed the 5 year projections, but not by a great amount. For example, for site 7029, the 5-year projection for all vehicles, single lane simple moments for 80' span is 4460 k-ft, while the corresponding 75-year projection is 4920 k-ft.

Tables F3-F5 provide projections for the combined sites (i.e. 1000 and 5000 ADTT levels), to provide averaged projection results used for design and rating. For example, once all site data has been projected, for each bridge case, the average $\overline{L}_{max}$ and V_{proj} values of all (20) sites for design are computed. Then, V_{site} is computed for each case as the COV of $\overline{L}_{max}$ across the sites. As noted earlier in this report, site 7169 contained a much larger proportion of heavy vehicles than any other site, and its projection values were much higher than any other site as well. However, since the WIM data associated with this site passed all checks, its load effects were included in the average of $\overline{L}_{max}$. But because its projection values were so anomalous, it was deemed not to represent the expected site-to-site variation of load effect, and the $\overline{L}_{max}$ values from this site were not included in the calculation of V_{site}. Note that if it were included in the V_{proj} calculation, V_{proj} would become unreasonably high (with most cases on the order of 0.4-0.6, nearly 2-4 times the

reasonable V_{proj} values computed without this site), causing a dramatic and unrealistic decrease in reliability.

This averaging process is repeated for the ~1000 ADTT sites and the sites with ADTT ≥ 5000, which are used for rating.

CHAPTER 7: Reliability Based Design Optimization

7.1 Genetic Algorithm

In its generic form, an RBDO problem seeks to minimize an objective function $f(\boldsymbol{X},\boldsymbol{Y})$, subject to a series of probabilistic constraints in the form $P_{f_i} = P\left[G_i(\boldsymbol{X},\boldsymbol{Y}) \le 0\right] \le P_{a_i}; i = 1, N_p$, side constraints on design variables $Y_k^l \le Y_k \le Y_k^u; k = 1, NDV$ with $\boldsymbol{X} = \{X_1, X_2, ..., X_n\}^T$ as vector of random variables. It is common to treat the mean values of random variables μ_X as the design variables. In this approach, the objective function can be written as $f(\boldsymbol{X},\boldsymbol{Y}) = a_1\mu_f(\boldsymbol{X},\boldsymbol{Y}) + a_2\tilde{\sigma}_f(\boldsymbol{X},\boldsymbol{Y})$, where μ_f and $\tilde{\sigma}_f$ represent the mean and standard deviation values of $f(\boldsymbol{X},\boldsymbol{Y})$, respectively, with coefficients a_1 and a_2 denoting scalar weighting factors that can be used to balance the requirements for efficiency and robustness in design (Rao 1992).

In this study, the design procedure optimization problem described above is solved with the Genetic Algorithm (GA) method. The GA is a heuristic global optimization model based on Darwin's theory of survival of the fittest and has a more global perspective than many of the competing optimization techniques in common usage (Koumousis and Georgiou 1994). The GA starts with a set of solutions called a population of individuals. Every datum in the set represents a point in the search space. Although these algorithms are randomized, the new set of populations to improve performance are produced by incorporating the information from previous generations based on their fitness in the design space (Koumousis and Georgiou 1994). This means that a population with better fitness has a higher chance to reproduce and thus be carried into the subsequent set for consideration. The genetic algorithm repeatedly modifies this population of individual solutions via iteration.

The GA is appropriate for a variety of optimization problems for which standard optimization algorithms cannot be effectively applied, such as problems where the objective function is discontinuous, non-differentiable, stochastic, or highly nonlinear.

Some differences between the GA and other normal search methods in engineering optimization as the following (Goldberg and Kuo, 1987):

1. Instead of searching from a single point, GAs search from a population of points. Many other methods use a decision rule to find a next point by moving cautiously from a single point in the decision space to the next. This may not work well if multiple peaks exist in the search space, as a local minimum may be found that is not the global minimum. On the other hand, GAs decreases the risk of finding a local peak by considering many peaks in parallel.
2. Instead of using derivative or other auxiliary data, GAs require only objective function information. This can help the GA to get appropriate results quickly.
3. Instead of using deterministic transition rules, GAs use probabilistic transition rules.

The general procedure for GA is shown in Figure 7.1.

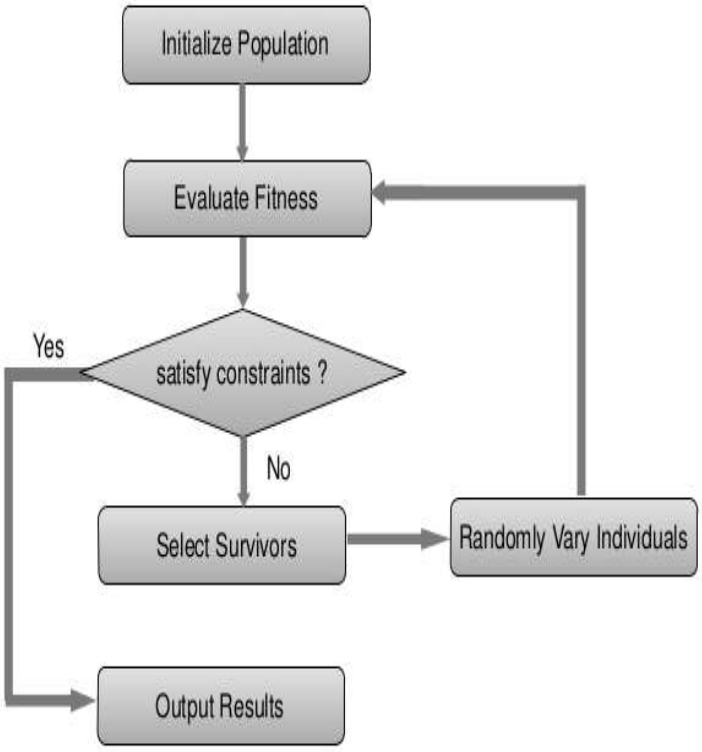

Figure 7.1 Genetic Algorithm flow chart

The summary outline of GA for this study is described as follow:

1. Generate random trucks (population) to meet the constraints which is given in Table 7.6. For this project, the population size is 40000.
2. The fitness function is evaluated as describe in section 7.2-7.6. The lowest fitness function is selected.
3. Generate the new set of trucks base on the truck which has the selected fitness function using the same number of population as step one.
4. Steps 2 and 3 are repeated based on chosen number of iteration. Number of iteration for this study is 1000.
5. Truck with the lowest fitness value through all iterations is elected as the optimized final truck.

7.2 Design Variables

For trucks with "n" number of axles, "2n" design variables are defined which include "n" design variables for axle weights, "n-1" design variables for axle spacing and one variable for the number of axles.

$Y = (Y_1, Y_2, Y_{3, \ldots,} Y_{2n-2}, Y_{2n-1}, Y_{2n}) = (w_1, s_1, w_2, \ldots, s_{n-1}, w_n, N)$

Where w_1 to w_n represent axle weights, s_1 to s_{n-1} represent axle spacing and N shows the number of axles.

Table 7.1 shows the design variables and their description.

Table 7.1 Design variables

Design Variable	Description
Y_1	First axle weight, w_1
Y_2	Axle spacing between 1th and 2nd axle, s_1
Y_3	Second axle weight, w_2
.	.
.	.
.	.
Y_{2n-2}	last axle spacing, s_{n-1}
Y_{2n-1}	last axle weight, w_n
Y_{2n}	Number of Axles, N

To find accurate results more quickly, two different scenarios are considered:

1- The number of axles (x_{2n}) is treated as a random variable. In other words, any trucks between 3 to 13 can be generated for each iteration.

2- The number of axles is treated as a constant. In this case, 11 different cases (trucks from 3 to 13 axles) are generated individually with the same population size for each iteration. In other words, this scenario includes "2n-1" variables.

A uniform lane load was also considered as a design variable, but this was found to produce less optimal results for the number of simulations considered as compared to applying a constant

value for lane load as specified in AASHTO LRFD of 0.64 kips/ft for each span length. Note that using higher or lower value for lane load leads to increase or decrease the GVW of final truck which does not make any significant difference in reliability index discrepancy along the span length (more below).

7.3 Load Effects Calculation

Once the truck population is generated, for each iteration, simple span load effects (moment and shear) are calculated. For this study, span lengths of 20, 50, 80, 100 and 200 ft are used for two-lane bridges with composite steel and prestressed concrete (PC) girders. Structures with girder spacing from 6 to 12 ft with a 2 ft increment were analyzed.

All required parameters for the bridge designs are described earlier.

7.4 Reliability Analysis

Reliability indices (and corresponding load factors) are calculated for both 1-lane (following trucks) as well as 2-lane (side by side trucks) projected load effects for each span and girder spacing configuration. From these two results, the lowest reliability index value is taken for each case. For example, considering a bridge with span length of 20 ft with 6 ft girder spacing, β is calculated for both side-by-side and following load cases, and the lowest value for β is reported as the result.

For the reliability analysis, nominal dead loads loads include the wearing surface (D_w), prefabricated (D_P), and site-cast (D_S) components, and can be found in Tables D1, D3 and D4, respectively.

As mentioned earlier, live load statistics, which are used to generate the maximum live load effect on a girder, V_{LLmax}, are based on values found in Table 6.1 and F5 for design and F7 for rating. Live load coefficient of variation is calculated as follows:

$V_{LLmax} = (V_{proj}^2 + V_{site}^2 + V_{data}^2 + V_{IM}^2 + V_{DF}^2)^{1/2}$

where V_{proj} is the uncertainty in future data projection, V_{site} is uncertainty in mean maximum load effects among different sites, V_{data} is uncertainty in mean maximum load effect (L_{max}) based on the WIM data at a particular site, V_{IM} is uncertainty in impact factor and V_{DF} is uncertainty in load distribution.

Mean resistances include distribution factor (DF) from eq. 6.5,6.6 and bias factor (λ) from Table 6.2.

Once the above parameters are determined, total load effect mean value and standard deviation are calculated as follows:

m total DL = (mDp + mDw + mDs)

σ total DL = $((m\ Dp*V\ Dp)^2 + (m\ Dw*V\ Dw)^2 + (m\ Ds*V\ Ds)^2\ )^{0.5}$

m total load = m total DL + m total LL

With the above parameters, the load Factor (LF) can be determined by equation 7.1 as:

$$LF = \frac{-B+\sqrt{B^2-4AC}}{2A} \qquad \text{eq. 7.1}$$

where:

$A = R_L^2 - \beta^2 V_R^2 R_L^2$ eq. 7.2

$B = 2R_L R_D - 2QR_L - 2\beta^2 V_R^2 R_L R_D$ eq. 7.3

$C = R_D^2 - 2QR_D - \beta^2 V_R^2 R_D^2 + Q^2 - \beta^2 \sigma_Q^2$ eq. 7.4

R_L == vehicular design live-load effect on the girder, not including the live-load factor = $\lambda * D_F *$generated truck's load effects.

R_D = design dead-load effect on the girder, including the load factors = $\lambda*(1.25(D_P+D_S) +1.5(D_W))$.

V_R = COV of resistance.

Q = mean total load effect.

σ_Q = standard deviation of total load effect.

LF = in this study, load factor is considered as 1.75 based on AASHTO LRFD.

β = the desired target reliability index., as modified by the FOSM adjustment factor for improved accuracy. For a target reliability index of 3.50 for design, the adjustment factor is 1.07, such that β = 3.50/1.07 =3.27 while a target reliability index of 2.50/1.04=2.4 for rating, the adjustment factor is 1.04.

7.5 Objective Function

7.5.1 Optimize Beta Value When LF is Constant

For each iteration, β values are calculated for each girder spacing for each span. (4 β values for each span). Then by minimizing the mean square error of all β as the objective (fitness) function, the optimal truck for each iteration is found. In mean square error formula, instead of mean value of β, 3.27 is used for design and 2.4 for rating to come up with trucks having the most desirable β. as it can be seen in equations 7.5 and 7.6.

The Fitness function for design is:

$$\sum_{s=6}^{s=12}\sum_{l=2}^{l=200}\frac{(\beta_{l.s}-3.27)^2}{n} \qquad \text{eq. 7.5}$$

The fitness function for rating is:

$$\sum_{s=6}^{s=12}\sum_{l=20}^{l=200}\frac{(\beta_{l.s}-2.4)^2}{n} \qquad \text{eq. 7.6}$$

Where

S = girder spacing from 6 ft. to 12 ft. with 2 ft. increment.

L = span length (20, 50, 80, 100, 200 ft.)

n = number of total cases which is found by multiplying number of span lengths by the number of girder spacings = 20.

$\beta_{l.s}$ = Reliability index as the function of span length and girder spacing. (i.e. $\beta_{20.6}$ indicates reliability index for 20 ft. span length with 6 ft. girder spacing).

The objective is to minimize the fitness function:

Min f(x) = Min (Fitness function)

Then, the Genetic Algorithm generates the next iteration of trucks based on the truck with lowest fitness value. This process will continue until the last iteration, where the optimal trucks with the minimum fitness value are found.

7.6 Constraint

The constraints described in Table 7.2 are applied during the optimization.

Table 7.2 Constraints

Parameters	Description	Constraint
Y_1	First axle weight, w_1	2 (kips) $\leq Y_1 \leq$ 100 (kips)
Y_2	Axle spacing between 1th and 2nd axle, s_1	2 (ft.) $\leq Y_2 \leq$ 100 (ft.)
Y_3	Second axle weight, w_2	2 (kips) $\leq Y_3 \leq$ 100 (kips)
.	.	.
.	.	.
.	.	.
Y_{2n-2}	last axle spacing, s_{n-1}	2 (ft.) $\leq Y_{2n-2} \leq$ 100 (ft.)
Y_{2n-1}	last axle weight, w_n	2 (kips) $\leq Y_{2n-1} \leq$ 100 (kips)
Y_{2n}	Number of Axles, N	$3 \leq Y_{2n} \leq 13$
β Design	Reliability index for design	$\beta - 3.27 \geq 0$
β Rating	Reliability index for rating	$\beta - 2.5 \geq 0$

7.7 Results

As previously discussed, the optimization is conducted for both design and rating. For each case, two different bridge types are considered. Sections 7.7.1 and 7.7.2 discuss the results of design and rating.

7.7.1 Design

Steel girder and prestressed concrete bridge results for design are given in Section 7.7.1.1 and 7.7.1.2.

7.7.1.1 Steel girders bridge

Three different cases for load effects were considered. In first case, the effect of moment and shear are studied together, while in second and third case, moment and shear are studied separately. The results of these cases are shown in following sections.

a) Moment and Shear

Figure 7.2 represents the results of normalized reliability index when moment and shear are considered simultaneously. Normalized β for design refers to the reliability index divided by 3.27.

In the Figure, M and V represent moment and shear, respectively (i.e. M20G6 means simple moment for span = 20 ft. and girder spacing = 6 ft.).

A comparison of the 6-axle truck, HL93, and HL93mod for all spans is shown in Figure 7.2.

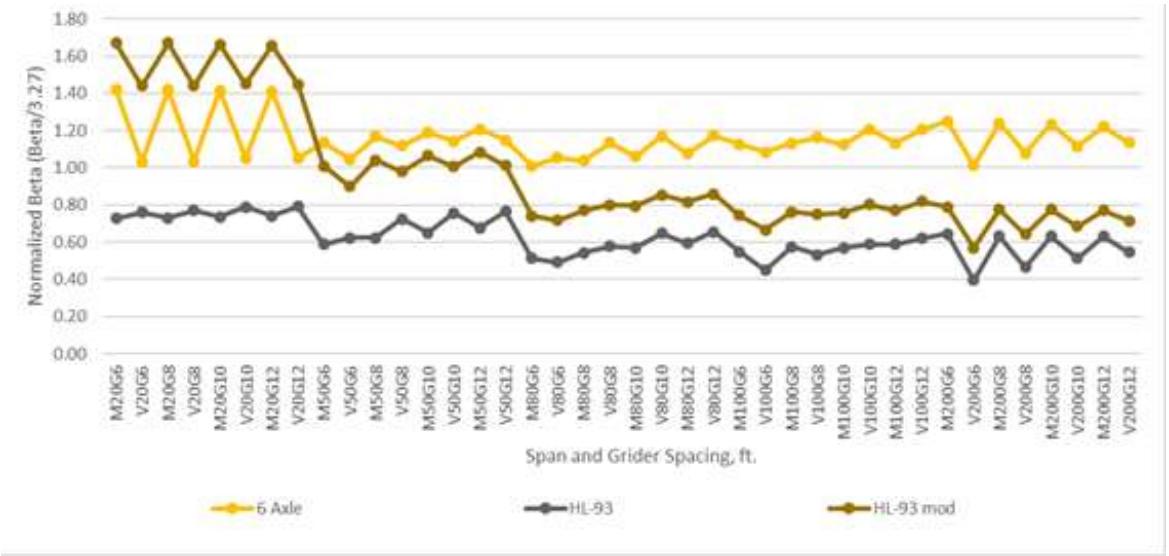

Figure 7.2 – Comparison of 6-axle truck, HL93 and HL93mod for all spans

The 6-axle truck configuration is shown in Figure 7.3.

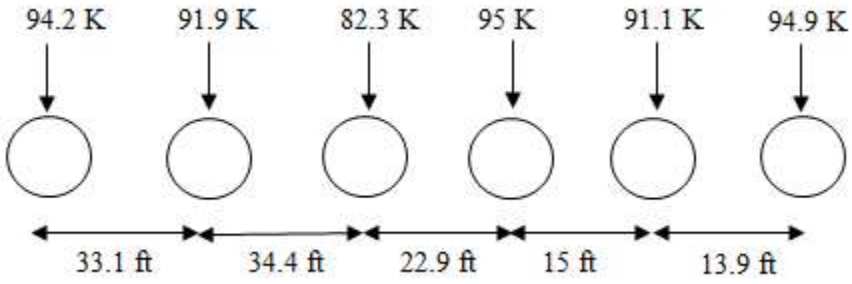

Figure 7.3 – 6 axle truck configurations

Table 7.3 compares the reliability index (β) statistics of mentioned trucks.

Table 7.3 Beta statistics

Truck	Min (β)	Max (β)	COV (β)
6-axle	1.009	1.42	0.95
HL93	0.4	0.8	0.16
HL93mod	0.57	1.67	0.334

Figure 7.2 shows that the 6 axles truck has more discrepancy than HL93 for shorter spans. To solve this issue, two categories are considered: 1- spans < 65 ft. (20 and 50 ft.) spans and 2- spans > 65 ft. (80,100 and 200 ft.). Each category is considered separately and for each case an optimize truck is calculated. The comparison of HL93, 6-axle truck for all spans and two 4-axle trucks for spans < 65 ft. and spans > 65 ft. is given in Figure 7.4.

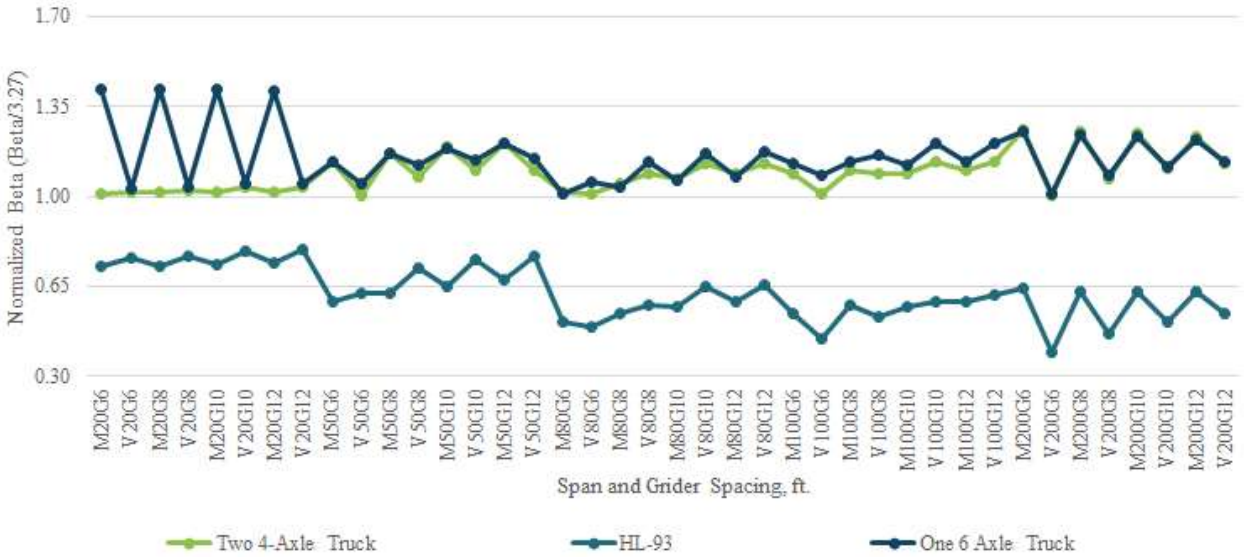

Figure 7.4 – Comparison of 6-axle truck, HL93 and two 4-axle trucks

The two 4-axle trucks configurations are given in Figure 7.5 and 7.6.

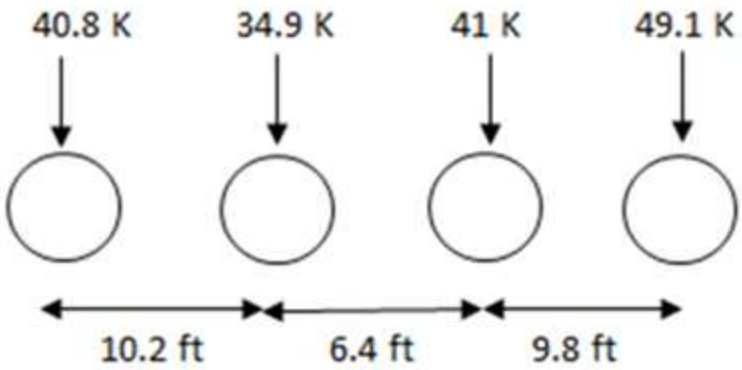

Figure 7.5 – 4-axle truck configuration for spans < 65 ft.

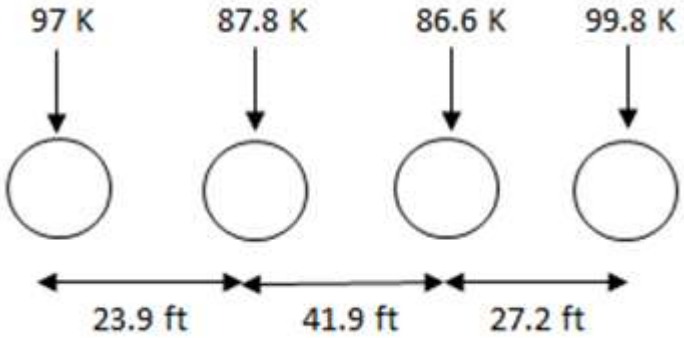

Figure 7.6 – 4-axle truck configuration for spans > 65 ft.

Table 7.4 compares the reliability index (β) statistics of above trucks.

Table 7.4 Beta statistics

Truck	Min (β)	Max (β)	COV (β)
6-axle	1.009	1.42	0.95
HL93	0.4	0.8	0.16
Two 4-Axle trucks	1	1.26	0.068

b) Moment

Figure 7.7 represents the results of normalized beta for moment only.

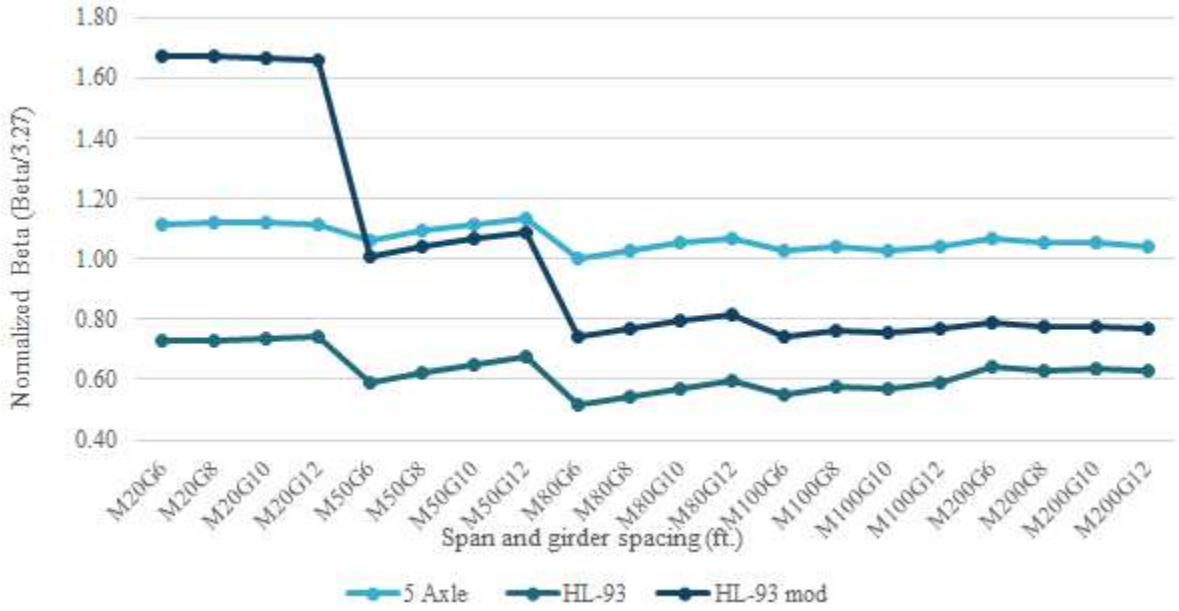

Figure 7.7 – Comparison of 5-axle truck, HL93 and HL93mod for all spans

Normalized beta for the 5-axle truck varies between 1-1.13, while this range for HL-93mod is between 0.7-1.65 and for HL-93 is between 0.5-0.75.

The 5-axle truck configuration is shown in Figure 7.8.

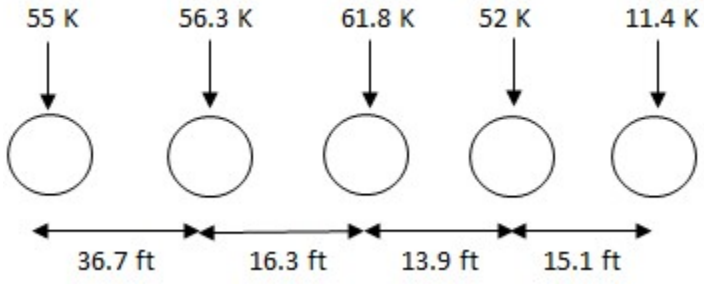

Figure 7.8 – 5 axle truck configurations

Table 7.5 compares the reliability index (β) statistics of mentioned trucks.

Table 7.5 Beta statistics

Truck	Min (β)	Max (β)	COV (β)
5-axle	1	1.13	0.037
HL93	0.51	0.74	0.109
HL93mod	0.74	1.67	0.354

In order to get more accurate results, two categories are considered: 1- spans < 65 ft. (20 and 50 ft.) spans and 2- spans > 65 ft. (80,100 and 200 ft.). Each category is considered separately and for each case an optimize truck is calculated. The comparison of HL93, 5-axle truck for all spans and two 3-axle trucks for spans < 65 ft. and spans > 65 ft. is given in Figure 7.9.

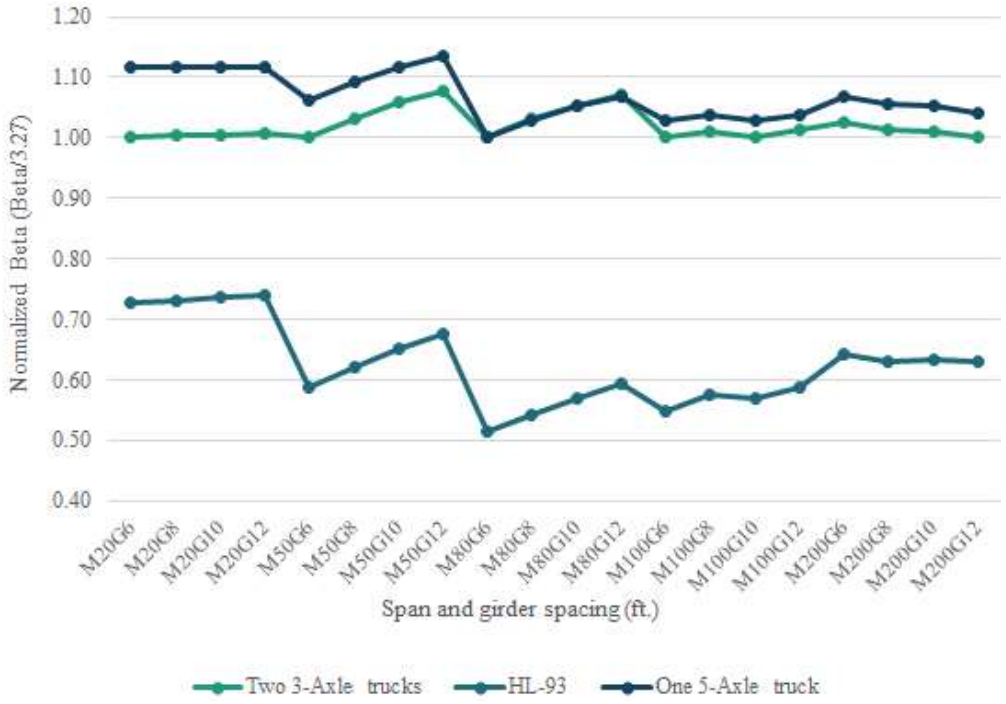

Figure 7.9 – Comparison of 5-axle truck, HL93 and two 3-axle trucks

The two 3-axle trucks configurations are given in Figure 7.10 and 7.11.

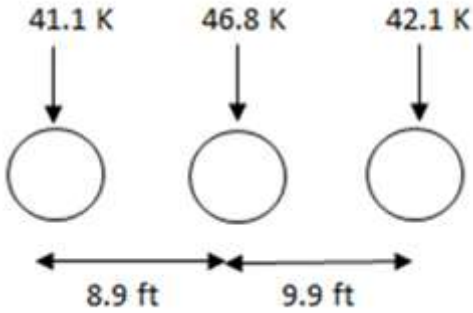

Figure 7.10 – 3-axle truck configuration for spans > 65 ft. (D1)

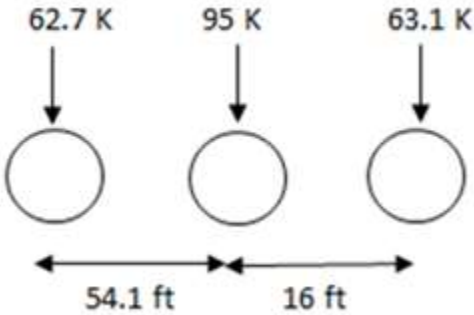

Figure 7.11 – 3-axle truck configuration for spans < 65 ft. (D2)

Table 7.6 compares the reliability index (β) statistics of above trucks.

Table 7.6 Beta statistics

Truck	Min (β)	Max (β)	COV (β)
5-axle	1	1.13	0.037
HL93	0.51	0.74	0.109
Two 3-Axle trucks	1	1.08	0.024

c) Shear

The comparison of HL93, 6-axle truck for all spans and two 4-axle trucks for spans < 65 ft. and spans > 65 ft. is given in Figure 7.12.

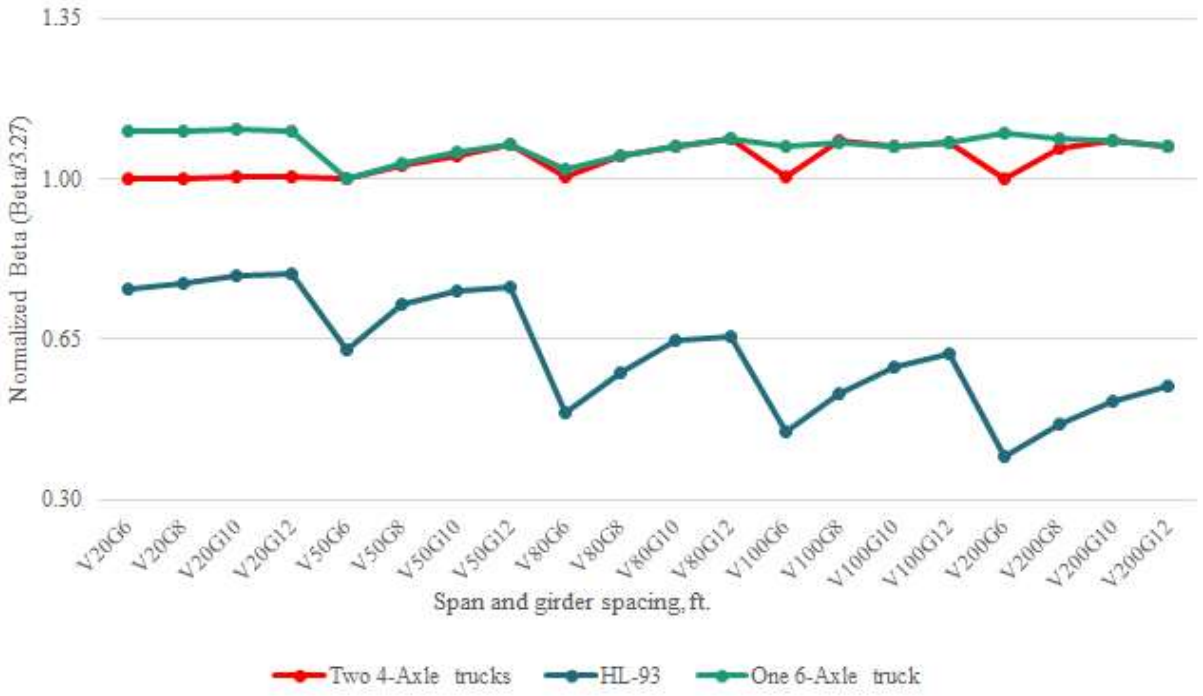

Figure 7.12 – Comparison of 6-axle truck, HL93 and two 4-axle trucks

The two 4-axle trucks configurations are given in Figure 7.13 and 7.14.

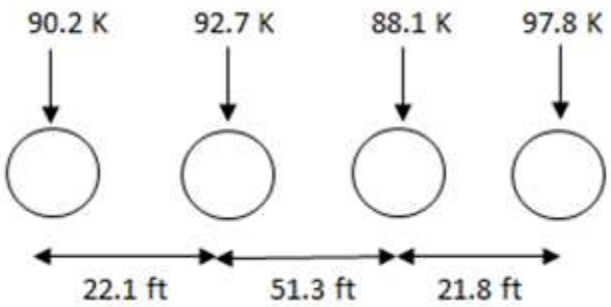

Figure 7.13 – 4-axle truck configuration for spans > 65 ft. (D3)

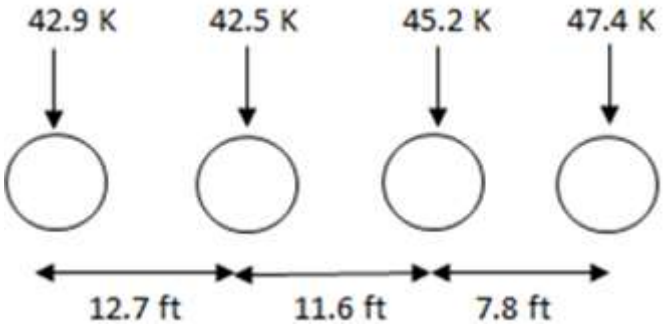

Figure 7.14 – 4-axle truck configuration for spans < 65 ft. (D4)

Table 7.7 compares the reliability index (β) statistics of above trucks.

Table 7.7 Beta statistics

Truck	Min (β)	Max (β)	COV (β)
6-axle	1	1.12	0.046
HL93	0.4	0.79	0.202
Two 4-Axle trucks	1	1.09	0.034

7.7.1.2 Prestressed concrete bridge

Two different cases for load effects were considered. In first case, the effect of moment is studied and for the second one only effect of shear is considered. The results of these cases are shown in following sections.

a) Moment

The same as the steel girder bridge two categories are considered: 1- spans < 65 ft. (20 and 50 ft.) spans and 2- spans > 65 ft. (80,100 and 200 ft.). Each category is considered separately and

for each case an optimize truck is calculated. The comparison of HL93, 10-axle truck for all spans and two 3-axle trucks for spans < 65 ft. and spans > 65 ft. is given in Figure 7.15.

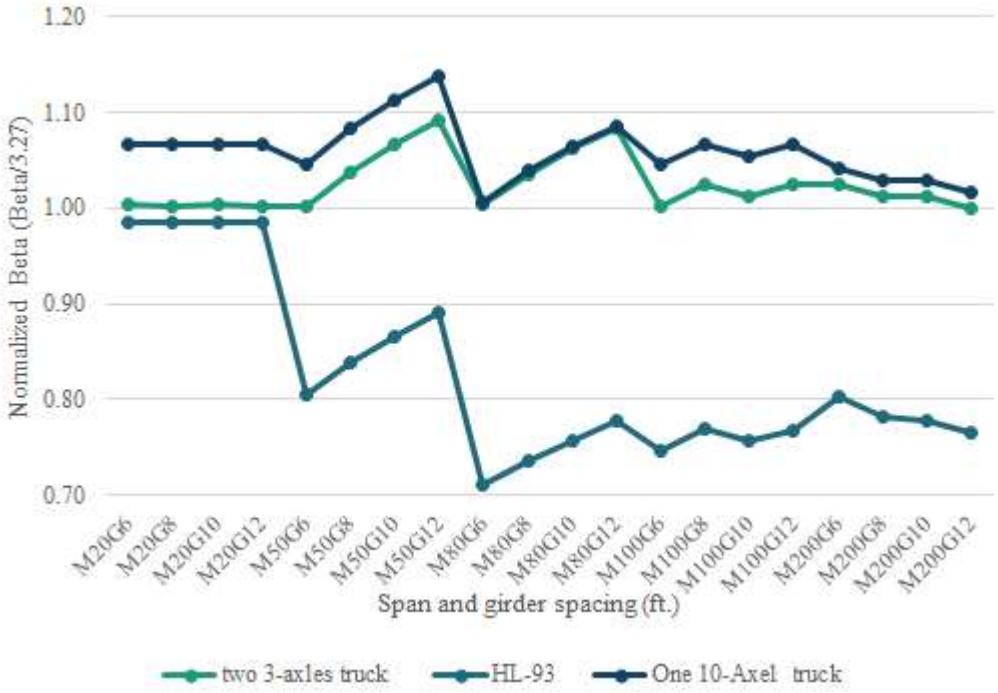

Figure 7.15 – Comparison of 10-axle truck, HL93 and two 3-axle trucks

The two 3-axle trucks configurations are given in Figure 7.16 and 7.17.

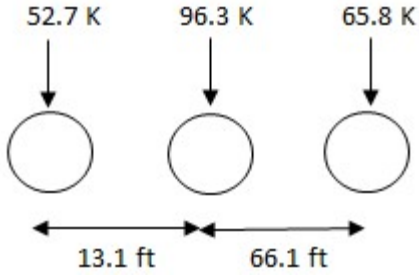

Figure 7.16 – 3-axle truck configuration for spans > 65 ft. (D5)

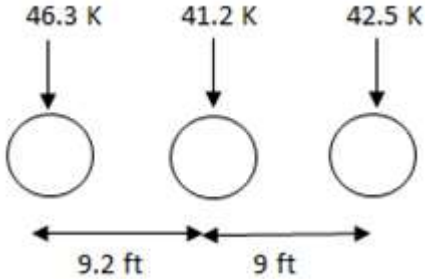

Figure 7.17 – 3-axle truck configuration for spans < 65 ft. (D6)

Table 7.8 compares the reliability index (β) statistics of above trucks.

Table 7.8 Beta statistics

Truck	Min (β)	Max (β)	COV (β)
10-axle	1.006	1.14	0.029
HL93	0.71	0.98	0.112
Two 3-Axle trucks	1	1.09	0.028

b) Shear

For shear, only one truck is considered for all spans. The comparison of HL93, HL93mod and 6-axle truck for all spans is given in Figure 7.18.

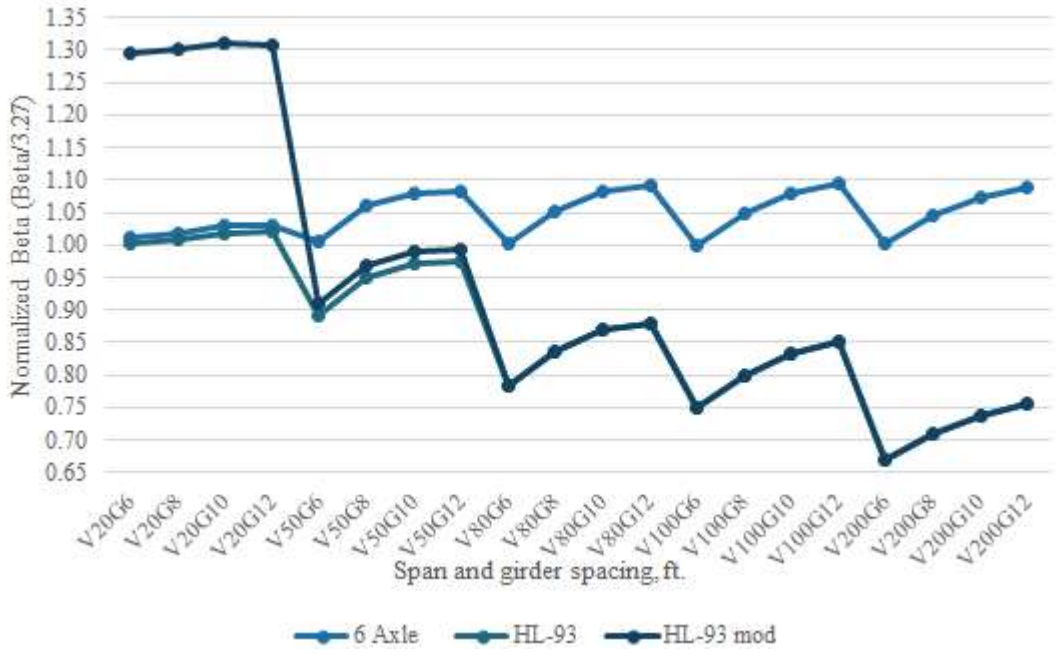

Figure 7.18 – Comparison of 6-axle truck, HL93 and HL93mod

The 6-axle truck configuration are given in Figure 7.19.

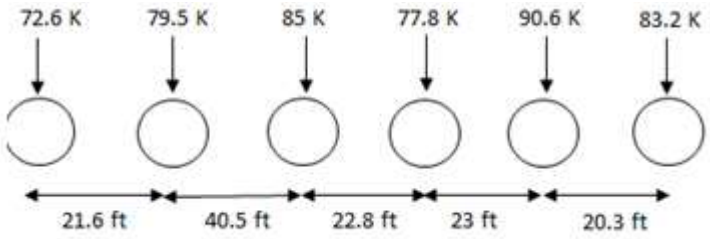

Figure 7.19 – 6-axle truck configuration for all spans (D7)

Table 7.9 compares the reliability index (β) statistics of above trucks.

Table 7.9 Beta statistics

Truck	Min (β)	Max (β)	COV (β)
6-axle	1	1.09	0.033
HL93	0.67	1.018	0.128
HL93-mod	0.67	1.31	0.228

7.7.2 Rating

Steel girder and prestressed concrete bridge results for rating are given in Section 7.7.2.1 and 7.7.2.2. For rating as discussed in section 6.2, legal load factors are considered for the set of 28 Michigan Legal trucks given in the Bridge Analysis Guide with AASHTO code rating procedure when the rating factor is set to 1.0.

The governing trucks for each load effect considering span length are given Table 7.10.

Table 7.10 Governing trucks through the 28 Michigan legal trucks

Load Effect	Span (ft.)	Governing Truck Number
Moment	20	16
	50	17
	80	17
	100	17
	200	25
Shear	20	16
	50	18
	80	17
	100	17
	200	18

7.7.2.1 Steel girders bridge

Two different cases for load effects were considered. In first case, the effect of moment is studied and for the second one only effect of shear is considered. For all rating cases one truck is used for all spans. The results of these cases are shown in following sections.

a) Moment

The comparison of Michigan govern legal trucks for different span and 4-axle truck for all spans is given in Figure 7.20.

Figure 7.20 – Comparison of 4-axle truck and Michigan govern trucks

The 4-axle truck configuration are given in Figure 7.21.

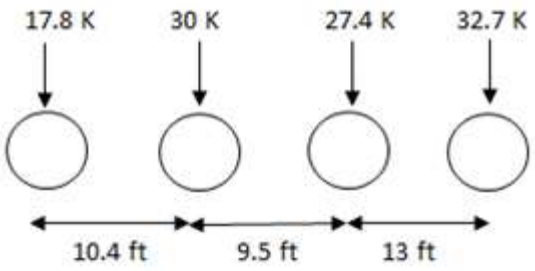

Figure 7.21 – 4-axle truck configuration for all spans (R1)

Table 7.11 compares the reliability index (β) statistics of above cases.

Table 7.11 Beta statistics

Truck	Min (β)	Max (β)	COV (β)
4-axle	1.04	1.15	0.03
MI 28 Legal trucks	1.34	1.6	0.049

b) Shear

The comparison of Michigan govern legal trucks for different span and 10-axle truck for all spans is given in Figure 7.22.

Figure 7.22 – Comparison of 4-axle truck and Michigan govern trucks

The 10-axle truck configuration are given in Figure 7.23.

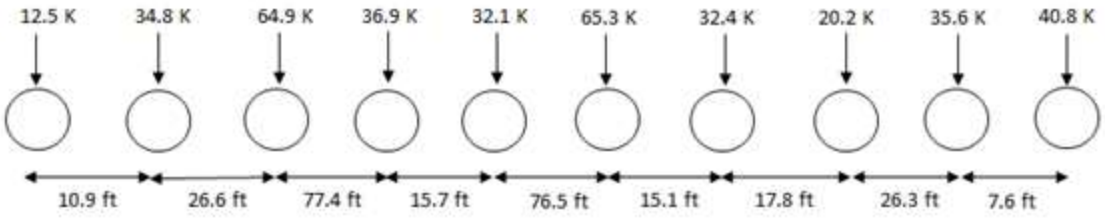

Figure 7.23 – 10-axle truck configuration for all spans (R2)

Table 7.12 compares the reliability index (β) statistics of above cases.

Table 7.12 Beta statistics

Truck	Min (β)	Max (β)	COV (β)
10-axle	1	1.28	0.071
MI 28 Legal trucks	1.21	1.79	0.105

7.7.2.2 Prestressed concrete bridge

a) Moment

The comparison of Michigan govern legal trucks for different span and 3-axle truck for all spans is given in Figure 7.24.

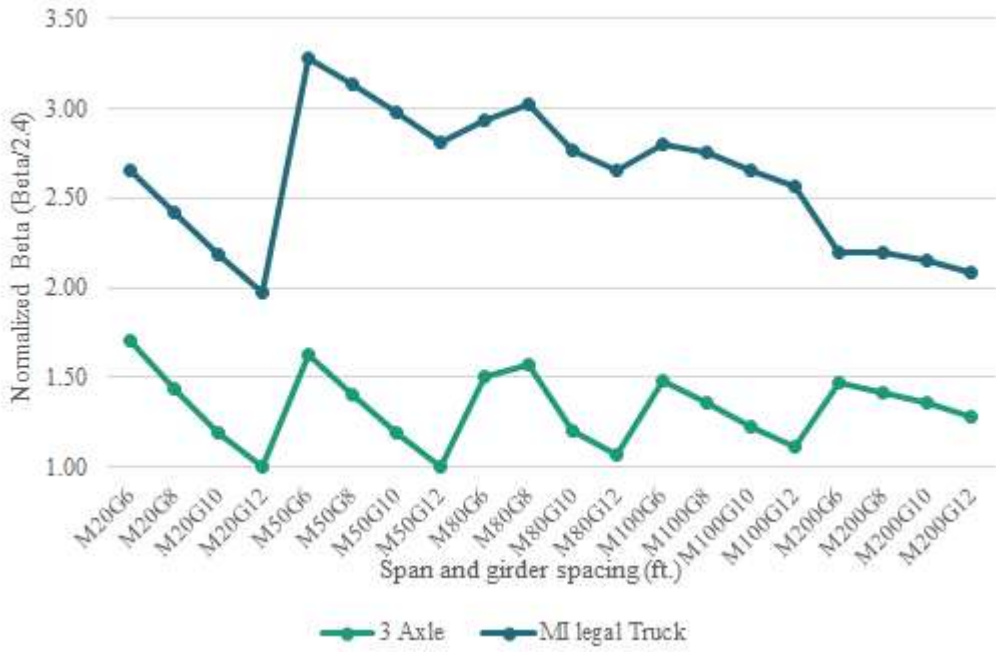

Figure 7.24 – Comparison of 3-axle truck and Michigan govern trucks

The 3-axle truck configuration are given in Figure 7.25.

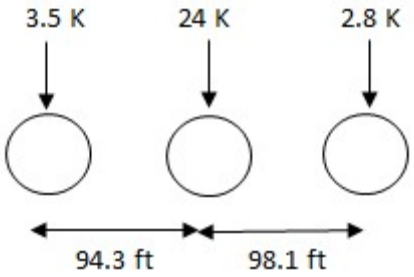

Figure 7.25 – 3-axle truck configuration for all spans (R3)

Table 7.13 compares the reliability index (β) statistics of above cases.

Table 7.13 Beta statistics

Truck	Min (β)	Max (β)	COV (β)
3-axle	1	1.7	0.153
MI 28 Legal trucks	1.98	3.29	0.145

b) Shear

The comparison of Michigan govern legal trucks for different span and 6-axle truck for all spans is given in Figure 7.26.

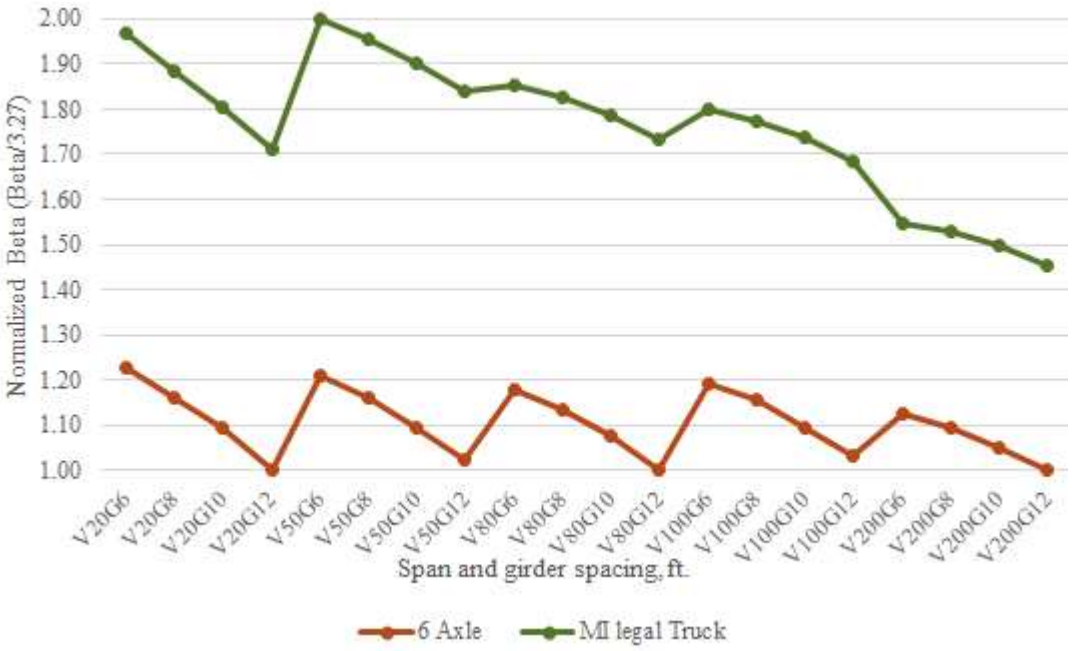

Figure 7.26 – Comparison of 4-axle truck and Michigan govern trucks

The 6-axle truck configuration are given in Figure 7.27.

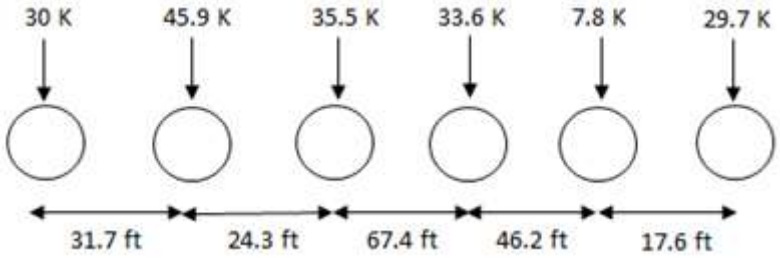

Figure 7.27 – 6-axle truck configuration for all spans (R4)

Table 7.14 compares the reliability index (β) statistics of above cases.

Table 7.14 Beta statistics

Truck	Min (β)	Max (β)	COV (β)
6-axle	1	1.23	0.066
MI 28 Legal trucks	1.45	1.99	0.089

The summary of design and rating trucks for each case is shown in Table 7.15.

Table 7.15 Design and Rating trucks summary

Design Trucks Summary							
Bridge Case	Load Effect	Spans	Truck	β range	COV β	HL93	
						β range	COV β
Steel Girder	Moment	> 65 ft.	D1 (3-Axle)	0.08	0.024	0.23	0.109
	Moment	< 65 ft.	D2 (3-Axle)	0.08	0.024	0.23	0.109
	Shear	> 65 ft.	D3 (4-Axle)	0.09	0.034	0.39	0.202
	Shear	< 65 ft.	D4 (4-Axle)	0.09	0.034	0.39	0.202
Prestressed concrete	Moment	> 65 ft.	D5 (3-Axle)	0.09	0.028	0.27	0.112
	Moment	< 65 ft.	D6 (3-Axle)	0.09	0.028	0.27	0.112
	Shear	All Spans	D7 (6-Axle)	0.09	0.033	0.35	0.128
Rating Trucks Summary							
Steel Girder	Moment	All Spans	R1 (4-Axle)	0.11	0.03	0.26	0.05
	Shear	All Spans	R2 (10-Axle)	0.028	0.07	0.58	1.11
Prestressed concrete	Moment	All Spans	R3 (3-Axle)	0.7	1.31	1.31	0.15
	Shear	All Spans	R4 (6-Axle)	0.23	0.07	0.54	0.09

CHAPTER 8: SUMMARY, CONCLUSIONS AND RECOMMENDATIONS

8.1 Summary

This study involves the reliability-based design optimization of a live load model for design and rating considering actual traffic loads in the State of Michigan. The objective of the study is to develop appropriate design and rating trucks such that target reliability levels for bridge members are consistently met. Steel girder and prestressed concrete bridges with span lengths from 20-200ft and girder spacing from 6-12 ft with simple span load effects (moment and shear) are considered. The objective of the study was achieved by:

1) Analysis of high-fidelity weigh-in-motion (WIM) data that was collected by the Michigan Department of Transportation (MDOT) over a two-year period across nearly 40 sites in Michigan. A total of 20 sites were chosen for consideration in the project. Filtering criteria were developed and used to remove fictitious vehicles that considered axle spacing and weight; speed; length; and number of axles. A series of quality control checks were implemented on the data, including verification of heavy vehicles against available permit data; as well as verification of 5-axle vehicle axle weights, spacing, and gross vehicle weight histograms, against expected values. Confidence intervals of the data were also considered, to judge the expected accuracy of their statistical parameters.
2) Load effects were generated from the filtered WIM data over a series of hypothetical bridge spans and girder live load distribution factors (for two-lane structures). Load effects were generated for simple moments and shears for spans from 20- 200 ft, for both single lane and two lane load effects.

3) Based on the load effect data generated from the WIM vehicle configurations, load effects were then statistically projected to 5 (for rating) and 75 (for design) years to obtain estimates for the maximum load effect statistics. An extreme type I projection was considered.

4) The major task of this study was to implement reliability based-design optimization to determine an optimal live load model for design and rating. A genetic algorithm was used as the optimization method, where the objective function considered minimization in variation of reliability index when the load model is used to design and rate bridges. Based on AASHTO LRFD/LRFR, the target reliability index of 3.5 and 2.5 were considered for design and rating, respectively.

8.2 Recommendations and Conclusions

1) For design, it is recommended to use the following trucks, with the load factor = 1.75 and the lane load = 0.64 k/ft.

   a) Steel girder bridge moment for span <65 ft. 3-Axle truck with the following configuration.

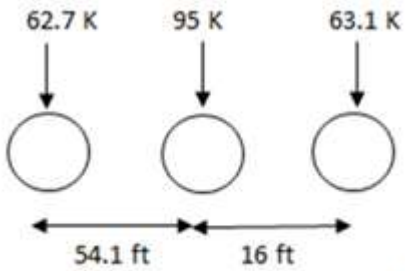

3-Axle truck configuration for span >65 ft. (D1)

b) Steel girder bridge moment for span > 65 ft. 3-Axle truck with the following configuration.

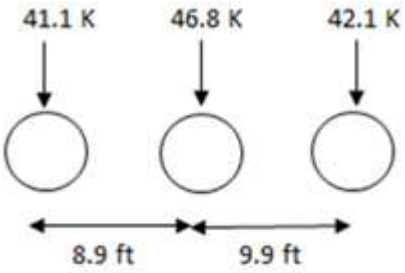

3-Axle truck configuration for span < 65 ft. (D2)

c) Steel girder bridge shear for span < 65 ft. 4-Axle truck with the following configuration.

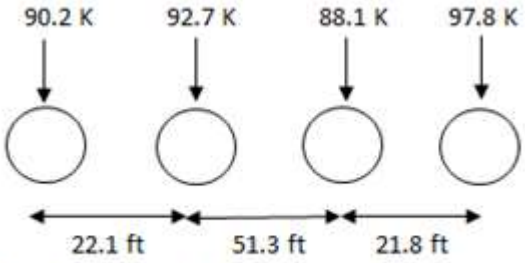

4-Axle truck configuration for spans > 65 ft. (D3)

d) Steel girder bridge shear for span > 65 ft. 4-Axle truck with the following configuration.

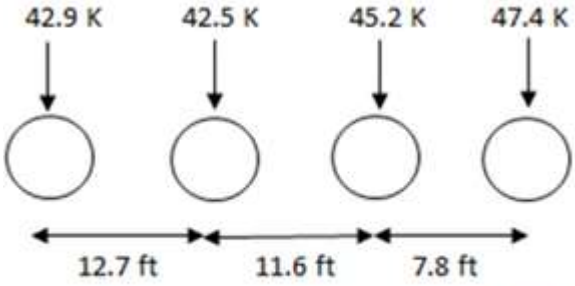

4-Axle truck configuration for spans < 65 ft. (D4)

e) Prestressed concrete bridge moment for span <65 ft. 3-Axle truck with the following configuration.

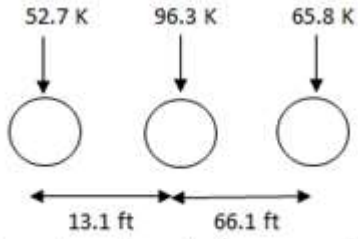

3-Axle truck configuration for spans > 65 ft. (D5)

f) Prestressed concrete bridge moment for span > 65 ft. 3-Axle truck with the following configuration.

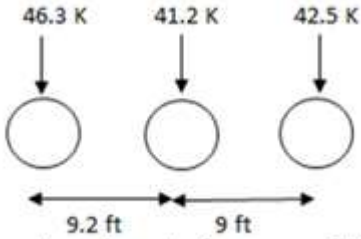

3-Axle truck configuration for spans < 65 ft. (D6)

g) Prestressed concrete bridge shear for all spans length, 6-Axle truck with the following configuration.

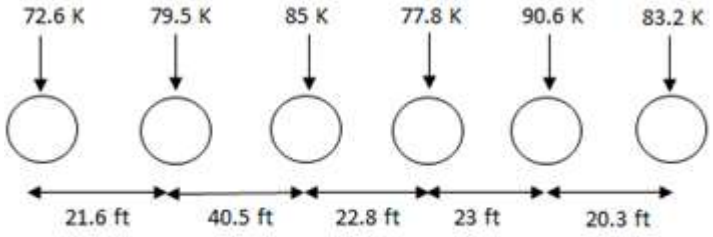

6-Axle truck configuration for all spans (D7)

2) For rating, it is recommended to use the following trucks, with the load factor = 1.75 and the lane load = 0.64 k/ft.

a) Steel girder bridge moment for all spans length, 4-Axle truck with the following configuration.

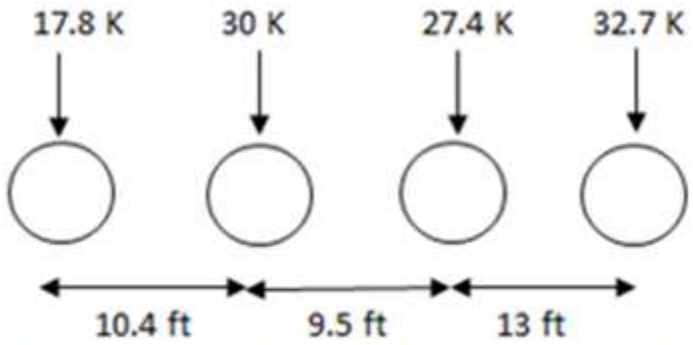

4-Axle truck configuration for all spans (R1)

b) Steel girder bridge shear for all spans length, 10-Axle truck with the following configuration.

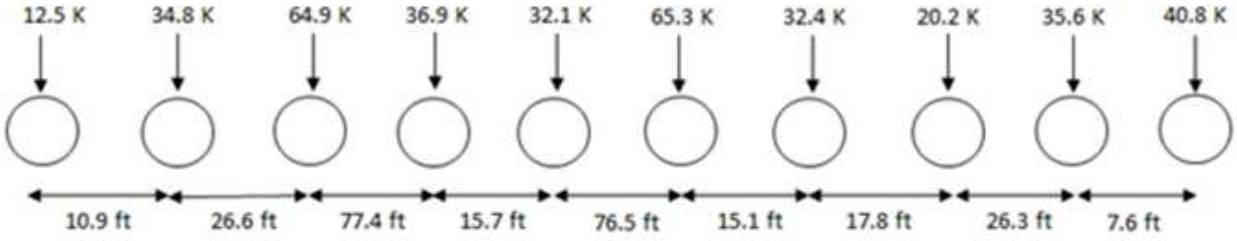

10-Axle truck configuration for all spans (R2)

c) Prestressed concrete bridge moment for all spans length, 3-Axle truck with the following configuration.

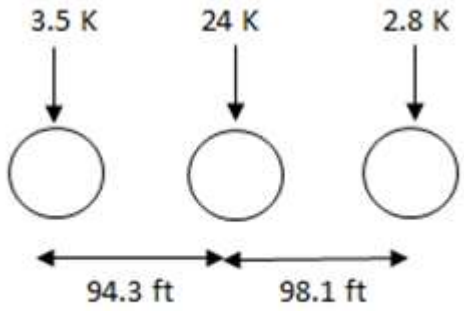

3-Axle truck configuration for all span (R3)

d) Prestressed concrete bridge shear for all spans length, 6-Axles truck with the following configuration.

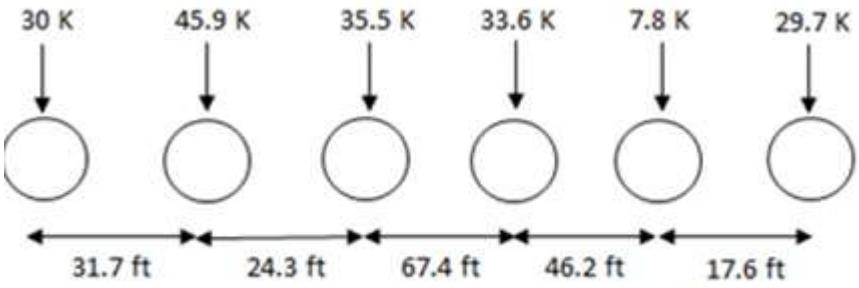

e) 6-Axle truck configuration for all spans (R4)

3) It is further recommended that the developed RBDO procedure is used for other bridge types such as reinforced concrete, prestressed concrete box beams (spaced) and prestressed concrete box beams (side-by-side), as well as for two-span continuous bridges.

4) It is further recommended that the developed RBDO procedure is used for other bridge types such as reinforced concrete, prestressed concrete box beams (spaced) and prestressed concrete box beams (side-by-side), as well as for two-span continuous bridges.

APPENDIX A. STATEWIDE MDOT WIM SENSOR LOCATIONS

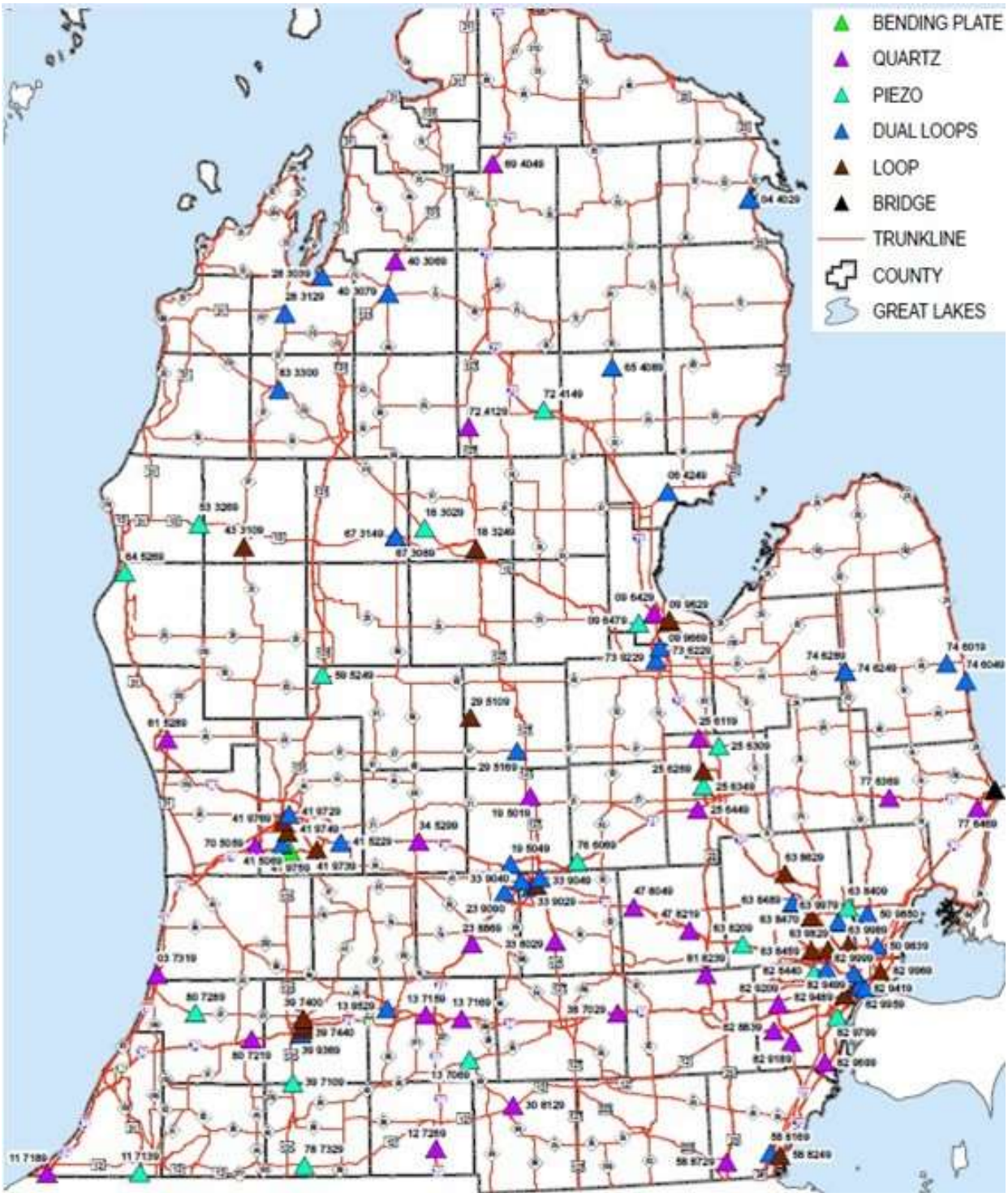

Figure A.1. WIM Stations, Lower Peninsula.

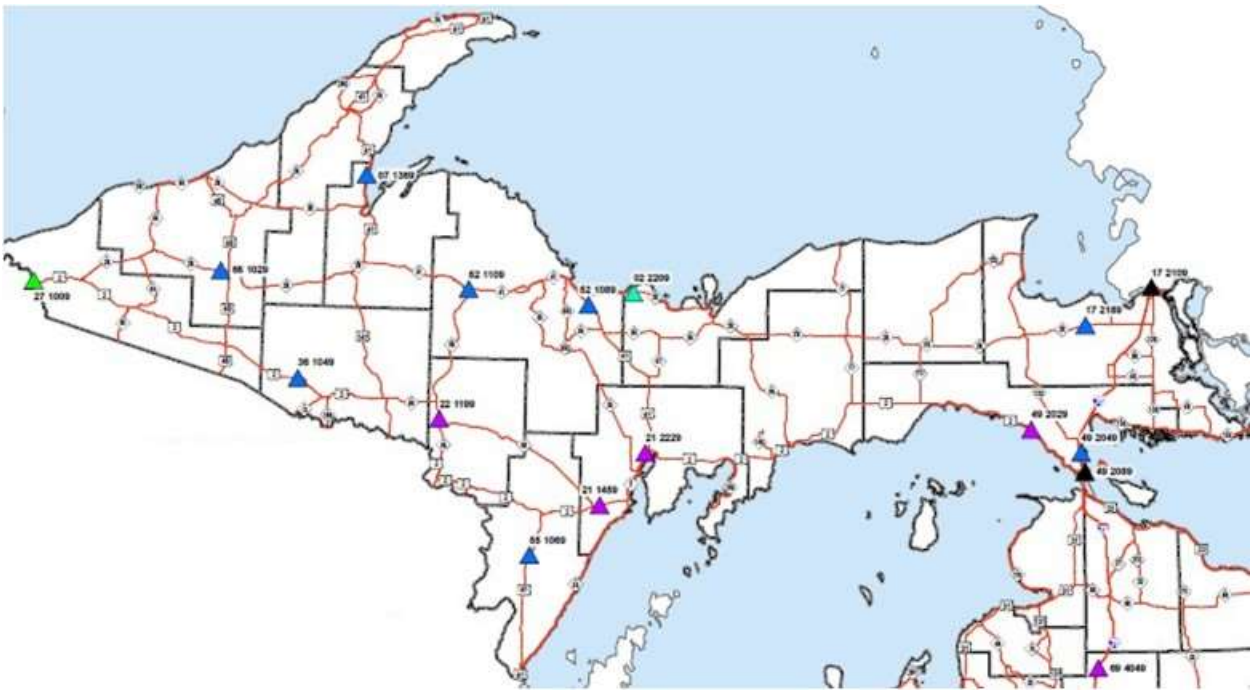

Figure A.2. WIM Stations, Upper Peninsula.

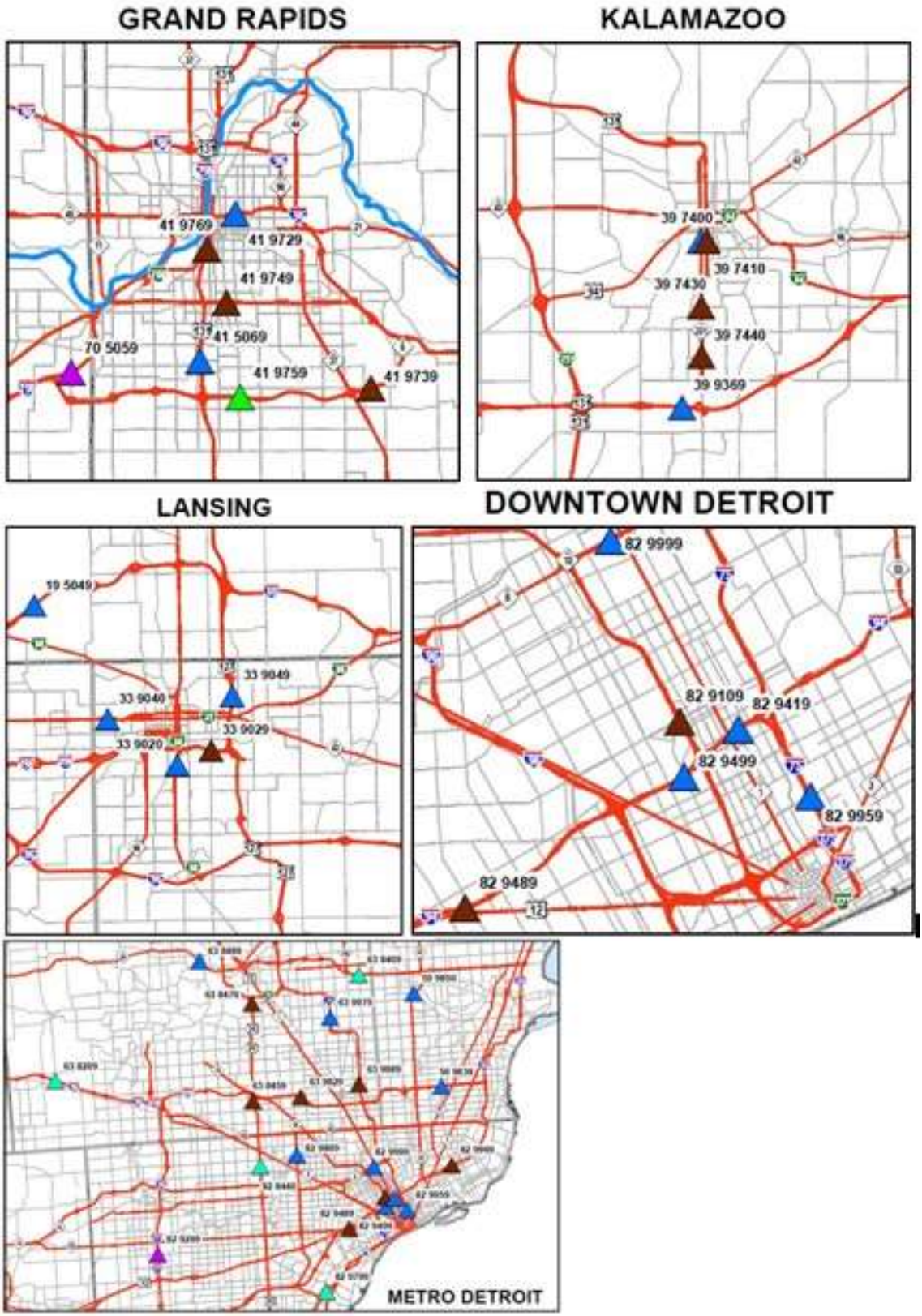

Figure A.3. WIM Stations, Cities.

Table A.1. Description of WIM Stations.

Station	Name	Description	Route	NFC	Calibrated	ADTT	Type of Pavement
1199	Sagola	1.67 miles north of south leg M-69	M-95	02	Oct-11	400	Bit over flex*
1459	Bark River	2 mi E of M-69	US-2	02	Oct-11	550	Bit over conc
2029	Cut River	US-2 1/2 mile West of Worth rd.	US-2	02	Oct-11	420	Bit over flex*
2229	Rapid River	1 mi S of US-41 - Brampton Twp	US-2	14	Oct-11	760	Concrete
3069	Kalkaska	0.5 mi SW of Twin Lk, Wallace	US-131	02	Oct-11	560	Bit over conc*
4049	Vanderbilt	S of Vanderbilt Exit	I-75	01	Oct-11	850	Bit Conc on Agg Base*
4129	Houghton Lk	5 mi S of M-55	US-127	02	Oct-11	510	Bit over flex*
4249	Omer	0.1 mi NE of Sterling Rd	US-23	02		100	Bit over conc
5019	St.Johns SHRP	100 ft. West of Scott Rd.	US-127	02	Nov-11	1300	Concrete
5059	Hudsonville	At 8th Ave (NE of Hudsonville)	I-196	11	Oct-11	2530	Bit over conc*
5099	Coopersville	1 MILE E. OF 68TH AVE	I-96	01	Dec-11	1350	Concrete
5289	Muskegeon	0.3 mi N of Laketon Av (0.7 mi	US-31	12	Nov-11	1050	Concrete
5299	Ionia SHRP	0.5 mi E of M-66	I-96	01	Feb-12	4210	Concrete
6119	Birch Run	I-75 @ Lake rd	I-75	01	Apr-06	3700	Concrete
6369	Capac	1 mi E of Capac Rd	I-69	01	Jan-11	2650	Concrete
6429	Kawkawlin	0.5 mi NW of Wilder Rd - Monit	I-75	01	Jan-12	1340	Concrete
6449	Swartz Creek	0.5 Mi SW of Linden Rd. overpass	I-69	11	Dec-11	4540	Concrete
6469	Port Huron	1 mi S of Range Rd	I-94	11	Nov-11	2640	Concrete
7029	Grass Lake	500 ft east of Whipple rd	I-94	01	May-06	4930	Concrete
7159	Battle Creek	350' W of Verona/ Emmett St	I-94	01	Dec-11	9900	Bit over conc
7169	Marshall	0.5 MI W of 22 1/2 Mile Rd.	I-94	01	Jan-11	6480	Concrete
7189	New Buffalo	.9 miles East of Indian Border	I-94	01	Jan-11	4870	Concrete WB Bit EB
7219	Mattawan	I-94 at CR 657	I-94	01	Oct-11	8440	Concrete
7269	Coldwater	S of Central/Btw T.I.C. ramps	I-69	01	Nov-11	5290	Concrete
7319	South Haven	I-196 1/2 North of North Shore Dr	I-196	01	Oct-11	4360	Concrete
8029	Mason	1.0 N of Barnes Rd - Vevay Twp	US-127	02	Nov-11	1560	Bit over Concrete
8049	Fowlerville	0.5 mi W of Fowlerville Rd	I-96	01	Dec-11	3615	Bit over conc
8129	Jonesville	0.3 mi SW of Dobson Rd	US-12	02	Dec-11	580	Bit over conc
8219	Howell	At Dorr Rd Overpass - Genoa Twp	I-96	11	Feb-12	4560	Concrete
8239	Whitmore Lake	US-23 1/2 mile south of Barker rd	US-23	12	Jan-11	4370	Bit over flex*
8729	Lambertville	S of US-223	US-23	02	Nov-11	4590	Concrete
8839	Belleville	I-94 1/2 mile East of Belleville rd	I-94	11	Jan-12	6340	Concrete
8869	Charlotte	1 mile south of M-50	I-69	01	Oct-11	4980	concrete
9189	275@Penn	At Romulus/Penn. Rd overpass	I-275	11	Feb-12	5120	Concrete
9209	275@CherryHi	At Cherry Hill Rd Overpass	I-275	11	Nov-11	4850	Bit over conc
9699	Vreeland	At the Vreeland Rd. overpass	I-75	11	Jan-12	11100	Concrete
9759	Cutlerville	1300 ft East of Kalamazoo Ave	M-6	12	Oct-11	4400	Concrete

*These stations are located on pavements classified as Flexible per the TWIS Pavement Code. All others are classified as Rigid. All stations have quartz sensors except Stations 9189 and 4249, which are Piezo BL.

APPENDIX B. SUMMARY OF WIM DATA

Table B1. Summary of Eliminated Vehicles.

	% of Total Vehicles at Each WIM Station		(# Elim. At Station) / (Total Elim. Vehicles)		(# Elim. At Station) / (Total Vehicles)	(# Elim. At Station) / (Total Vehicles at Station)
Station	# of vehicles	%	# of vehicles	%	%	%
7189	3054751	3.7	524131	2.04	0.64	17
7219	5411632	6.6	975784	3.80	1.19	18
7159	6260726	7.7	1308460	5.10	1.60	21
7319	2733228	3.3	637782	2.48	0.78	23
7029	3389386	4.1	835063	3.25	1.02	25
6369	1663087	2.0	410262	1.60	0.50	25
7269	3323885	4.1	849674	3.31	1.04	26
7049	44586	0.1	11916	0.05	0.01	27
8869	3121764	3.8	867423	3.38	1.06	28
9699	6931961	8.5	1931911	7.53	2.36	28
8049	2271355	2.8	640670	2.50	0.78	28
6469	1645503	2.0	489791	1.91	0.60	30
6449	2831544	3.5	864922	3.37	1.06	31
5059	1557362	1.9	497766	1.94	0.61	32
7169	4106689	5.0	1374719	5.36	1.68	33
5299	2622531	3.2	880281	3.43	1.08	34
8729	2895434	3.5	979660	3.82	1.20	34
8839	3942476	4.8	1352211	5.27	1.65	34
8129	362128	0.4	127377	0.50	0.16	35
8239	2713809	3.3	981978	3.83	1.20	36
5099	935895	1.1	340254	1.33	0.42	36
9189	3169012	3.9	1169929	4.56	1.43	37
4149	77165	0.1	28877	0.11	0.04	37
6119	2364972	2.9	891338	3.47	1.09	38
5289	721283	0.9	287771	1.12	0.35	40
9209	2863462	3.5	1174059	4.57	1.44	41
8219	2879496	3.5	1213670	4.73	1.48	42
3069	334172	0.4	145973	0.57	0.18	44
8029	967695	1.2	424211	1.65	0.52	44
2199	24669	0.0	10982	0.04	0.01	45
5019	787127	1.0	359341	1.40	0.44	46
4049	508122	0.6	245744	0.96	0.30	48
4129	307559	0.4	159504	0.62	0.20	52
6429	821004	1.0	428276	1.67	0.52	52
2029	253348	0.3	134235	0.52	0.16	53
2229	463261	0.6	245953	0.96	0.30	53
1199	244871	0.3	131481	0.51	0.16	54
9759	2733984	3.3	1485327	5.79	1.82	54
1459	332422	0.4	201557	0.79	0.25	61
4249	71639	0.1	47395	0.18	0.06	66
SUM:	81744995	100	25667658	100	31.4	AVE: 37.7

Table B2. Effect of Scrubbing Criteria on Heavy Weight Vehicles.

Statistic (GVW)	All data no scrubbing	All data Scrubbed	Upper 20% no scrubbing	Upper 20% Scrubbed	Over 150k Scrubbed	Over 280k Scrubbed
Total # of Data	92381307	66275263	18352767	13255185	52554	177
Mean	49.25	52.08	88.65	80.04	164.9	346.7
Median	44.9	49.5	76.7	75.8	158.1	338
Mode 1	30.88	35	72.9	72.9	150.2	338
Mode 2	70.7	74.25	--	--	--	--
Std. Dev	28.03	20	29.27	13.93	20.2	54.3
COV	0.57	0.38	0.33	0.17	0.12	0.16
Min.	1	12	70.3	71.1	150	280.1
Max.	655.3	543	655.3	280.8	543	543

*Note that vehicles may be eliminated by multiple criteria, so percentages will not add up to 100%

Table B3. Summary of Excluded Data.

Excluded data						
Statistic (GVW)	Excluded by Weight	Excluded by Length	Excluded by Speed	Excluded by # of Axles	Excluded by Axle Weight	Excluded by Axle Spacing
Total # of Data	4957293	361673	351853	12	14692762	13037235
Mean	6.44	6.56	42.31	267.16	38.38	38.03
Median	8.3	1.92	10.85	284.3	23.17	28.21
Mode 1	1.89	9.38	10.51	-----	12.18	27.32
Mode 2	9.14				143.71	131.95
Std. Dev	3.97	12.72	97.53	160.95	46.77	37.21
COV	0.62	1.94	2.31	0.60	1.22	0.98
Min.	1	1	1	33.3	1	1
Max.	11.9	571	655.3	571	655.3	655.3
Percentage Scrubbed	18.99	1.39	1.35	0.00005	56.28	49.94
Percentage Remaining	94.63	99.61	99.62	100.00	84.10	85.89

*Note that vehicles may be eliminated by multiple criteria, so percentages will not add up to 100%

Table B4. Summary of Top 20% of Data Excluded.

Upper 20% of Excluded data						
Statistic (GVW)	All exculded data	Excluded by Weight	Excluded by Length	Excluded by Speed	Excluded by Axle Weight	Excluded by Axle Spacing
Total # of Data	5221208	0	73653	72317	2972380	2612876
Mean	109.23	0	22.77	155.27	116.32	102.51
Median	109.5	0	17.21	79.25	120.58	90.93
Mode 1	70.44	0	10.34	75.1	71.68	72.11
Mode 2	141.29				146.25	131.18
Std. Dev	44.84	0	20.78	174.29	47.77	38.83
COV	0.41	0.00	0.91	1.12	0.41	0.38
Min.	57.7	0	3.5	1.6	60.4	56.1
Max.	655.3	0	571	655.3	655.3	655.3
Percentage Scrubbed	100.00	0.00	1.41	1.39	56.93	50.04
Percentage Remaining	71.84	100.00	99.60	99.61	83.97	85.91

*Note that vehicles may be eliminated by multiple criteria, so percentages will not add up to 100%

Table B5. Summary of Heavy Vehicles Excluded.

Excluded data			
Statistic (GVW)	All excluded data	Data above 280k excluded	Data above 150k excluded
Total # of Data	26106044	33994	627503
Mean	42.01	419.21	179
Median	29.7	382.15	159
Mode 1	26.9	310.77	150
Mode 2	134.4		
Std. Dev	41.3	119.23	66.99
COV	0.98	0.28	0.37
Min.	1	280.1	150
Max.	655.3	655.3	655.3
Percentage Scrubbed	100.00	0.13	2.40
Percentage Remaining	71.74	99.96	97.60

*Note that vehicles may be eliminated by multiple criteria, so percentages will not add up to 100%

Table B6. Summary of Data By Region.

Data Summary							
	Quantity	Mean	Std. Dev.	Mode1	Mode2	Min.	Max.
All Data	92381307	49.25	28.03	30.88	70.7	1	655.3
Correct Data	66275263	52.08	20.03	35.004	74.25	12	543.1
Top 20% of All Data	18352767	88.65	29.27	73.68		70.3	655.3
Top 20% of Correct Data	13255185	86.13	19.76	73.12		71.1	543.1
Correct Data over 150 kips	52554	164.9	20.21			150	543.1
Correct Data over 280 kips	177	346.65	54.33			280.1	543.1
5-axle Trucks	50594764	54.48	15.51	35.42	72.96	16.4	278
Top 5% of 5-axle Trucks	2530407	81.19	3.62	78.8		78	278
Interstate WIM Stations	53508179	52.8	19.54	35	72.82	12	280.8
Top 5% of Interstate WIM Stations	2689938	95.67	20.5	80.78		79.4	280.8
Other Principal Arterial WIM Stations	5069531	52.08	21.08	33.98	72.78	12	280.1
Top 5% of Other Principal Arterial WIM Statio	254281	99	21.67	80.44		79.8	280.1
Metro Region WIM Stations	15308153	51.99	20.44	35.67	72.36	12	280.2
Top 5% of Metro Region WIM Stations	772107	99.98	21.496	81.83		80.1	280.2
University Region WIM Stations	14317815	51.52	19.78	35.67	72.78	12	279.8
Top 5% of University Region WIM Stations	718121	94.47	19.26	81.83		80	279.8
Southwest Region WIM Stations	20939545	54.78	17.87	36.27	72.96	12	280.8
Top 5% of Southwest Region WIM Stations	1049154	89.9	19.16	79.02		78	280.8
Superior Region WIM Stations	732051	54.47	26.8	33.18	72.95	12	280.1
Top 5% of Superior Region WIM Stations	36605	125.6	18.2			104.6	280.1
North Region WIM Stations	790569	50.84	26.15	35.69	74.62	12	273.2
Top 5% of North Region WIM Stations	39587	126.87	15.72	126.76		102.3	273.2
Grand Region WIM Stations	5776603	48.07	20.56	33.98	77	12	278
Top 5% of Grand Region WIM Stations	289727	95.98	18.26	82.88		81.3	278
Bay Region WIM Stations	4312109	51.14	21.51	34.83	72.78	12	270.1
Top 5% of Bay Region WIM Stations	216470	103.79	20.19	80.09		80	270.1

Table B7. Comparison of Original and Reduced WIM Data Statistics.

Statistic (GVW)	Original WIM	Reduced	Original over 150k	Reduced over 150k	Original over 280k	Reduced over 280k
Total # of Data	66275263	66243352	52554	20643	177	146
Mean	52.08	52.03	165	176	347	346
Median	49.5	49.5	158	159	338	337
Mode	34.6	34.6	150	155	338	338
Std. Dev	20.03	19.90	20.2	27.7	54.3	54.1
COV	0.385	0.385	0.12	0.157	0.156	0.156
Min.	12.0	12.0	150	155	280.1	280.1
Max.	543	543	543	543	543	543

Table B8. Total Legal and Non-legal Vehicles.

	Data Analyzed	Percentage
All trucks	45183078	100.0
Legal	42697297	94.5
Legal, above 80k	1235748	2.7
Legal, below 80k	41461549	91.8
Non-legal	2485781	5.5
Non-legal, above 80k	1535088	3.4
Non-legal, below 80k	950693	2.1

*note that vehicle classes 1-3 are not included in these counts..

Table B9. Legal and Non-Legal Vehicles, k= GVW/Length

Legal below 80		**41261549**
GVW/Length	Quantity	Percentage
k < 0.5	2037644	4.94
0.5 ≤ k <1.0	24891376	60.33
1.0 ≤ k <2.0	14123040	34.23
2.0 ≤ k <3.0	199048	0.482
3.0 ≤ k <4.0	10148	0.025
4.0 ≤ k <5.0	239	0.001
5.0 ≤ k	54	0.0001

Legal above 80		**1035748**
GVW/Length	Quantity	Percentage
k < 0.5	268	0.03
0.5 ≤ k <1.0	11142	1.08
1.0 ≤ k <2.0	677838	65.44
2.0 ≤ k <3.0	346314	33.44
3.0 ≤ k <4.0	160	0.02
4.0 ≤ k <5.0	0	0.00
5.0 ≤ k	26	0.003

Non-Legal below 80		**1150693**
GVW/Length	Quantity	Percentage
k < 0.5	22941	1.99
0.5 ≤ k <1.0	94734	8.23
1.0 ≤ k <2.0	913140	79.36
2.0 ≤ k <3.0	100072	8.70
3.0 ≤ k <4.0	19341	1.68
4.0 ≤ k <5.0	299	0.026
5.0 ≤ k	166	0.014

Non-Legal above 80		**1735088**
GVW/Length	Quantity	Percentage
k < 0.5	214	0.01
0.5 ≤ k <1.0	7543	0.43
1.0 ≤ k <2.0	970822	55.95
2.0 ≤ k <3.0	743524	42.85
3.0 ≤ k <4.0	12747	0.73
4.0 ≤ k <5.0	176	0.01
5.0 ≤ k	62	0.004

Table B10. Vehicle Checking Statistics by Site.

	5-AXLE VEHICLES			ALL VEHICLES		
	Mean Weight			Mean Weight		
SITE	Drive Axle (k)	Steering Axle (k)	Tandem Axle Spacing (ft)	Drive Axle (k)	Steering Axle (k)	Tandem Axle Spacing (ft)
4049	11.6	11.0	4.5	12.0	10.9	5.3
5019	11.5	10.4	4.8	11.9	10.3	5.8
5099	11.0	11.5	4.4	11.9	11.5	6.0
5289	11.5	11.0	4.5	12.0	11.1	6.1
6429	11.1	10.4	4.6	11.8	10.3	5.3
7029	11.8	10.7	4.7	11.9	10.6	5.3
7159	11.8	11.0	4.6	11.9	10.9	5.1
7169	11.8	10.8	4.6	11.9	10.8	5.2
7219	11.7	10.5	4.6	11.8	10.4	4.8
7269	11.7	10.7	4.9	11.8	10.6	5.5
8029	10.9	10.8	4.7	11.7	10.5	7.0
8839	11.3	10.7	4.8	11.6	10.5	5.3
8869	11.8	11.0	4.5	11.9	10.9	4.9
9189	11.0	10.5	4.9	11.2	10.4	5.3
9209	10.5	11.0	4.5	11.1	10.6	5.8
9699	11.5	10.9	4.5	11.6	10.8	4.7

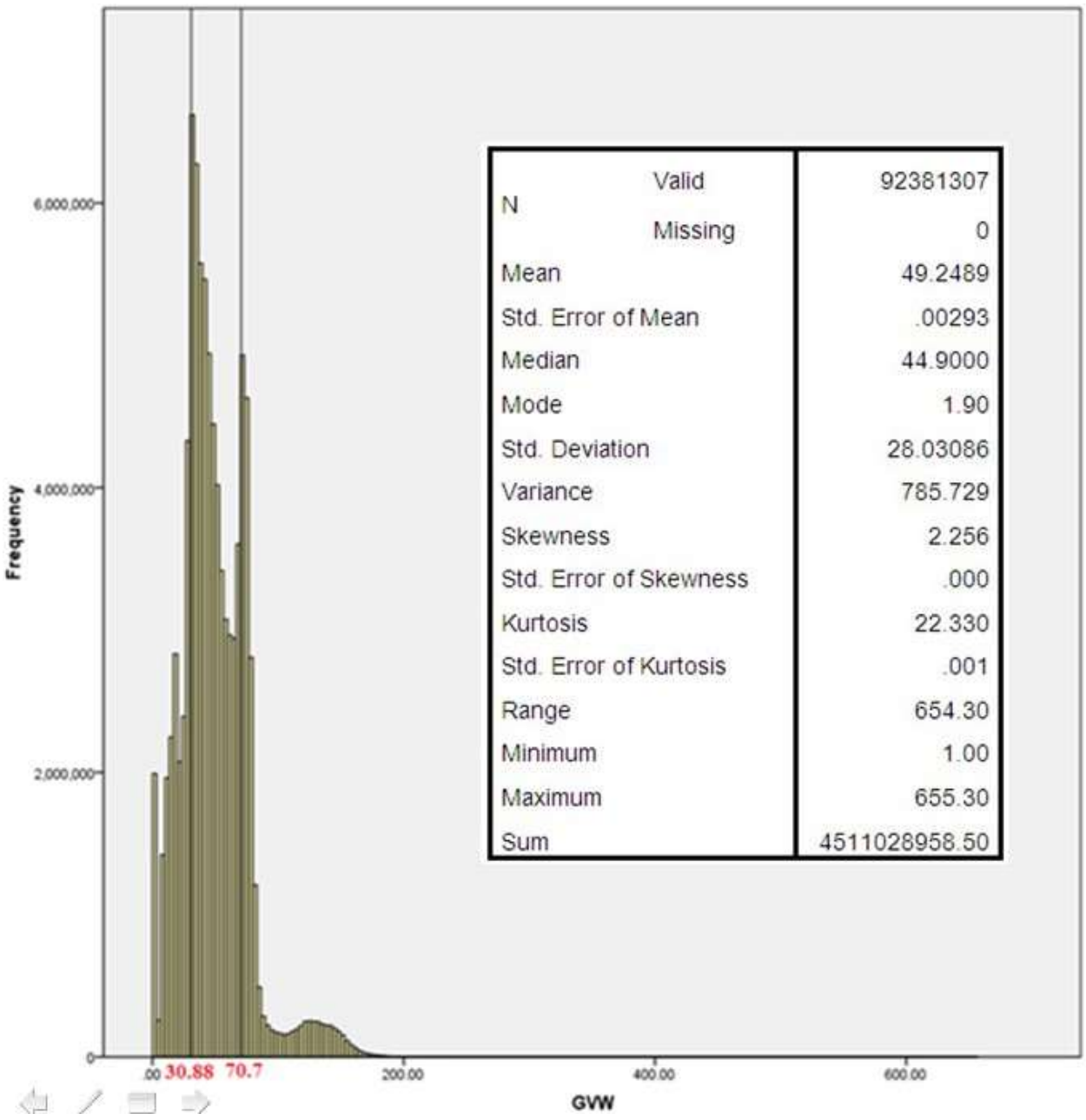

N	Valid	92381307
	Missing	0
Mean		49.2489
Std. Error of Mean		.00293
Median		44.9000
Mode		1.90
Std. Deviation		28.03086
Variance		785.729
Skewness		2.256
Std. Error of Skewness		.000
Kurtosis		22.330
Std. Error of Kurtosis		.001
Range		654.30
Minimum		1.00
Maximum		655.30
Sum		4511028958.50

Figure B1. Frequency Histogram for All Data, Prior to Scrubbing.

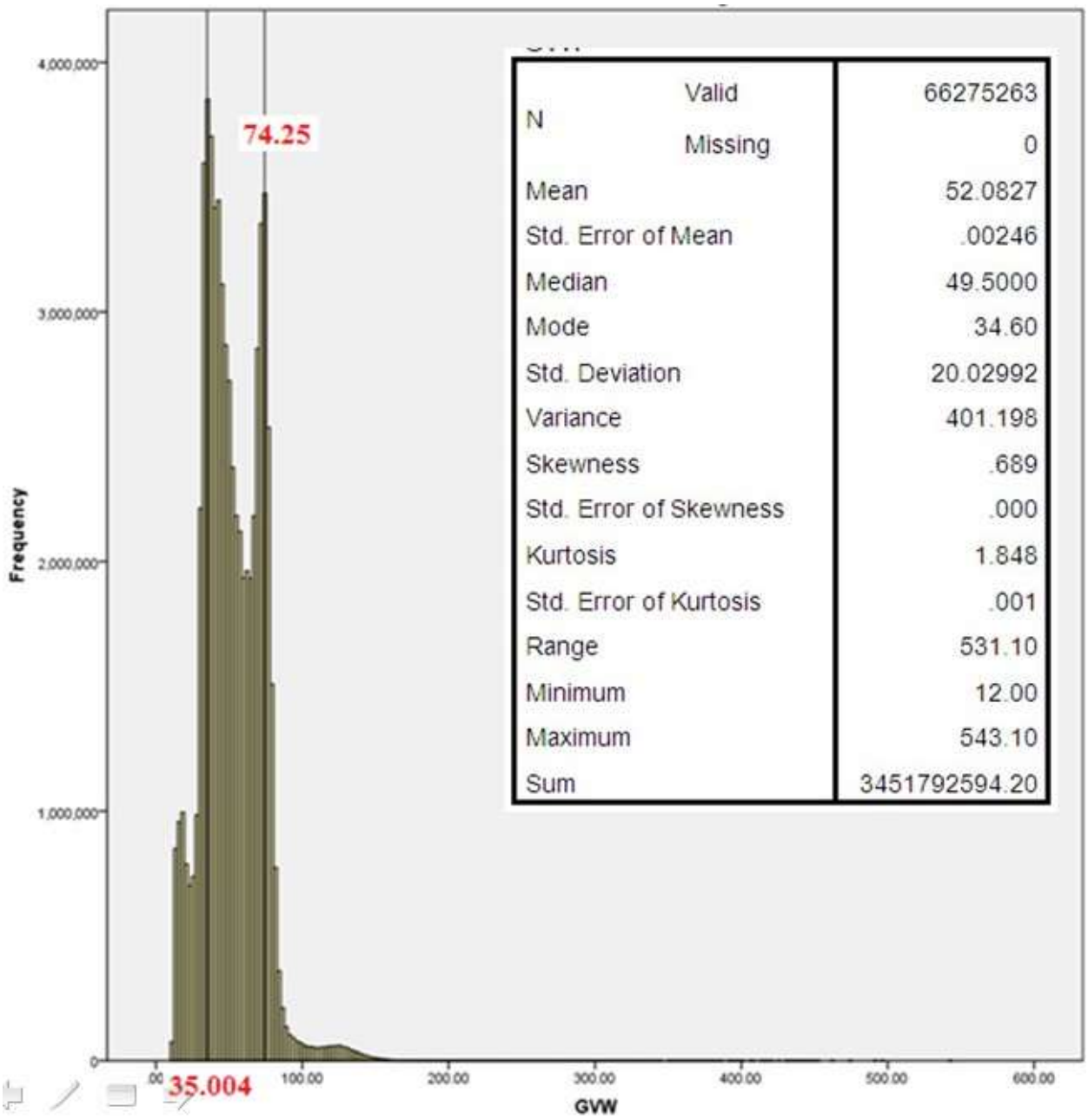

N	Valid	66275263
	Missing	0
Mean		52.0827
Std. Error of Mean		.00246
Median		49.5000
Mode		34.60
Std. Deviation		20.02992
Variance		401.198
Skewness		.689
Std. Error of Skewness		.000
Kurtosis		1.848
Std. Error of Kurtosis		.001
Range		531.10
Minimum		12.00
Maximum		543.10
Sum		3451792594.20

Figure B2. Frequency Histogram for All Correct Data.

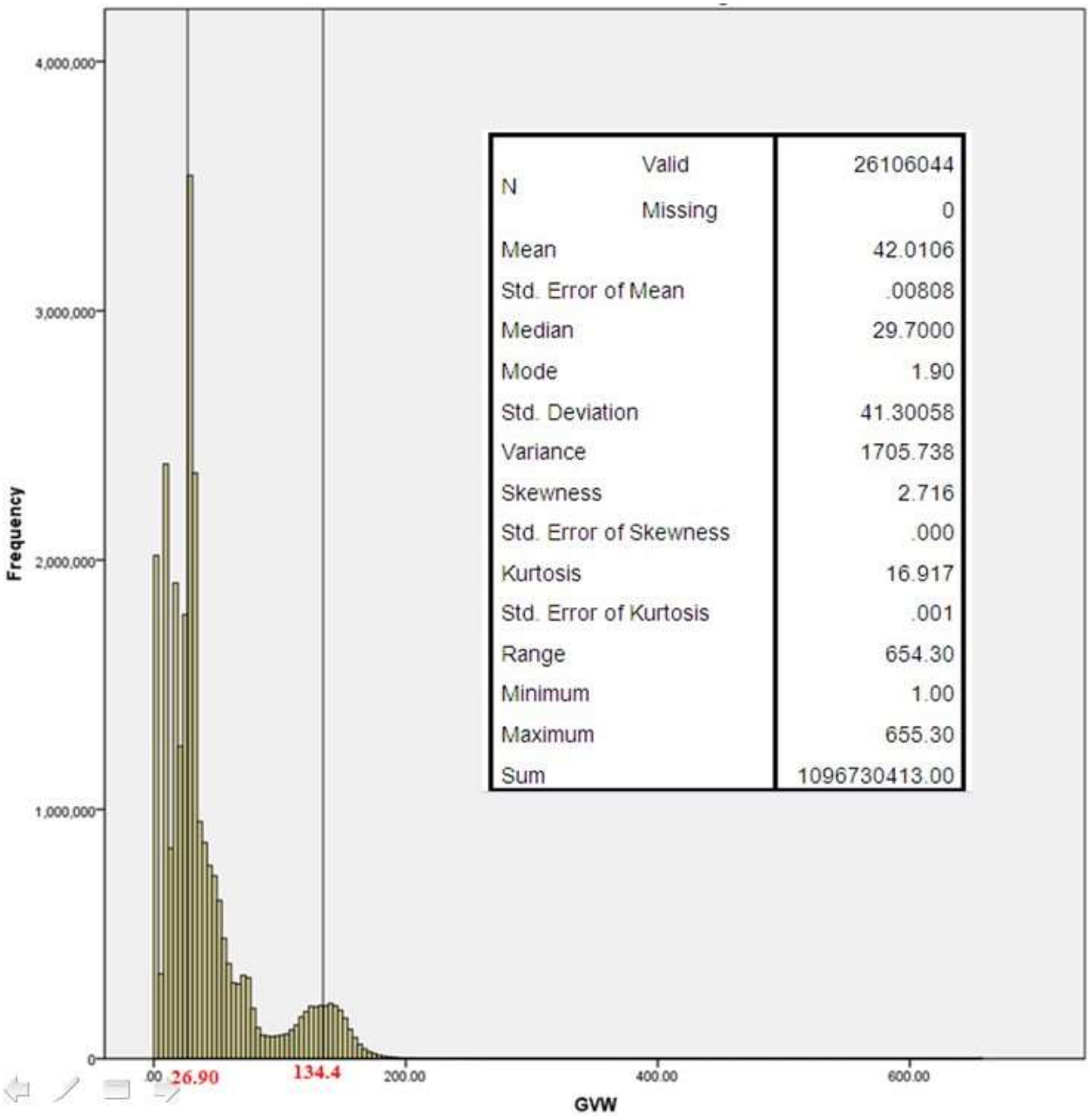

N	Valid	26106044
	Missing	0
Mean		42.0106
Std. Error of Mean		.00808
Median		29.7000
Mode		1.90
Std. Deviation		41.30058
Variance		1705.738
Skewness		2.716
Std. Error of Skewness		.000
Kurtosis		16.917
Std. Error of Kurtosis		.001
Range		654.30
Minimum		1.00
Maximum		655.30
Sum		1096730413.00

Figure B3. Frequency Histogram for Incorrect Data.

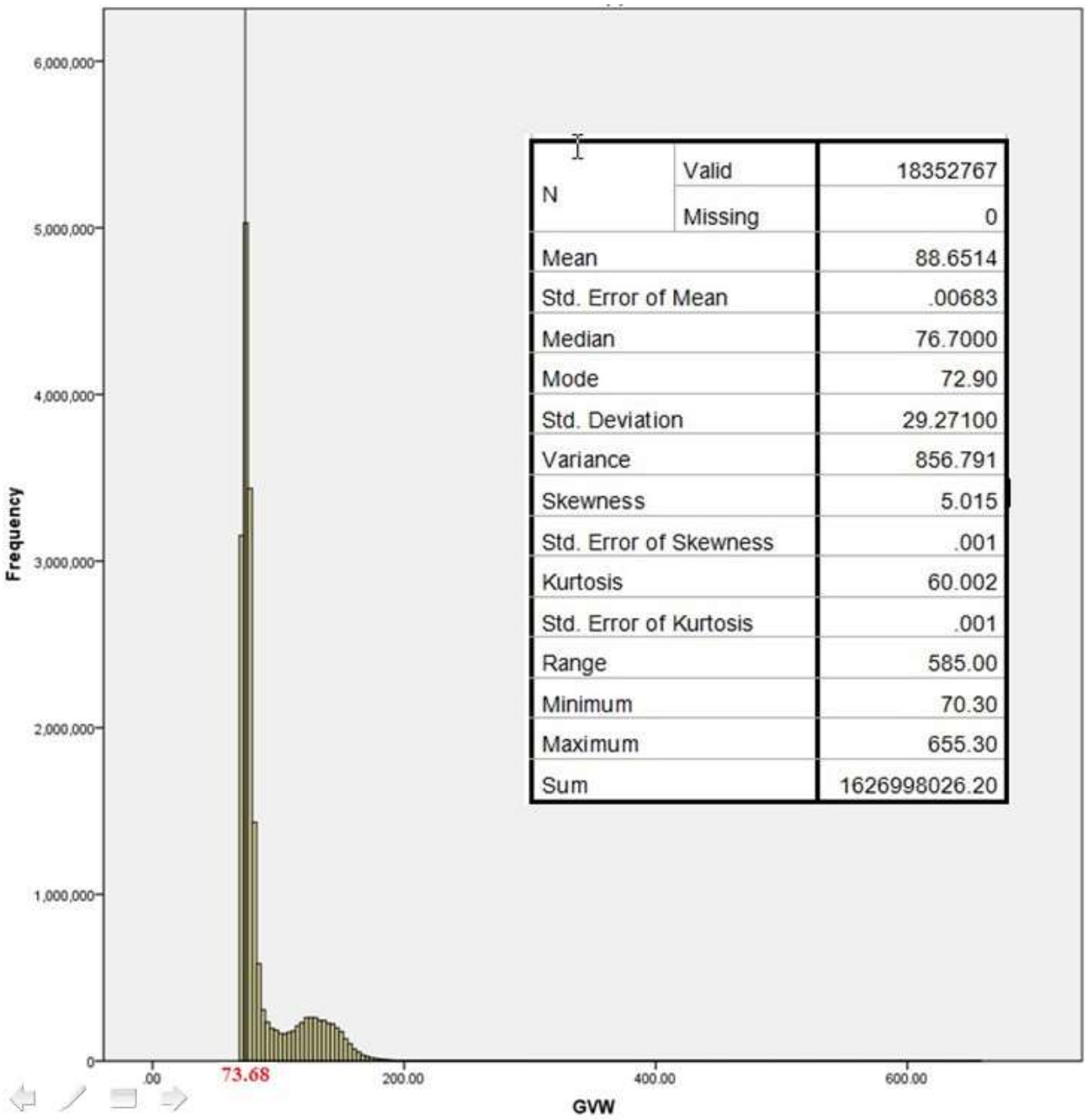

N	Valid	18352767
	Missing	0
Mean		88.6514
Std. Error of Mean		.00683
Median		76.7000
Mode		72.90
Std. Deviation		29.27100
Variance		856.791
Skewness		5.015
Std. Error of Skewness		.001
Kurtosis		60.002
Std. Error of Kurtosis		.001
Range		585.00
Minimum		70.30
Maximum		655.30
Sum		1626998026.20

Figure B4. Frequency Histogram for Top 20% of All Data, Prior to Scrubbing.

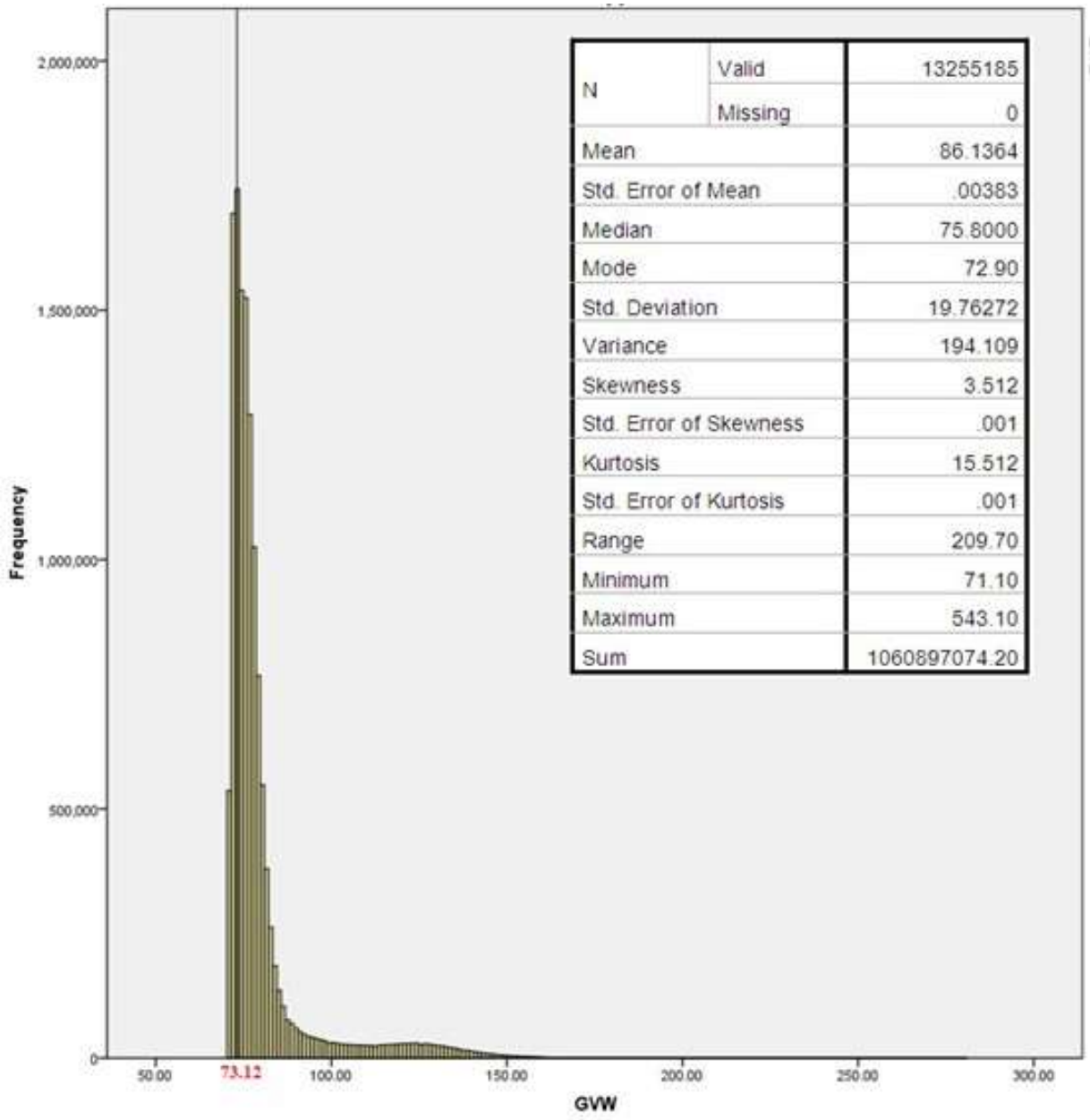

N	Valid	13255185
	Missing	0
Mean		86.1364
Std. Error of Mean		.00383
Median		75.8000
Mode		72.90
Std. Deviation		19.76272
Variance		194.109
Skewness		3.512
Std. Error of Skewness		.001
Kurtosis		15.512
Std. Error of Kurtosis		.001
Range		209.70
Minimum		71.10
Maximum		543.10
Sum		1060897074.20

Figure B5. Frequency Histogram for Top 20% of Correct Data.

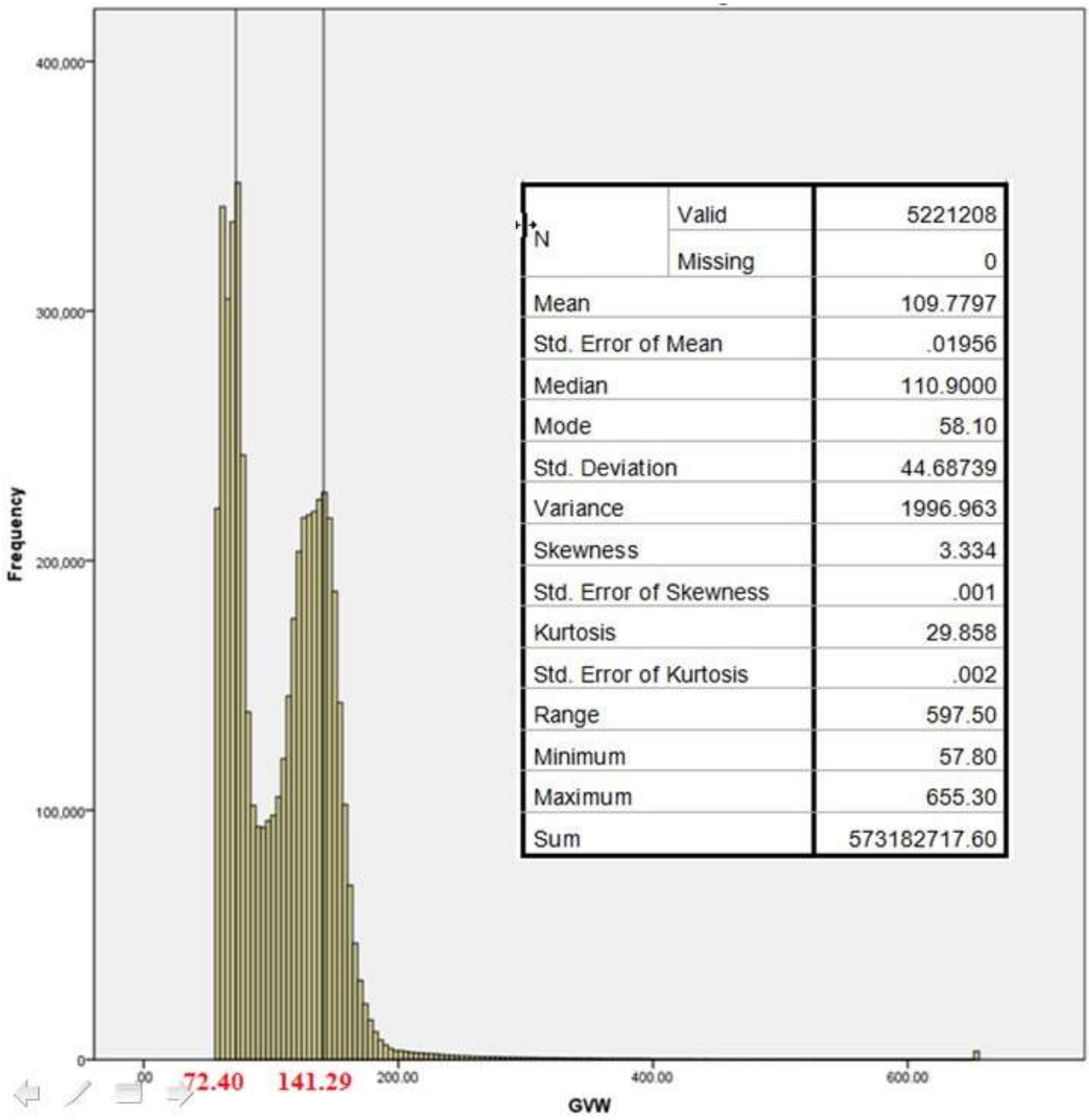

N	Valid	5221208
	Missing	0
Mean		109.7797
Std. Error of Mean		.01956
Median		110.9000
Mode		58.10
Std. Deviation		44.68739
Variance		1996.963
Skewness		3.334
Std. Error of Skewness		.001
Kurtosis		29.858
Std. Error of Kurtosis		.002
Range		597.50
Minimum		57.80
Maximum		655.30
Sum		573182717.60

Figure B6. Frequency Histogram for Top 20% of Incorrect Data.

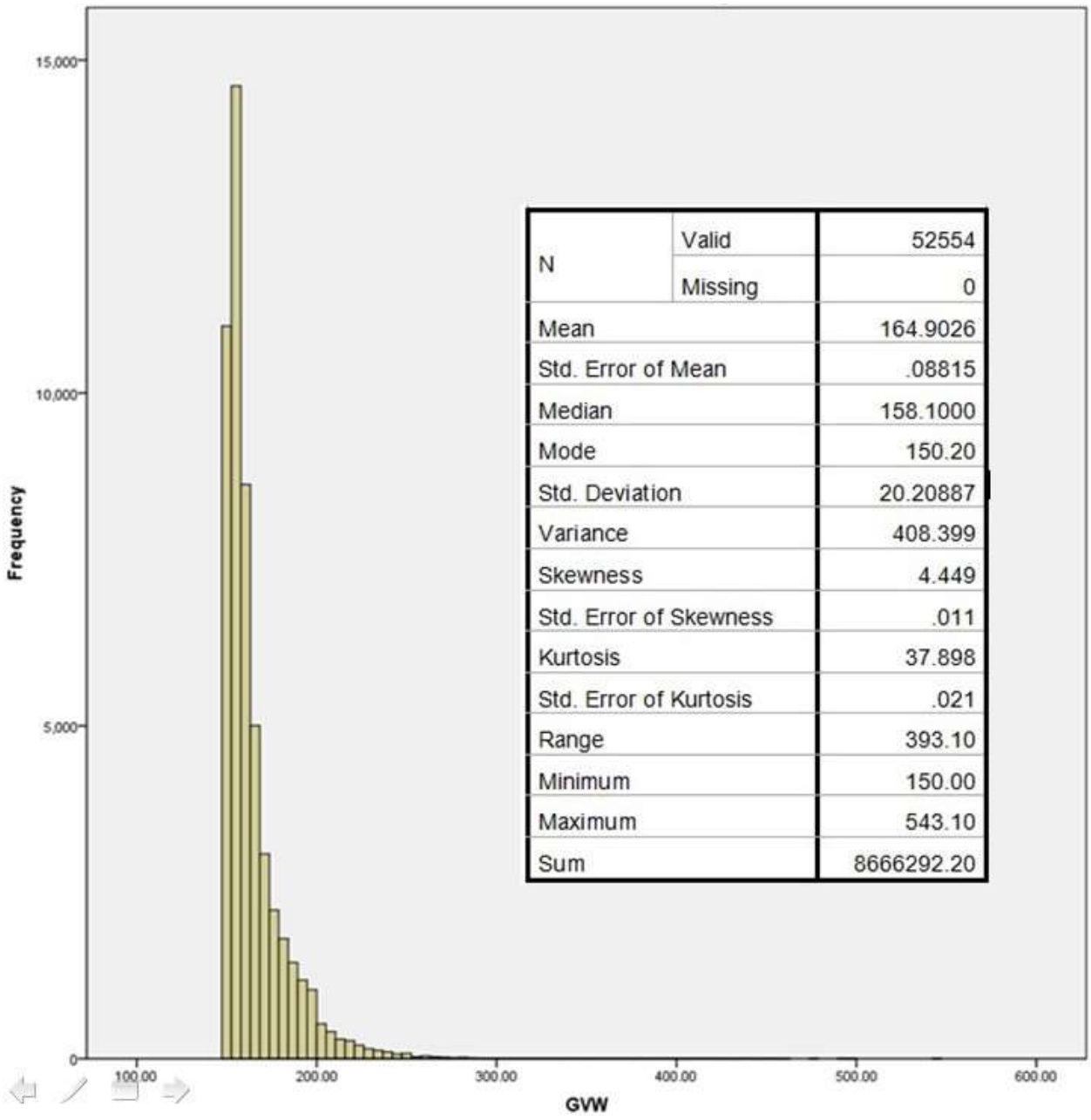

N	Valid	52554
	Missing	0
Mean		164.9026
Std. Error of Mean		.08815
Median		158.1000
Mode		150.20
Std. Deviation		20.20887
Variance		408.399
Skewness		4.449
Std. Error of Skewness		.011
Kurtosis		37.898
Std. Error of Kurtosis		.021
Range		393.10
Minimum		150.00
Maximum		543.10
Sum		8666292.20

Figure B7. Frequency Histogram for Correct Data over 150 kips.

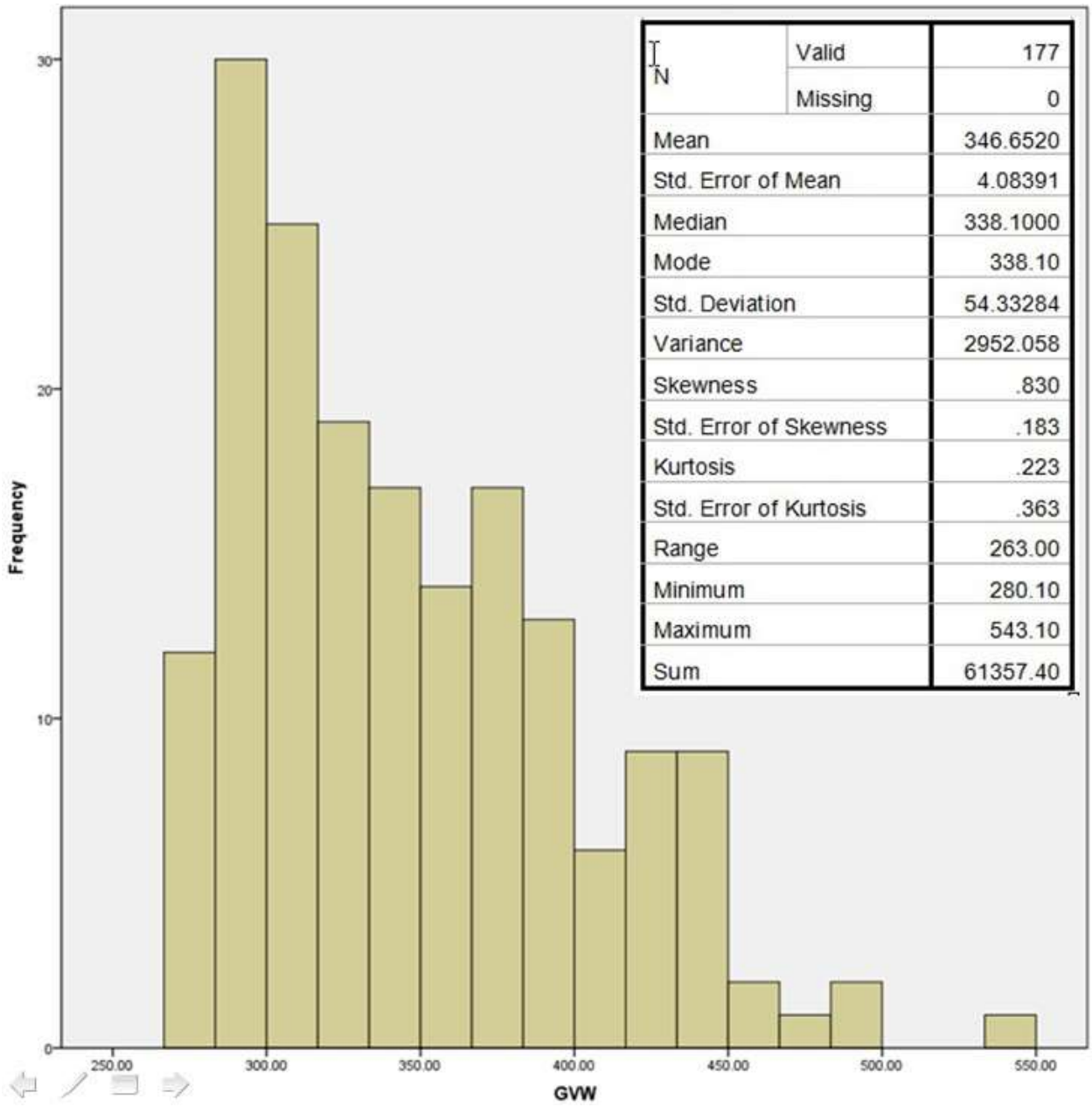

N	Valid	177
	Missing	0
Mean		346.6520
Std. Error of Mean		4.08391
Median		338.1000
Mode		338.10
Std. Deviation		54.33284
Variance		2952.058
Skewness		.830
Std. Error of Skewness		.183
Kurtosis		.223
Std. Error of Kurtosis		.363
Range		263.00
Minimum		280.10
Maximum		543.10
Sum		61357.40

Figure B8. Frequency Histogram for Correct Data over 280 kips.

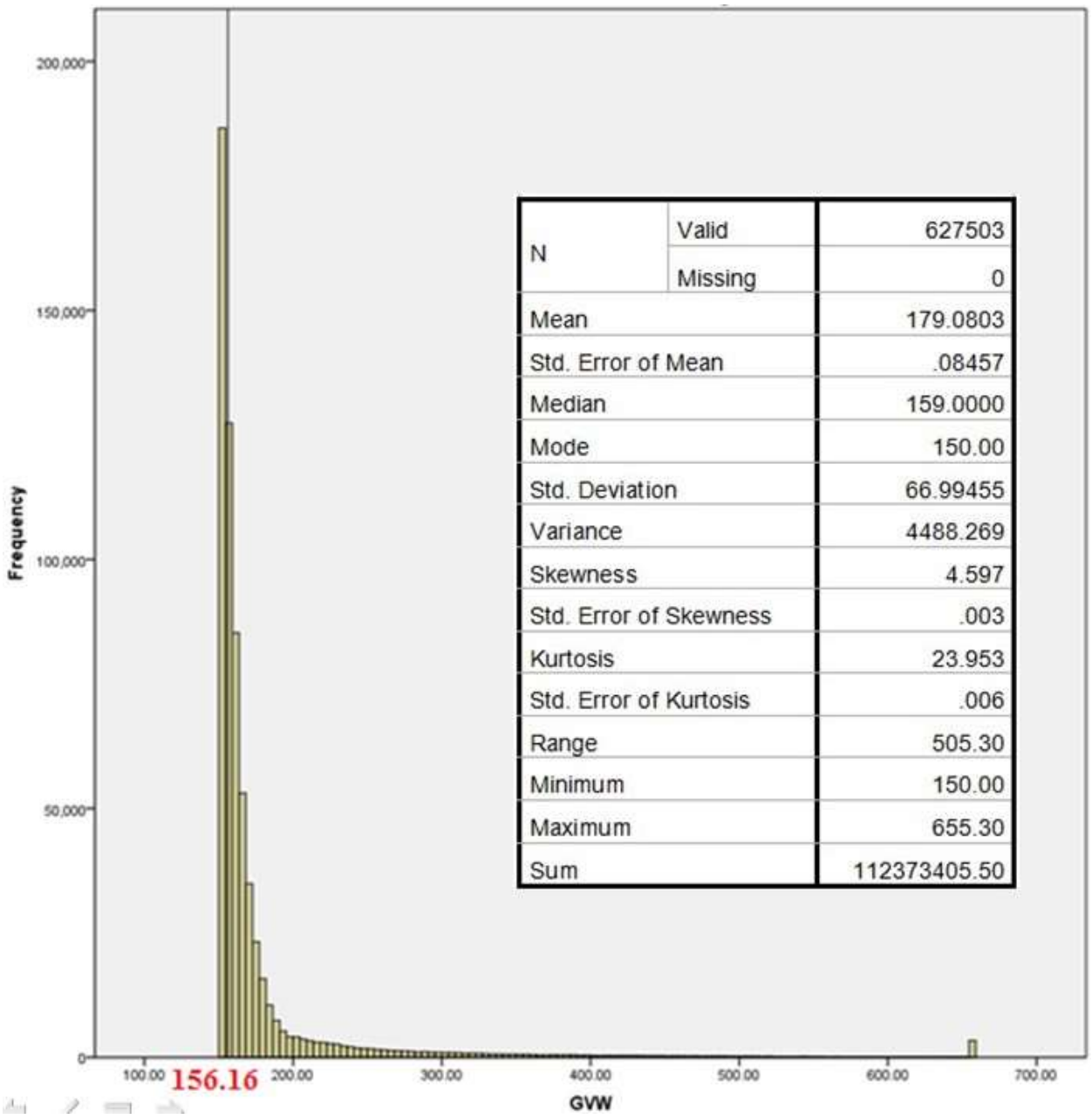

N	Valid	627503
	Missing	0
Mean		179.0803
Std. Error of Mean		.08457
Median		159.0000
Mode		150.00
Std. Deviation		66.99455
Variance		4488.269
Skewness		4.597
Std. Error of Skewness		.003
Kurtosis		23.953
Std. Error of Kurtosis		.006
Range		505.30
Minimum		150.00
Maximum		655.30
Sum		112373405.50

Figure B9. Frequency Histogram for Incorrect Data over 150 kips.

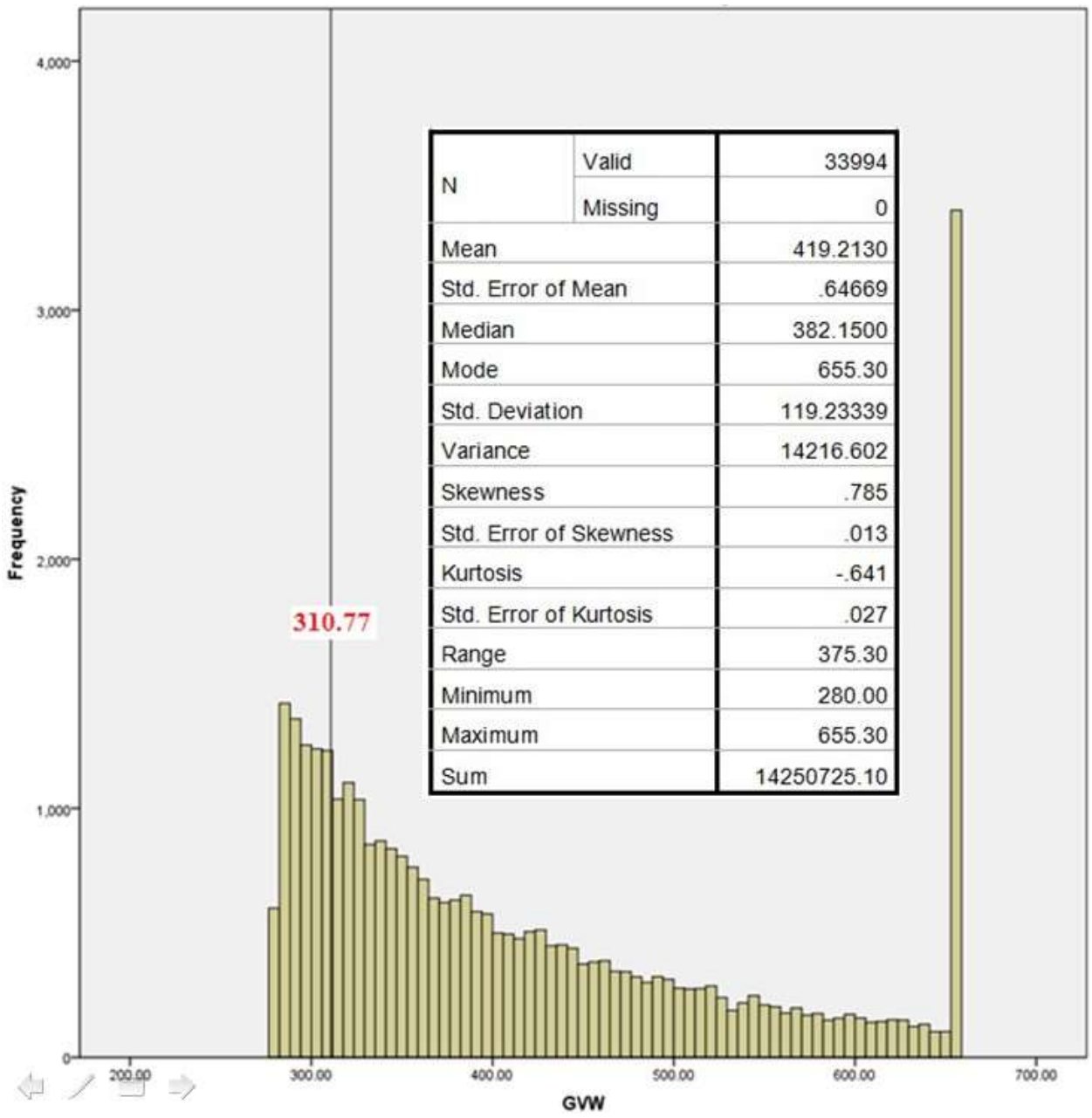

N	Valid	33994
	Missing	0
Mean		419.2130
Std. Error of Mean		.64669
Median		382.1500
Mode		655.30
Std. Deviation		119.23339
Variance		14216.602
Skewness		.785
Std. Error of Skewness		.013
Kurtosis		-.641
Std. Error of Kurtosis		.027
Range		375.30
Minimum		280.00
Maximum		655.30
Sum		14250725.10

Figure B10. Frequency Histogram for Incorrect Data over 280 kips.

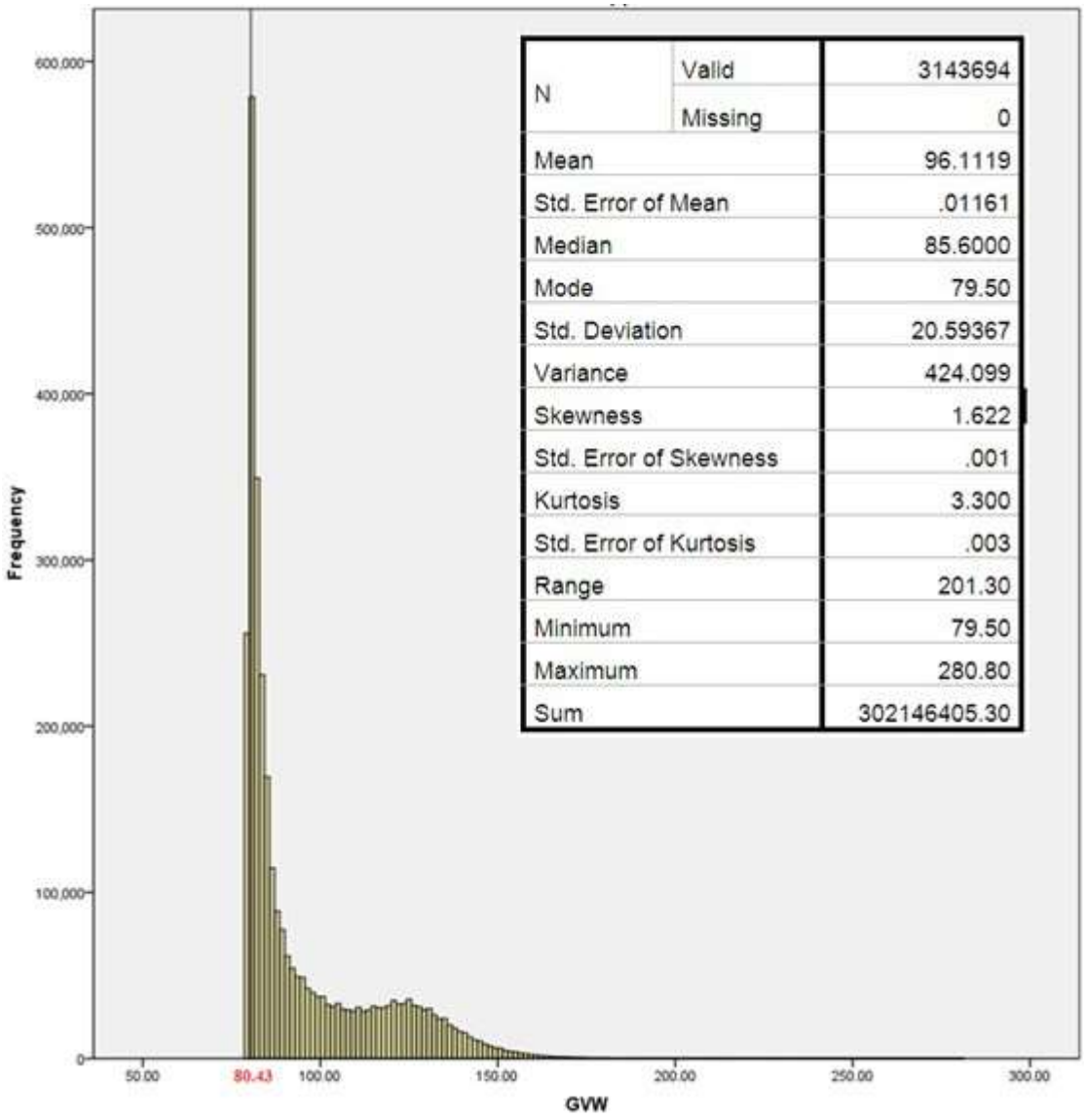

N	Valid	3143694
	Missing	0
Mean		96.1119
Std. Error of Mean		.01161
Median		85.6000
Mode		79.50
Std. Deviation		20.59367
Variance		424.099
Skewness		1.622
Std. Error of Skewness		.001
Kurtosis		3.300
Std. Error of Kurtosis		.003
Range		201.30
Minimum		79.50
Maximum		280.80
Sum		302146405.30

Figure B11. Frequency Histogram for Top 5% of Correct Data.

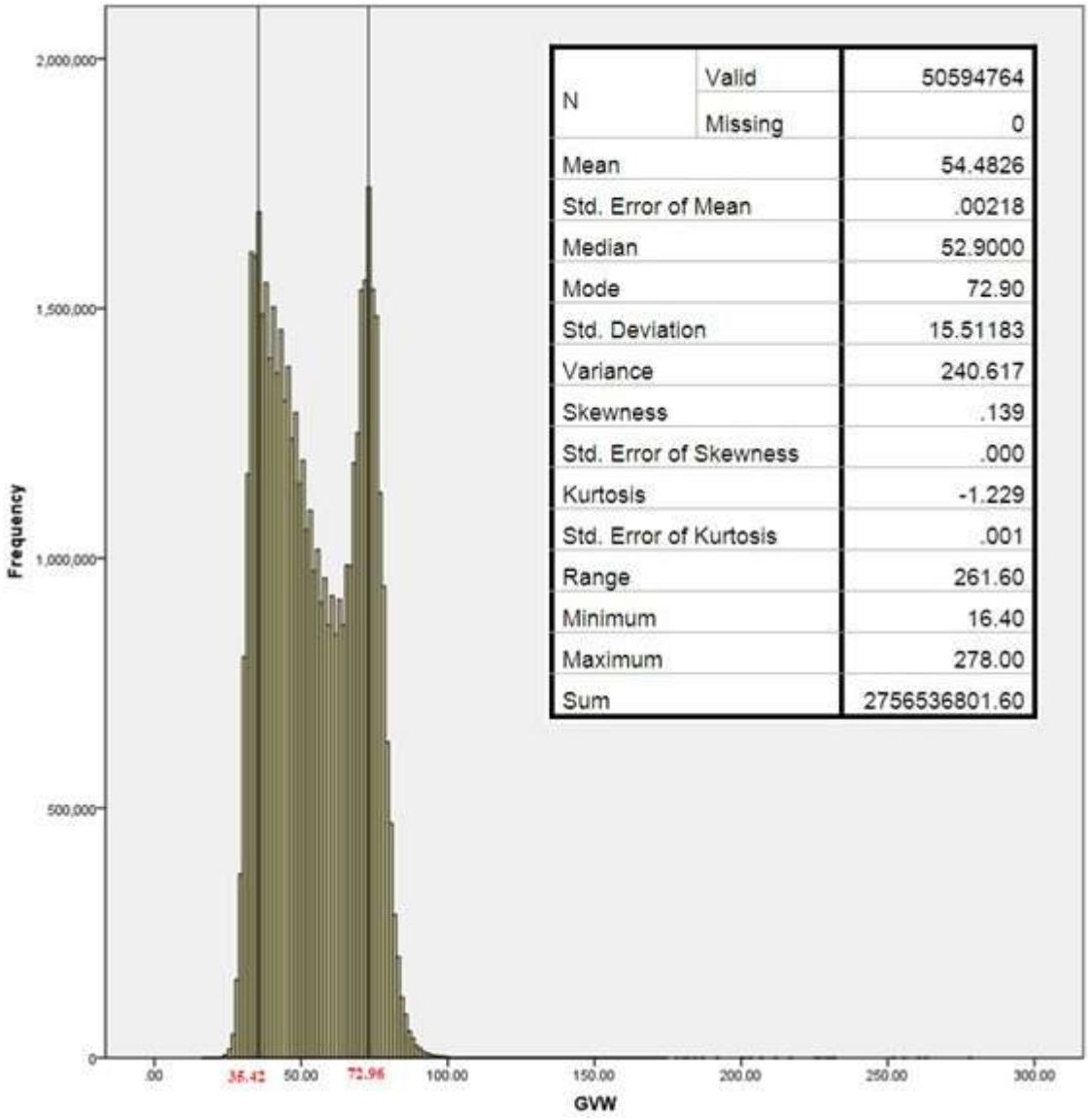

N	Valid	50594764
	Missing	0
Mean		54.4826
Std. Error of Mean		.00218
Median		52.9000
Mode		72.90
Std. Deviation		15.51183
Variance		240.617
Skewness		.139
Std. Error of Skewness		.000
Kurtosis		-1.229
Std. Error of Kurtosis		.001
Range		261.60
Minimum		16.40
Maximum		278.00
Sum		2756536801.60

Figure B12. Frequency Histogram for 5-axle Trucks (Correct Data).

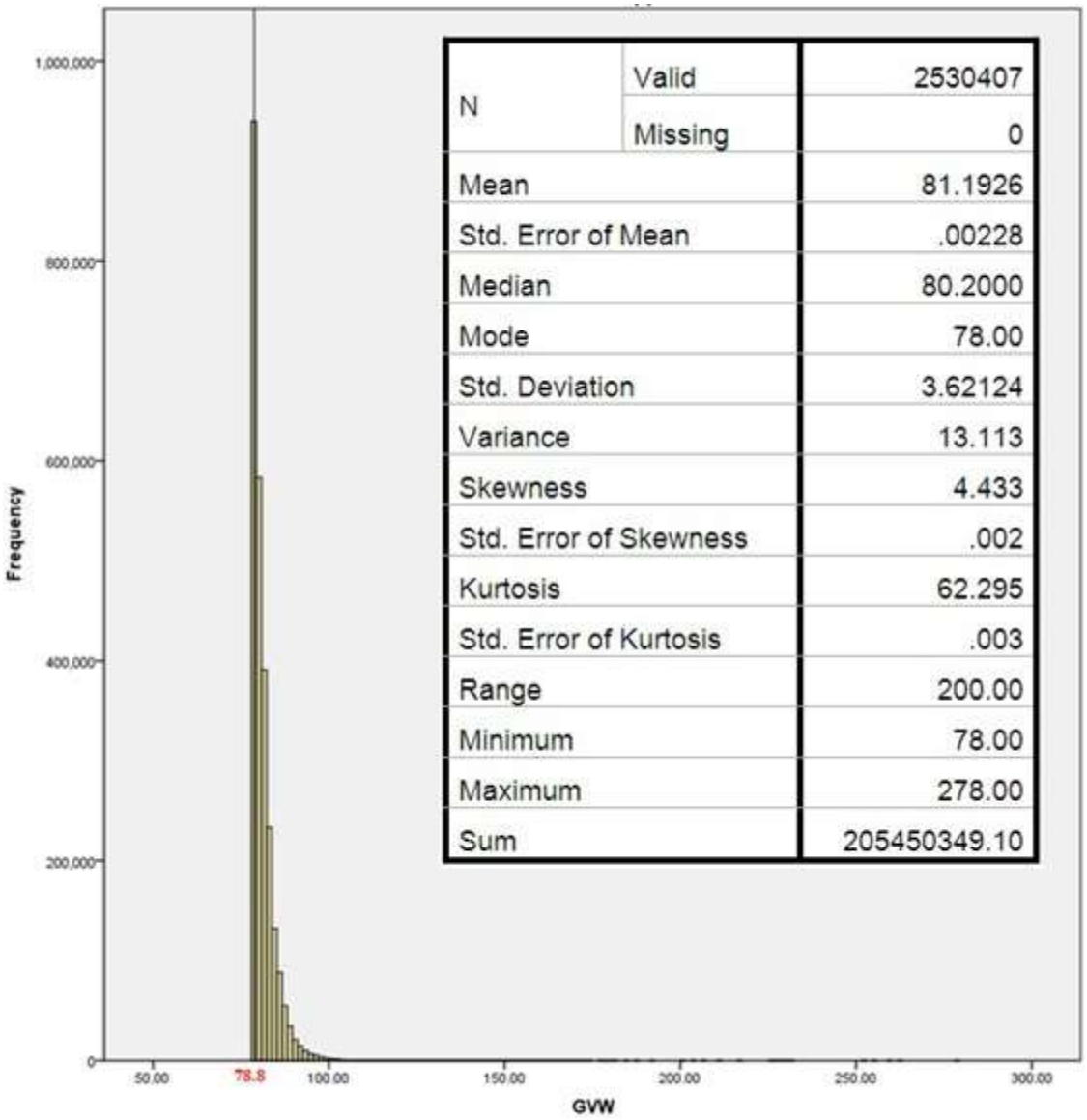

N	Valid	2530407
	Missing	0
Mean		81.1926
Std. Error of Mean		.00228
Median		80.2000
Mode		78.00
Std. Deviation		3.62124
Variance		13.113
Skewness		4.433
Std. Error of Skewness		.002
Kurtosis		62.295
Std. Error of Kurtosis		.003
Range		200.00
Minimum		78.00
Maximum		278.00
Sum		205450349.10

Figure B13. Frequency Histogram for Top 5% of 5-axle Trucks (Correct Data).

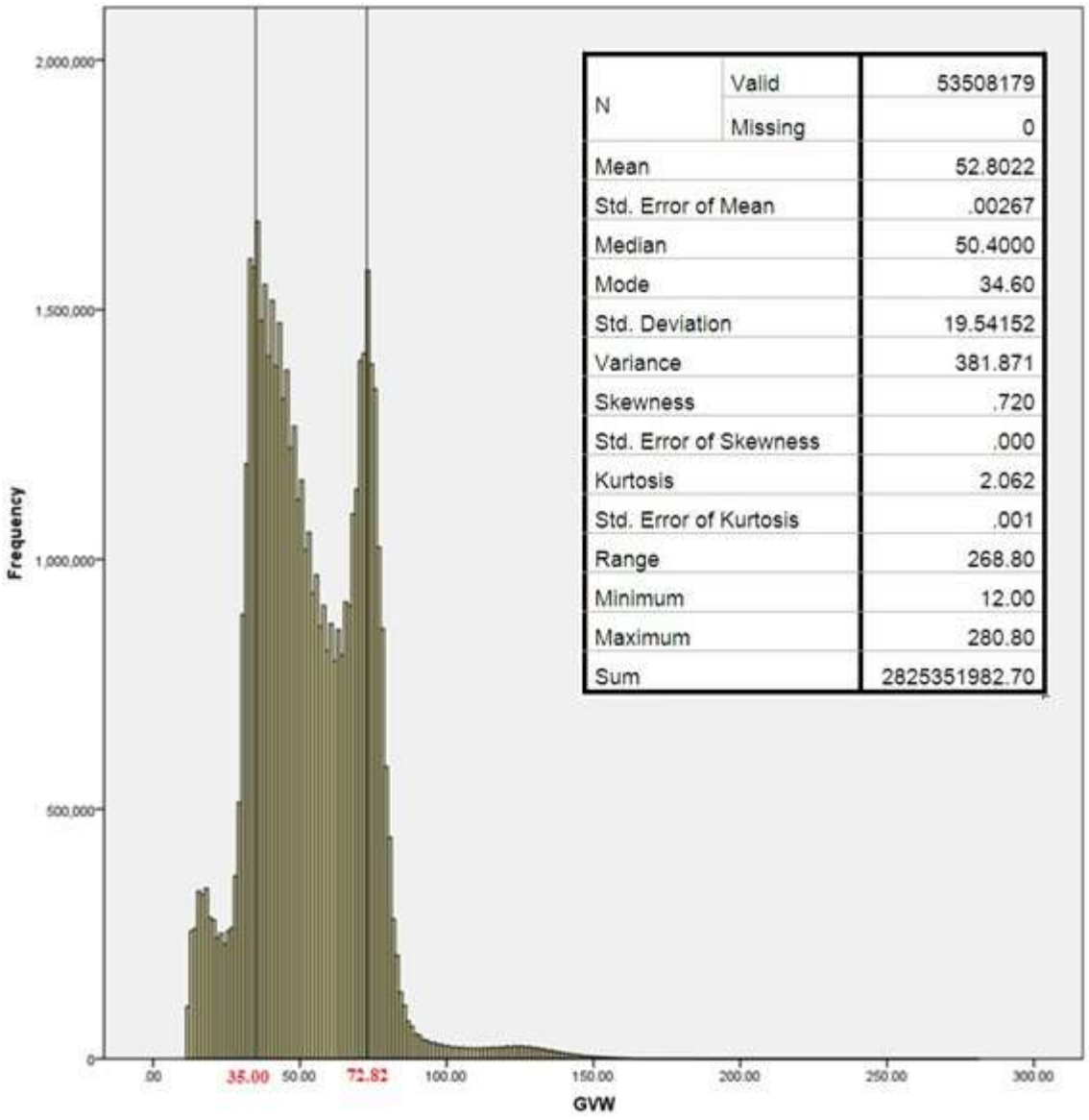

N	Valid	53508179
	Missing	0
Mean		52.8022
Std. Error of Mean		.00267
Median		50.4000
Mode		34.60
Std. Deviation		19.54152
Variance		381.871
Skewness		.720
Std. Error of Skewness		.000
Kurtosis		2.062
Std. Error of Kurtosis		.001
Range		268.80
Minimum		12.00
Maximum		280.80
Sum		2825351982.70

Figure B14. Frequency Histogram for Interstate WIM Stations (Correct Data).

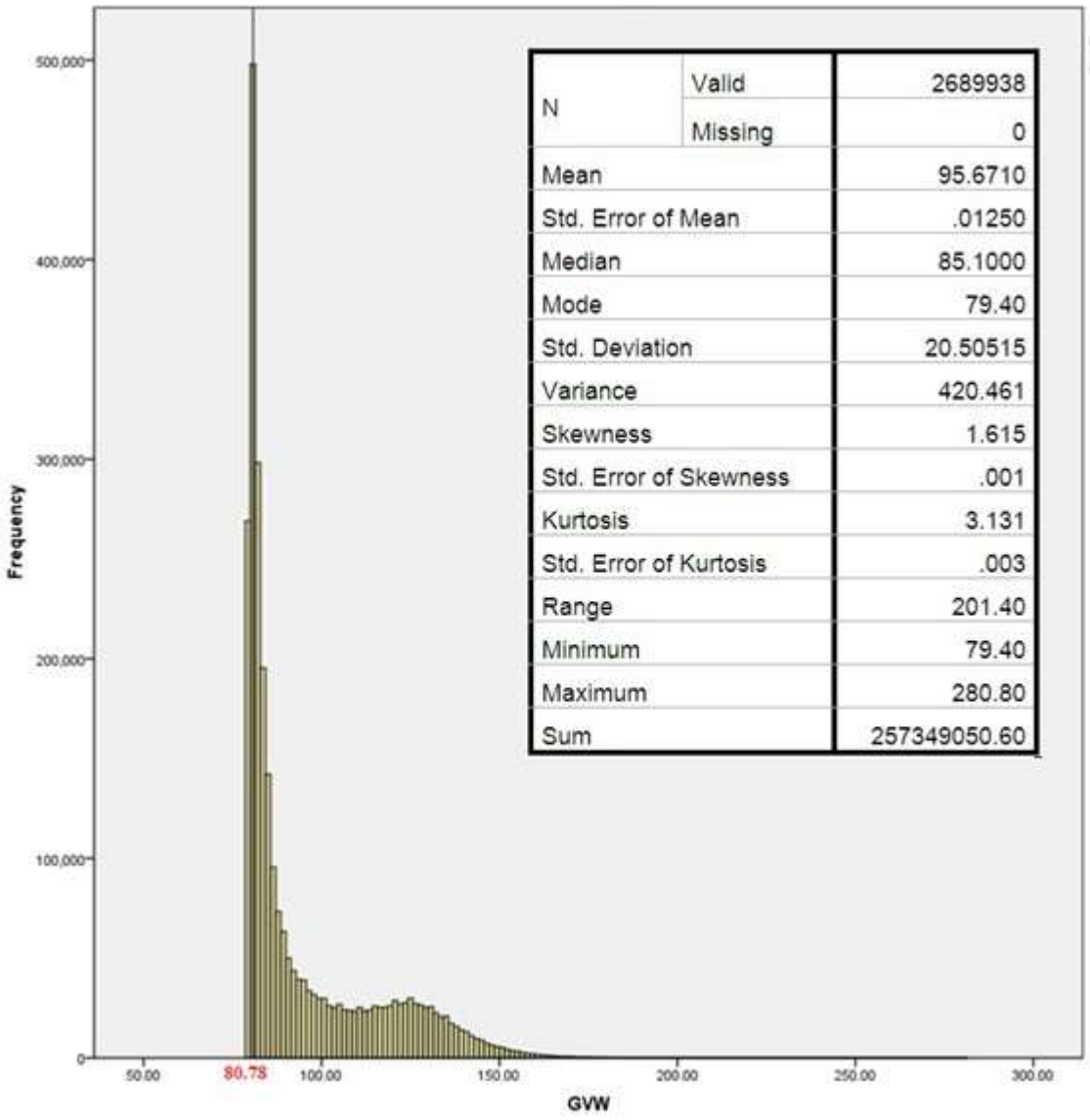

N	Valid	2689938
	Missing	0
Mean		95.6710
Std. Error of Mean		.01250
Median		85.1000
Mode		79.40
Std. Deviation		20.50515
Variance		420.461
Skewness		1.615
Std. Error of Skewness		.001
Kurtosis		3.131
Std. Error of Kurtosis		.003
Range		201.40
Minimum		79.40
Maximum		280.80
Sum		257349050.60

Figure B15. Frequency Histogram for Top 5% of Interstate WIM Stations (Correct Data).

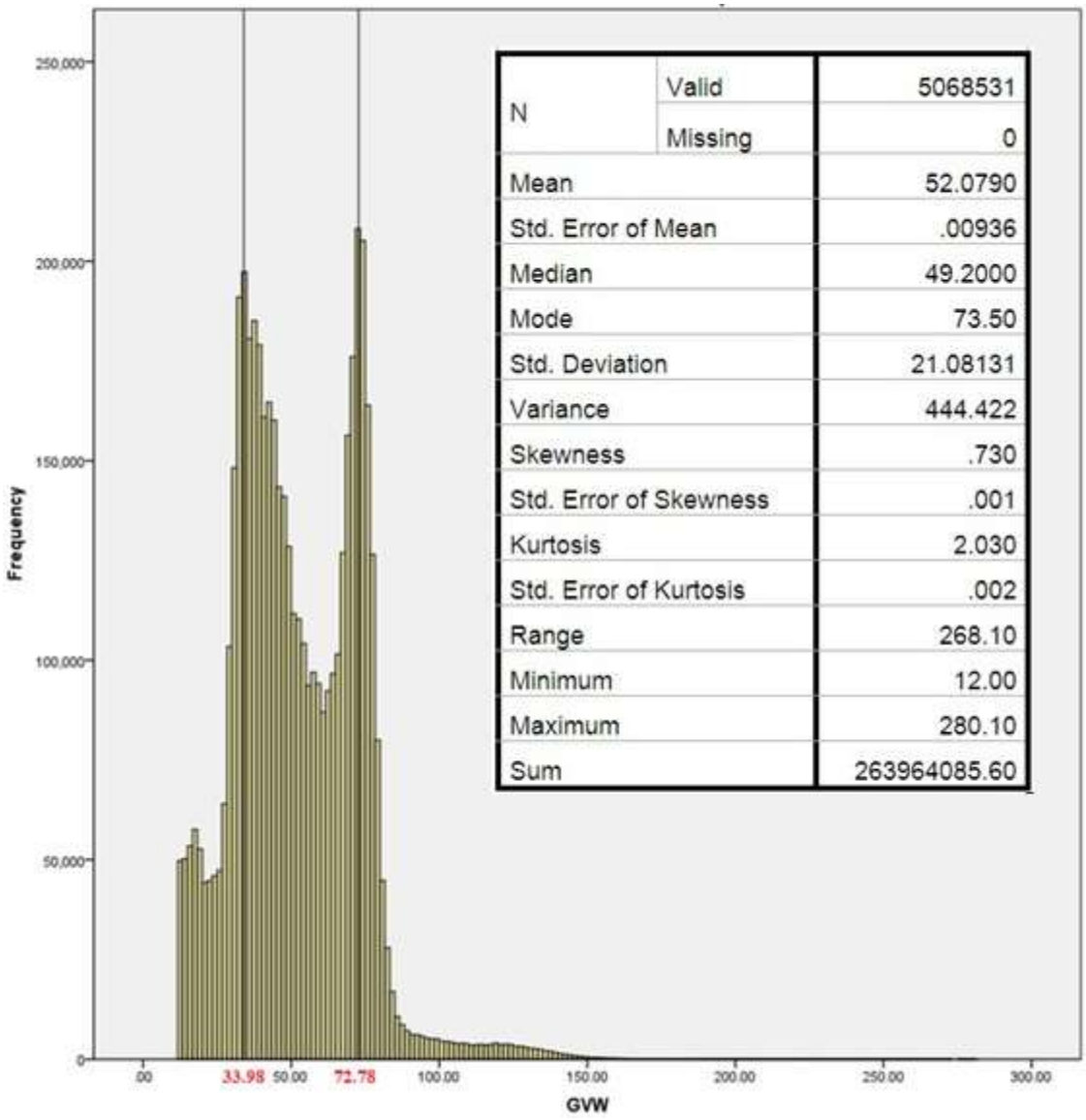

N	Valid	5068531
	Missing	0
Mean		52.0790
Std. Error of Mean		.00936
Median		49.2000
Mode		73.50
Std. Deviation		21.08131
Variance		444.422
Skewness		.730
Std. Error of Skewness		.001
Kurtosis		2.030
Std. Error of Kurtosis		.002
Range		268.10
Minimum		12.00
Maximum		280.10
Sum		263964085.60

Figure B16. Frequency Histogram for Other Principal Arterial WIM Stations (Correct Data).

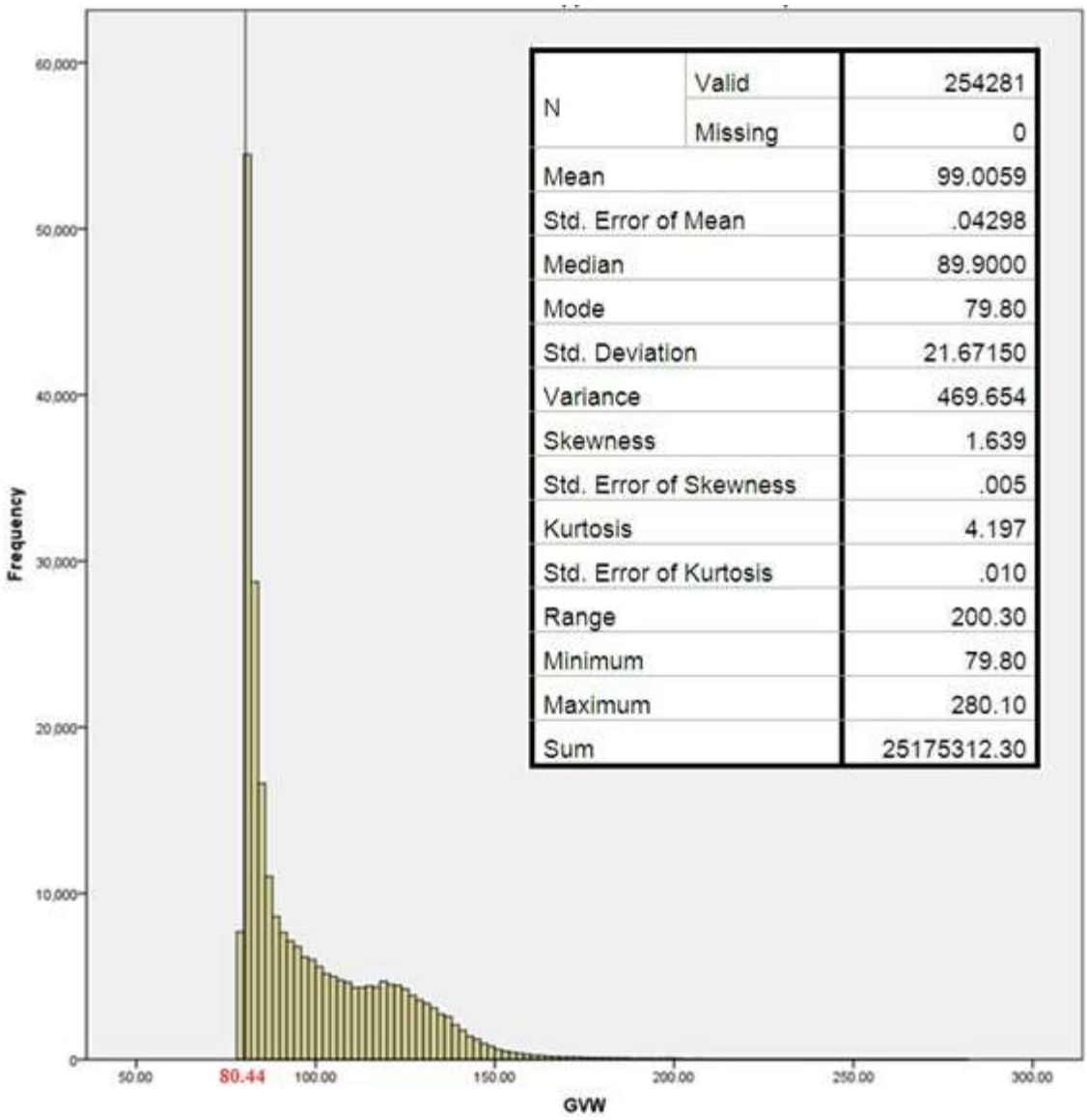

N	Valid	254281
	Missing	0
Mean		99.0059
Std. Error of Mean		.04298
Median		89.9000
Mode		79.80
Std. Deviation		21.67150
Variance		469.654
Skewness		1.639
Std. Error of Skewness		.005
Kurtosis		4.197
Std. Error of Kurtosis		.010
Range		200.30
Minimum		79.80
Maximum		280.10
Sum		25175312.30

Figure B17. Frequency Histogram for Top 5% of Other Principal Arterial WIM Stations (Correct Data).

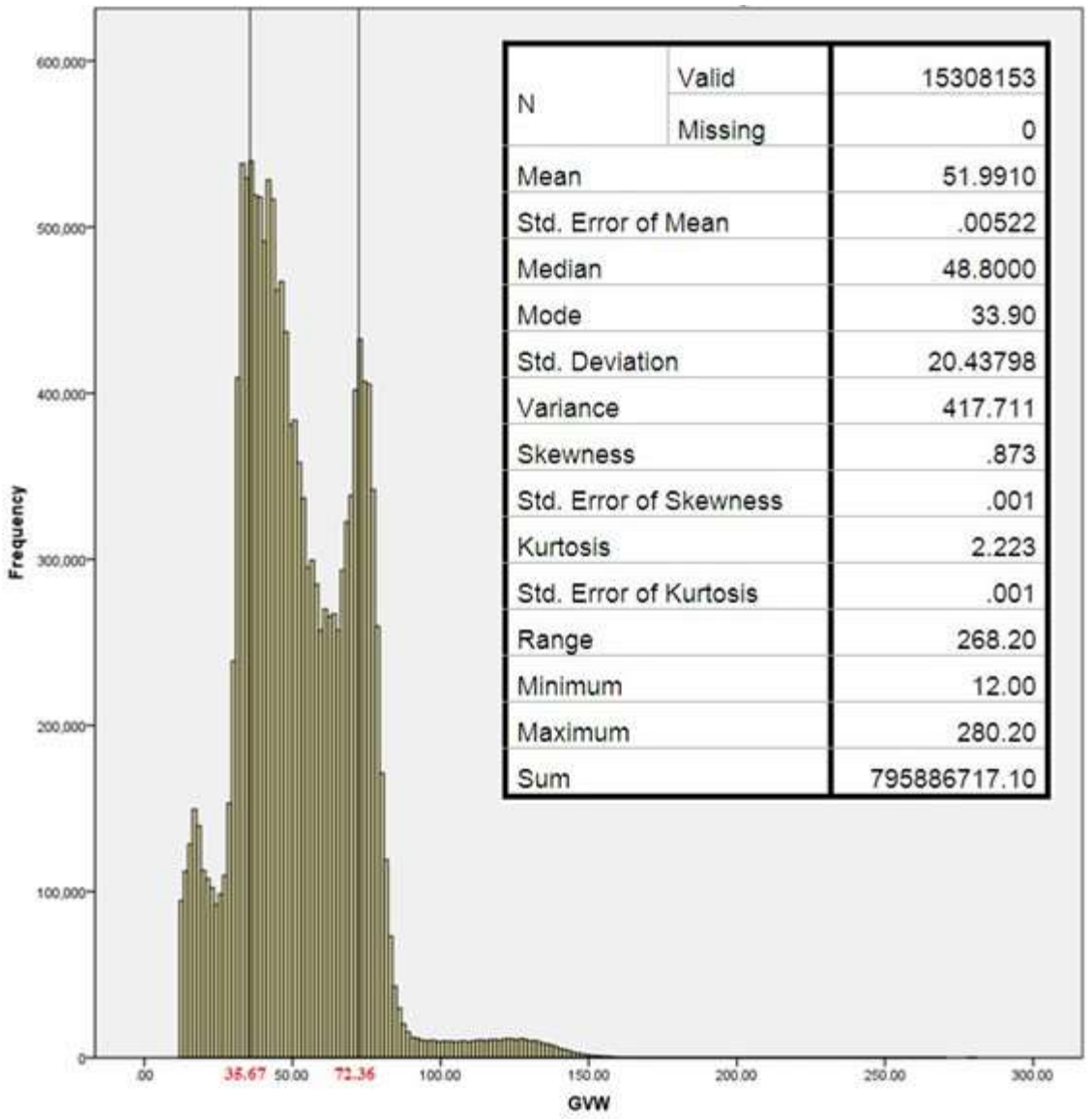

N	Valid	15308153
	Missing	0
Mean		51.9910
Std. Error of Mean		.00522
Median		48.8000
Mode		33.90
Std. Deviation		20.43798
Variance		417.711
Skewness		.873
Std. Error of Skewness		.001
Kurtosis		2.223
Std. Error of Kurtosis		.001
Range		268.20
Minimum		12.00
Maximum		280.20
Sum		795886717.10

Figure B18. Frequency Histogram for Metro Region WIM Stations (Correct Data).

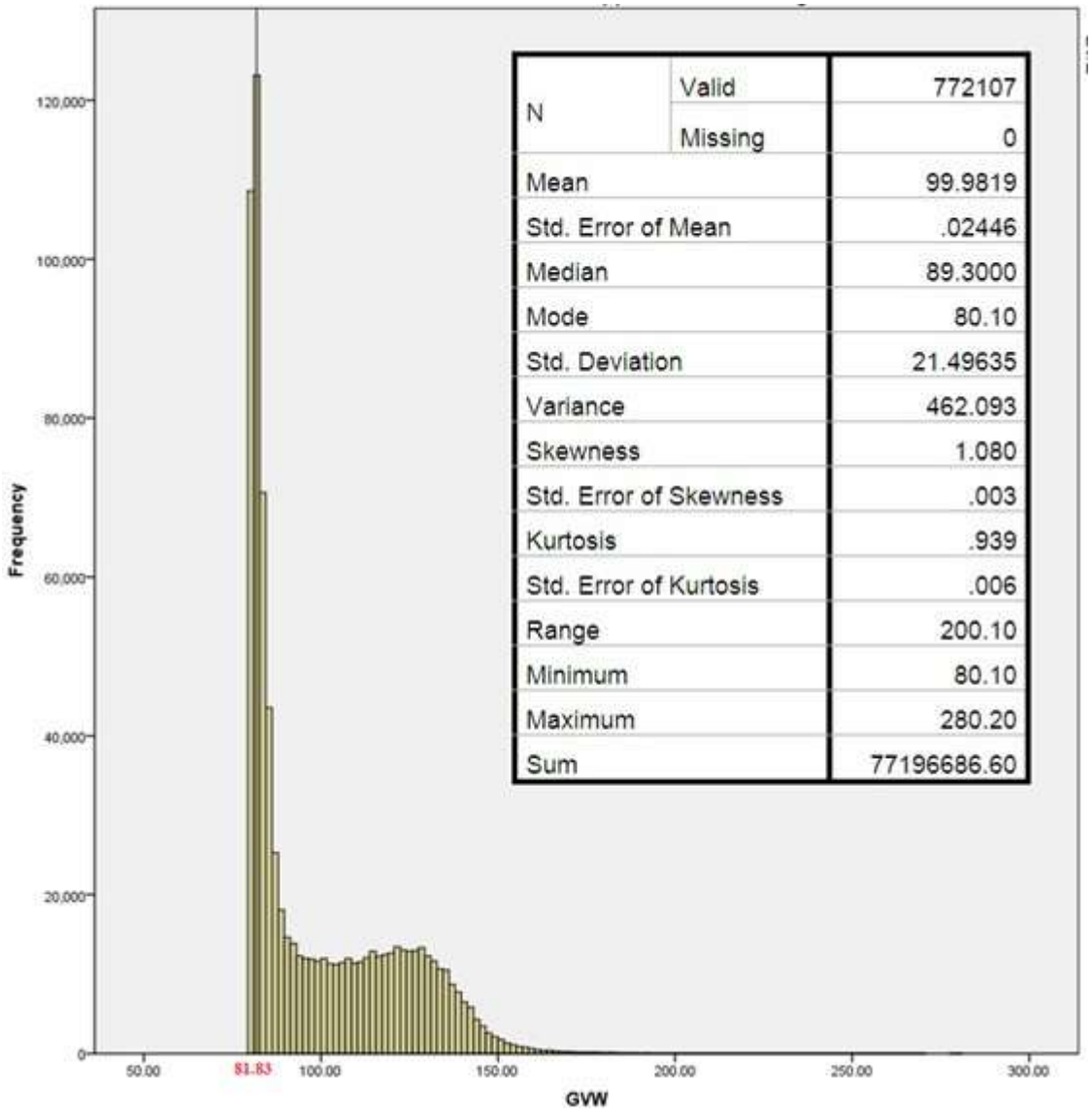

N	Valid	772107
	Missing	0
Mean		99.9819
Std. Error of Mean		.02446
Median		89.3000
Mode		80.10
Std. Deviation		21.49635
Variance		462.093
Skewness		1.080
Std. Error of Skewness		.003
Kurtosis		.939
Std. Error of Kurtosis		.006
Range		200.10
Minimum		80.10
Maximum		280.20
Sum		77196686.60

Figure B19. Frequency Histogram for Top 5% of Metro Region WIM Stations (Correct Data).

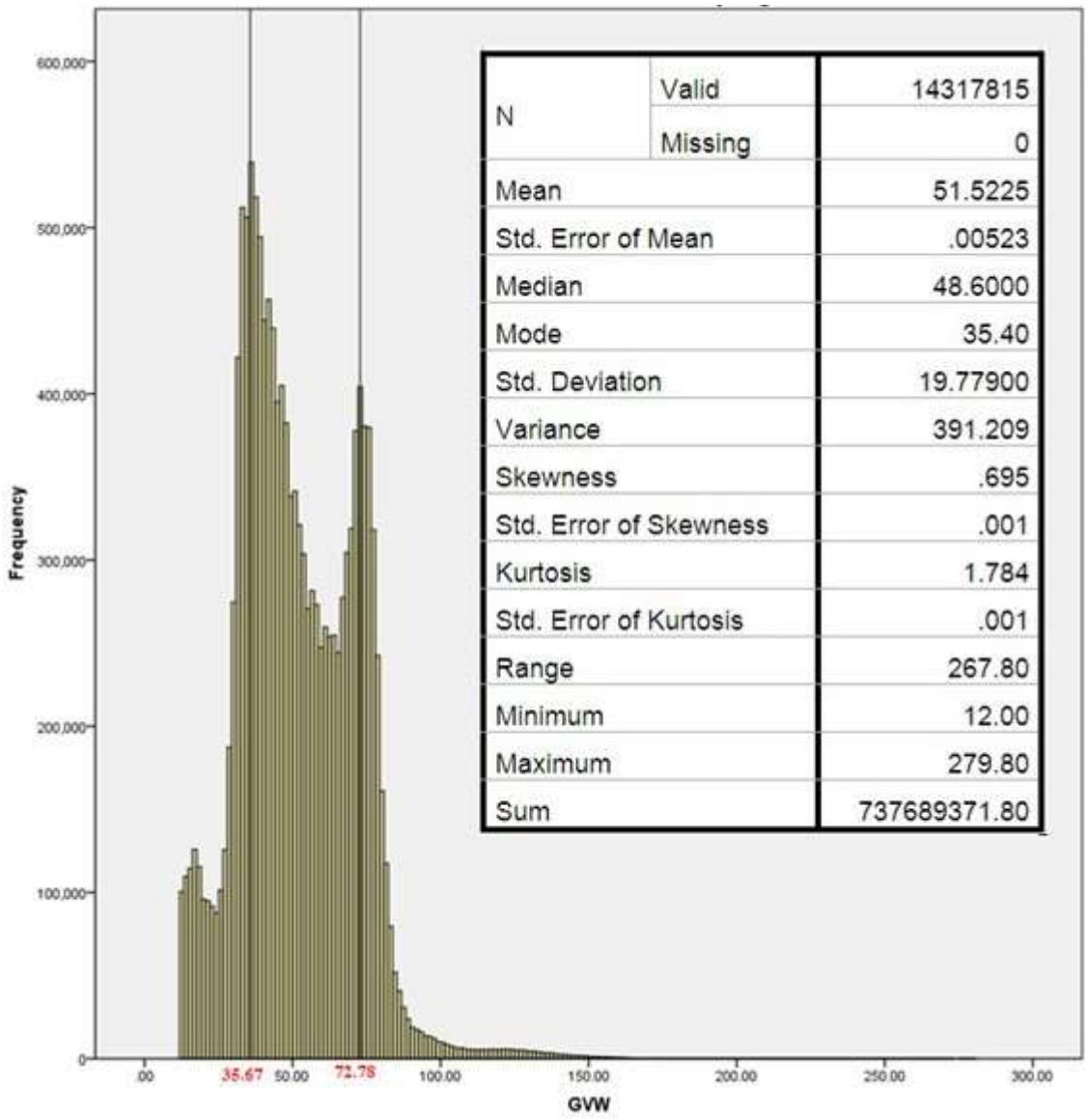

N	Valid	14317815
	Missing	0
Mean		51.5225
Std. Error of Mean		.00523
Median		48.6000
Mode		35.40
Std. Deviation		19.77900
Variance		391.209
Skewness		.695
Std. Error of Skewness		.001
Kurtosis		1.784
Std. Error of Kurtosis		.001
Range		267.80
Minimum		12.00
Maximum		279.80
Sum		737689371.80

Figure B20. Frequency Histogram for University Region WIM Stations (Correct Data).

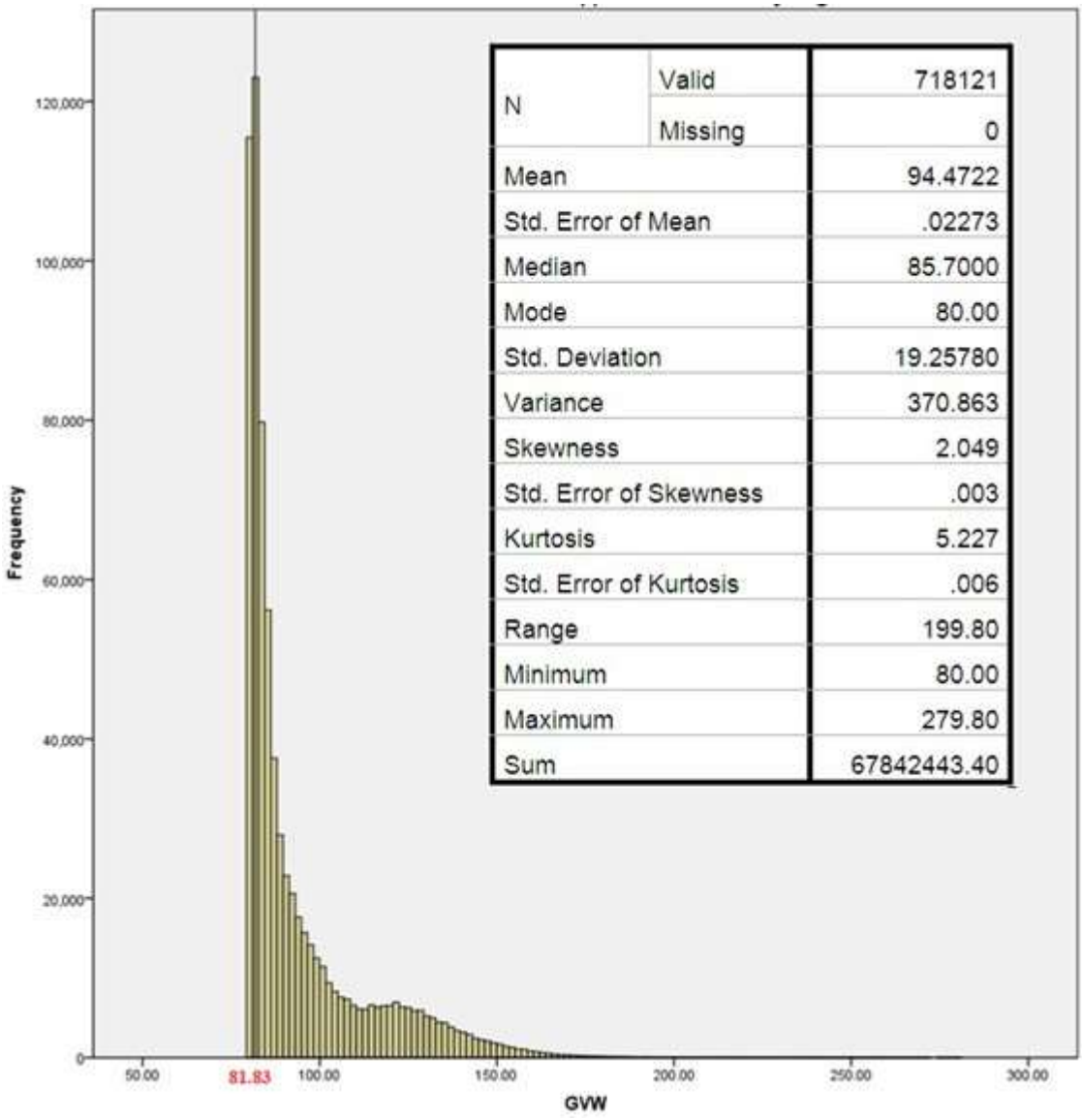

N	Valid	718121
	Missing	0
Mean		94.4722
Std. Error of Mean		.02273
Median		85.7000
Mode		80.00
Std. Deviation		19.25780
Variance		370.863
Skewness		2.049
Std. Error of Skewness		.003
Kurtosis		5.227
Std. Error of Kurtosis		.006
Range		199.80
Minimum		80.00
Maximum		279.80
Sum		67842443.40

Figure B21. Frequency Histogram for Top 5% of University Region WIM Stations (Correct Data).

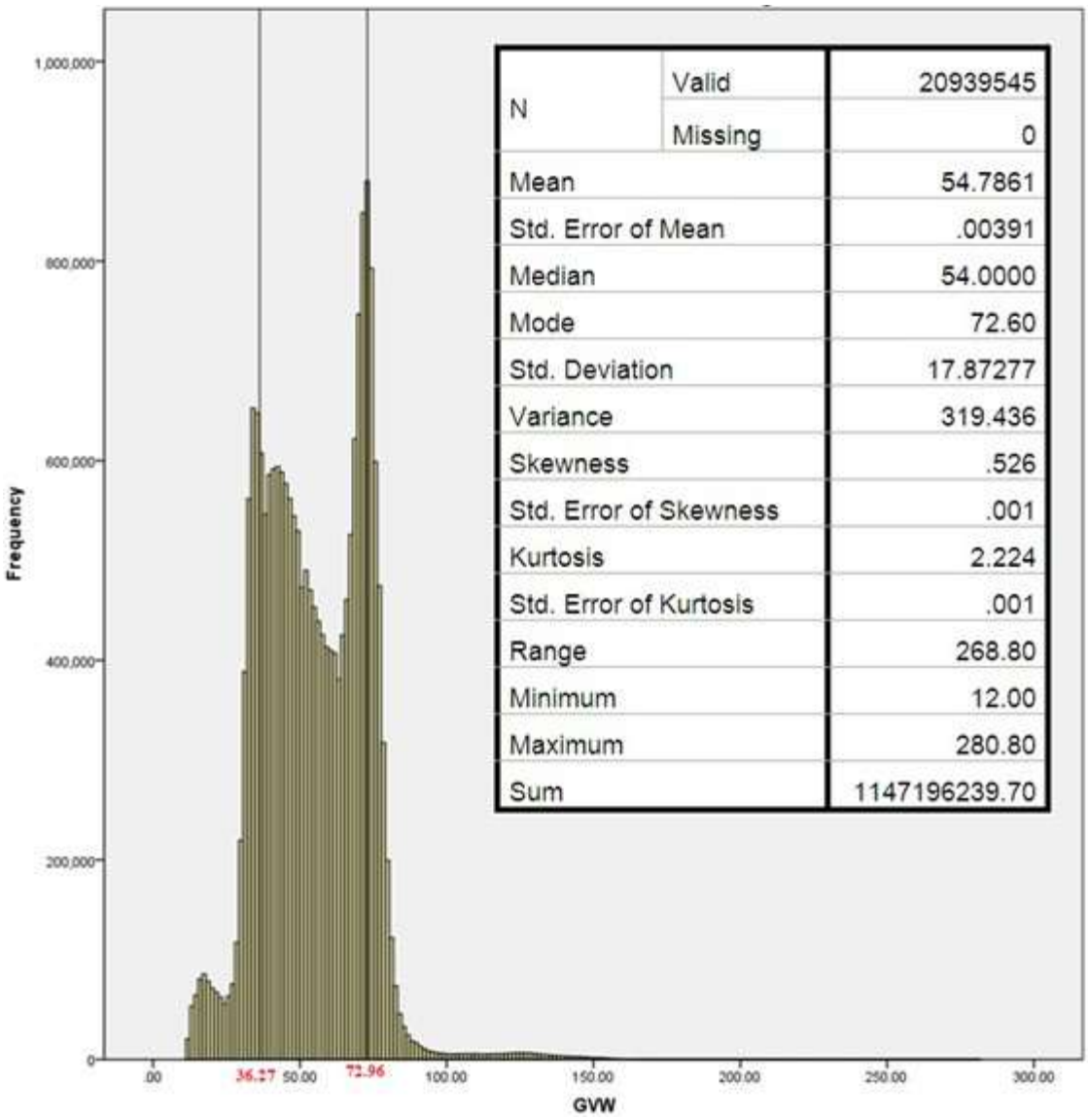

N	Valid	20939545
	Missing	0
Mean		54.7861
Std. Error of Mean		.00391
Median		54.0000
Mode		72.60
Std. Deviation		17.87277
Variance		319.436
Skewness		.526
Std. Error of Skewness		.001
Kurtosis		2.224
Std. Error of Kurtosis		.001
Range		268.80
Minimum		12.00
Maximum		280.80
Sum		1147196239.70

Figure B22. Frequency Histogram for Southwest Region WIM Stations (Correct Data).

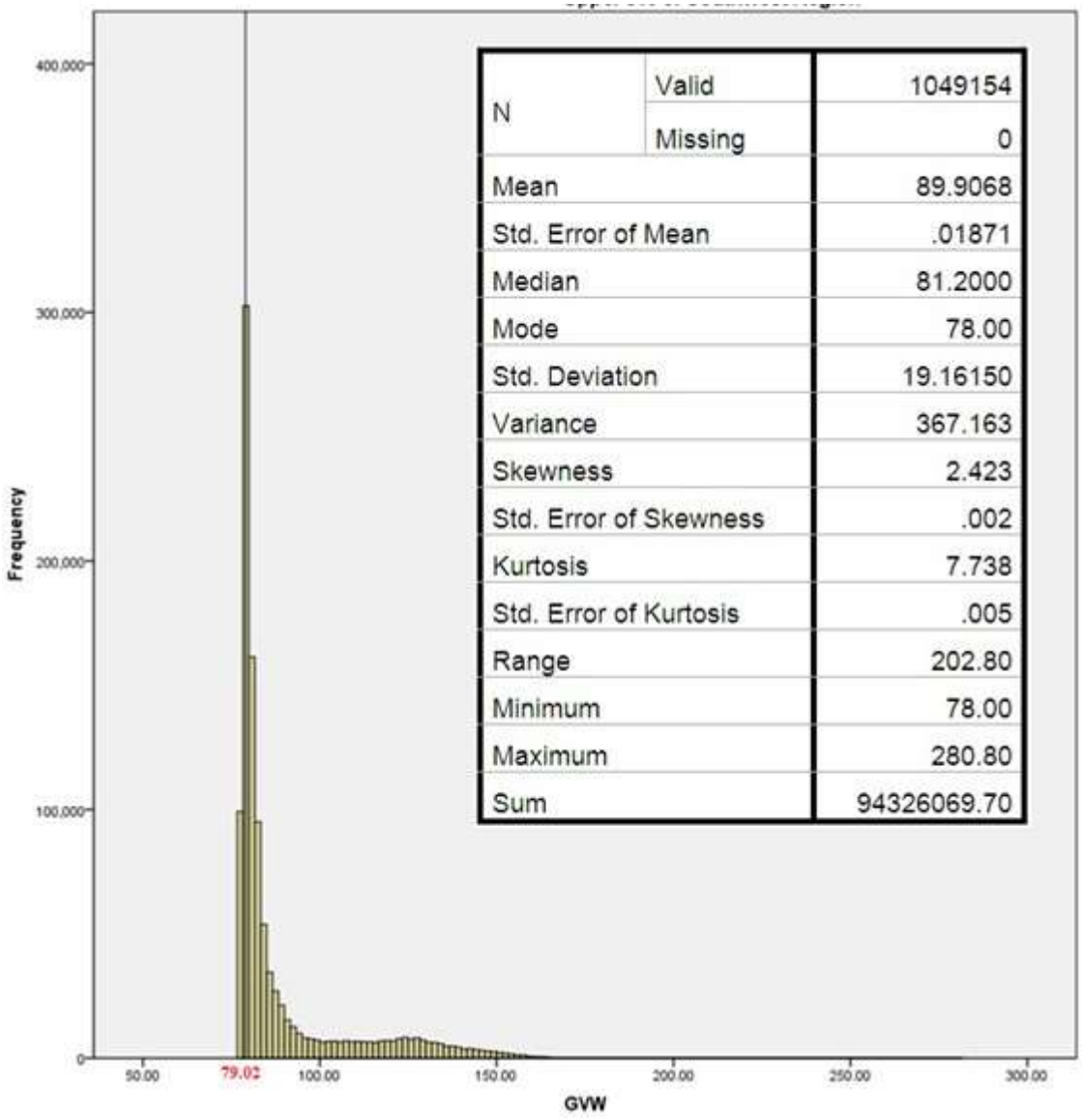

N	Valid	1049154
	Missing	0
Mean		89.9068
Std. Error of Mean		.01871
Median		81.2000
Mode		78.00
Std. Deviation		19.16150
Variance		367.163
Skewness		2.423
Std. Error of Skewness		.002
Kurtosis		7.738
Std. Error of Kurtosis		.005
Range		202.80
Minimum		78.00
Maximum		280.80
Sum		94326069.70

Figure B23. Frequency Histogram for Top 5% of Southwest Region WIM Stations (Correct Data).

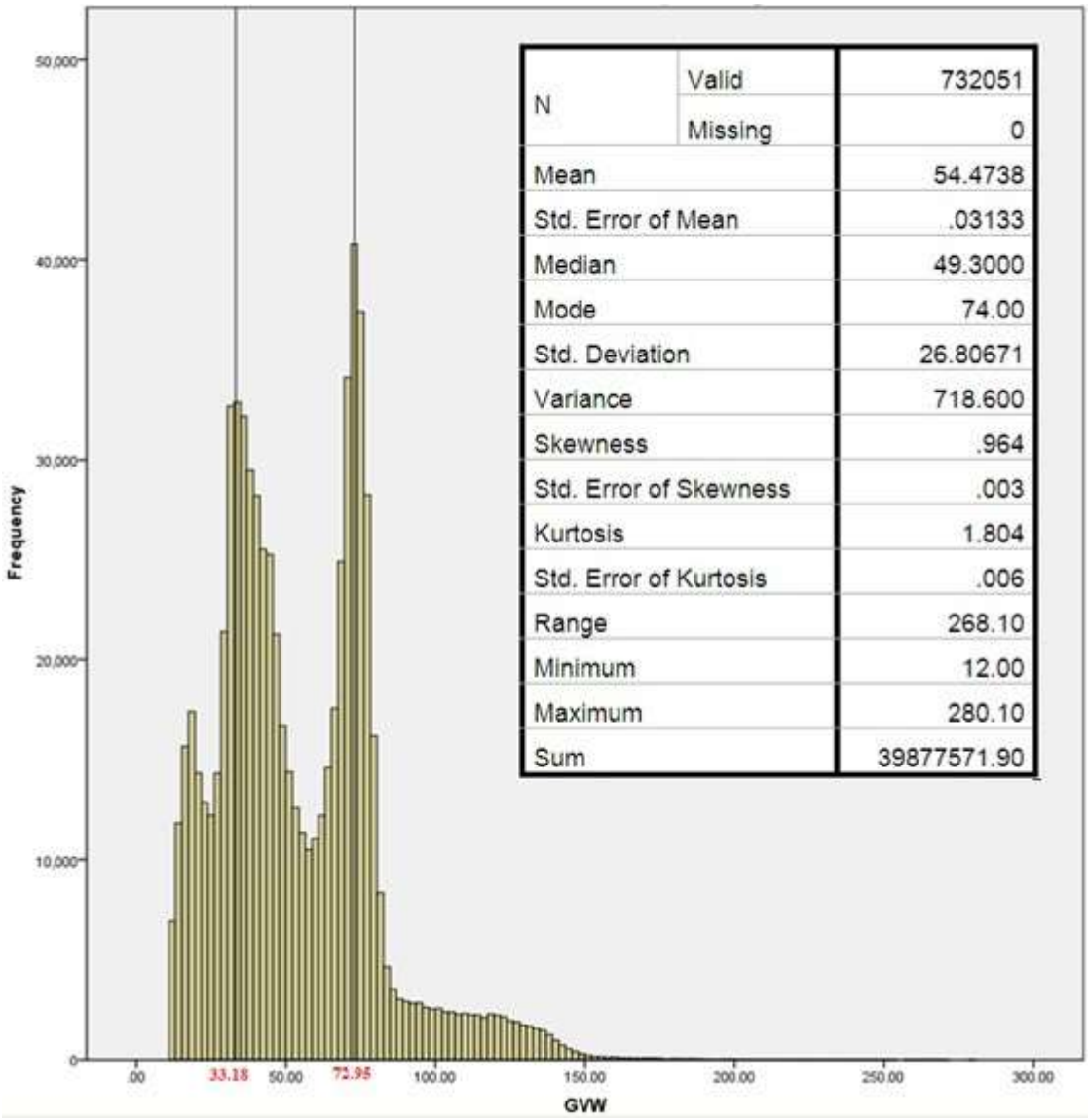

N	Valid	732051
	Missing	0
Mean		54.4738
Std. Error of Mean		.03133
Median		49.3000
Mode		74.00
Std. Deviation		26.80671
Variance		718.600
Skewness		.964
Std. Error of Skewness		.003
Kurtosis		1.804
Std. Error of Kurtosis		.006
Range		268.10
Minimum		12.00
Maximum		280.10
Sum		39877571.90

Figure B24. Frequency Histogram for Superior Region WIM Stations (Correct Data).

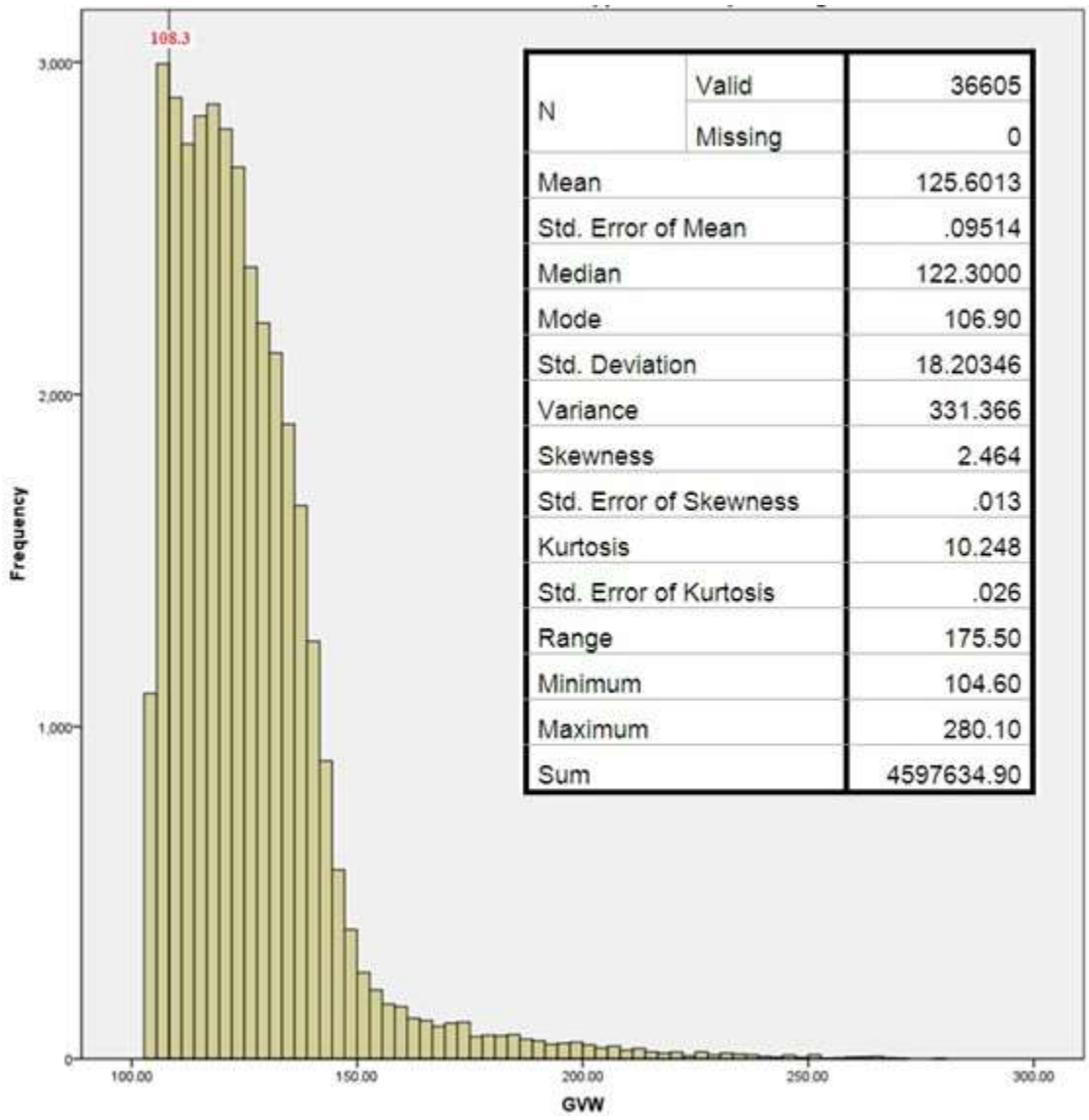

N	Valid	36605
	Missing	0
Mean		125.6013
Std. Error of Mean		.09514
Median		122.3000
Mode		106.90
Std. Deviation		18.20346
Variance		331.366
Skewness		2.464
Std. Error of Skewness		.013
Kurtosis		10.248
Std. Error of Kurtosis		.026
Range		175.50
Minimum		104.60
Maximum		280.10
Sum		4597634.90

Figure B25. Frequency Histogram for Top 5% of Superior Region WIM Stations (Correct Data).

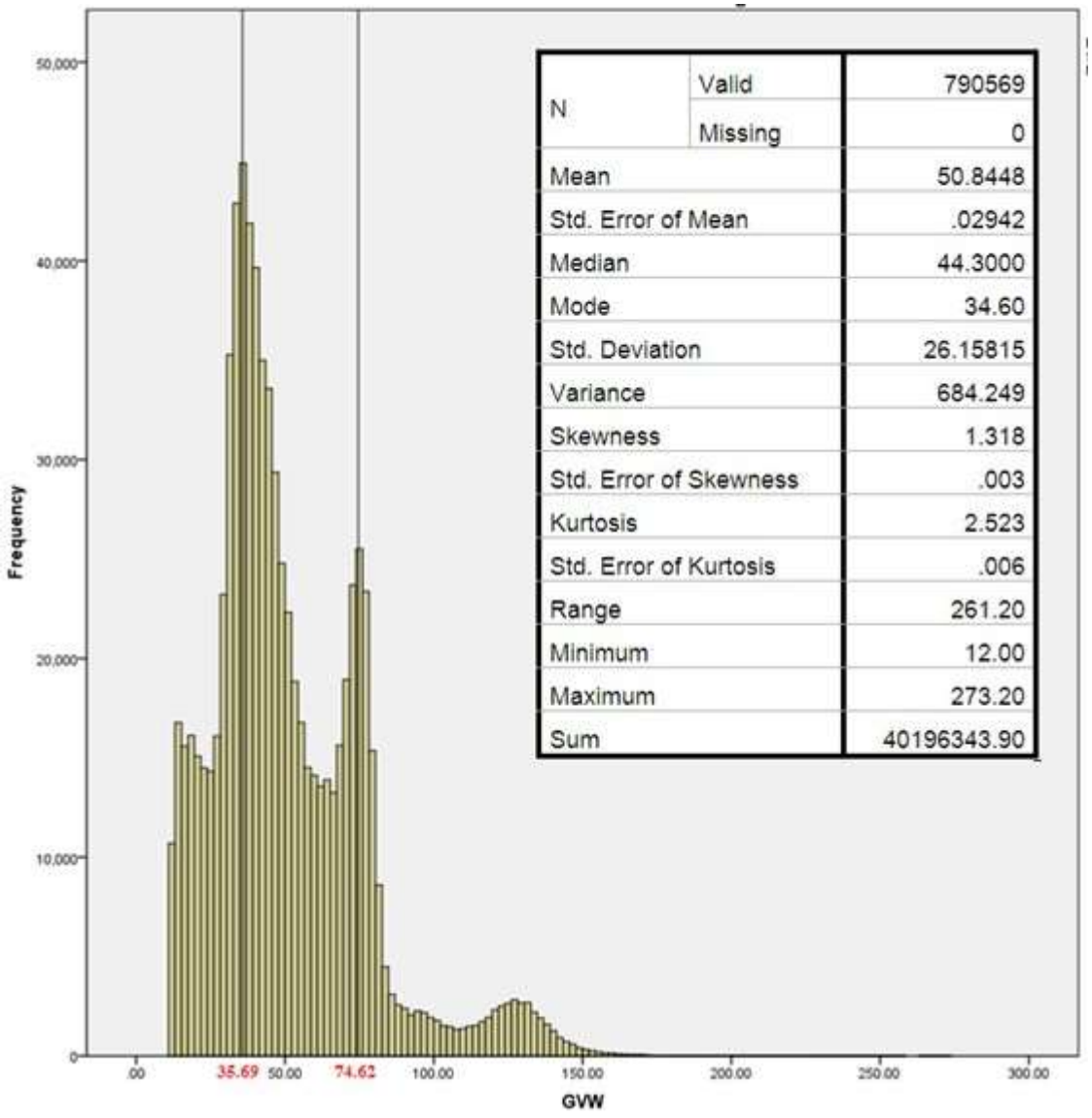

N	Valid	790569
	Missing	0
Mean		50.8448
Std. Error of Mean		.02942
Median		44.3000
Mode		34.60
Std. Deviation		26.15815
Variance		684.249
Skewness		1.318
Std. Error of Skewness		.003
Kurtosis		2.523
Std. Error of Kurtosis		.006
Range		261.20
Minimum		12.00
Maximum		273.20
Sum		40196343.90

Figure B26. Frequency Histogram for North Region WIM Stations (Correct Data).

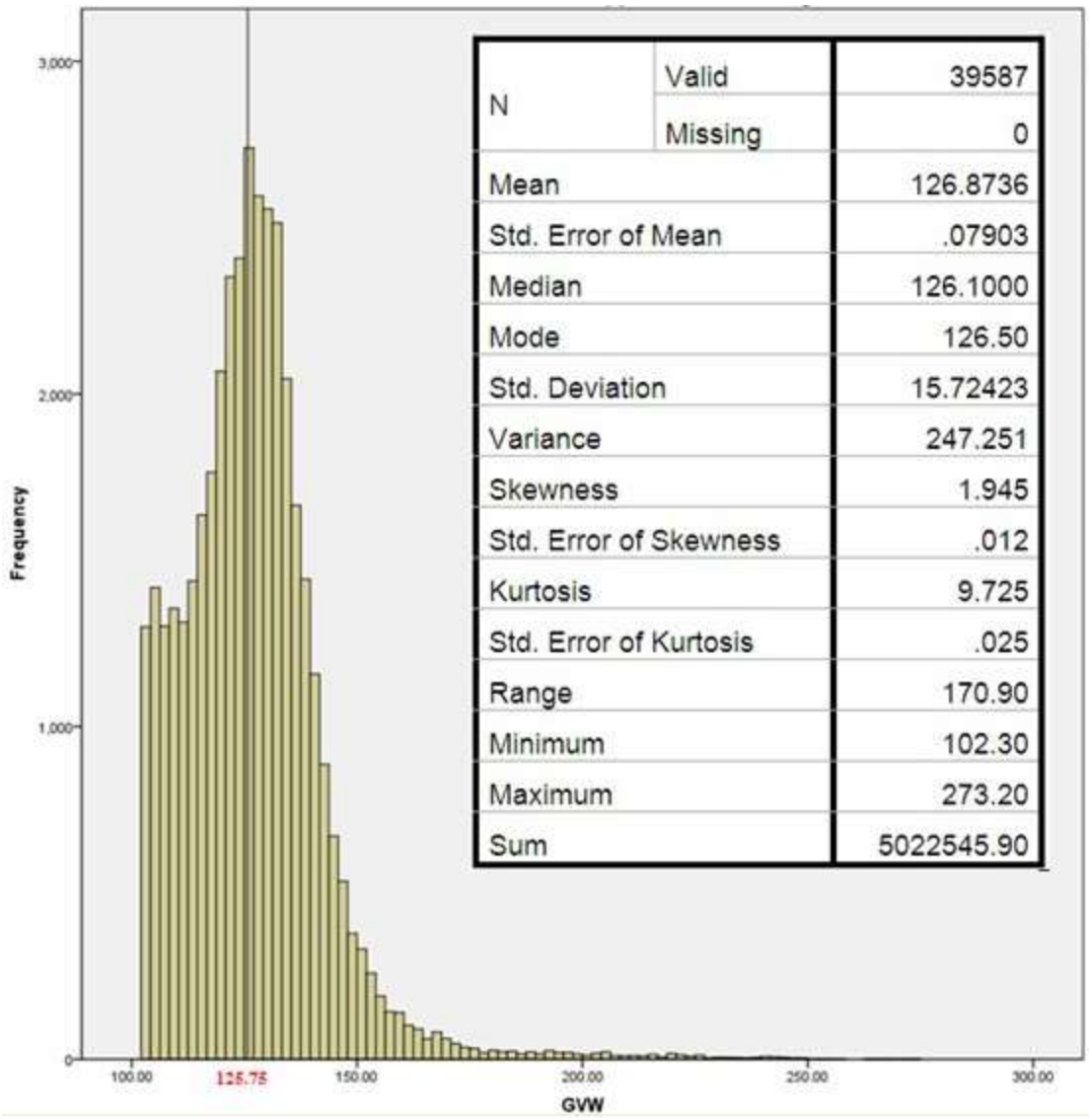

N	Valid	39587
	Missing	0
Mean		126.8736
Std. Error of Mean		.07903
Median		126.1000
Mode		126.50
Std. Deviation		15.72423
Variance		247.251
Skewness		1.945
Std. Error of Skewness		.012
Kurtosis		9.725
Std. Error of Kurtosis		.025
Range		170.90
Minimum		102.30
Maximum		273.20
Sum		5022545.90

Figure B27. Frequency Histogram for Top 5% of North Region WIM Stations (Correct Data).

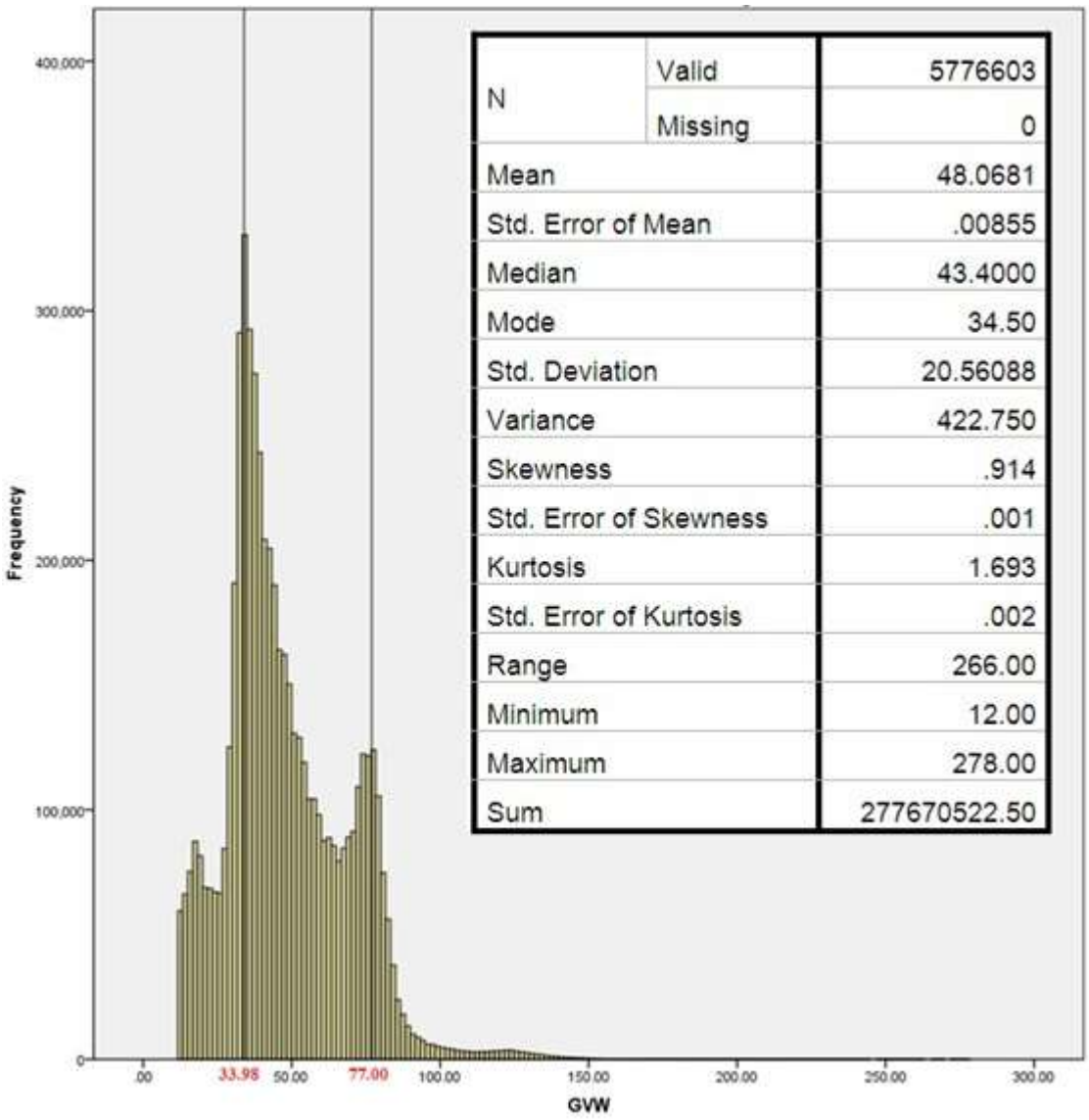

N	Valid	5776603
	Missing	0
Mean		48.0681
Std. Error of Mean		.00855
Median		43.4000
Mode		34.50
Std. Deviation		20.56088
Variance		422.750
Skewness		.914
Std. Error of Skewness		.001
Kurtosis		1.693
Std. Error of Kurtosis		.002
Range		266.00
Minimum		12.00
Maximum		278.00
Sum		277670522.50

Figure B28. Frequency Histogram for Grand Region WIM Stations (Correct Data).

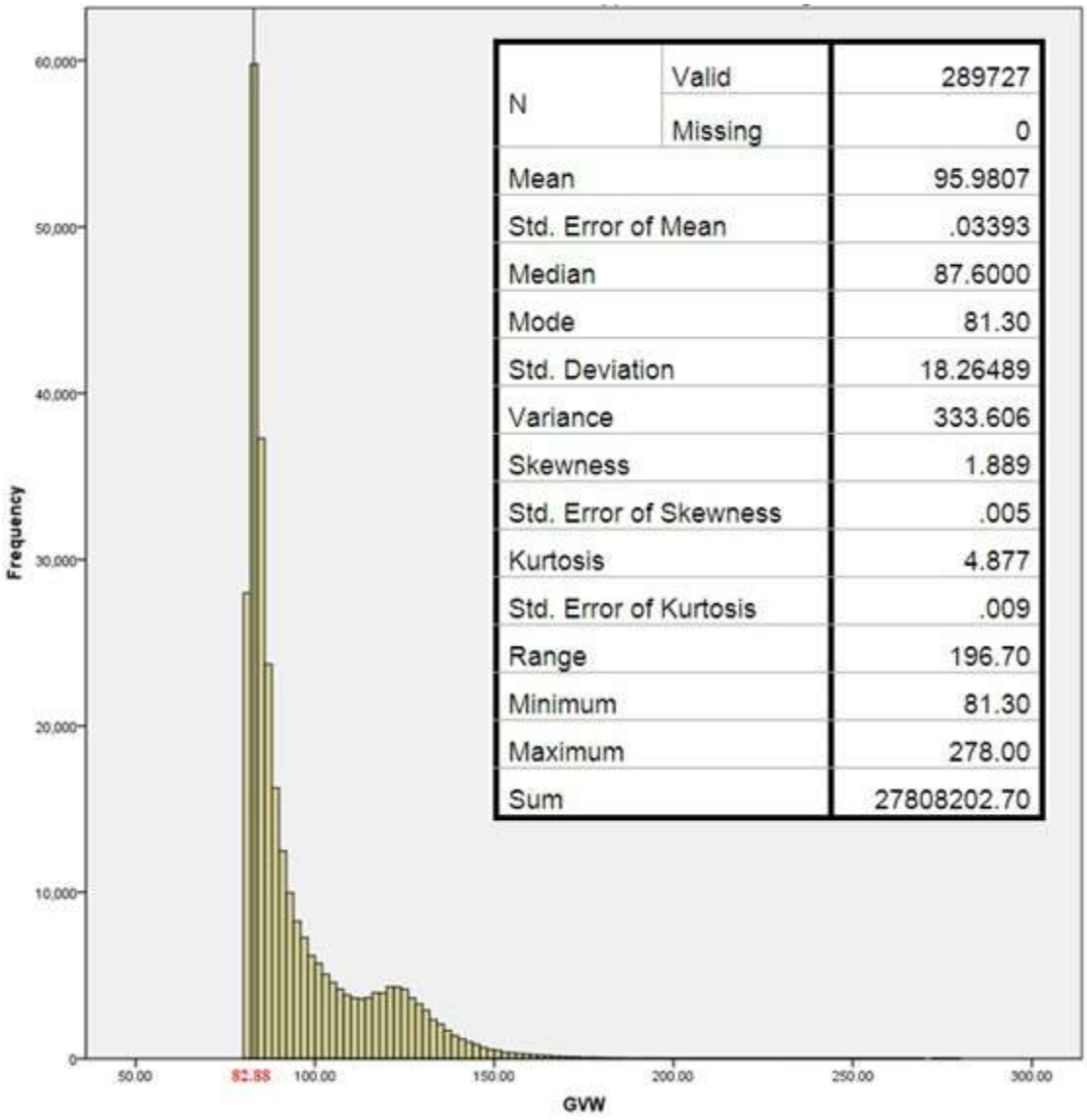

N	Valid	289727
	Missing	0
Mean		95.9807
Std. Error of Mean		.03393
Median		87.6000
Mode		81.30
Std. Deviation		18.26489
Variance		333.606
Skewness		1.889
Std. Error of Skewness		.005
Kurtosis		4.877
Std. Error of Kurtosis		.009
Range		196.70
Minimum		81.30
Maximum		278.00
Sum		27808202.70

Figure B29. Frequency Histogram for Top 5% of Grand Region WIM Stations (Correct Data).

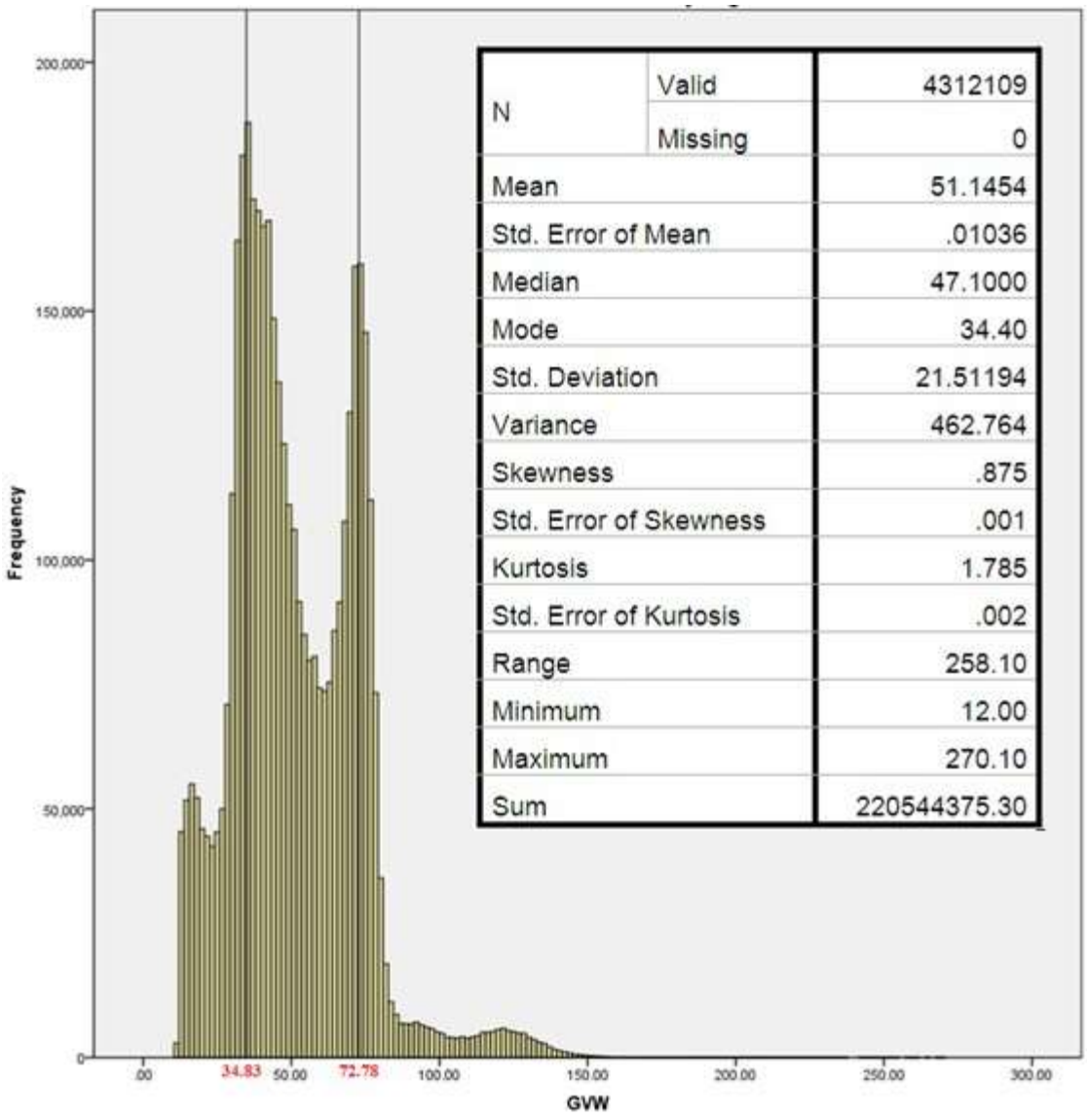

N	Valid	4312109
	Missing	0
Mean		51.1454
Std. Error of Mean		.01036
Median		47.1000
Mode		34.40
Std. Deviation		21.51194
Variance		462.764
Skewness		.875
Std. Error of Skewness		.001
Kurtosis		1.785
Std. Error of Kurtosis		.002
Range		258.10
Minimum		12.00
Maximum		270.10
Sum		220544375.30

Figure B30. Frequency Histogram for Bay Region WIM Stations (Correct Data).

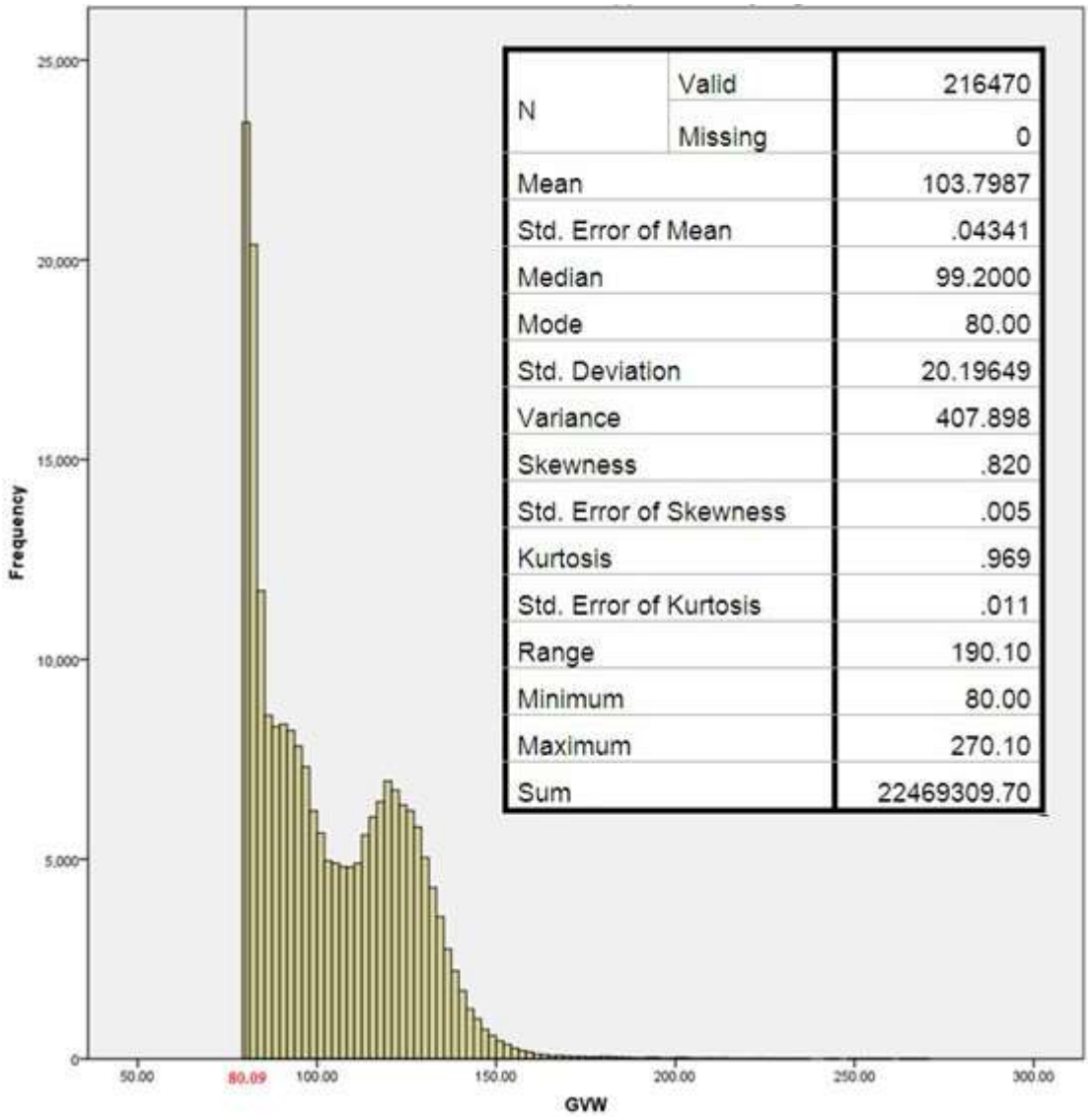

N	Valid	216470
	Missing	0
Mean		103.7987
Std. Error of Mean		.04341
Median		99.2000
Mode		80.00
Std. Deviation		20.19649
Variance		407.898
Skewness		.820
Std. Error of Skewness		.005
Kurtosis		.969
Std. Error of Kurtosis		.011
Range		190.10
Minimum		80.00
Maximum		270.10
Sum		22469309.70

Figure B31. Frequency Histogram for Top 5% of Bay Region WIM Stations (Correct Data).

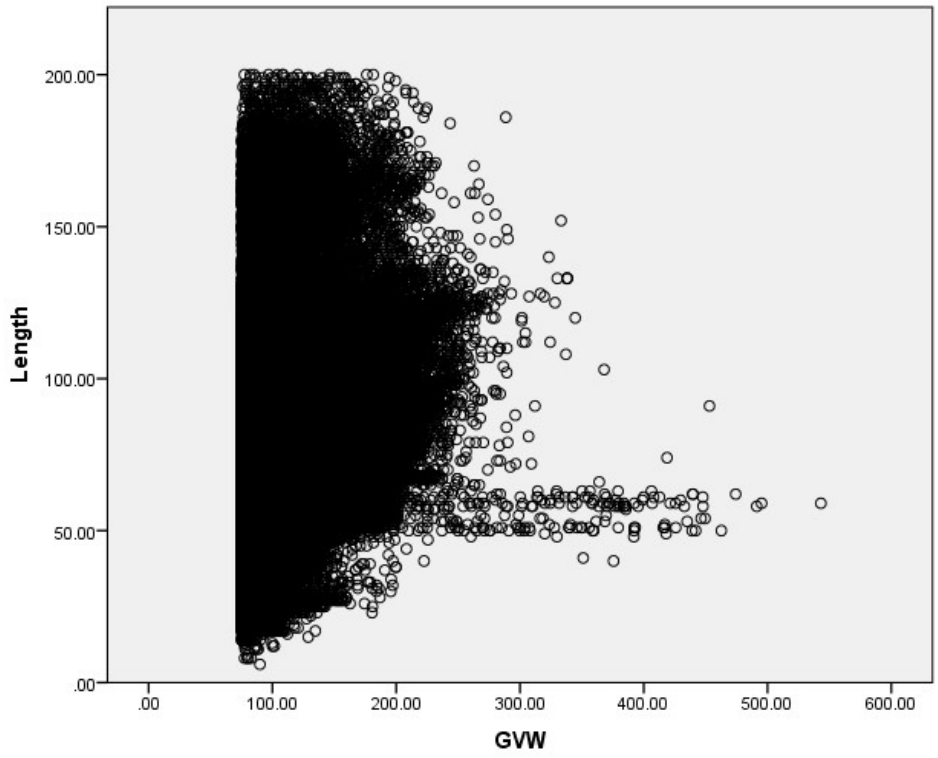

Figure B32. GVW-Length Relationship for Vehicles over 75 kips.

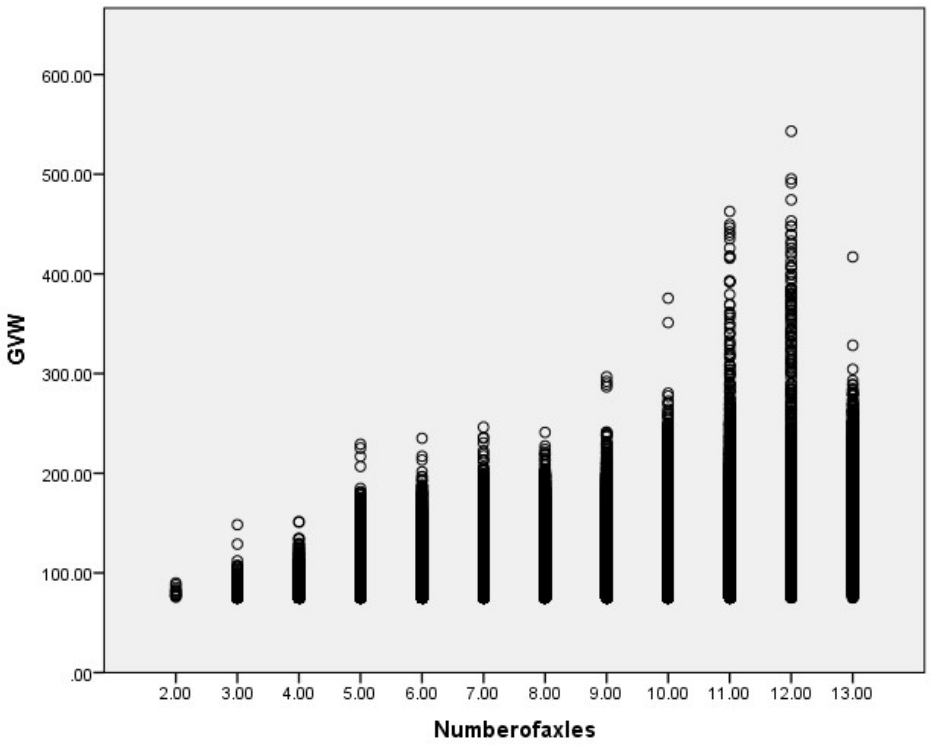

Figure B33. GVW-Number-of-Axles Relationship for Vehicles over 75 kips.

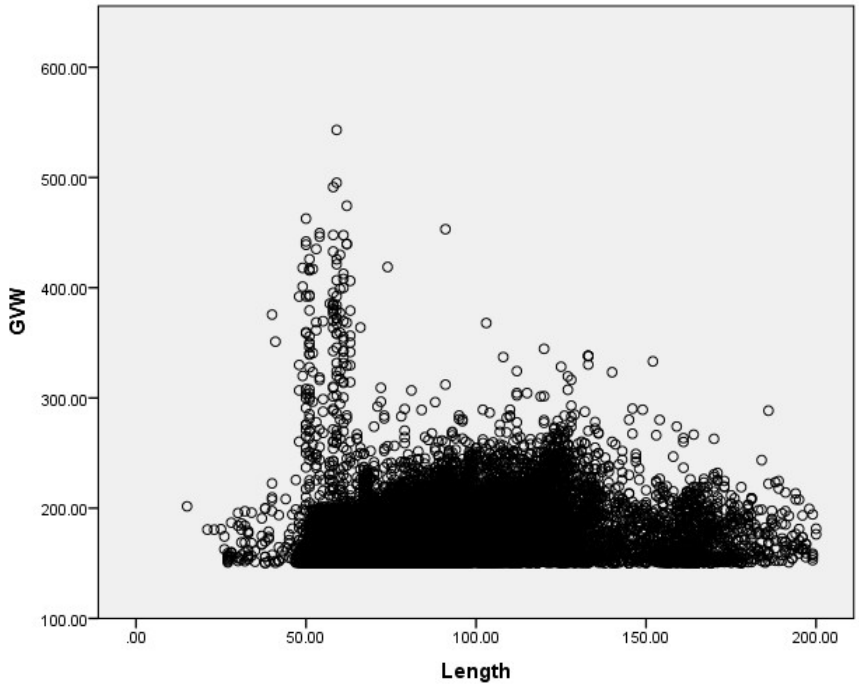

Figure B34. GVW-Length Relationship for Vehicles over 150 kips.

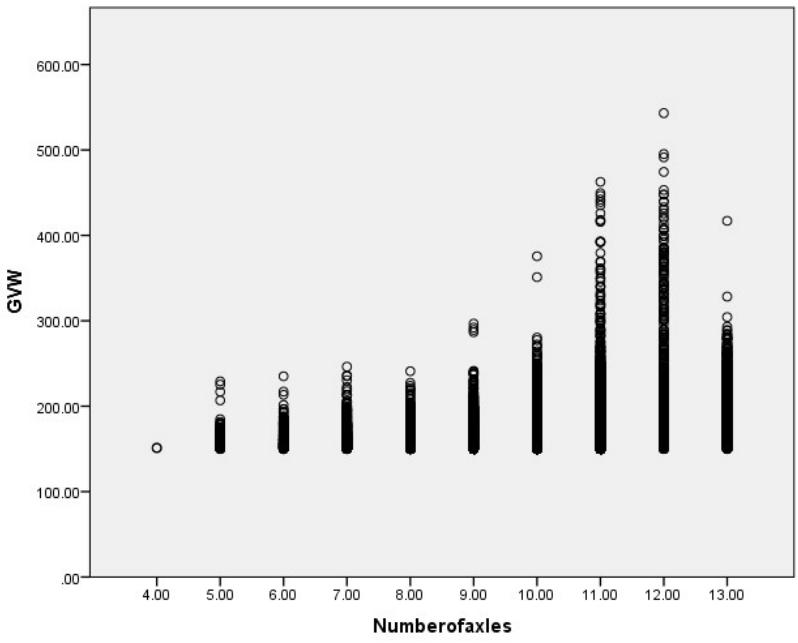

Figure B35. GVW-Number-of-Axles Relationship for Vehicles over 150 kips.

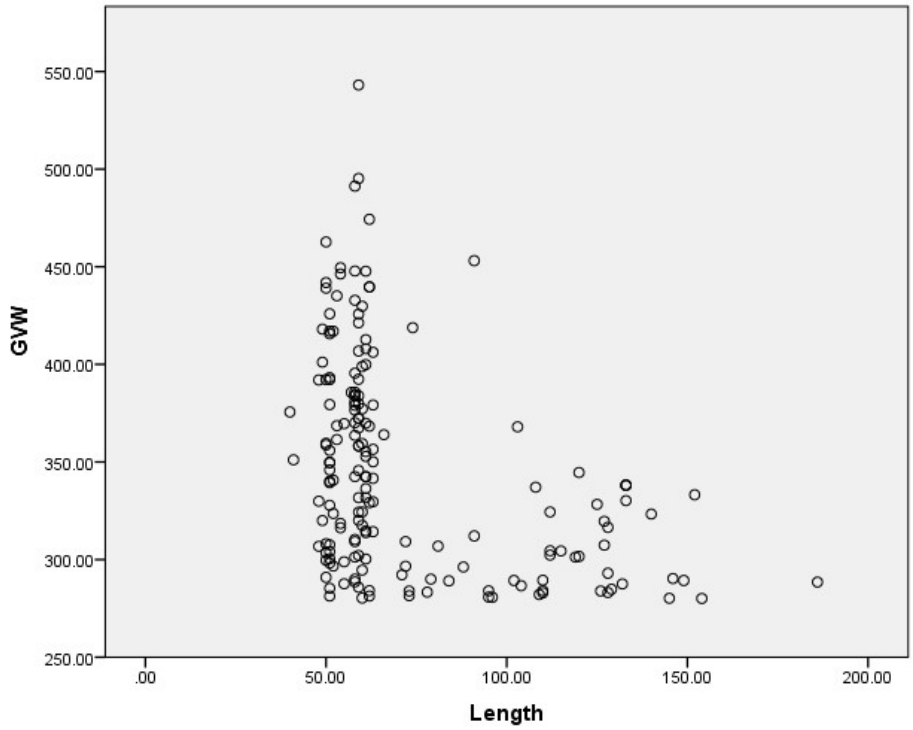

Figure B36. GVW-Length Relationship for Vehicles over 280 kips.

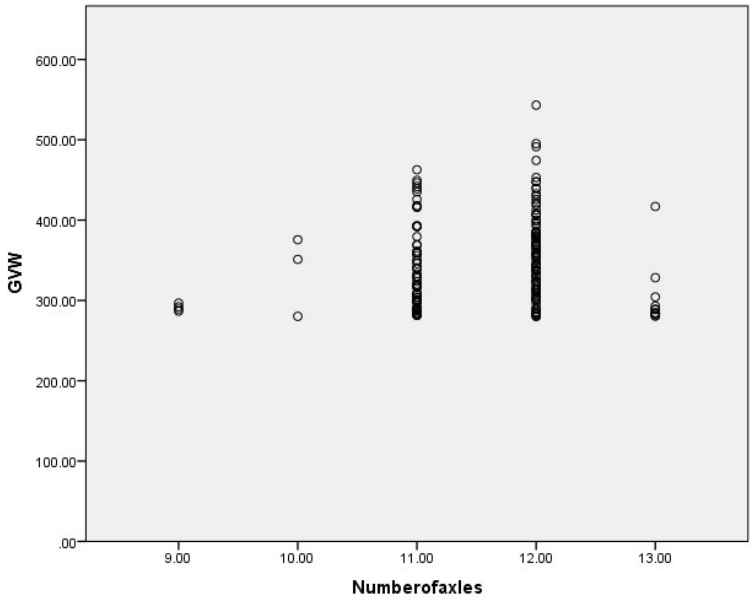

Figure B37. GVW-Number-of-Axles Relationship for Vehicles over 280 kips.

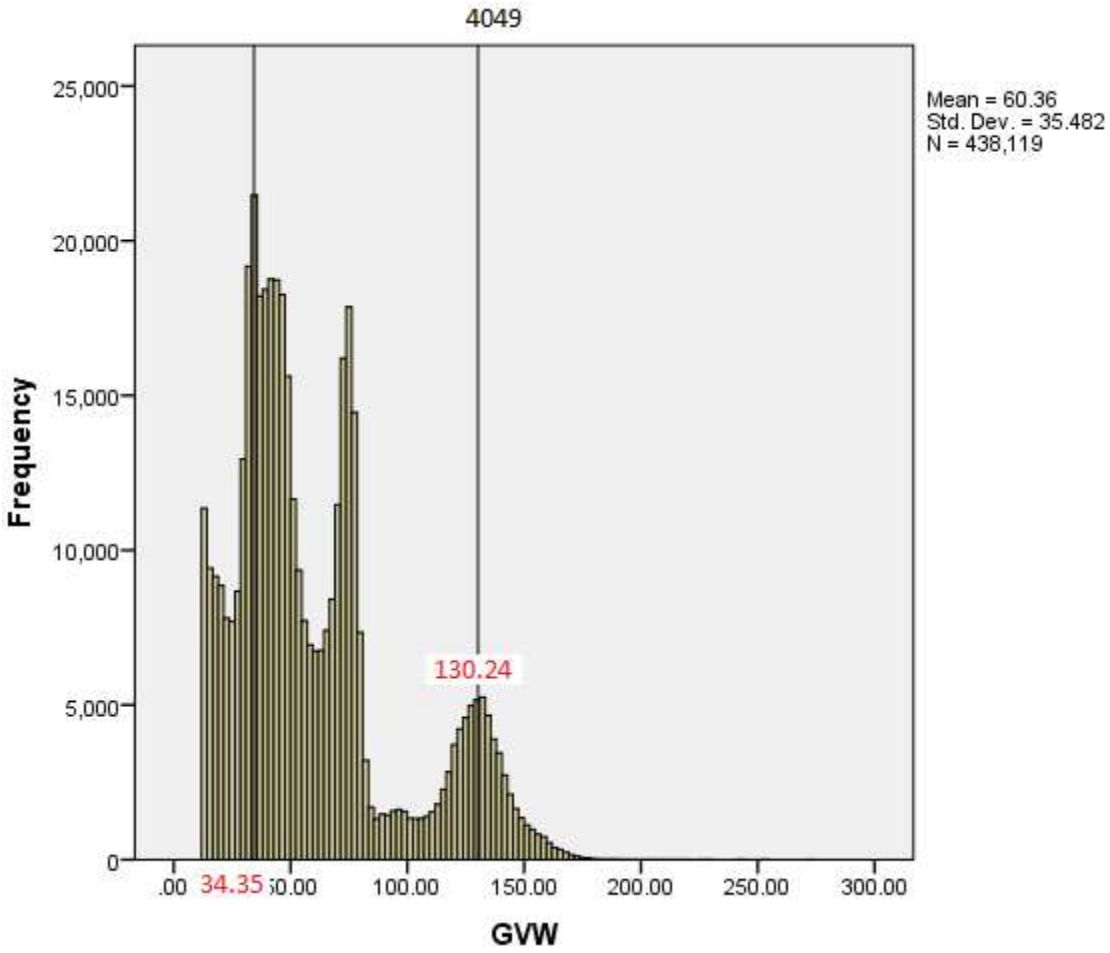

GVW

N	Valid	438119
	Missing	0
Mean		60.3607
Std. Error of Mean		.05361
Median		49.1000
Mode		34.20
Std. Deviation		35.48185
Variance		1258.962
Minimum		12.00
Maximum		273.20
Sum		26445166.50

Figure B38. Frequency Histogram of All Vehicles, Site 4049.

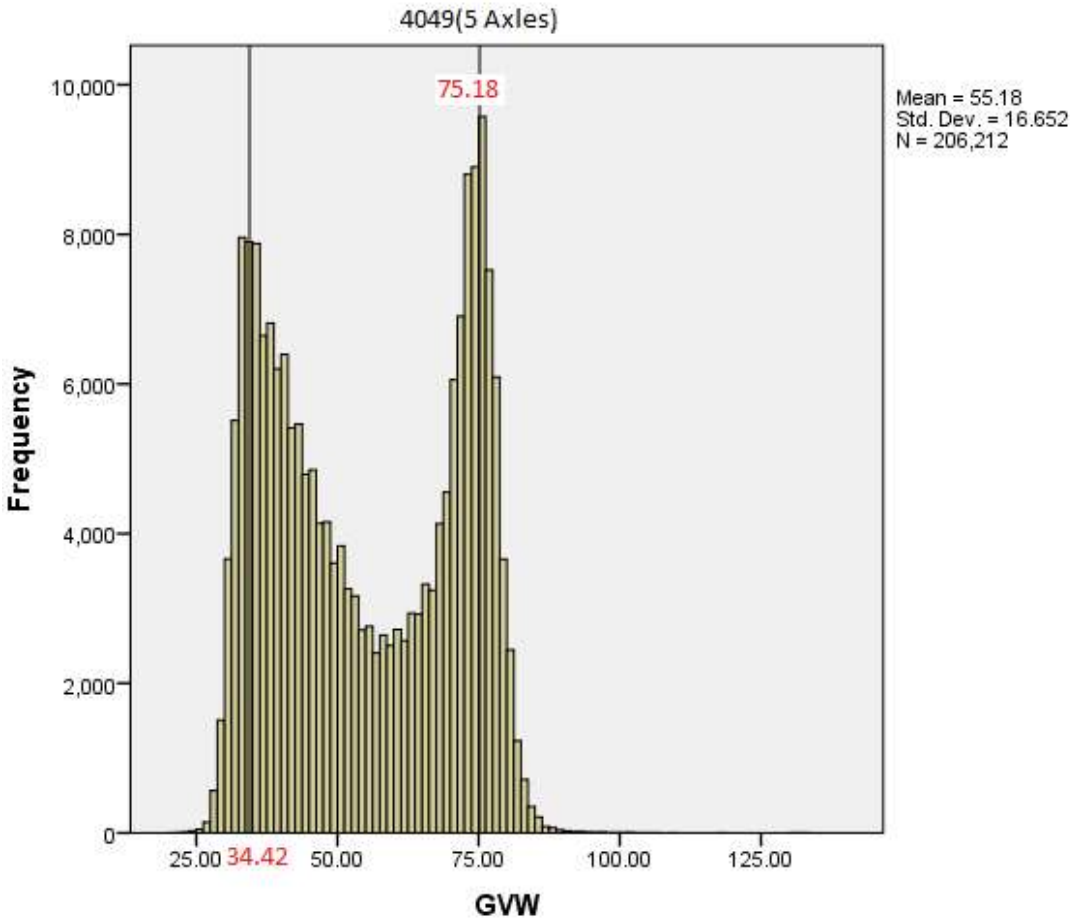

Statistics

GVW

N	Valid	206212
	Missing	0
Mean		55.1800
Std. Error of Mean		.03667
Median		53.4000
Mode		74.60
Std. Deviation		16.65207
Variance		277.292
Minimum		20.10
Maximum		133.20
Sum		11378775.30

Figure B39. Frequency Histogram of 5-Axle Vehicles, Site 4049.

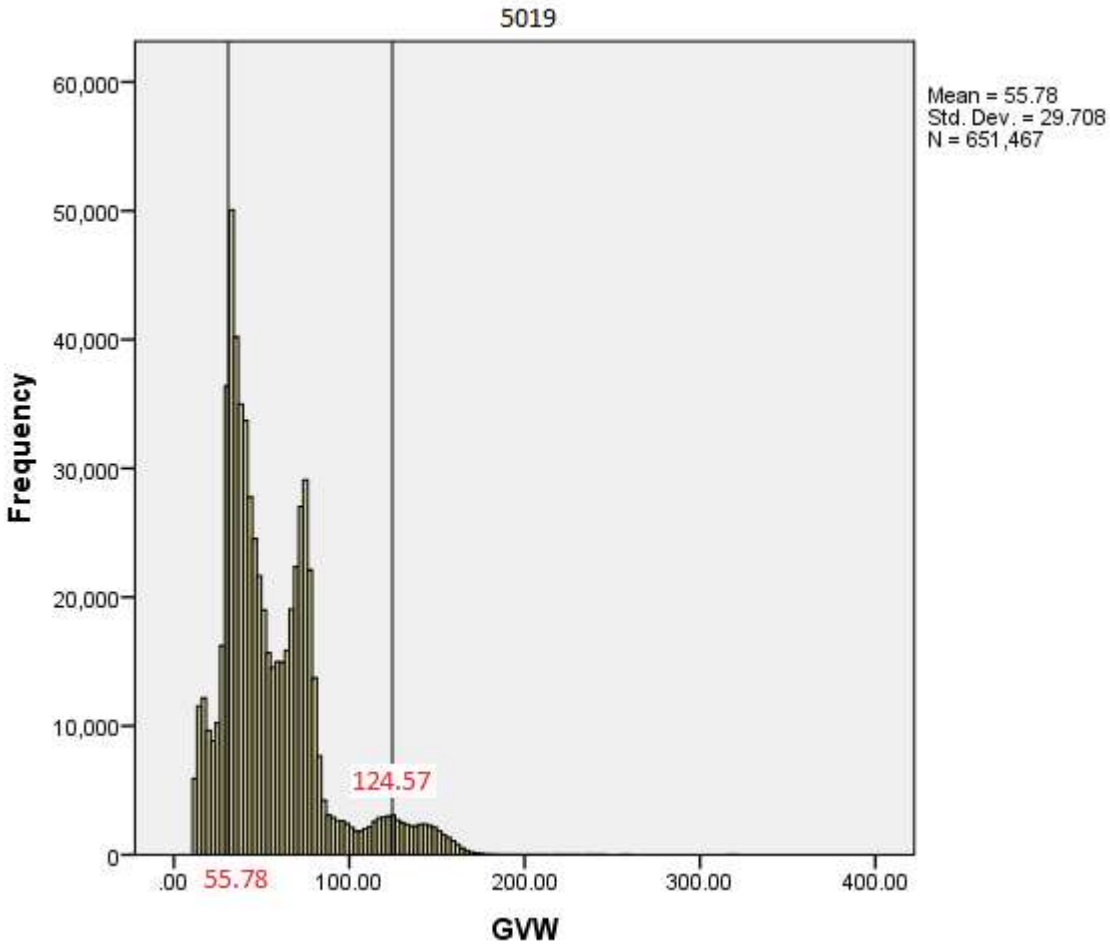

Statistics

GVW

N	Valid	651467
	Missing	0
Mean		55.7835
Std. Error of Mean		.03681
Median		47.8000
Mode		32.50
Std. Deviation		29.70838
Variance		882.588
Minimum		12.00
Maximum		319.60
Sum		36341127.00

Figure B40. Frequency Histogram of All Vehicles, Site 5019.

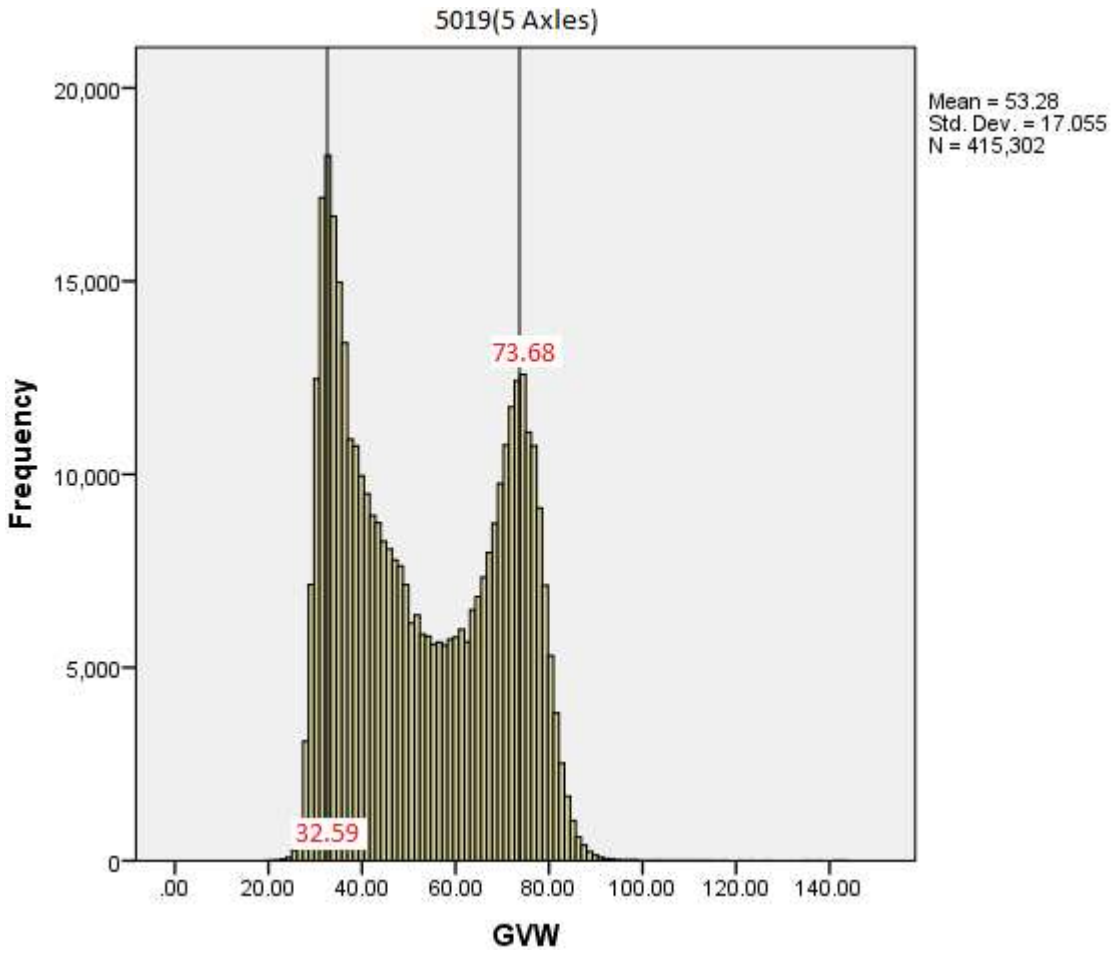

Statistics

GVW

N	Valid	415302
	Missing	0
Mean		53.2839
Std. Error of Mean		.02646
Median		51.0000
Mode		32.50
Std. Deviation		17.05468
Variance		290.862
Minimum		19.80
Maximum		143.00
Sum		22128927.10

Figure B41. Frequency Histogram of 5-Axle Vehicles, Site 5019.

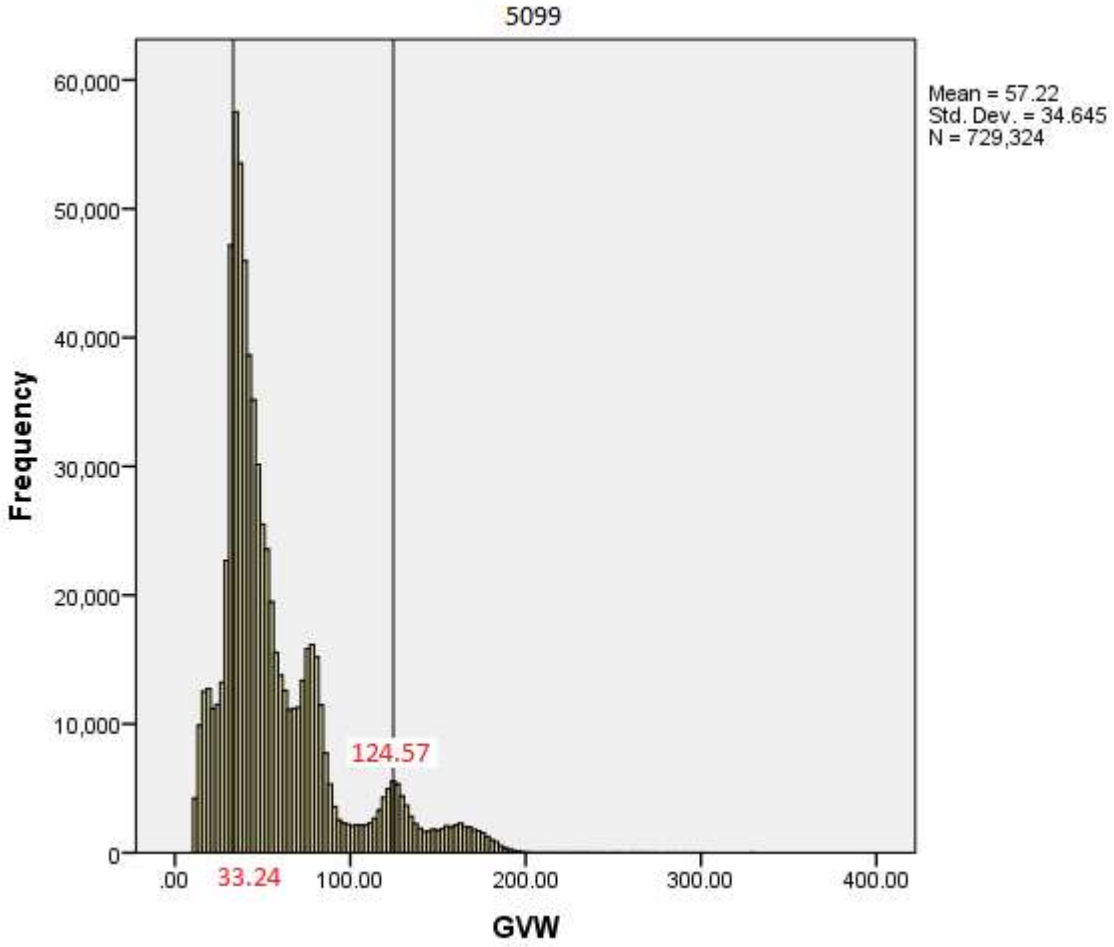

Statistics

GVW

N	Valid	729324
	Missing	0
Mean		57.2222
Std. Error of Mean		.04057
Median		45.3000
Mode		34.60
Std. Deviation		34.64522
Variance		1200.292
Minimum		12.00
Maximum		329.50
Sum		41733494.30

Figure B42. Frequency Histogram of All Vehicles, Site 5099.

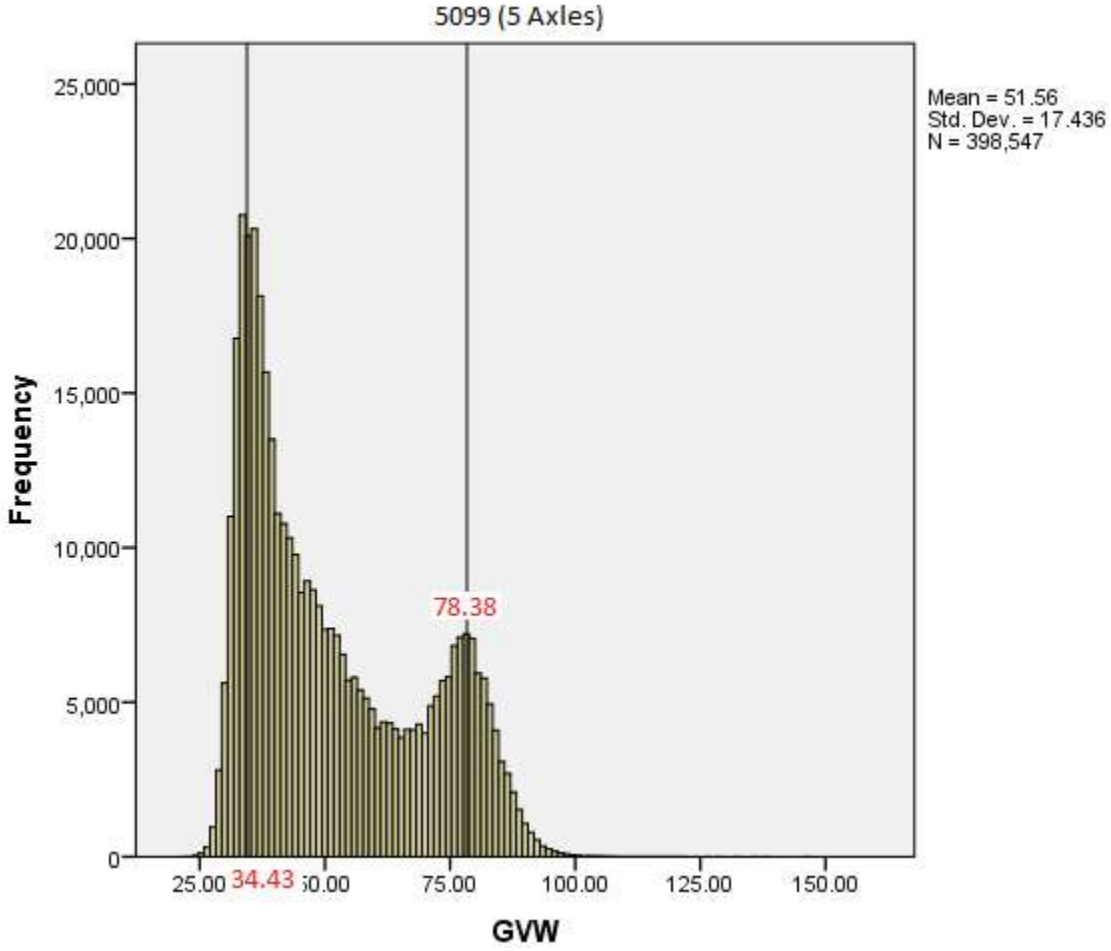

Statistics

GVW

N	Valid	398547
	Missing	0
Mean		51.5596
Std. Error of Mean		.02762
Median		46.2000
Mode		34.40
Std. Deviation		17.43638
Variance		304.028
Minimum		21.80
Maximum		146.00
Sum		20548937.60

Figure B43. Frequency Histogram of 5-Axle Vehicles, Site 5099.

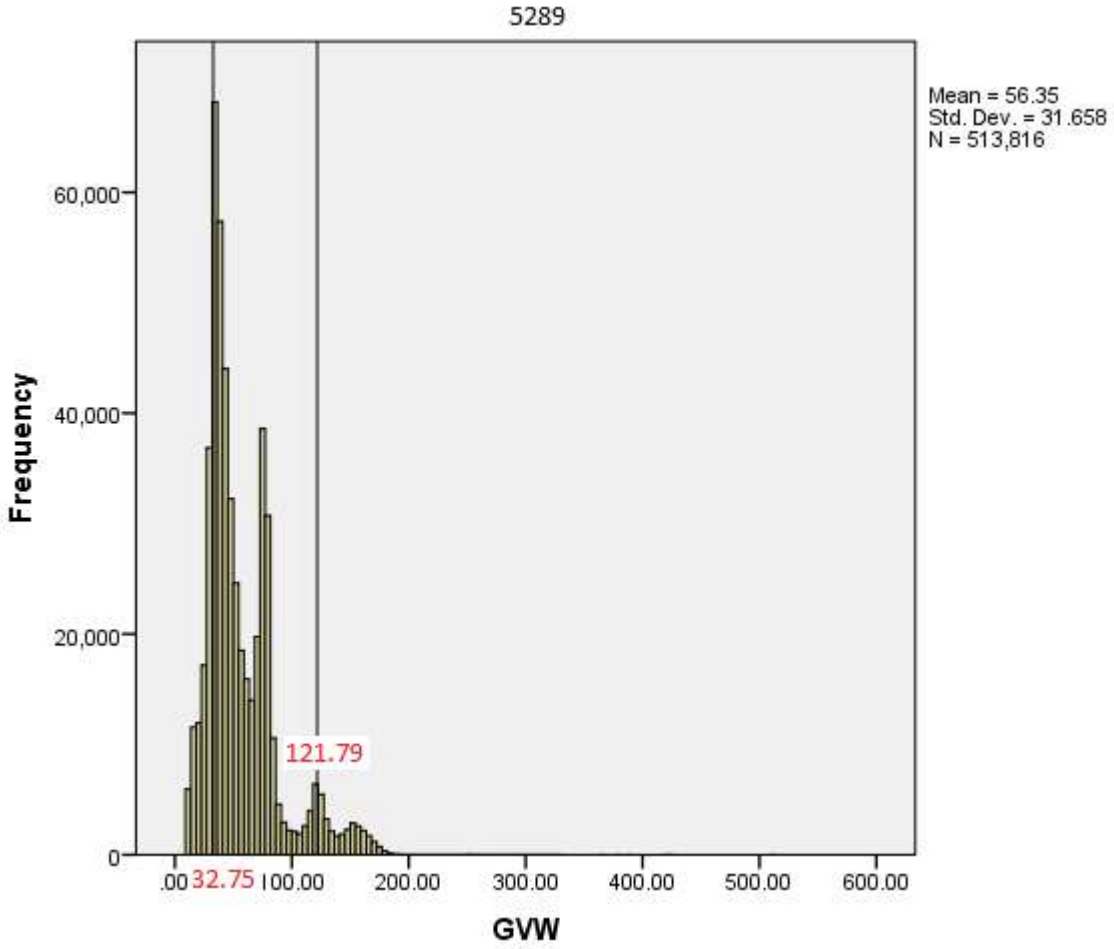

Statistics

GVW

N	Valid	513816
	Missing	0
Mean		56.3525
Std. Error of Mean		.04416
Median		45.9000
Mode		33.50
Std. Deviation		31.65786
Variance		1002.220
Minimum		12.00
Maximum		510.20
Sum		28954814.70

Figure B44. Frequency Histogram of All Vehicles, Site 5289.

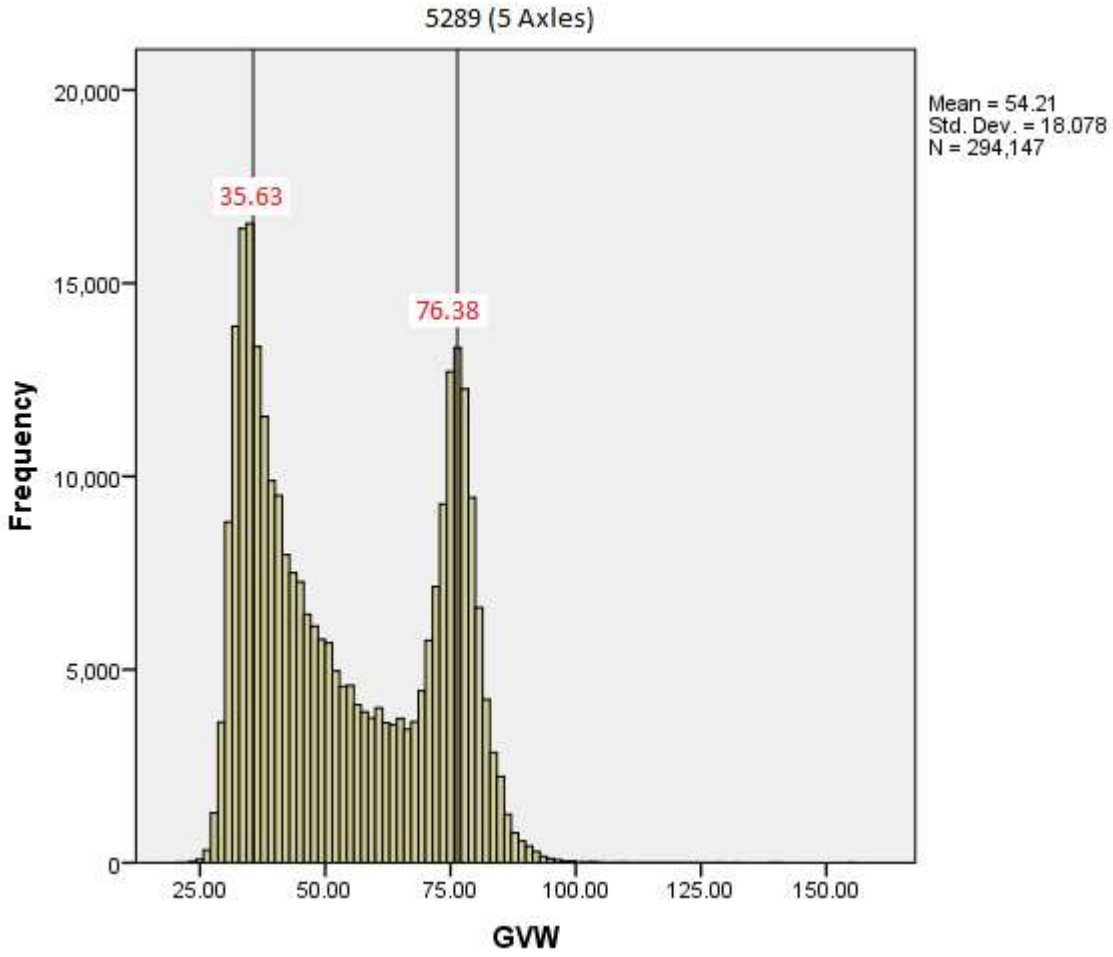

Statistics

GVW

N	Valid	294147
	Missing	0
Mean		54.2129
Std. Error of Mean		.03333
Median		50.1000
Mode		33.50
Std. Deviation		18.07803
Variance		326.815
Minimum		21.20
Maximum		154.70
Sum		15946571.40

Figure B45. Frequency Histogram of 5-Axle Vehicles, Site 5289.

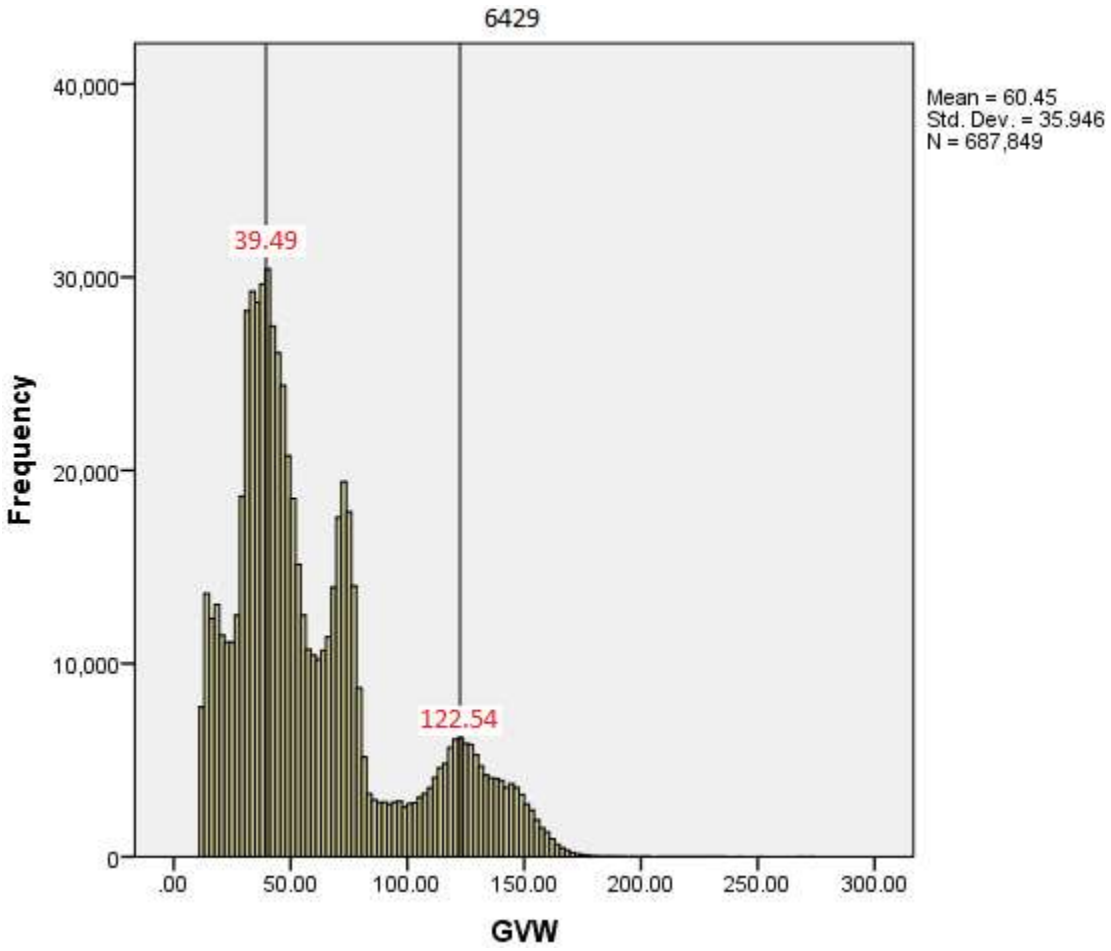

Statistics

GVW

N	Valid	687849
	Missing	0
Mean		60.4526
Std. Error of Mean		.04334
Median		48.6000
Mode		32.80
Std. Deviation		35.94620
Variance		1292.129
Minimum		12.00
Maximum		272.70
Sum		41582253.30

Figure B46. Frequency Histogram of All Vehicles, Site 6429.

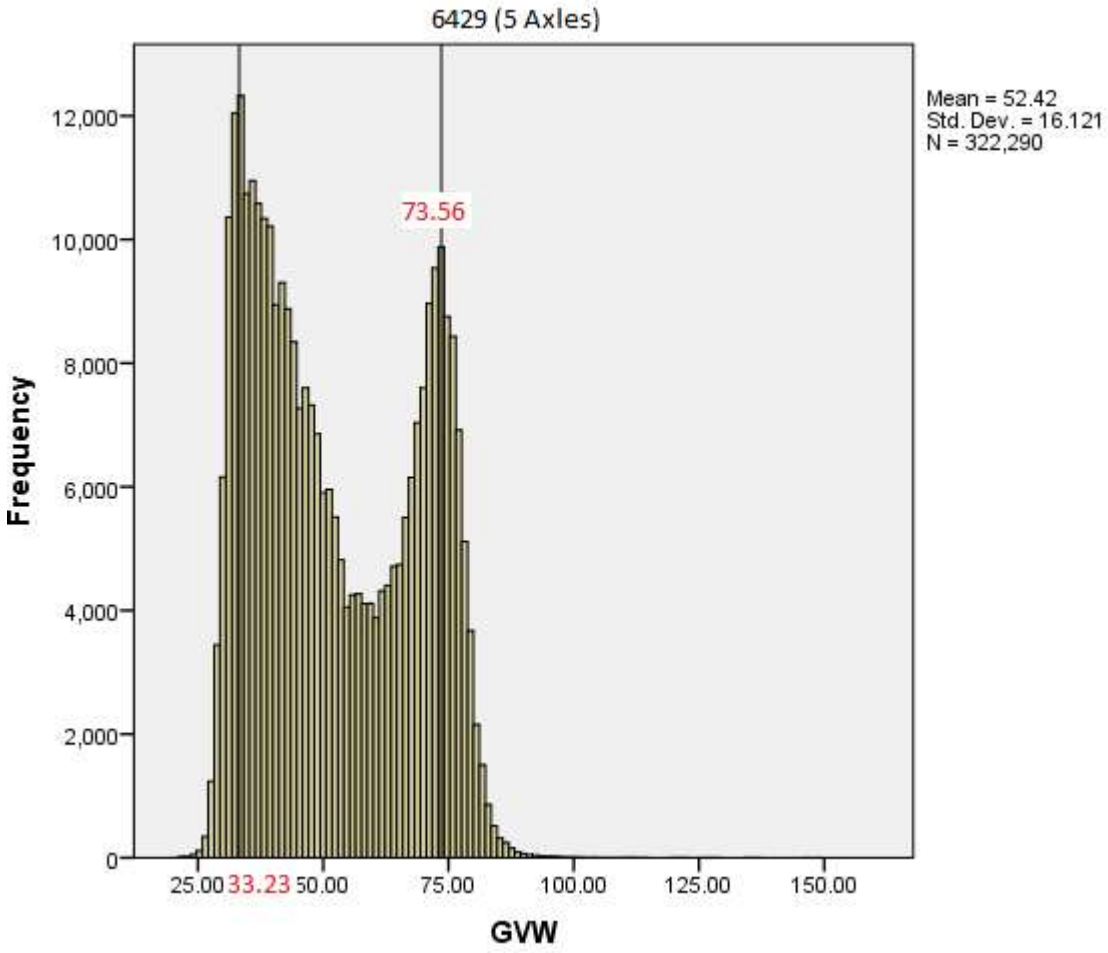

Statistics

GVW

N	Valid	322290
	Missing	0
Mean		52.4166
Std. Error of Mean		.02840
Median		49.0000
Mode		32.80
Std. Deviation		16.12101
Variance		259.887
Minimum		20.20
Maximum		148.70
Sum		16893360.10

Figure B47. Frequency Histogram of 5-Axle Vehicles, Site 6429.

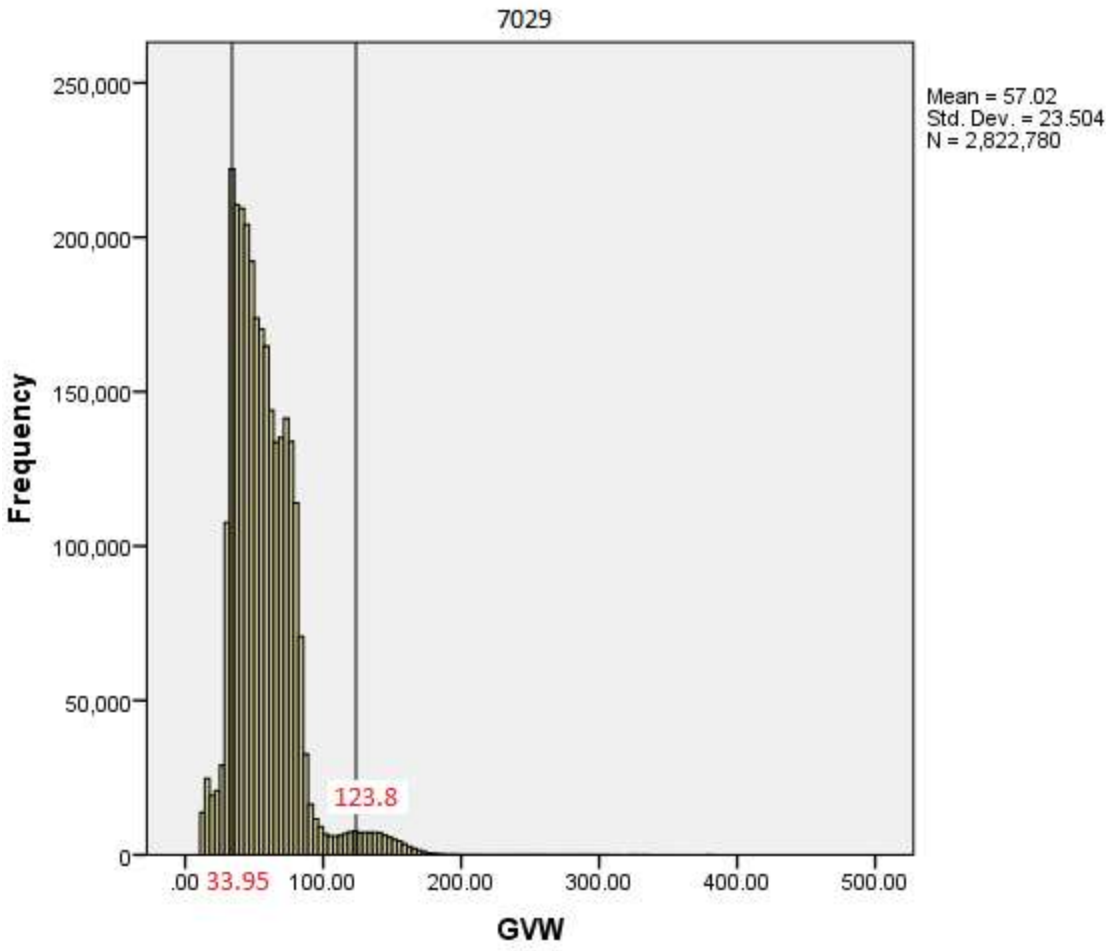

Statistics

GVW

N	Valid	2822780
	Missing	0
Mean		57.0184
Std. Error of Mean		.01399
Median		53.2000
Mode		34.10
Std. Deviation		23.50351
Variance		552.415
Minimum		12.00
Maximum		493.50
Sum		160950337.70

Figure B48. Frequency Histogram of All Vehicles, Site 7029.

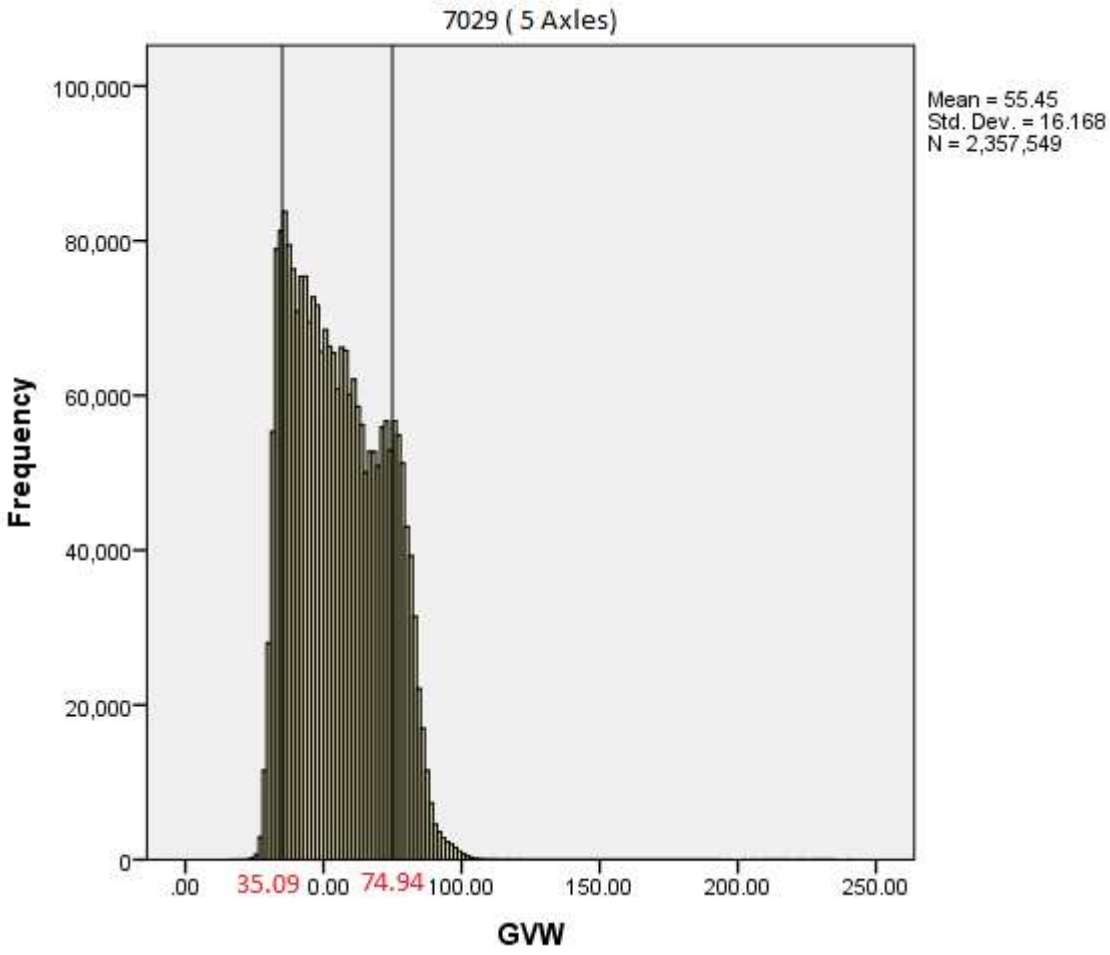

Statistics

GVW

N	Valid	2357549
	Missing	0
Mean		55.4514
Std. Error of Mean		.01053
Median		54.0000
Mode		34.60
Std. Deviation		16.16800
Variance		261.404
Minimum		17.30
Maximum		240.10
Sum		130729350.40

Figure B49. Frequency Histogram of 5-Axle Vehicles, Site 7029.

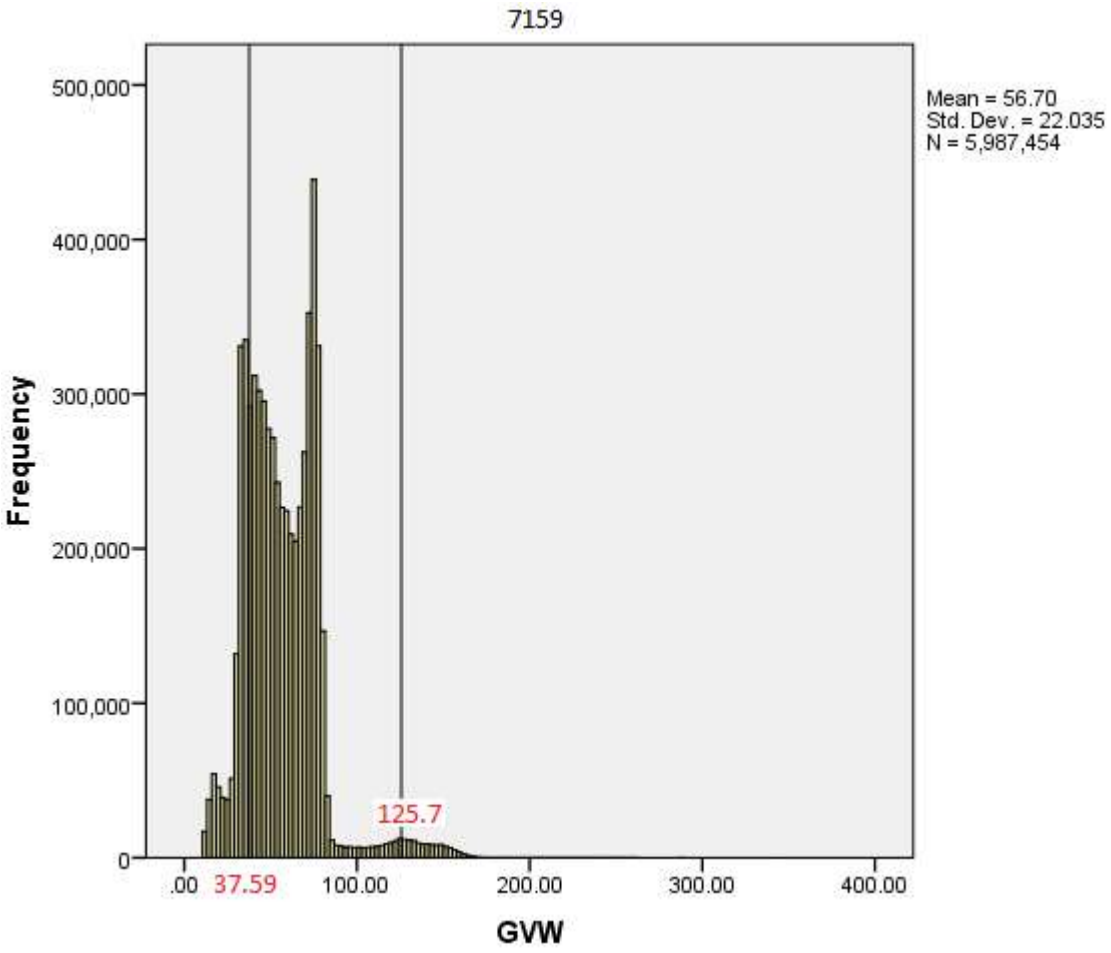

Statistics

GVW

N	Valid	5987454
	Missing	0
Mean		56.7040
Std. Error of Mean		.00901
Median		54.4000
Mode		75.10
Std. Deviation		22.03487
Variance		485.536
Minimum		12.00
Maximum		394.30
Sum		339512872.40

Figure B50. Frequency Histogram of All Vehicles, Site 7159.

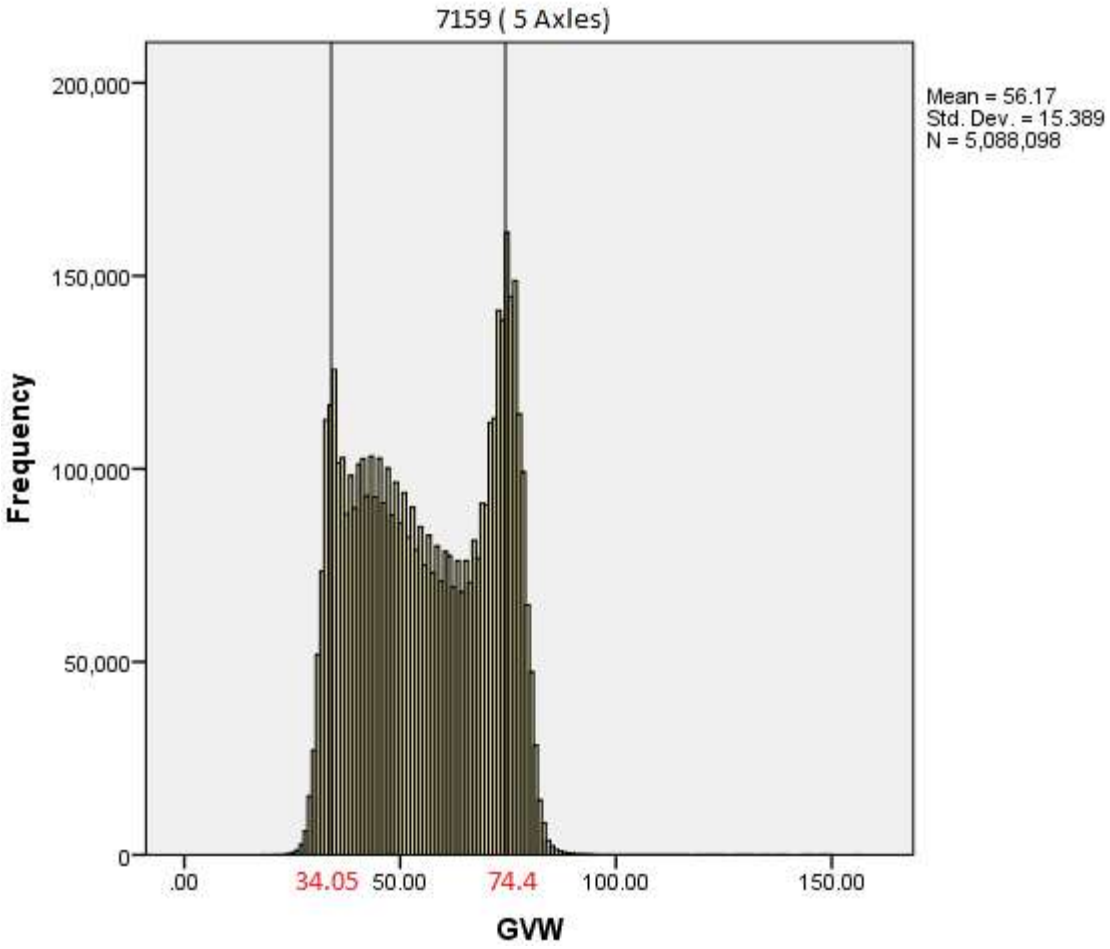

Statistics

GVW

N	Valid	5088098
	Missing	0
Mean		56.1711
Std. Error of Mean		.00682
Median		55.7000
Mode		75.10
Std. Deviation		15.38909
Variance		236.824
Minimum		19.00
Maximum		156.10
Sum		285804181.40

Figure B51. Frequency Histogram of 5-Axle Vehicles, Site 7159.

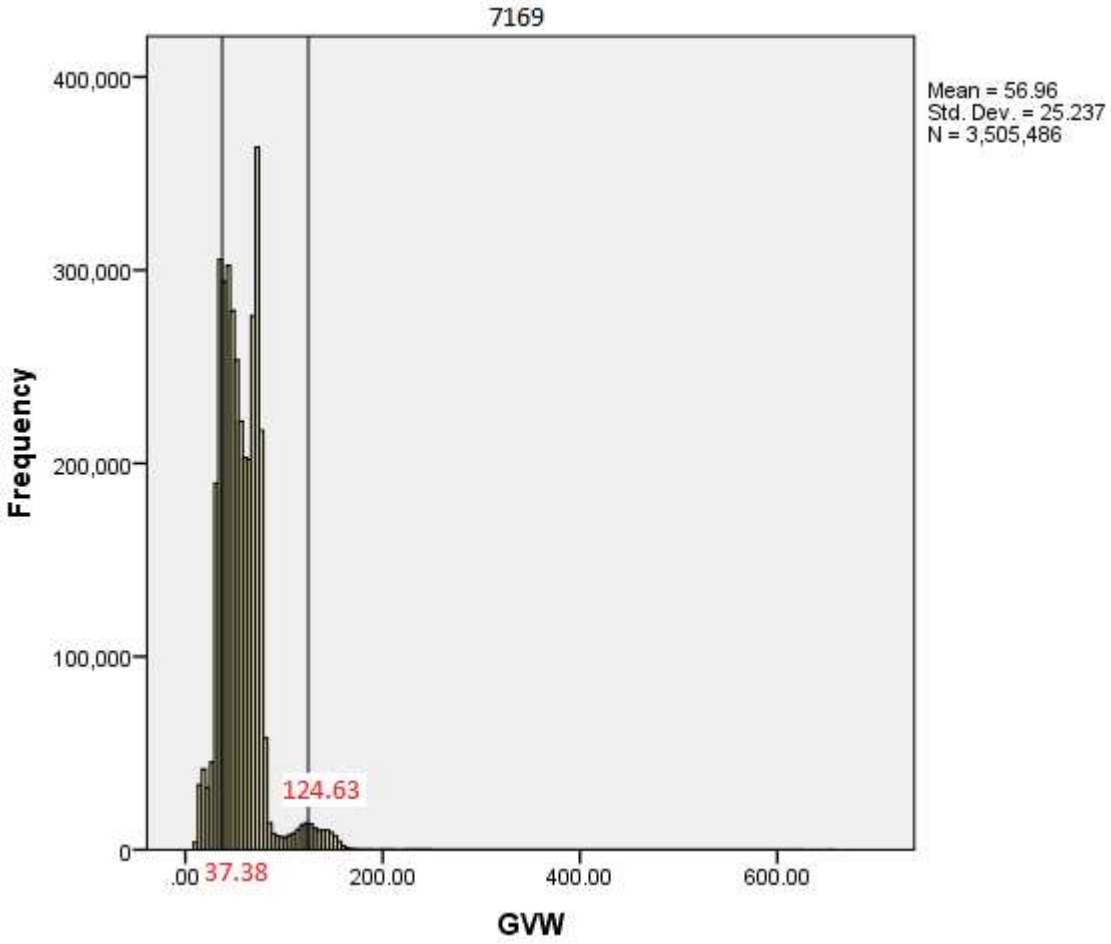

Statistics

GVW

N	Valid	3505486
	Missing	0
Mean		56.9629
Std. Error of Mean		.01348
Median		53.6000
Mode		73.10[a]
Std. Deviation		25.23733
Variance		636.923
Minimum		12.00
Maximum		655.30
Sum		199682549.70

Figure B52. Frequency Histogram of All Vehicles, Site 7169.

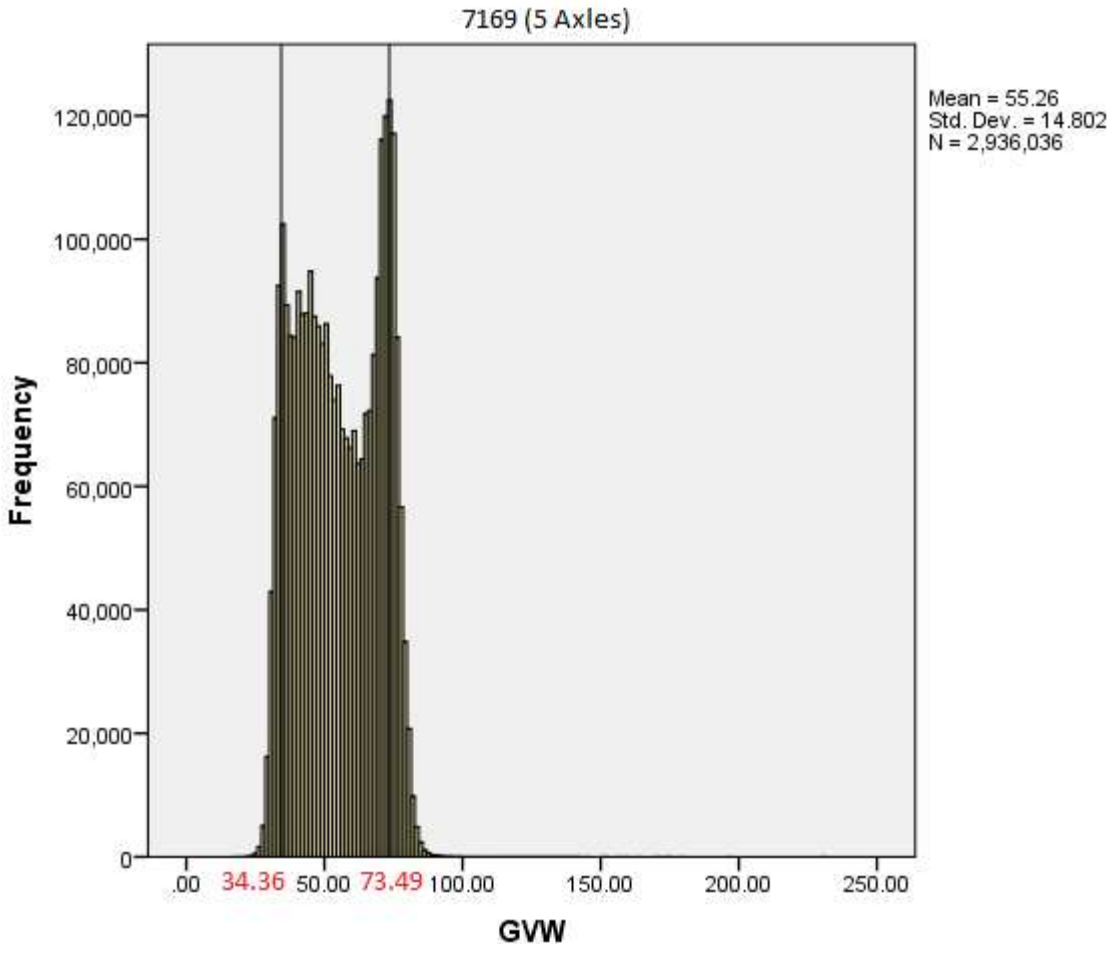

Statistics

GVW

N	Valid	2936036
	Missing	0
Mean		55.2650
Std. Error of Mean		.00864
Median		54.6000
Mode		73.20
Std. Deviation		14.80179
Variance		219.093
Minimum		18.40
Maximum		230.10
Sum		162259983.70

Figure B52. Frequency Histogram of 5-Axle Vehicles, Site 7169.

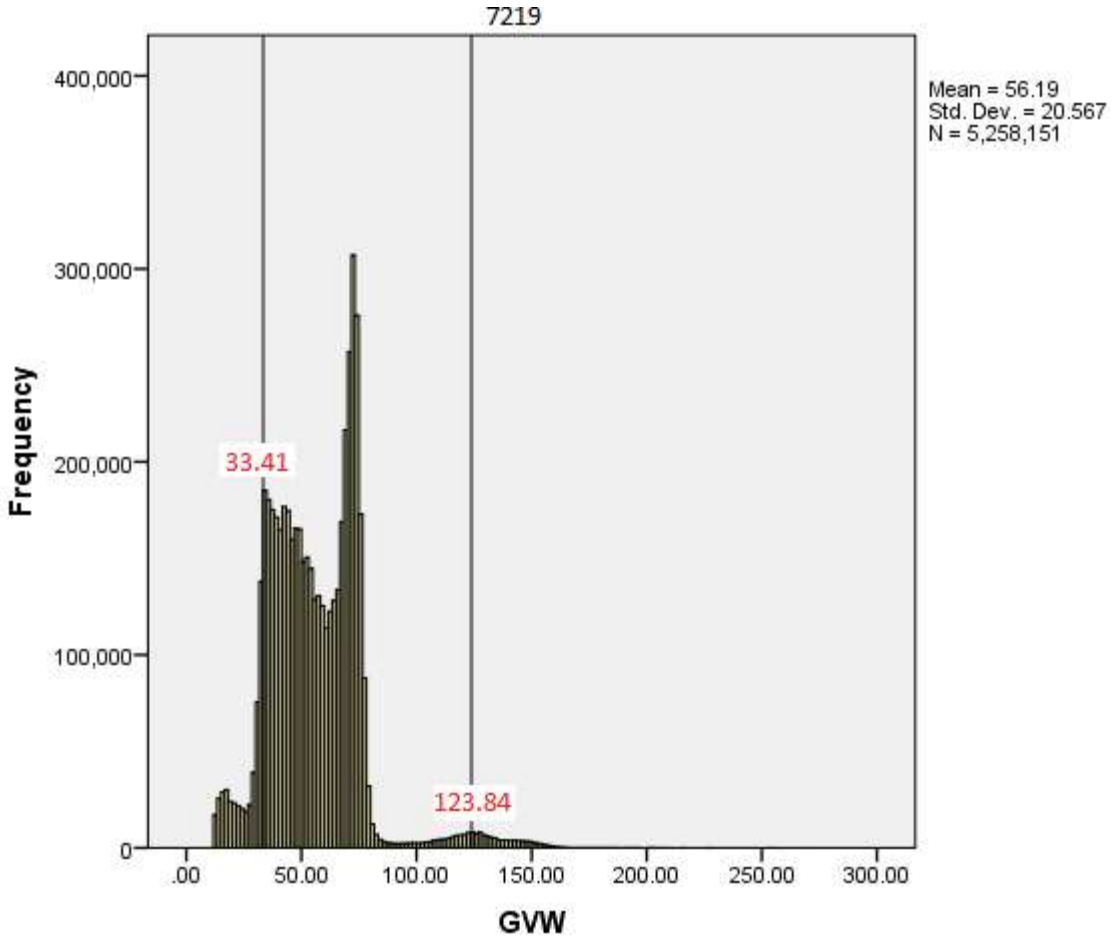

Statistics

GVW

N	Valid	5258151
	Missing	0
Mean		56.1946
Std. Error of Mean		.00897
Median		54.8000
Mode		72.80
Std. Deviation		20.56709
Variance		423.005
Minimum		12.00
Maximum		270.30
Sum		295479447.20

Figure B53. Frequency Histogram of All Vehicles, Site 7219.

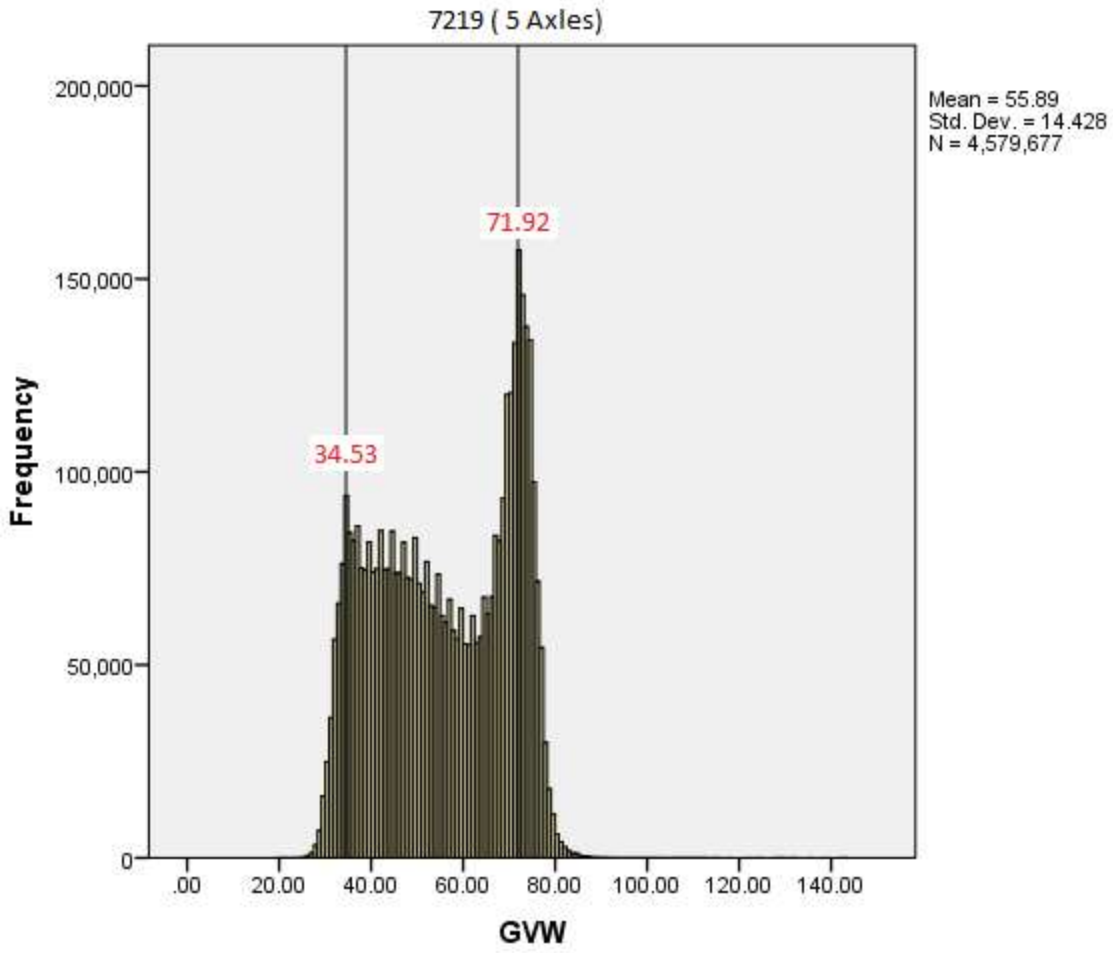

Statistics

GVW

N	Valid	4579677
	Missing	0
Mean		55.8926
Std. Error of Mean		.00674
Median		56.0000
Mode		72.80
Std. Deviation		14.42798
Variance		208.167
Minimum		19.60
Maximum		143.30
Sum		255970219.90

Figure B54. Frequency Histogram of 5-Axle Vehicles, Site 7219.

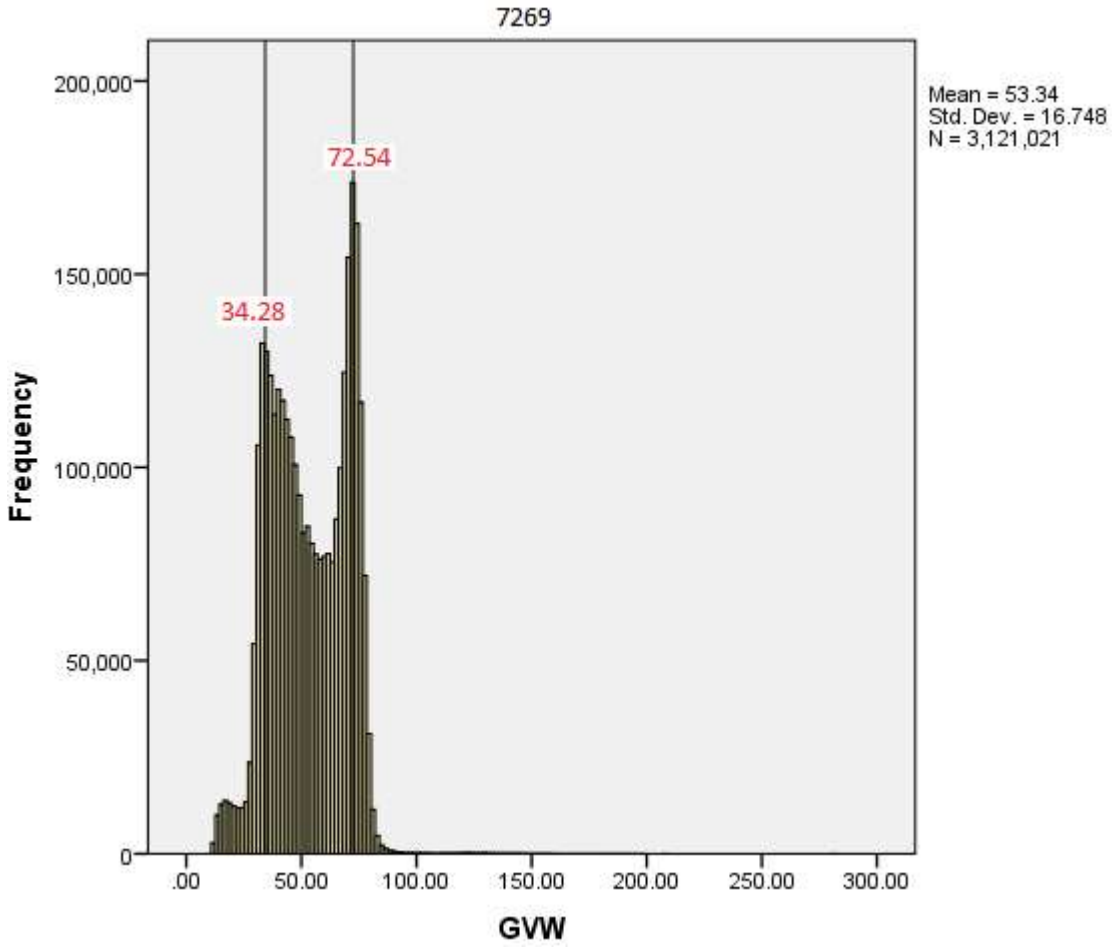

Statistics

GVW

N	Valid	3121021
	Missing	0
Mean		53.3391
Std. Error of Mean		.00948
Median		52.6000
Mode		72.60
Std. Deviation		16.74772
Variance		280.486
Minimum		12.00
Maximum		282.10

Figure B55. Frequency Histogram of All Vehicles, Site 7269.

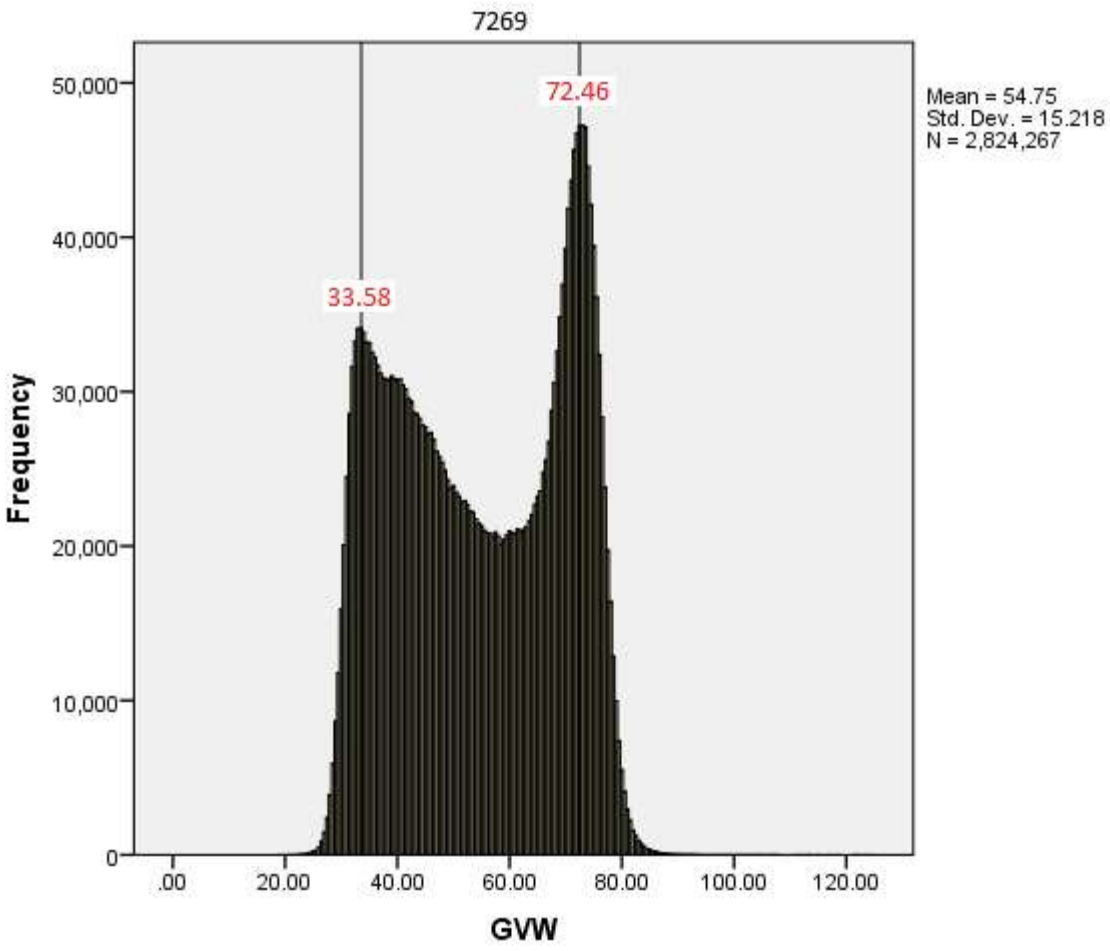

Statistics

GVW

N	Valid	2824267
	Missing	0
Mean		54.7484
Std. Error of Mean		.00906
Median		54.5000
Mode		72.60
Std. Deviation		15.21841
Variance		231.600
Minimum		19.00
Maximum		124.60
Sum		154624191.40

Figure B56. Frequency Histogram of 5-Axle Vehicles, Site 7269.

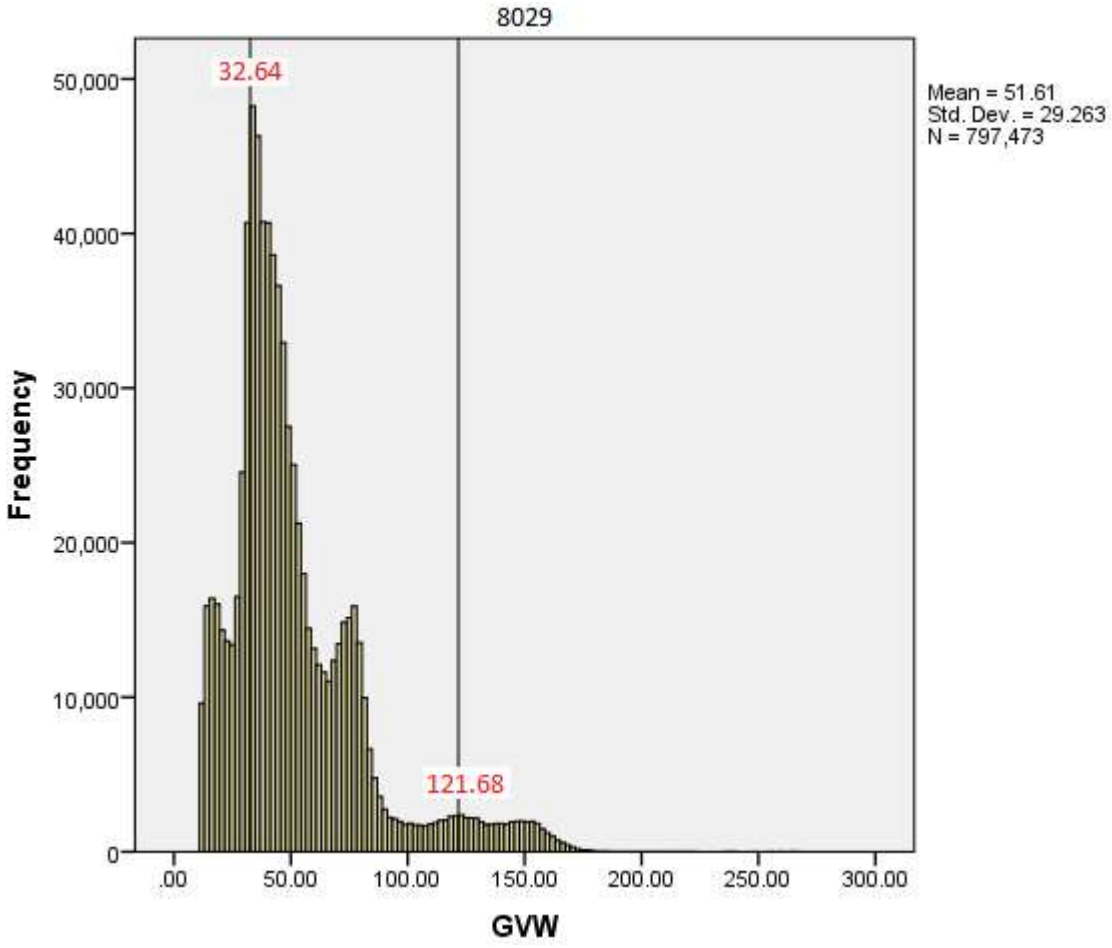

Statistics

GVW

N	Valid	797473
	Missing	0
Mean		51.6122
Std. Error of Mean		.03277
Median		43.6000
Mode		34.10
Std. Deviation		29.26319
Variance		856.334
Minimum		12.00
Maximum		266.50
Sum		41159375.80

Figure B57. Frequency Histogram of All Vehicles, Site 8029.

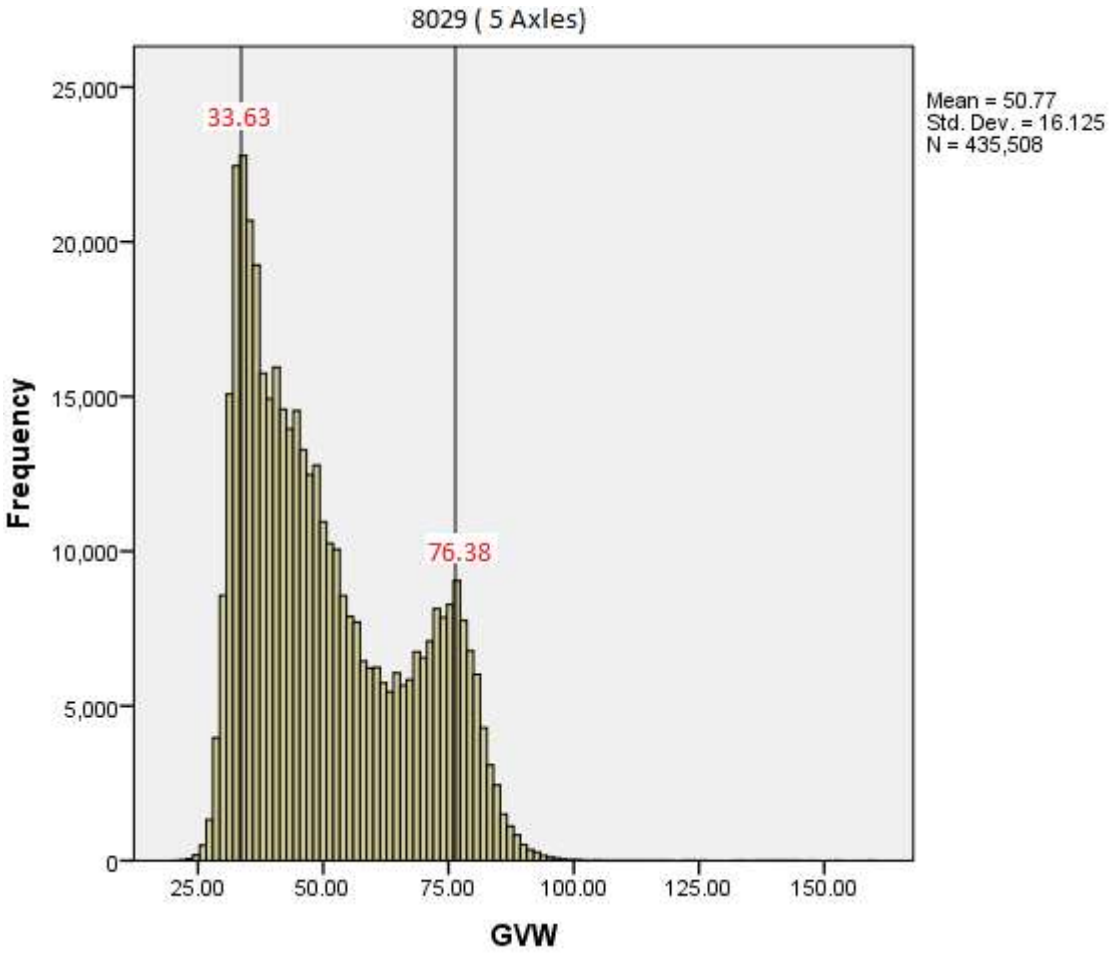

Statistics

GVW

N	Valid	435508
	Missing	0
Mean		50.7652
Std. Error of Mean		.02444
Median		46.6000
Mode		33.70
Std. Deviation		16.12545
Variance		260.030
Minimum		20.20
Maximum		159.90
Sum		22108666.70

Figure B58. Frequency Histogram of 5-Axle Vehicles, Site 8029.

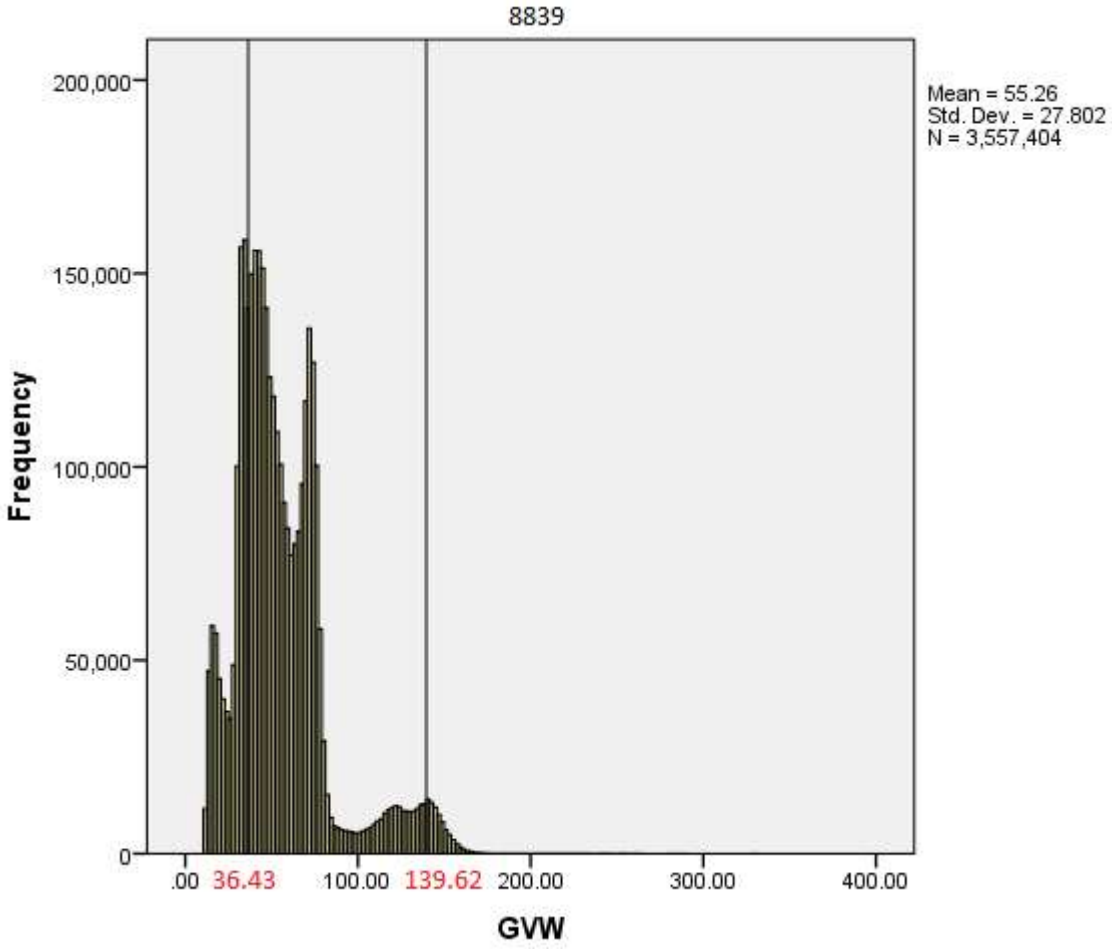

Statistics

GVW

N	Valid	3557404
	Missing	0
Mean		55.2649
Std. Error of Mean		.01474
Median		49.4000
Mode		32.80
Std. Deviation		27.80224
Variance		772.965
Minimum		12.00
Maximum		330.20
Sum		196599610.60

Figure B59. Frequency Histogram of All Vehicles, Site 8839.

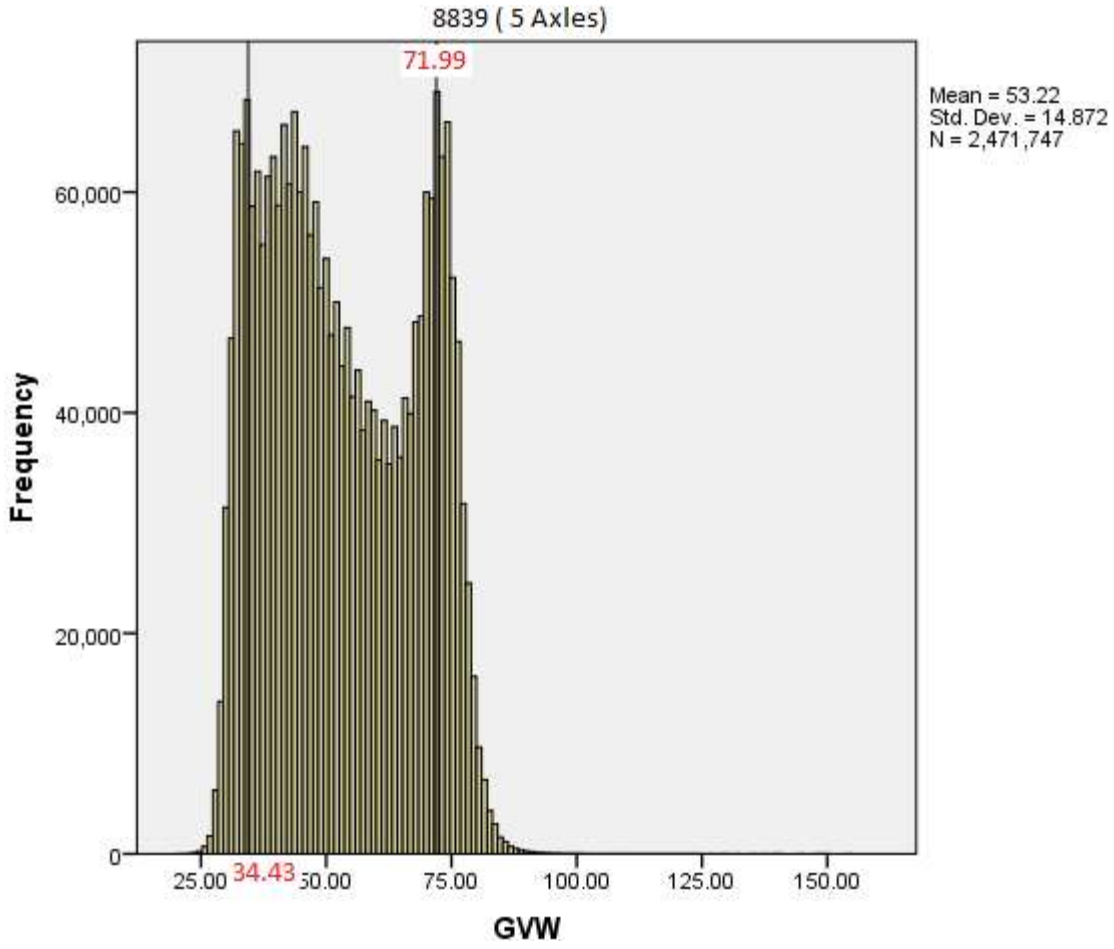

Statistics

GVW

N	Valid	2471747
	Missing	0
Mean		53.2220
Std. Error of Mean		.00946
Median		51.4000
Mode		32.80
Std. Deviation		14.87220
Variance		221.182
Minimum		20.20
Maximum		154.70
Sum		131551373.20

Figure B60. Frequency Histogram of 5-Axle Vehicles, Site 8839.

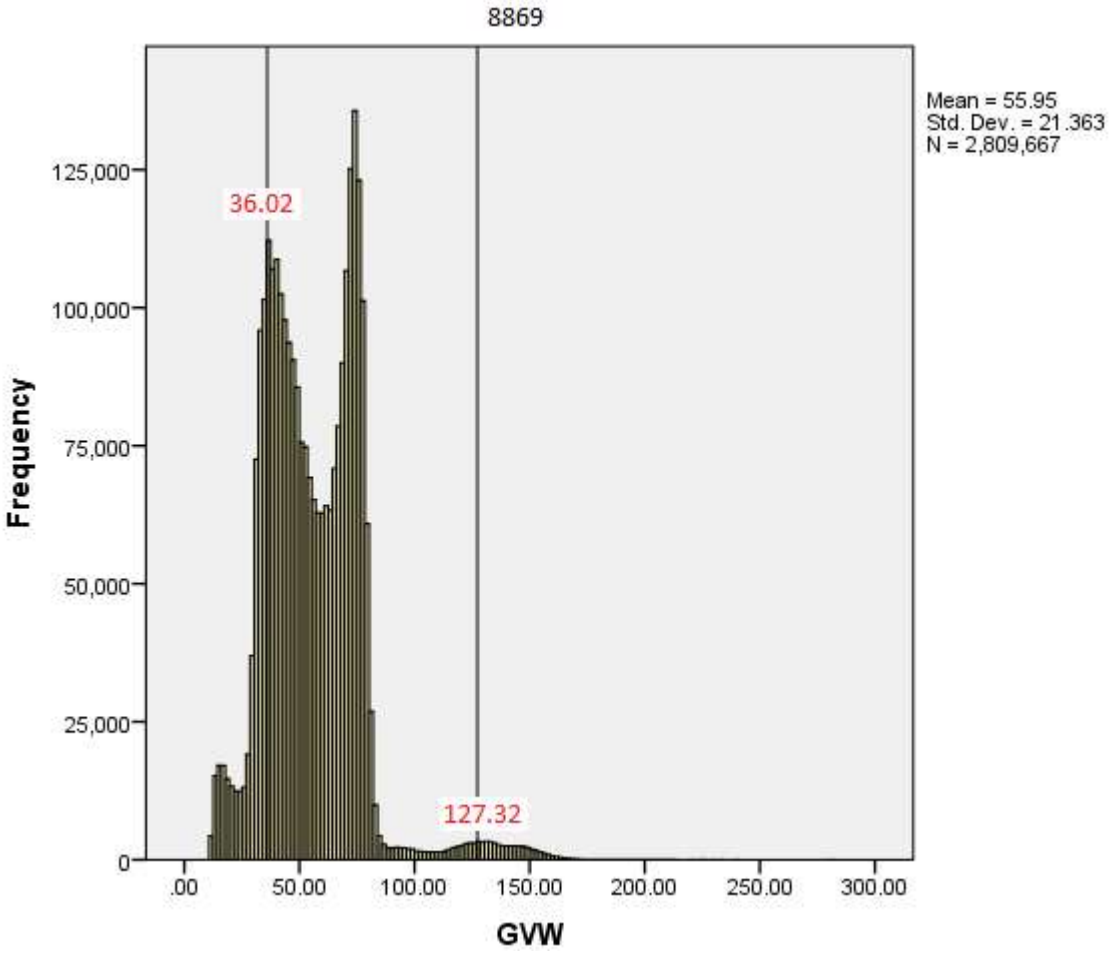

Statistics

GVW

N	Valid	2809667
	Missing	0
Mean		55.9528
Std. Error of Mean		.01275
Median		53.8000
Mode		74.60
Std. Deviation		21.36349
Variance		456.399
Minimum		12.00
Maximum		281.60
Sum		157208696.80

Figure B61. Frequency Histogram of All Vehicles, Site 8869.

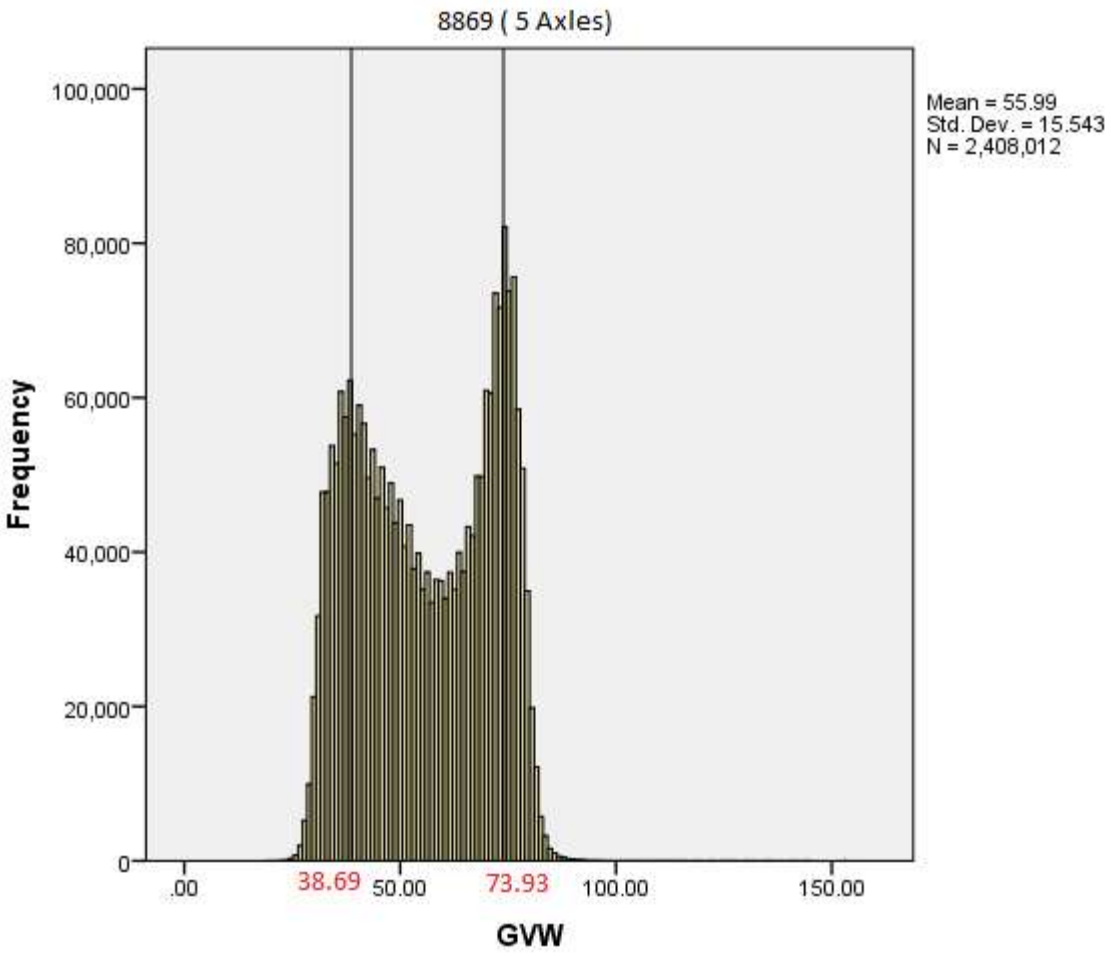

Statistics

GVW

N	Valid	2408012
	Missing	0
Mean		55.9884
Std. Error of Mean		.01002
Median		55.7000
Mode		74.60
Std. Deviation		15.54317
Variance		241.590
Minimum		19.80
Maximum		152.70
Sum		134820756.90

Figure B62. Frequency Histogram of 5-Axle Vehicles, Site 8869.

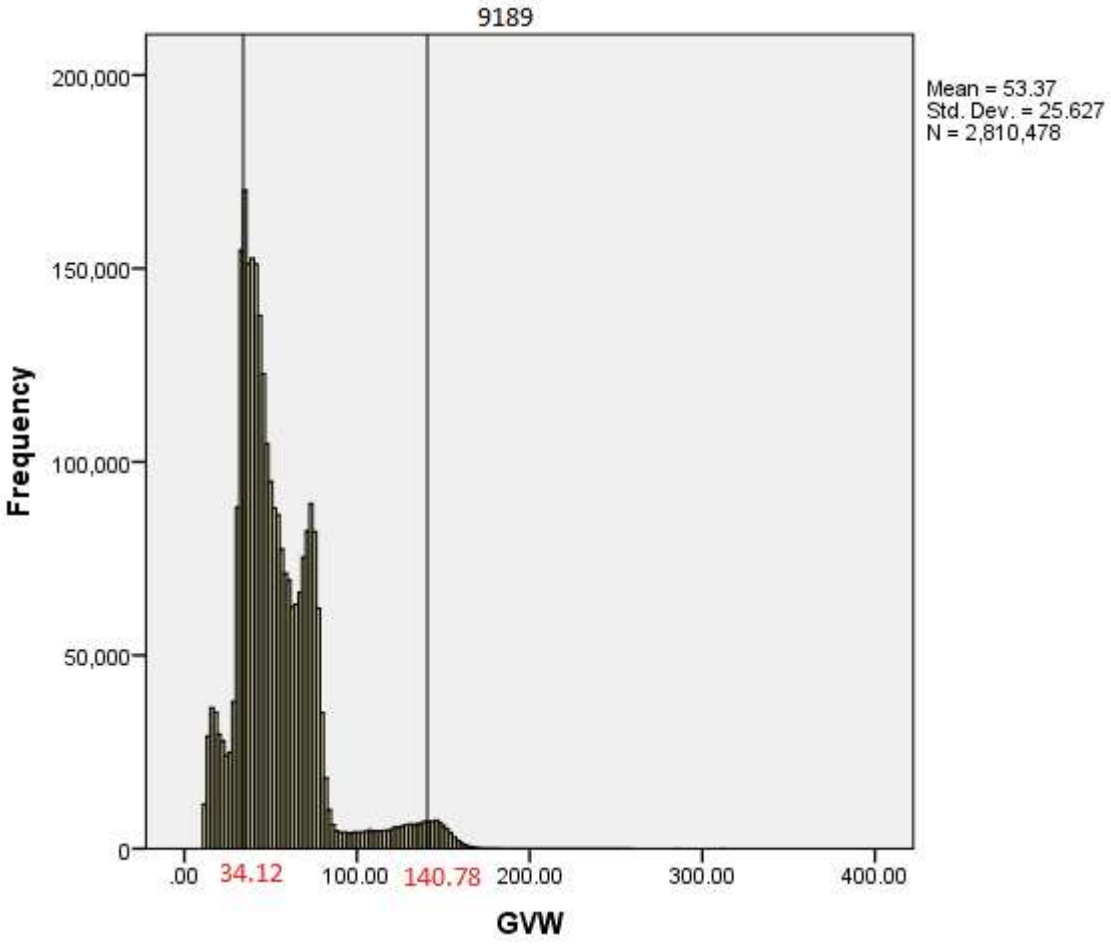

Statistics

GVW

N	Valid	2810478
	Missing	0
Mean		53.3726
Std. Error of Mean		.01529
Median		47.2000
Mode		34.10
Std. Deviation		25.62662
Variance		656.724
Minimum		12.00
Maximum		311.70
Sum		150002426.90

Figure B63. Frequency Histogram of All Vehicles, Site 9189.

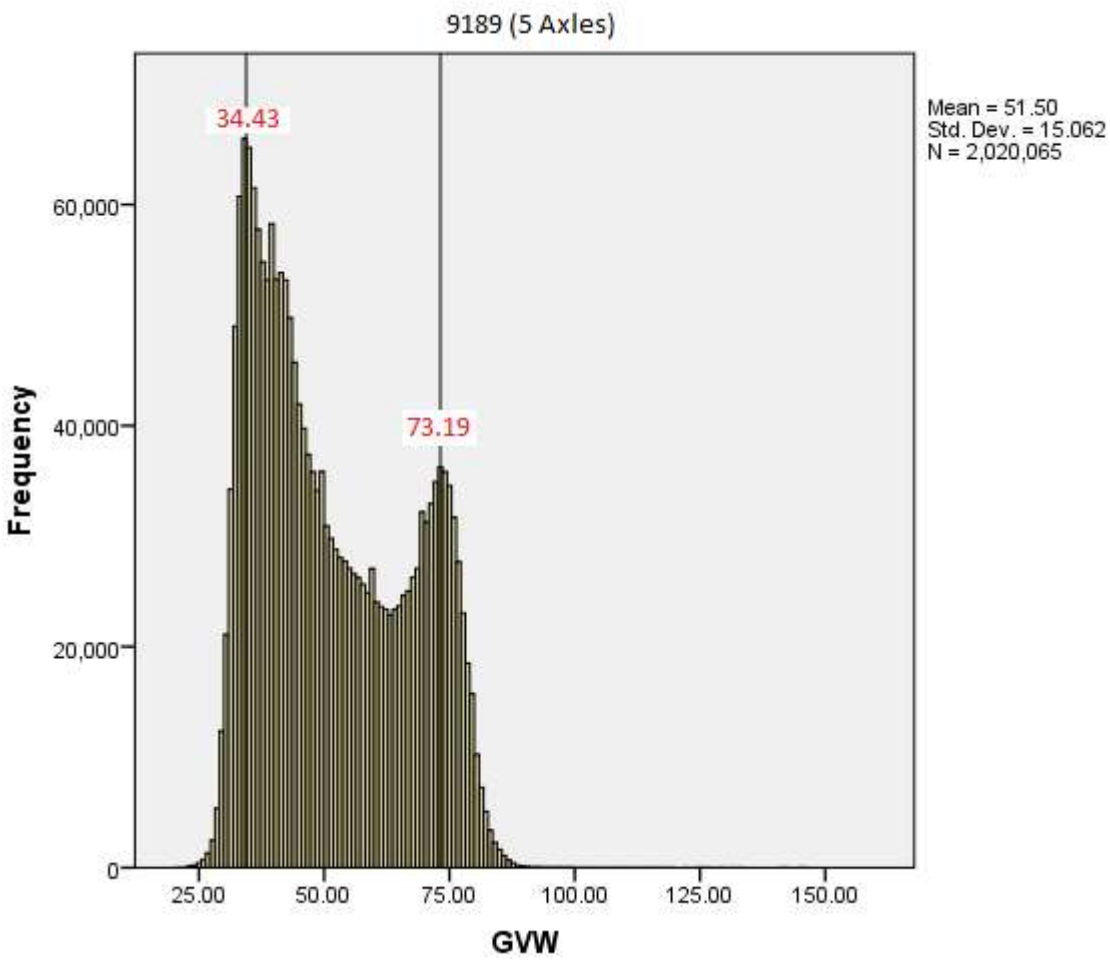

Statistics

GVW

N	Valid	2020065
	Missing	0
Mean		51.5039
Std. Error of Mean		.01060
Median		48.0000
Mode		34.10
Std. Deviation		15.06212
Variance		226.868
Minimum		20.40
Maximum		146.30
Sum		104041173.00

Figure B64. Frequency Histogram of 5-Axle Vehicles, Site 9189.

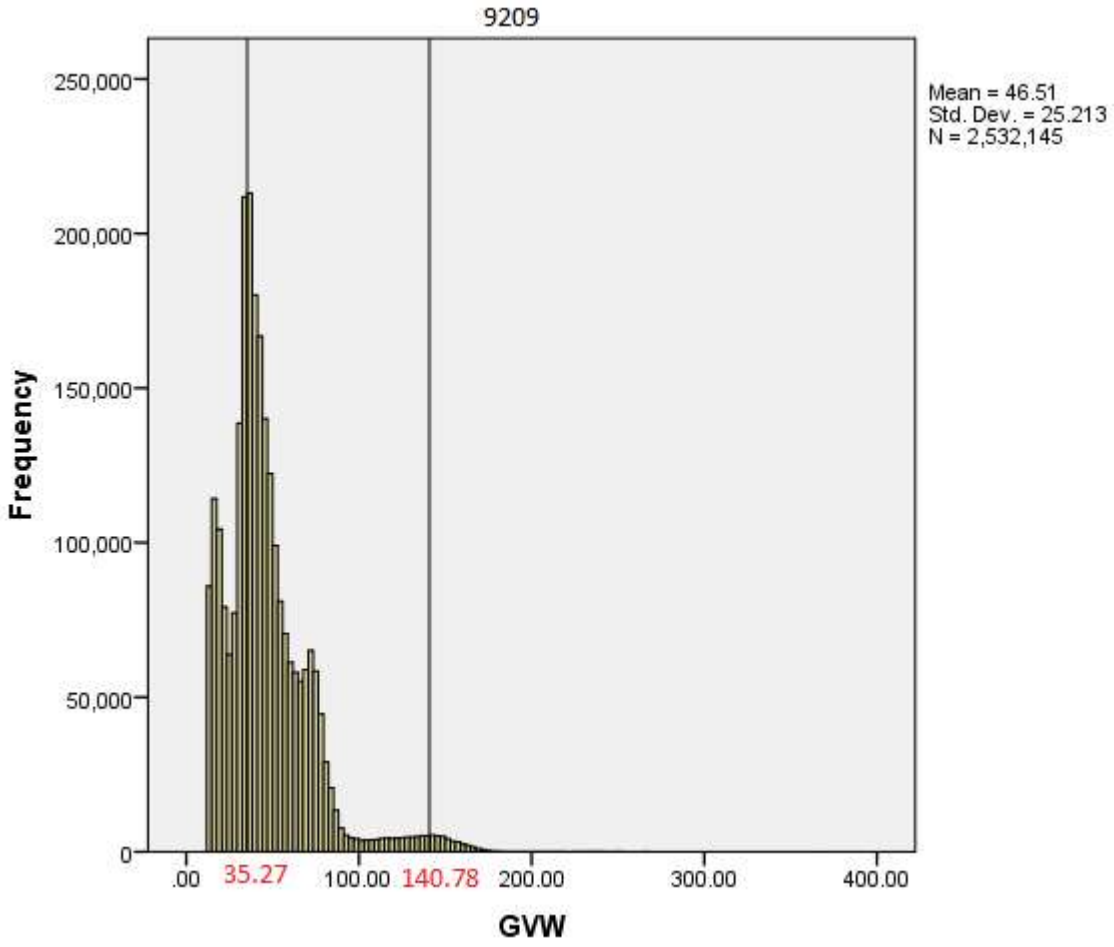

Statistics

GVW

N	Valid	2532145
	Missing	0
Mean		46.5107
Std. Error of Mean		.01584
Median		41.1000
Mode		34.60
Std. Deviation		25.21322
Variance		635.706
Minimum		12.00
Maximum		368.00
Sum		117771897.00

Figure B65. Frequency Histogram of All Vehicles, Site 9209.

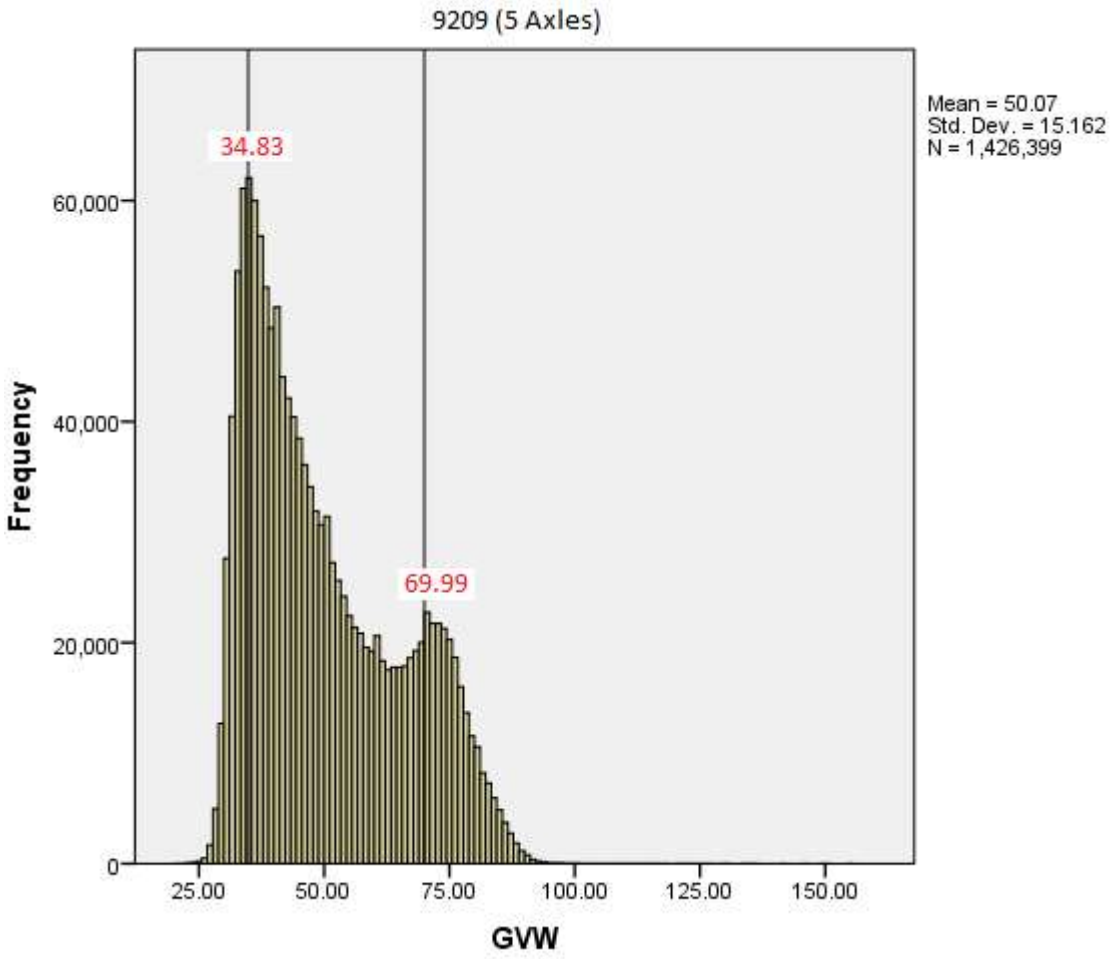

Statistics

GVW

N	Valid	1426399
	Missing	0
Mean		50.0682
Std. Error of Mean		.01270
Median		46.0000
Mode		34.60
Std. Deviation		15.16247
Variance		229.901
Minimum		20.00
Maximum		154.70
Sum		71417267.80

Figure B66. Frequency Histogram of 5-Axle Vehicles, Site 9209.

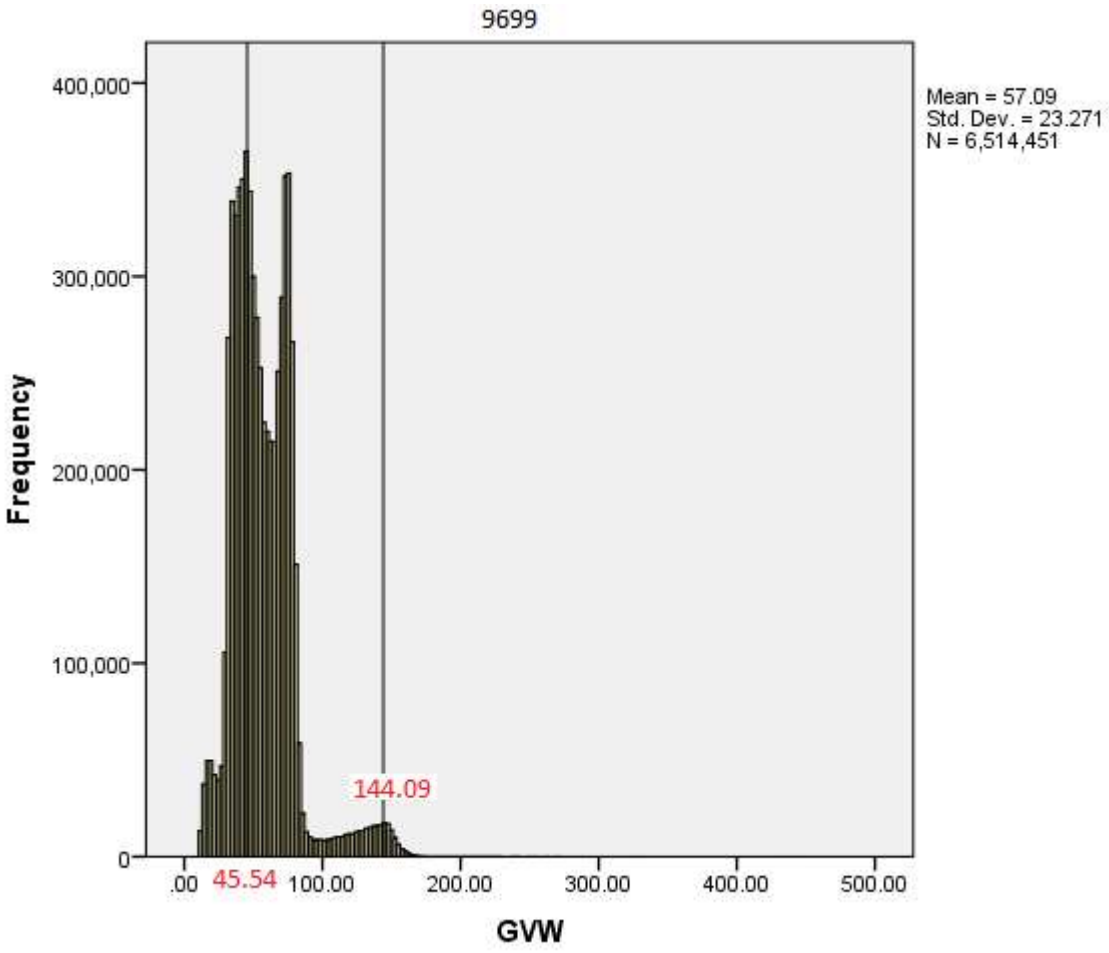

Statistics

GVW

N	Valid	6514451
	Missing	0
Mean		57.0938
Std. Error of Mean		.00912
Median		53.3000
Mode		43.50
Std. Deviation		23.27135
Variance		541.556
Minimum		12.00
Maximum		437.80
Sum		371934812.00

Figure B67. Frequency Histogram of All Vehicles, Site 9699.

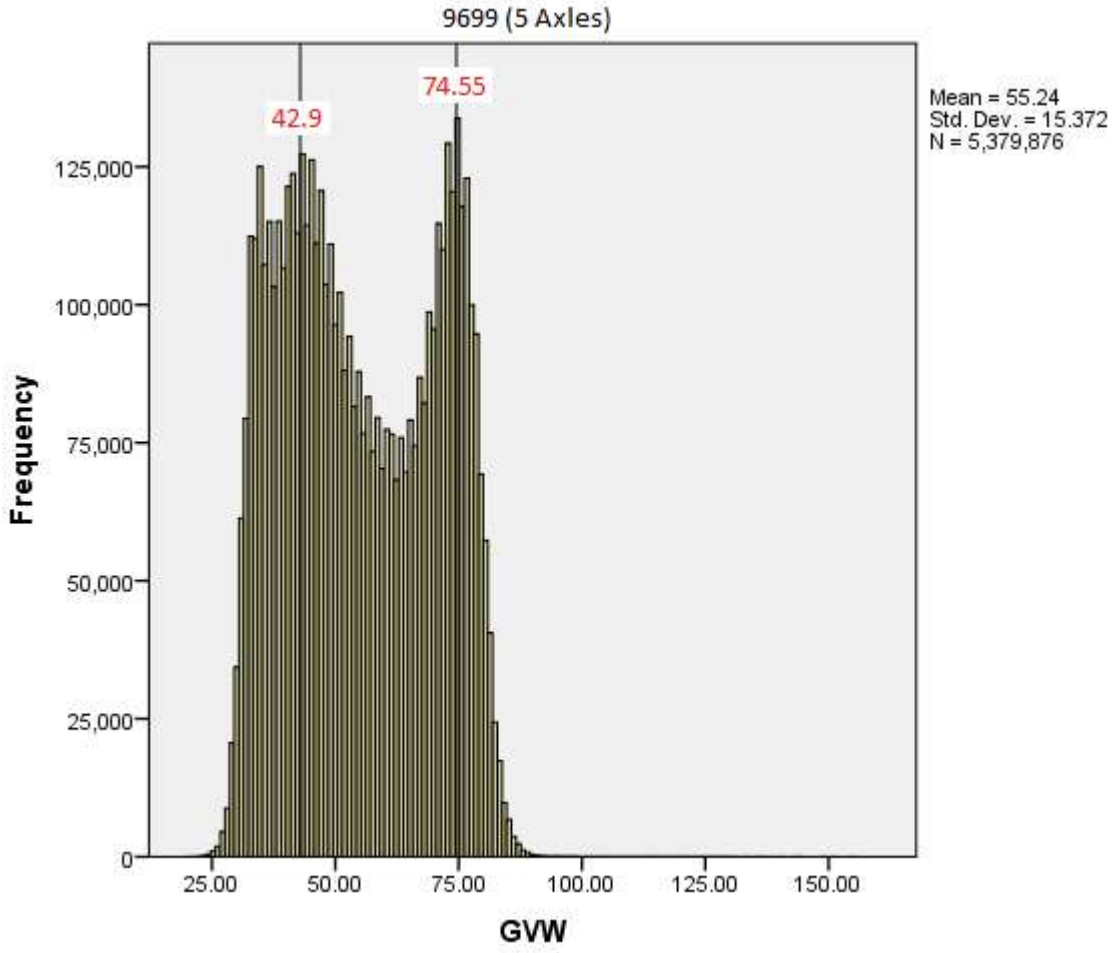

Statistics

GVW

N	Valid	5379876
	Missing	0
Mean		55.2406
Std. Error of Mean		.00663
Median		53.6000
Mode		74.30
Std. Deviation		15.37201
Variance		236.299
Minimum		20.00
Maximum		154.60
Sum		297187542.90

Figure B68. Frequency Histogram of 5-Axle Vehicles, Site 9699.

APPENDIX C: VEHICLE LOAD EFFECTS

Table C1. Vehicle Load Effects Summary.

			Single Lane (Following) Load Effects, Simple Span					
	Moment				Shear			
Span	Mean	COV	Min.	Max.	Mean	COV	Min.	Max.
20	92	0.39	28	717	22	0.38	5	158
100	936	0.45	148	7088	39	0.46	10	247
400	8355	0.40	1016	39199	60	0.52	23	628
			Single Lane (Following) Load Effects Continuous Span					
	Moment				Shear			
Span	Mean	COV	Min.	Max.	Mean	COV	Min.	Max.
20	69	0.38	6	333	22	0.36	6	124
100	433	0.47	15	1330	40	0.43	10	296
400	2651	0.53	150	18097	62	0.52	12	624
			Two Lane Load Effects, Simple Span					
	Moment				Shear			
Span	Mean	COV	Min.	Max.	Mean	COV	Min.	Max.
20	39	0.38	4	500	8	0.44	1	123
100	249	0.42	27	2835	18	0.44	2	242
400	11002	0.41	875	96040	108	0.41	9	971
			Two Lane Load Effects Continuous Span					
	Moment				Shear			
Span	Mean	COV	Min.	Max.	Mean	COV	Min.	Max.
20	26	0.42	3	272	8	0.40	1	99
100	190	0.41	16	1659	16	0.50	1	226
400	4762	0.41	366	39950	101	0.41	9	928

Table C2. Comparison of Single Vehicle and Following Load Effects.

Single Vehicle Simple Moment				
Span	Mean	COV	Minimum	Maximum
20	93	0.35	28	620
50	317	0.39	71	2458
100	895	0.44	141	5891
200	2267	0.43	284	12777
300	3646	0.43	425	19678
400	5024	0.43	561	26605

Following Vehicles Simple Moment				
Span	Mean	COV	Minimum	Maximum
20	93	0.39	28	717
50	318	0.43	71	2698
100	936	0.45	148	7088
200	3500	0.39	392	18416
300	5929	0.40	637	29330
400	8355	0.40	1016	39199

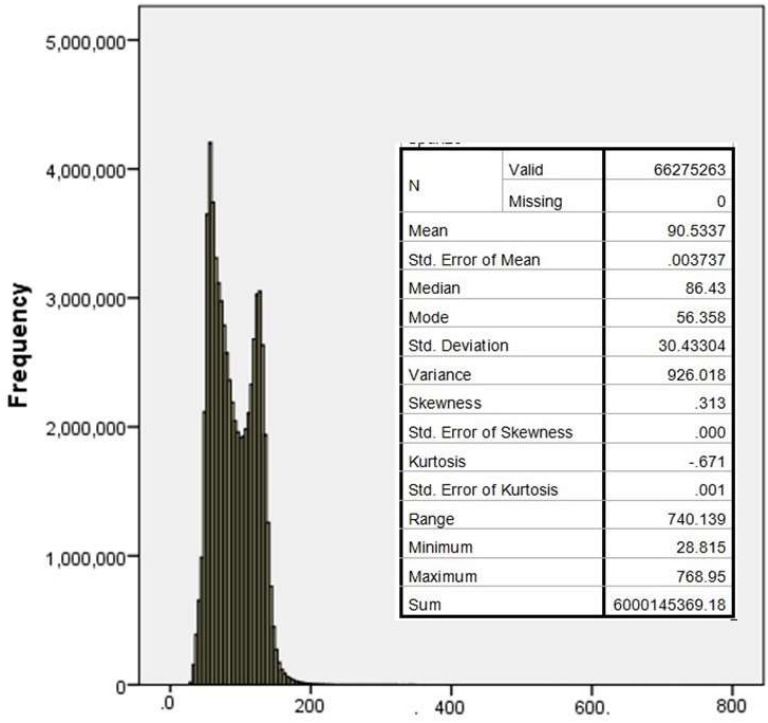

Figure C1. Frequency Histogram of Single Vehicle Moments, 20 ft Simple Span.

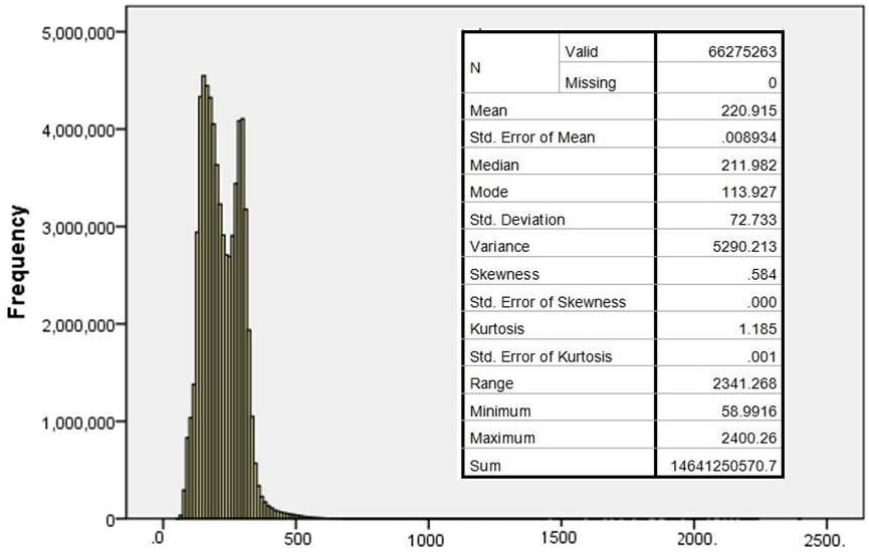

N	Valid	66275263
	Missing	0
Mean		220.915
Std. Error of Mean		.008934
Median		211.982
Mode		113.927
Std. Deviation		72.733
Variance		5290.213
Skewness		.584
Std. Error of Skewness		.000
Kurtosis		1.185
Std. Error of Kurtosis		.001
Range		2341.268
Minimum		58.9916
Maximum		2400.26
Sum		14641250570.7

Figure C2. Frequency Histogram of Single Vehicle Moments, 40 ft Simple Span.

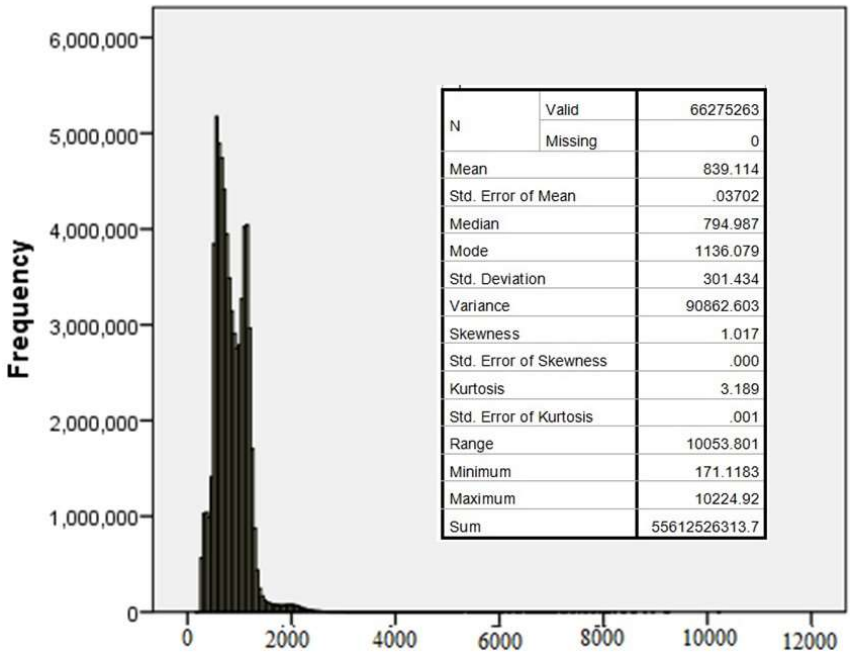

N	Valid	66275263
	Missing	0
Mean		839.114
Std. Error of Mean		.03702
Median		794.987
Mode		1136.079
Std. Deviation		301.434
Variance		90862.603
Skewness		1.017
Std. Error of Skewness		.000
Kurtosis		3.189
Std. Error of Kurtosis		.001
Range		10053.801
Minimum		171.1183
Maximum		10224.92
Sum		55612526313.7

Figure C3. Frequency Histogram of Single Vehicle Moments, 100 ft Simple Span.

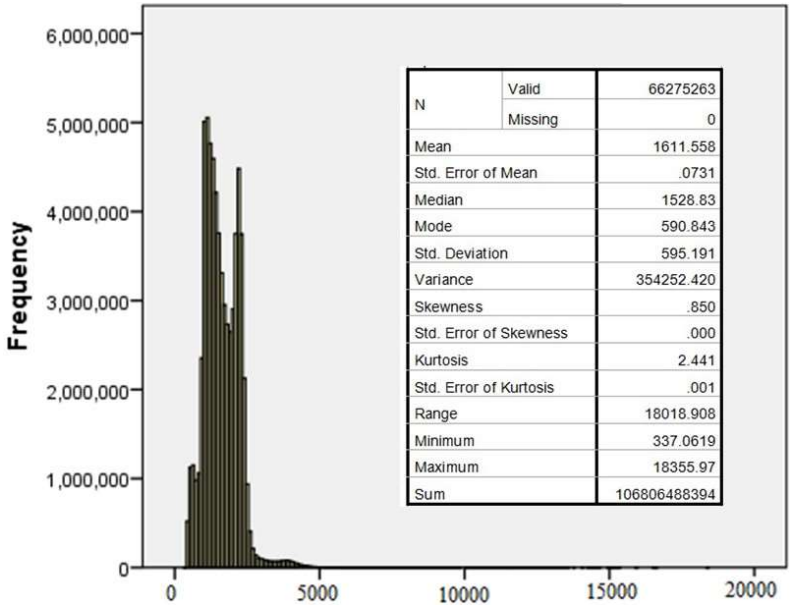

N	Valid	66275263
	Missing	0
Mean		1611.558
Std. Error of Mean		.0731
Median		1528.83
Mode		590.843
Std. Deviation		595.191
Variance		354252.420
Skewness		.850
Std. Error of Skewness		.000
Kurtosis		2.441
Std. Error of Kurtosis		.001
Range		18018.908
Minimum		337.0619
Maximum		18355.97
Sum		106806488394

Figure C4. Frequency Histogram of Single Vehicle Moments, 160 ft Simple Span.

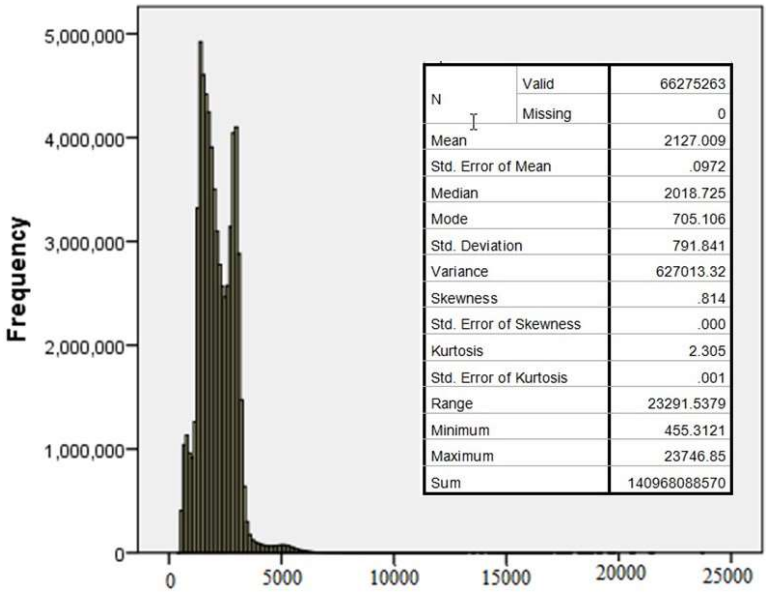

N	Valid	66275263
	Missing	0
Mean		2127.009
Std. Error of Mean		.0972
Median		2018.725
Mode		705.106
Std. Deviation		791.841
Variance		627013.32
Skewness		.814
Std. Error of Skewness		.000
Kurtosis		2.305
Std. Error of Kurtosis		.001
Range		23291.5379
Minimum		455.3121
Maximum		23746.85
Sum		140968088570

Figure C5. Frequency Histogram of Single Vehicle Moments, 200 ft Simple Span.

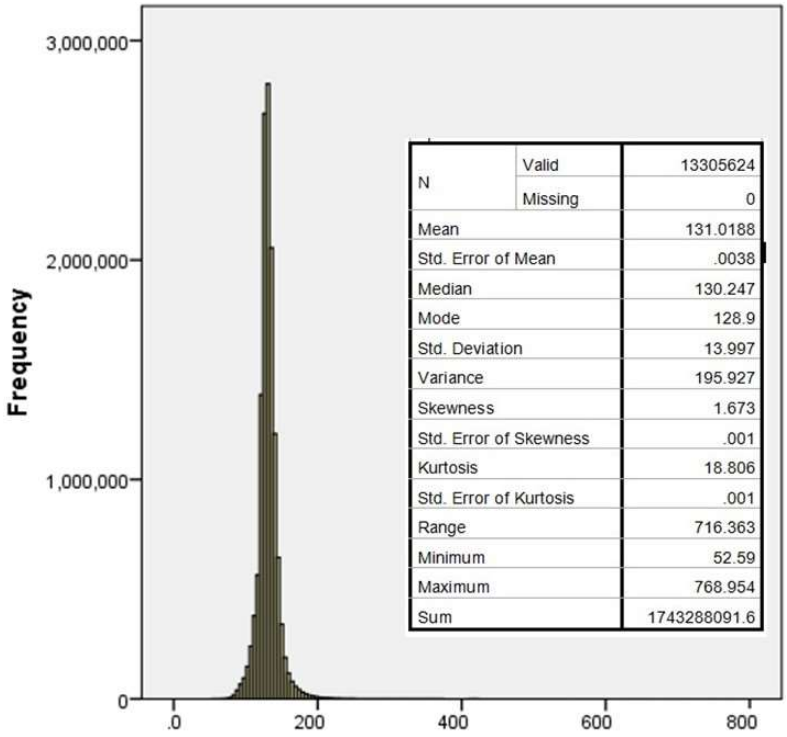

N	Valid	13305624
	Missing	0
Mean		131.0188
Std. Error of Mean		.0038
Median		130.247
Mode		128.9
Std. Deviation		13.997
Variance		195.927
Skewness		1.673
Std. Error of Skewness		.001
Kurtosis		18.806
Std. Error of Kurtosis		.001
Range		716.363
Minimum		52.59
Maximum		768.954
Sum		1743288091.6

Figure C6. Frequency Histogram of Top 20% of Single Vehicle Moments, 20 ft Simple Span.

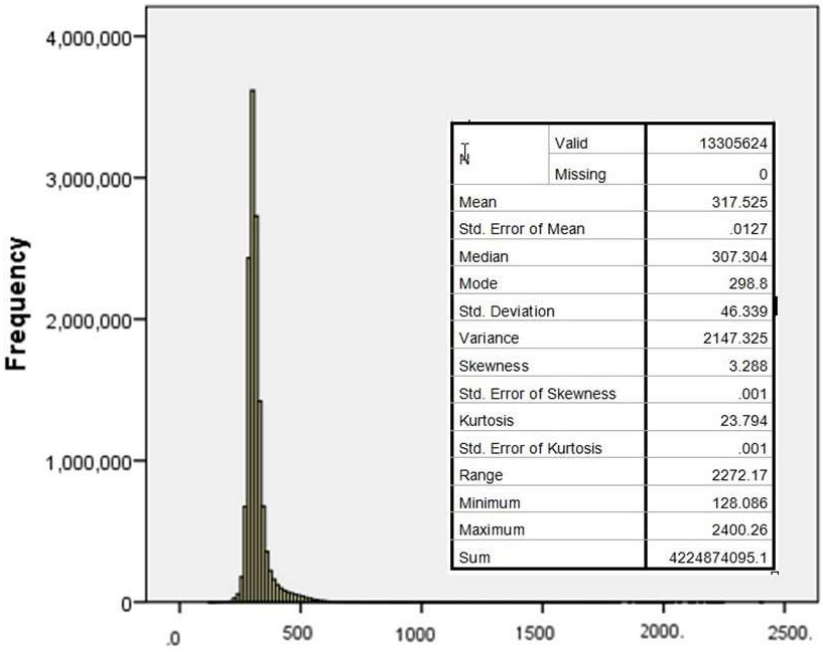

T N	Valid	13305624
	Missing	0
Mean		317.525
Std. Error of Mean		.0127
Median		307.304
Mode		298.8
Std. Deviation		46.339
Variance		2147.325
Skewness		3.288
Std. Error of Skewness		.001
Kurtosis		23.794
Std. Error of Kurtosis		.001
Range		2272.17
Minimum		128.086
Maximum		2400.26
Sum		4224874095.1

Figure C7. Frequency Histogram of Top 20% of Single Vehicle Moments, 40 ft Simple Span.

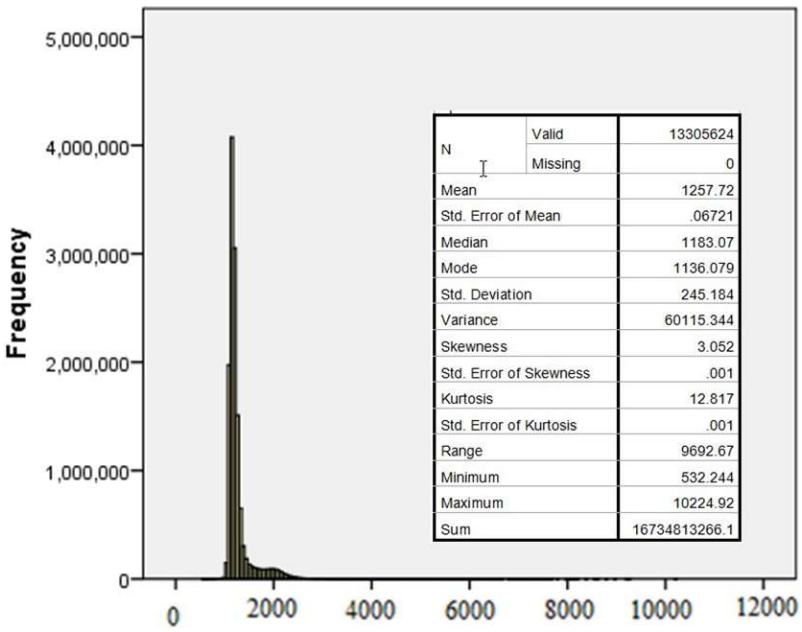

N	Valid	13305624
	Missing	0
Mean		1257.72
Std. Error of Mean		.06721
Median		1183.07
Mode		1136.079
Std. Deviation		245.184
Variance		60115.344
Skewness		3.052
Std. Error of Skewness		.001
Kurtosis		12.817
Std. Error of Kurtosis		.001
Range		9692.67
Minimum		532.244
Maximum		10224.92
Sum		16734813266.1

Figure C8. Frequency Histogram of Top 20% of Single Vehicle Moments, 100 ft Simple Span.

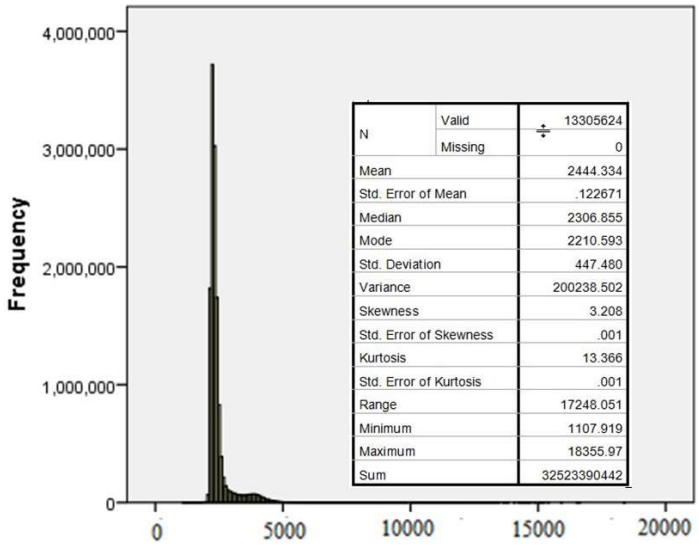

N	Valid	13305624
	Missing	0
Mean		2444.334
Std. Error of Mean		.122671
Median		2306.855
Mode		2210.593
Std. Deviation		447.480
Variance		200238.502
Skewness		3.208
Std. Error of Skewness		.001
Kurtosis		13.366
Std. Error of Kurtosis		.001
Range		17248.051
Minimum		1107.919
Maximum		18355.97
Sum		32523390442

Figure C9. Frequency Histogram of Top 20% of Single Vehicle Moments, 160 ft Simple Span.

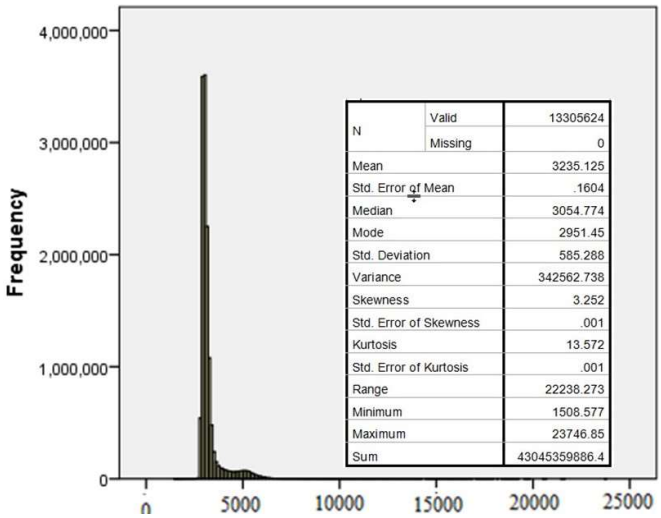

Figure C10. Frequency Histogram of Top 20% of Single Vehicle Moments, 200 ft Simple Span.

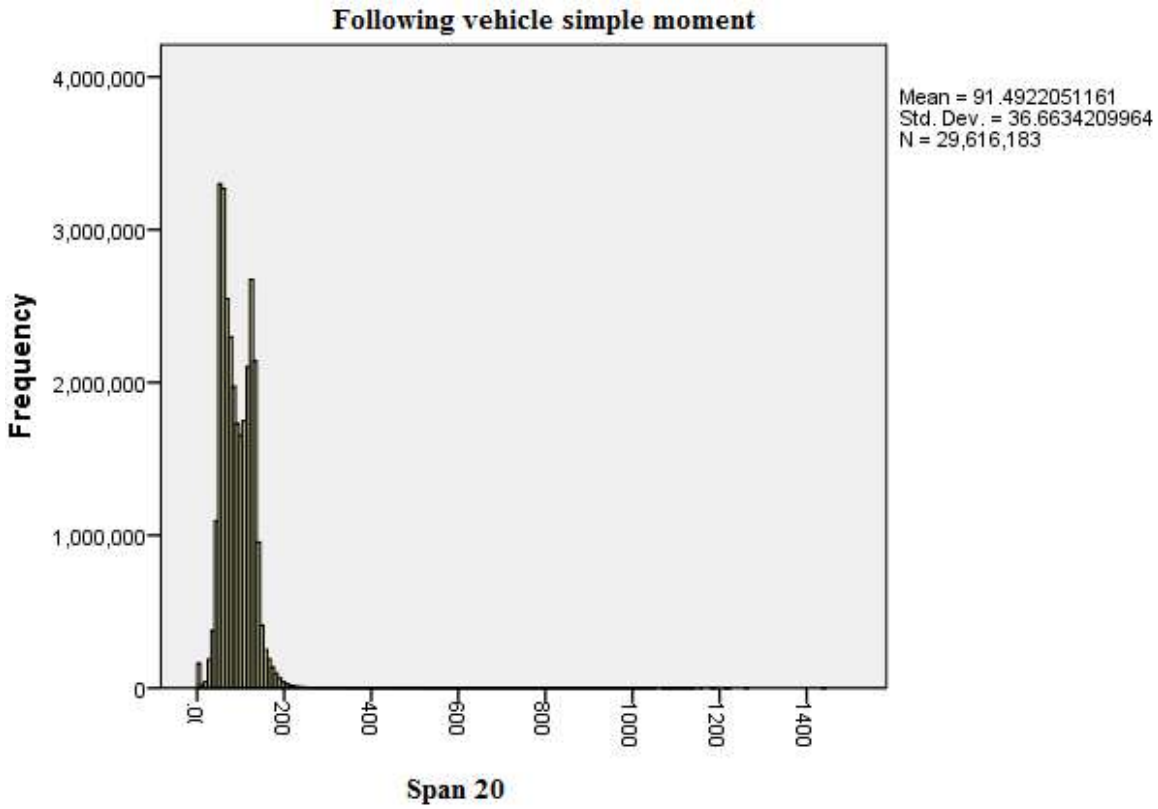

Statistics

Span20

N	Valid	29314766
	Missing	0
Mean		92.2845
Median		87.34475
Mode		55.86
Std. Deviation		35.7285
Variance		1276.527
Range		688.6745
Minimum		28.1815
Maximum		716.856

Figure C11. Single Lane (Following) Moment, 20’ Simple Span.

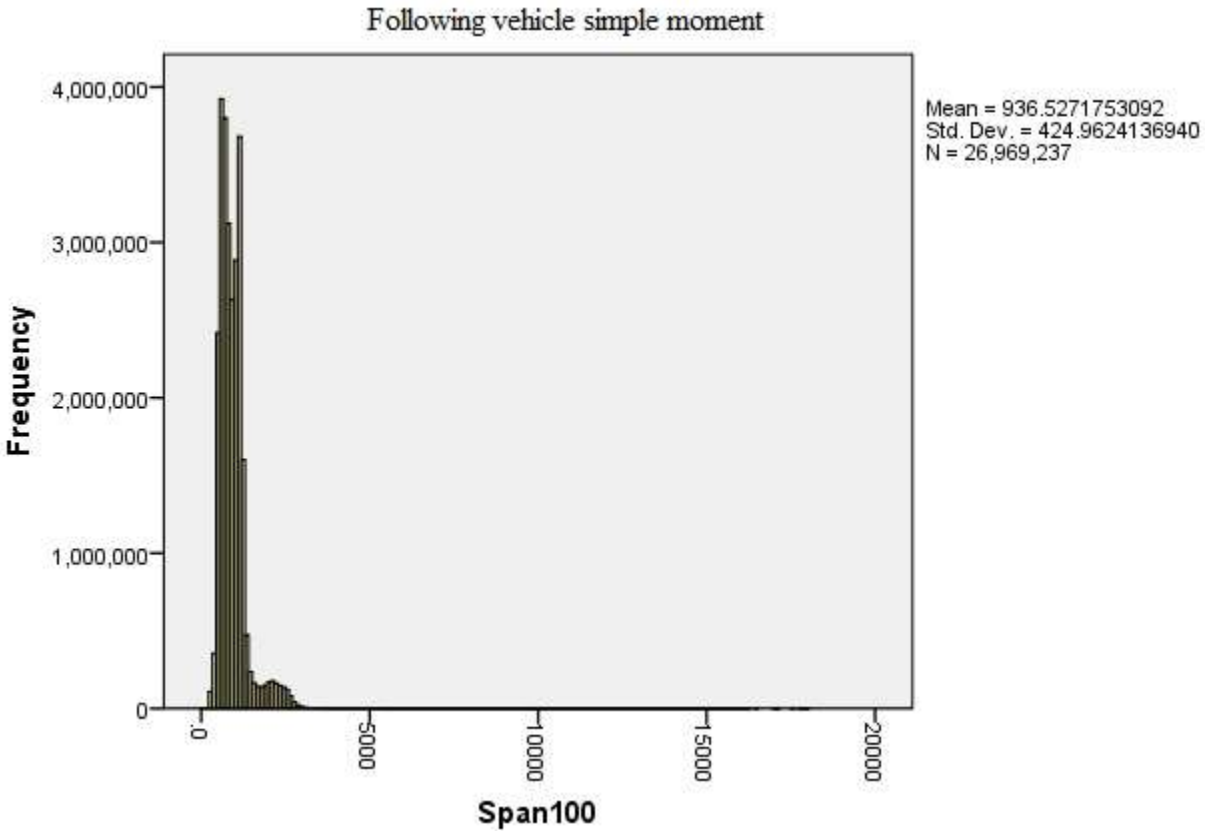

Statistics

Span100

N	Valid	26962016
	Missing	0
Mean		936.03384
Median		859.77975
Mode		1106.497
Std. Deviation		417.92848
Variance		174664.217
Range		6940.1895
Minimum		148.0295
Maximum		7088.219

Figure C12. Single Lane (Following) Moment, 100’ Simple Span.

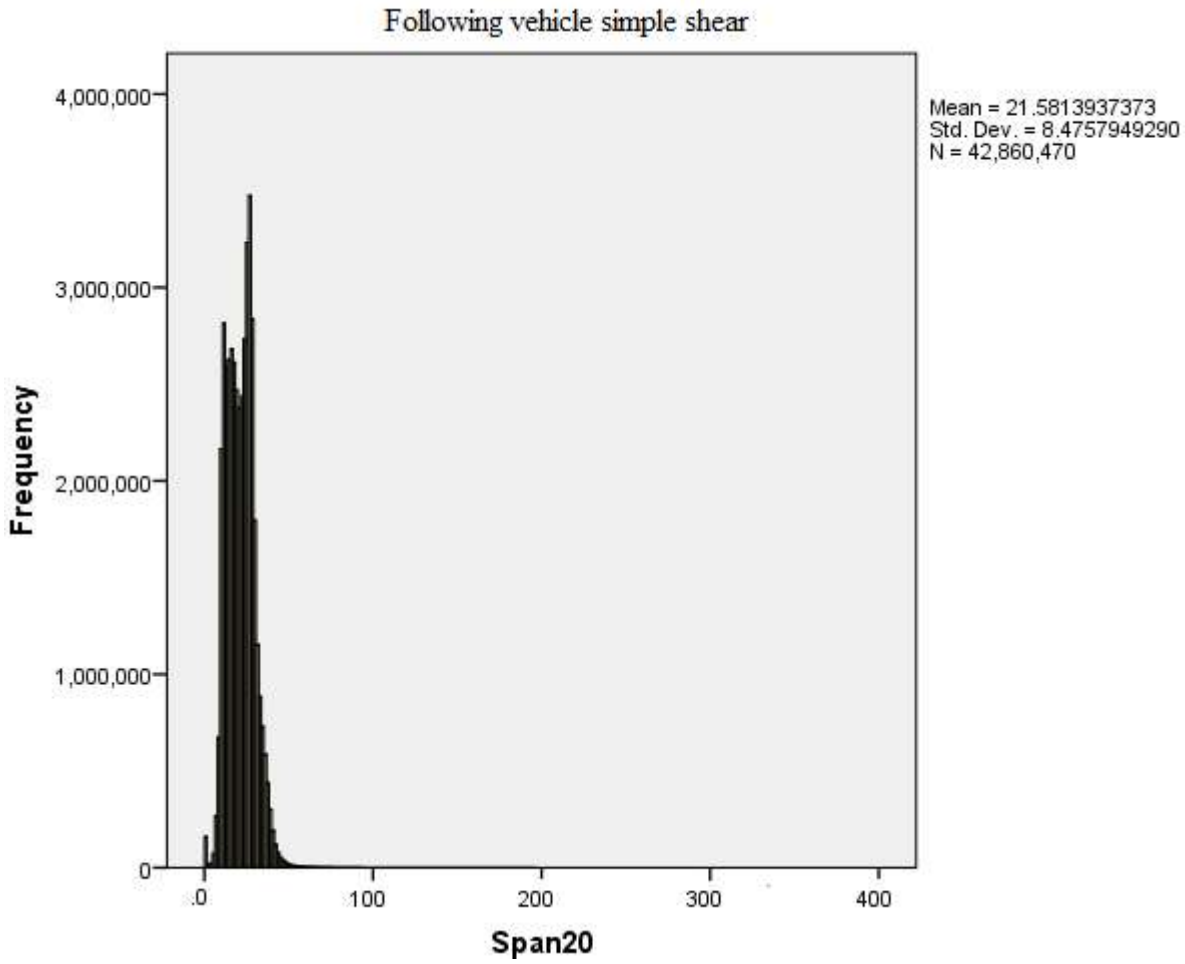

Statistics

Span20

N	Valid	42643736
	Missing	0
Mean		21.6783
Median		21.5203
Mode		10.27425
Std. Deviation		8.326430
Variance		69.329
Range		152.680687
Minimum		5.009213
Maximum		157.6899

Figure C13. Single Lane (Following) Shear, 20’ Simple Span.

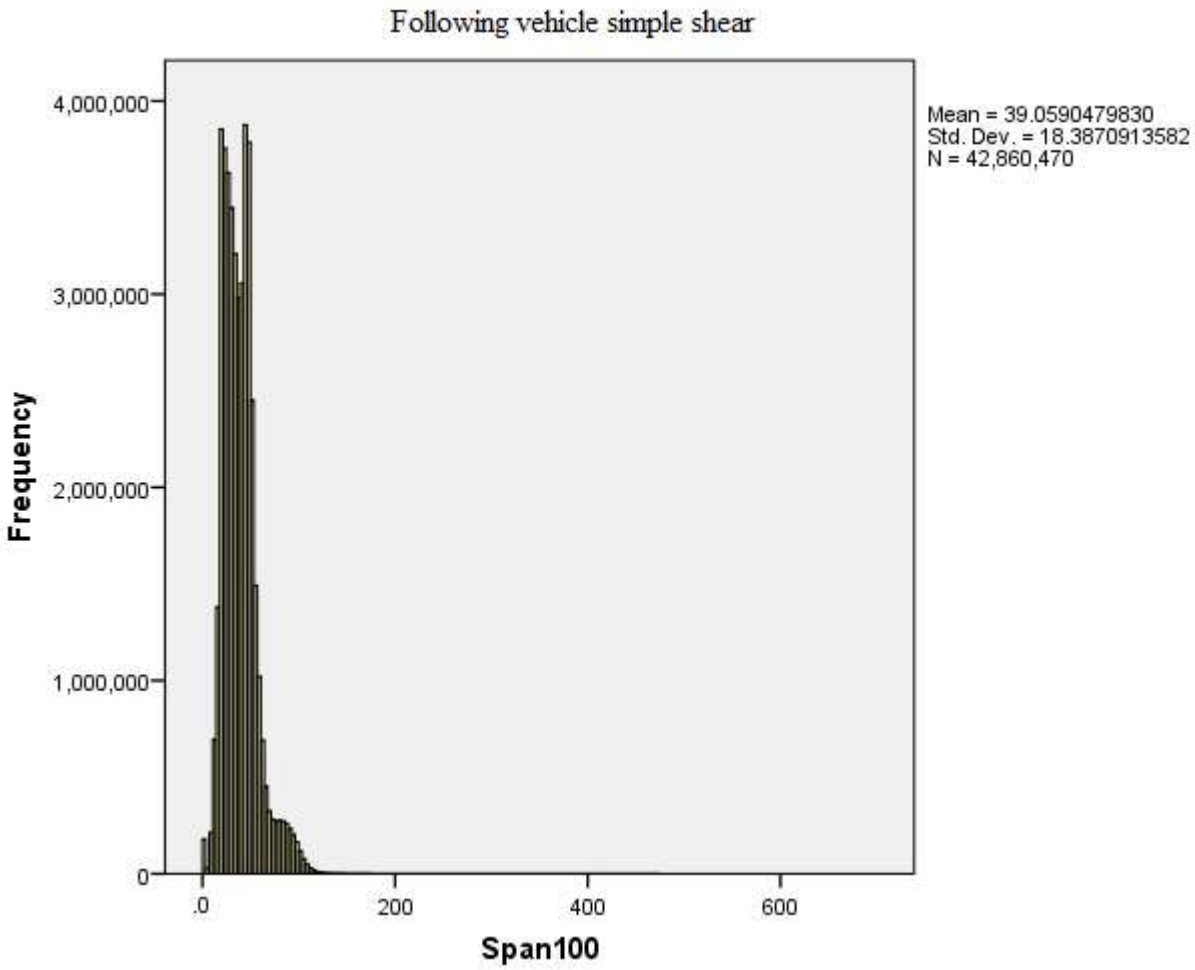

Statistics

Span100

N	Valid	42471020
	Missing	0
Mean		39.32824
Median		37.1555
Mode		27.24753
Std. Deviation		17.851
Variance		318.686
Range		236.5455
Minimum		10.2392
Maximum		246.7848

Figure C14. Single Lane (Following) Shear, 100’ Simple Span.

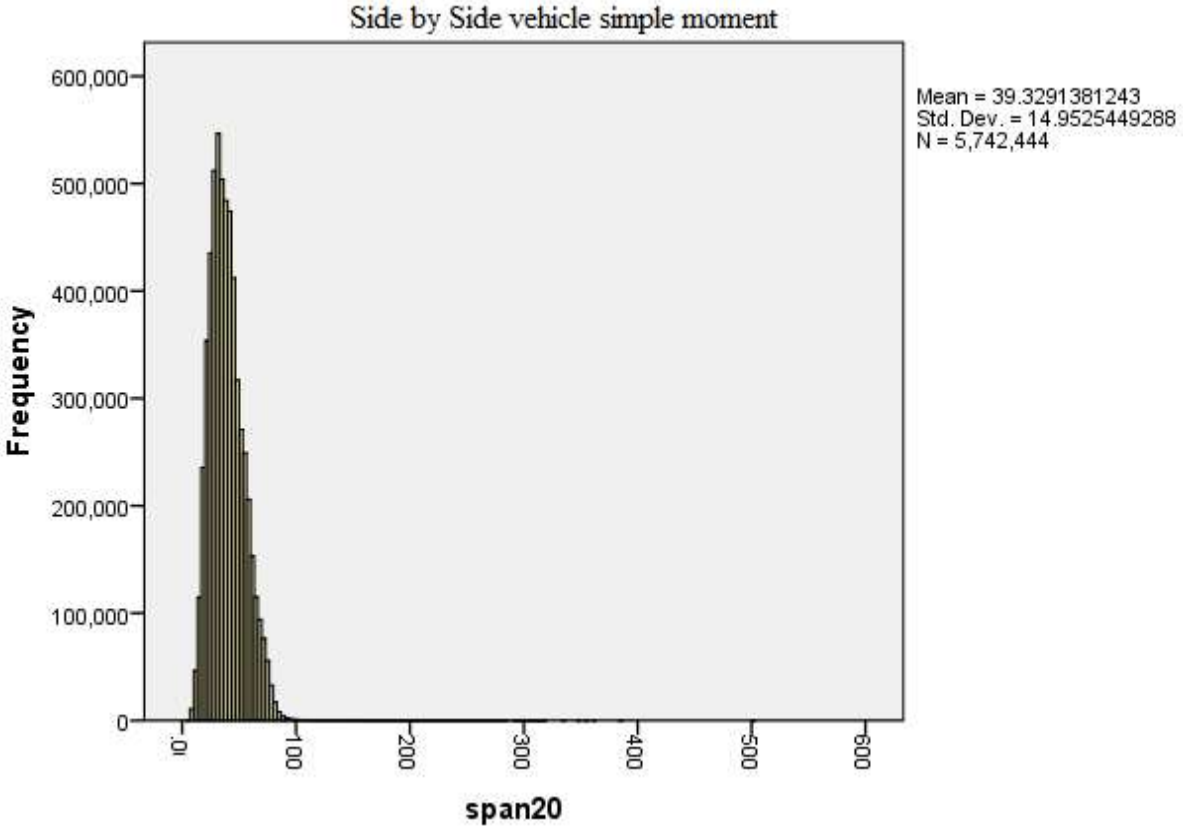

Statistics

span20

N	Valid	5742444
	Missing	0
Mean		39.3291
Std. Error of Mean		.006239
Median		37.427093
Mode		39.228443
Std. Deviation		14.95254712
Variance		223.579
Minimum		3.9134401000
Maximum		500.283260
Sum		225845373.246

Figure C15. Two Lane Moment, 20’ Simple Span.

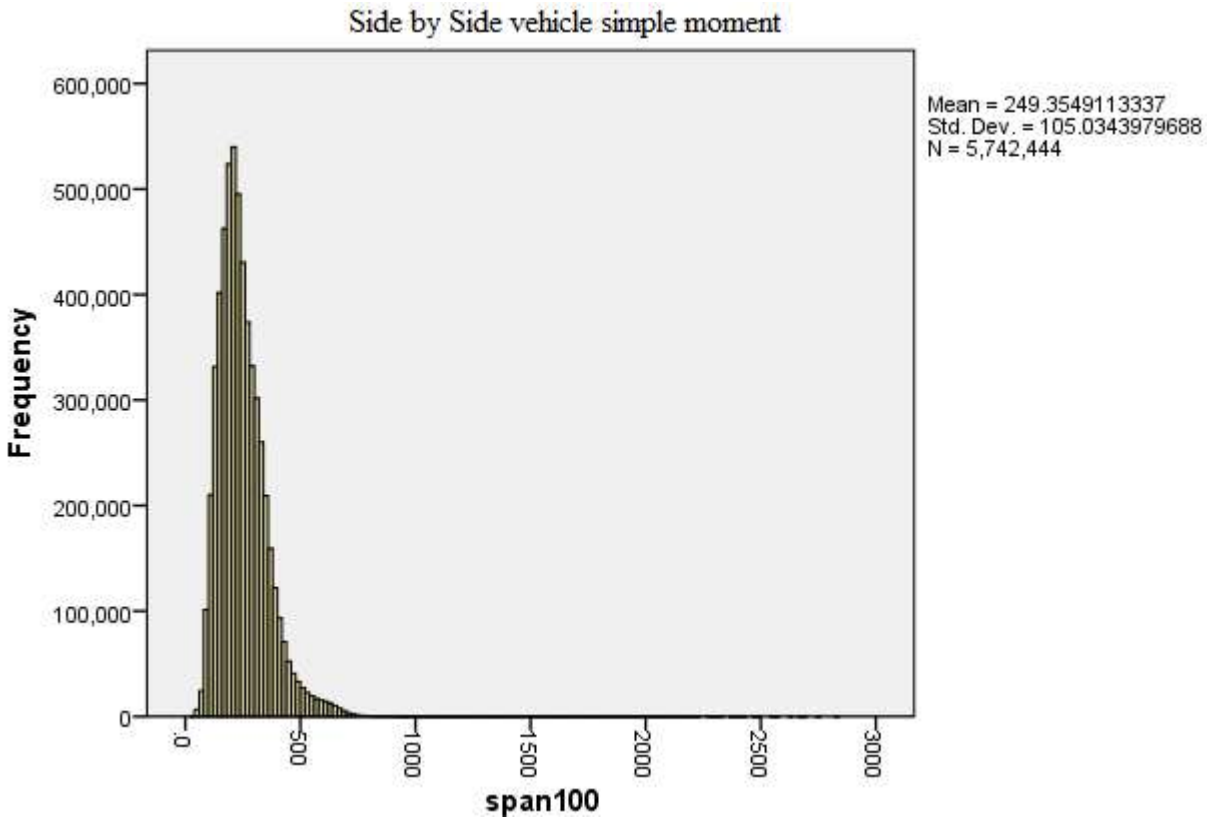

Statistics

span100

N	Valid	5742444
	Missing	0
Mean		249.35491
Std. Error of Mean		.04383111
Median		230.5138455
Mode		289.734312
Std. Deviation		105.03439
Variance		11032.225
Minimum		26.5046
Maximum		2834.5623
Sum		1431906614.45

Figure C16. Two Lane Moment, 100’ Simple Span.

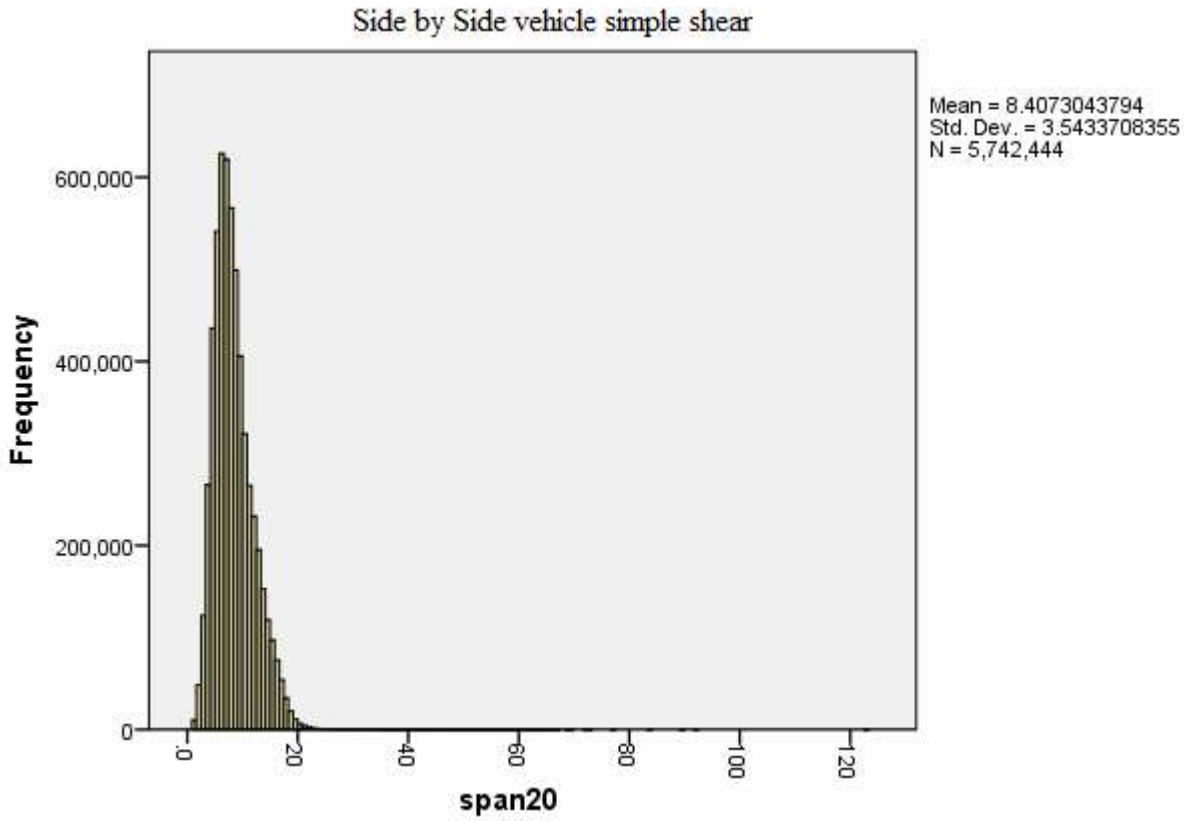

Statistics

span20

N	Valid	5742444
	Missing	0
Mean		8.407
Std. Error of Mean		.001478
Median		7.7848
Mode		7.22
Std. Deviation		3.54332
Variance		12.555
Minimum		.89371
Maximum		123.203
Sum		48278474.58

Figure C17. Two Lane Shear, 20’ Simple Span.

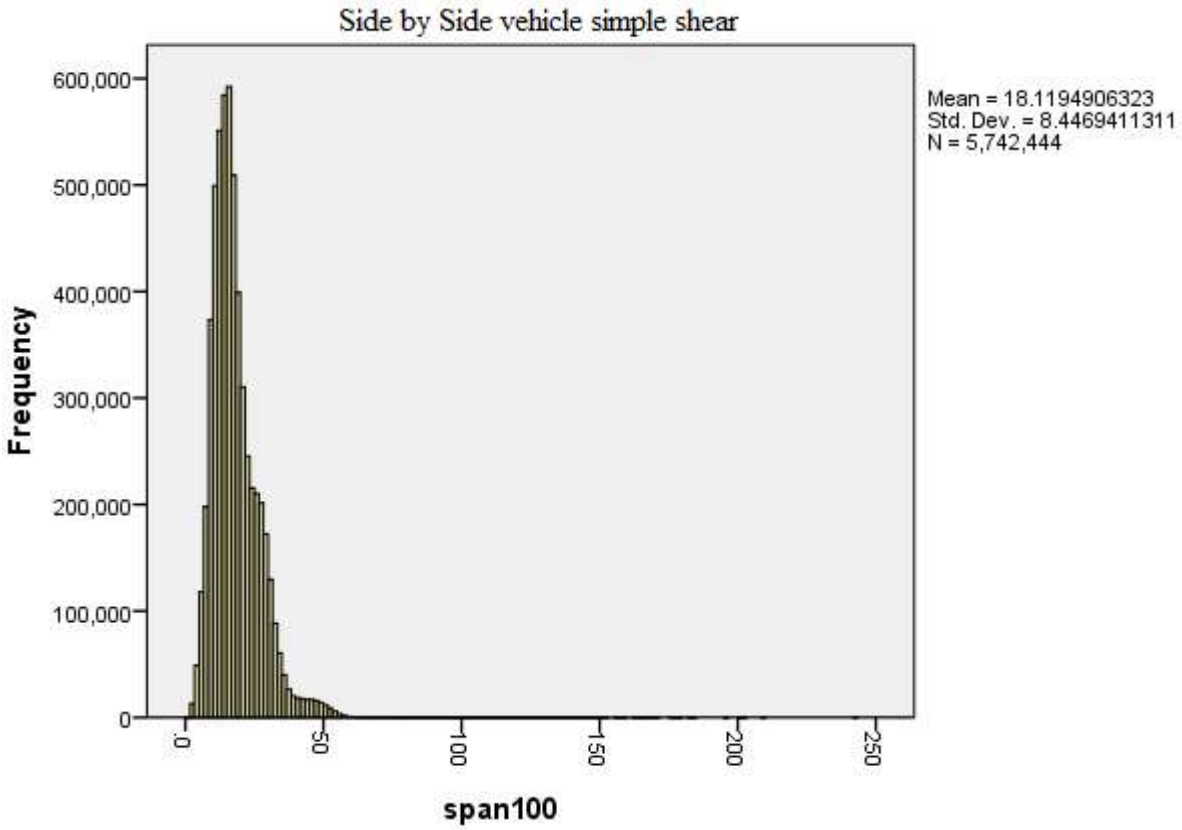

Statistics

span100

N	Valid	5742444
	Missing	0
Mean		18.1194
Std. Error of Mean		.0035249
Median		16.3531240
Mode		15.7166
Std. Deviation		8.4469
Variance		71.351
Minimum		1.3582
Maximum		241.817
Sum		104050160.26

Figure C18. Two Lane Shear, 100’ Simple Span.

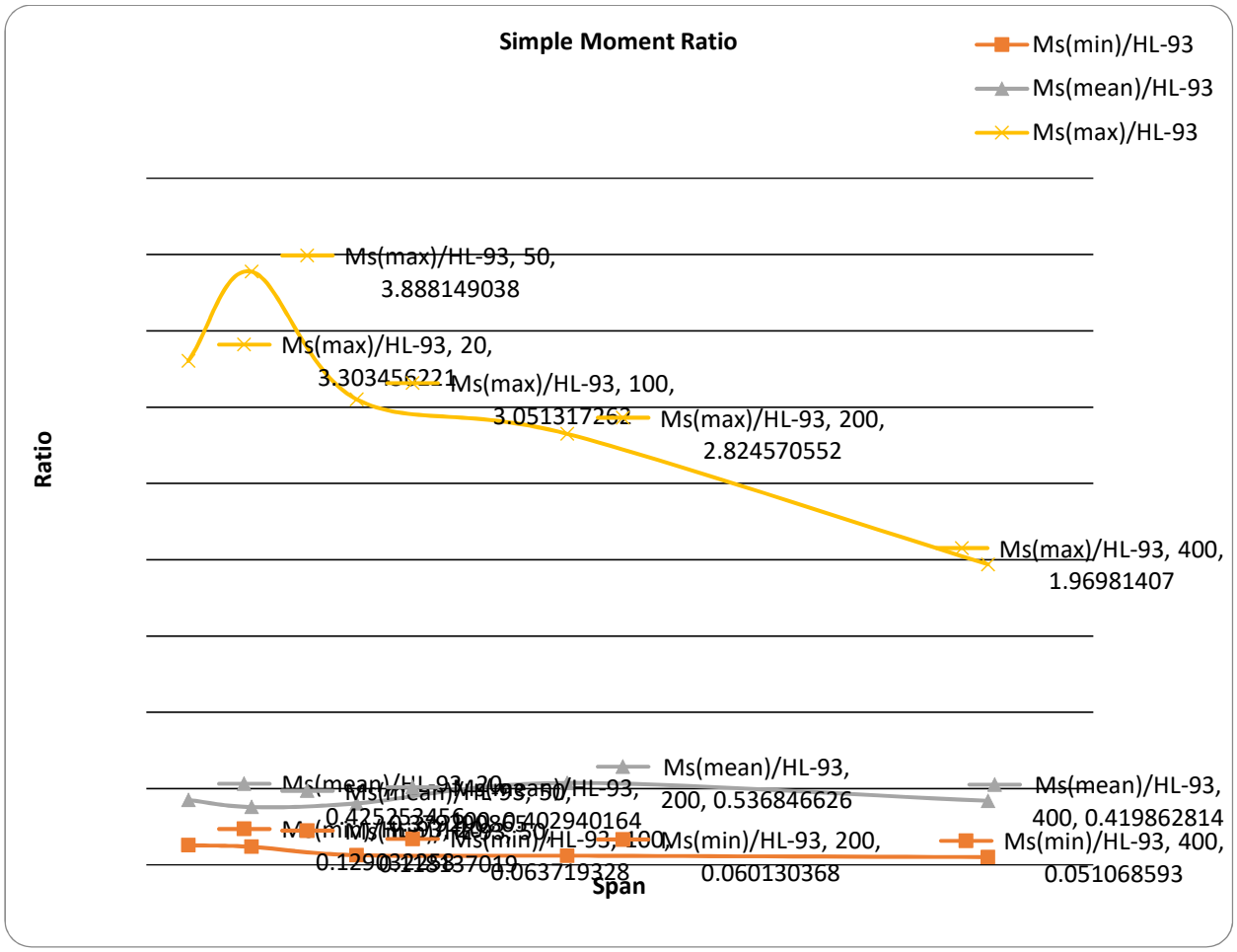

Figure C19. Simple Span Moment Ratios.

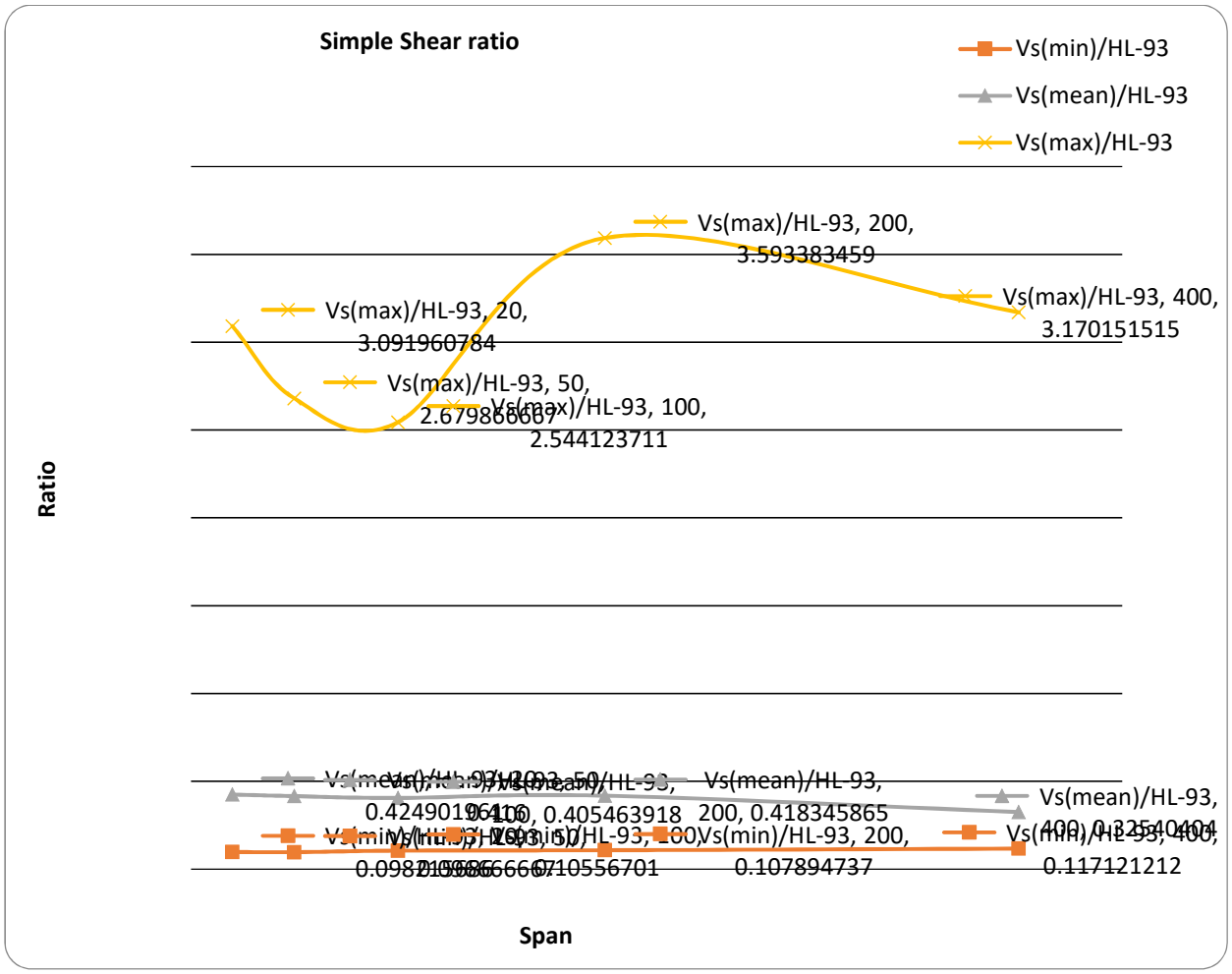

Figure C20. Simple Span Shear Ratios.

APPENDIX D: BRIDGE STRUCTURE DEAD LOADS

Table D1. Nominal Load Effects for Wearing Surface (Dw) (all bridges).

		SIMPLE SPAN		CONTINUOUS SPAN	
		moment	shear	moment	shear
L	S	Dw (kip-ft)	Dw (kips)	Dw (kip-ft)	Dw (kips)
20	4	5.4	1.1	5.4	1.4
20	6	8.1	1.6	8.1	2.0
20	8	10.8	2.2	10.8	2.7
20	10	13.5	2.7	13.5	3.4
20	12	16.2	3.2	16.2	4.1
50	4	33.8	2.7	33.8	3.4
50	6	50.7	4.1	50.7	5.1
50	8	67.6	5.4	67.6	6.8
50	10	84.5	6.8	84.5	8.4
50	12	101.4	8.1	101.4	10.1
80	4	86.5	4.3	86.5	5.4
80	6	129.8	6.5	129.8	8.1
80	8	173.0	8.6	173.0	10.8
80	10	216.3	10.8	216.3	13.5
80	12	259.5	13.0	259.5	16.2
100	4	135.2	5.4	135.2	6.8
100	6	202.8	8.1	202.8	10.1
100	8	270.3	10.8	270.3	13.5
100	10	337.9	13.5	337.9	16.9
100	12	405.5	16.2	405.5	20.3
200	4	540.7	10.8	540.7	13.5
200	6	811.0	16.2	811.0	20.3
200	8	1081.3	21.6	1081.3	27.0
200	10	1351.7	27.0	1351.7	33.8
200	12	1622.0	32.4	1622.0	40.6

Table D2. Nominal Load Effects for Prefabricated Components (Dp), Prestressed Concrete I-Beam Bridge.

Prestressed Conc. I-Girder Bridge		MOMENT (S & C)	SHEAR Simple	SHEAR Continuous
L	S	Dp (kip-ft)	Dp (kips)	Dp (kips)
20	all spacing	47.9	4.3	5.4
50		190.9	15.3	19.1
80		816.4	40.8	51.0
100		1237.9	49.5	61.9
200		5650.0	113.0	141.3

Table D3. Nominal Load Effects for Prefabricated Components (Dp), Steel Girder Bridge.

Steel Girder Bridge		MOMENT (S & C)	SHEAR Simple	SHEAR Continuous
L	S	Dp (kip-ft)	Dp (kips)	Dp (kips)
20	4	7.0	0.7	0.9
50	4	27.0	2.2	2.7
80	4	184.0	9.2	11.5
100	4	329.0	13.2	16.5
200	4	2780.0	55.6	69.5
20	6	7.5	0.8	0.9
50	6	32.0	2.6	3.2
80	6	205.0	10.3	12.8
100	6	361.0	14.4	18.1
200	6	3303.0	66.1	82.6
20	8	10.0	1.0	1.3
50	8	45.0	3.6	4.5
80	8	228.0	11.4	14.3
100	8	386.0	15.4	19.3
200	8	3790.0	75.8	94.8
20	10	12.0	1.2	1.4
50	10	54.0	4.3	5.4
80	10	246.0	12.3	15.4
100	10	407.0	16.3	20.4
200	10	4190.0	83.8	104.8
20	12	14.0	1.4	1.7
50	12	65.0	5.2	6.5
80	12	281.0	14.1	17.6
100	12	773.0	25.8	32.2
200	12	4875.0	97.5	121.9

Table D4. Nominal Load Effects for Site-cast Components (Ds), All Girder Bridges Except RC.

Girder Bridge (all but RC)		MOMENT (S & C)	SHEAR Simple	SHEAR Continuous
L	S	Ds (kip-ft)	Ds (kips)	Ds (kips)
20	4	55.0	5.5	6.8
50	4	183.0	14.6	18.3
80	4	463.0	23.2	28.9
100	4	681.0	27.2	34.1
200	4	2725.0	54.5	68.1
20	6	75.0	7.5	9.3
50	6	242.0	19.4	24.2
80	6	633.0	31.7	39.6
100	6	931.0	37.2	46.6
200	6	3725.0	74.5	93.1
20	8	93.0	9.3	11.6
50	8	300.0	24.0	30.0
80	8	782.0	39.1	48.9
100	8	1150.0	46.0	57.5
200	8	4600.0	92.0	115.0
20	10	116.0	11.6	14.4
50	10	376.0	30.1	37.6
80	10	984.0	49.2	61.5
100	10	1447.0	57.9	72.4
200	10	5788.0	115.8	144.7
20	12	142.0	14.2	17.8
50	12	462.0	37.0	46.2
80	12	1207.0	60.4	75.4
100	12	1775.0	71.0	88.8
200	12	7100.0	142.0	177.5

REFERENCES

AASHTO LRFD Bridge Design Specifications, 5st ed. American Association of State Highway and Transportation Officials, Washington, D.C., 2010.

AASHTO Manual for Bridge Evaluation, 2nd ed. American Association of State Highway and Transportation Officials, Washington, D.C., 2011.

AASHTO Manual for Condition Evaluation and Load and Resistance Factor Rating (LRFR) of Highway Bridges, American Association of State Highway and Transportation Officials, Washington, D.C., 2003.

AASHTO Manual for Condition Evaluation of Bridges, American Association of State Highway and Transportation Officials, Washington, D.C., 1998.

Aguwa, C., Olya, M. H., & Monplaisir, L. (2017). Modeling of fuzzy-based voice of customer for business decision analytics. Knowledge-Based Systems, 125, 136–145.

Ang, A. H-S. and Tang, W.H. "Probability Concepts in Engineering." Wiley, 2007.

Au, S.K. and Beck, J.L. "Estimation of small failure probabilities in high dimensions by subset simulation." Probabilistic Engineering Mechanics, Vol. 16, No. 4, pp. 263-277, 2001.

Au, S.K., Ching, J., and Beck, J.L., "Application of subset simulation methods to reliability benchmark problems." Structural Safety, Vol. 29, No. 3, pp. 183-193, 2007.

Ayyub, B.M., and Haldar, A. "Practical Structural Reliability Techniques." Journal of Structural Engineering, ASCE, Vol. 110, No. 8, pp. 1707-1724, 1984.

Breitung, K. "Asymptotic Approximations for Multinormal Integrals." Journal of Engineering Mechanics, ASCE, Vol. 110, No. 3, pp 357-366, 1984.

Bruls A, Croce P, Sanpaolesi L, Sedlacek O. ENV1991 - Part 3: traffic loads on bridges; calibration of load models for road bridges. In: Proceedings of IABSE colloquium, Delft, The Netherlands: IABSE-AIPC-IVBH; pp. 439-53, 1996.

Bucher, C.G. and Bourgund, U. "Fast and efficient response surface approach for structural reliability problems." Structural Safety, Vol. 7, No. 1, pp. 57-66, 1990.

Chen, X. and Lind, N.C. "Fast Probability Integration by Three-Parameter Normal Tail Approximation." Structural Safety, Vol. 1, pp. 269-276, 1983.

Cheng, J. and Li, Q.S. "Application of the response surface methods to solve inverse reliability problems with implicit response functions." Computational Mechanics, Vol. 43, No. 4, pp. 451-459, 2009.

Croce, P. and Salvatore, W. "Stochastic model for multilane traffic effects on bridges." ASCE Journal of Bridge Engineering, Vol. 6, No.2, pp. 136-143, 2001.

Curtis, R. and Till, R. "Recommendations for Michigan Specific Load and Resistance Factor Design Loads and Load and Resistance Factor Rating Procedures." MOOT Research Report R-1511, April 2008.

Data Collection Guide for SPS WIM Sites, 1st ed. Federal Highway Administration, Turner-Fairbank Highway Research Center Pavement Performance Division, Virginia, 2001.

Dawe P. Research perspectives: traffic loading on highway bridges. London: Thomas Telford, 2003.

Der Kiureghian, A., Lin, H.Z., and Hwang, S.J. "Second-Order Reliability Approximations," Journal of Engineering Mechanics, ASCE, Vol. 113, No. 8, pp. 1208-1225, 1987.

Eamon, C. and Charumas, B. “Reliability Estimation of Complex Numerical Problems using Modified Conditional Expectation Method,” Computers and Structures, No. 89, pp. 181-188, 2011.

Eamon, Christopher D., Valid Kamjoo, and Kazuhiko Shinki. "Design Live-Load Factor Calibration for Michigan Highway Bridges." Journal of Bridge Engineering 21.6 (2016): 04016014.

Eamon, Christopher D., and Masoud Rais-Rohani. "Integrated reliability and sizing optimization of a large composite structure." *Marine structures* 22.2 (2009): 315-334.

Eamon, C., Thompson, M., and Liu, Z. “Evaluation of Accuracy and Efficiency of some Simulation and Sampling Methods in Structural Reliability Analysis,” Journal of Structural Safety, Vol. 27 No. 4, pp. 356-392, 2005.

Eamon, C. D., Wu, H., Makkawy, A. A., & Siavashi, S. (2014). Design and construction guidelines for strengthening bridges using fiber reinforced polymers (FRP). Wayne State University, Michigan Department of Transportation, 368.

ECI. Eurocode 1: actions on structures. Part 2: Traffic loads on bridges. Brussels: European Standard EN 1991-2:2003: European Committee for Standardization, TC250, 2003.

Elicegui, M., Stefonowicz, T., and Severns, D. “Loads and Load Factors." NDOT Structures Manual, Chapter 12, Nevada Department of Transportation, 2008.

Elkins, L., and Higgins, Ch. “Development of Truck Axle Spectra from Oregon Weight-in-Motion Data for use in Pavement Design and Analysis." FHWA, Report no. OR-RD-08-06, Oregon Department of Transportation and Federal Highway Administration, 2008.

Engelund, S. and Rackwitz, R. “A benchmark study on importance sampling techniques in structural reliability, Structural Safety, Vol. 12, No. 4, pp. 255-276, 1993.

Fazlollahtabar, H., & Olya, M. H. (2013). A cross-entropy heuristic statistical modeling for determining total stochastic material handling time. The International Journal of Advanced Manufacturing Technology, 67(5–8), 1631–1641.

Fiessler, B., Neumann, H.J., and Rackwitz, R. "Quadratic Limit States in Structural Reliability." Journal of Engineering Mechanics, ASCE, Vol. 1095, No. 4, pp. 661-676, 1979.

Folwell, M. and Stephens, Jerry. "System for Processing and Analyzing WIM and AVC Data." FHWA, Report no. MT-97/8117-3, Montana Department of Transportation 1997.

Fu, G. and Hag-Elsafi, O. "Vehicular Overloads: Load Model, Bridge Safety, and Permit Checking." ASCE Journal of Bridge Engineering, Vol. 5, No.1, pp. 49-57, 2000.

Fu, G., Feng, J., Dekelbab, W., Moses, F., Cohen, H., Meliz, D., and Thompson, P. "Effect of Truck Weight on Bridge Network Costs." NCHRP Report 495. Washington, D.C., Transportation Research Board, 2003.

Fu, O. and Van de Lindt, 1. "LRFD Load Calibration for State of Michigan Trunkline Bridges." MDOT Research Report RC-1466, August, 2006.

Fu, O. and You, J. "Truck Loads and Bridge Capacity Evaluation in China." ASCE Journal of Bridge Engineering, Vol. 14, No.5, pp. 327-335, 2009.

Garambois, Pierre, Sébastien Besset, and Louis Jézéquel. "Multi-objective structural robust optimization under stress criteria based on mixed plate super-elements and genetic algorithms." Structural and Multidisciplinary Optimization 53, no. 2 (2016): 205-213.

Gelman, A., Carlin, J. B., Stern, H. S., & Rubin, D. B. (2014). Bayesian data analysis (Vol. 2). Boca Raton, FL, USA: Chapman & Hall/CRC.

Ghosn, M. "Development of Truck Weight Regulations Using Bridge Reliability Model." ASCE Journal of Bridge Engineering, Vol. 5, No.4, pp. 293-303, 2008.

Ghosn, M. and Moses, F. "Reliability Calibration of Bridge Design Code." Journal of Structural Engineering, Vol. 112, no. 4, 1986.

Ghosn, M., Sivakumar, B., and Miao, F. "Load and Resistance Factor Rating (LRFR) in NYS, Volume II, Final Report." NYSDOT Report C-06-13., 2011.

Ghosn, M., Sivakumar, B., and Moses, F. "Modeling maximum live load effects on highway bridges." Proceedings from the First International Symposium on Live-Cycle Civil Engineering, Varenna, Italy, June, pp. 335-341, 2008.

Ghosn, M., Sivakumar, B., and Moses, F. "Using weigh-in-motion data for modeling maximum live load effects on highway bridges." Proceedings of the Fifth International IABMAS Conference, Philadelphia, USA, July, 2010.

Gindy, M., and Nassif, H.H. "Multiple presence statistics for bridge live load base on weigh-in-motion data." Transportation research board 86th annual meeting, Washington, D.C., 2006.

Goldberg, David E., and Chie Hsiung Kuo. "Genetic algorithms in pipeline optimization." Journal of Computing in Civil Engineering 1.2 (1987): 128-141.

Gomes, H. M. and Awruch, A. M. "Comparison of response surface and neural network with other methods for structural reliability analysis." Structural Safety, Vol. 26, No. 1, pp. 49-67, 2004.

Hair, J. F., Anderson, R. E., Babin, B. J., & Black, W. C. (2010). Multivariate data analysis: A global perspective (Vol. 7). Upper Saddle River, NJ: Pearson.

Hohenbichler, M., Gollwitzer, S., Kruse, W., and Rackwitz, R. "New Light on First- and Second-Order Reliability Methods. "Structural Safety, Vol. 4, pp. 267-284, 1987.

Karaboga, D., & Basturk, B. (2007). A powerful and efficient algorithm for numerical function optimization: artificial bee colony (ABC) algorithm. Journal of global optimization, 39(3), 459-471.

Kaveh, A., and S. Shojaee. "Discrete-sizing optimal design of scissor-link foldable structures using genetic algorithm." Asian Journal of Civil Engineering (building and housing) 4, no. 2-4 (2003): 115-133.

Kennedy, James. "Particle swarm optimization." Encyclopedia of machine learning. Springer US, 2011. 760-766.

Koumar, A., Tysmansb, T., Coelhoc, R.F. and De Temmermand, N., An Automated Structural Optimization Methodology for Scissor Structures Using a Genetic Algorithm (2003).

Kordani, A., Molan, A., Monajjem, S., and Sadeghvaziri, E. (2014). ‘‘New Formulas of the Side Friction Factor on Three-Dimensional Horizontal Curves for Various Vehicles’’. The 2nd Congress of T&DI, ASCE, 2014, Orlando, Florida.

Kordani, A., Molan, A., and Monajjem, S. (2014). ‘‘Simulation Modeling of Dynamic Response of Vehicles to Different Types of Speed Control Humps’’. The 2nd Congress of T&DI, ASCE, 2014, Orlando, Florida.

Lu, Q., Harvey, J., Le, J., Quinley, R., Redo, D., and Avis, J. “Truck Traffic Analysis using Weigh-In-Motion (WIM) Data in California." University of California, Berkeley Institute of Transportation Studies, Pavement Research Center, 2002.

MDOT Bridge Analysis Guide, 2005 Ed, with 2009 Interim Update, Parts 1 and 2. MDOT Construction and Technology Support Area, 2009.

MDOT Maximum Legal Truck Loadings and Dimensions, T-1. MDOT, 2011.

Miao, T.J. and Chan. T.H.T. “Bridge live load models from WIM data.” Engineering Structures, Vol. 24, No. 8, pp. 1071-1084. 2002.

Molan, A., and Abdi, A. (2014). ‘‘Optimization of Speed Hump Profiles by Simulation Modeling of Vehicle Dynamic Performance’’. Journal of Transportation Engineering, ASCE, 140(8).

Molan, A., and Abdi, A. (2014). ‘‘Multi-Body Simulation Modeling of Vehicle Skidding and Roll Over for Horizontal Curves on Longitudinal Grades’’. 93rd Annual Meeting of TRB, 2014, Washington D.C.

Monsere, L., Higgins, Ch. and Nichols, A. “Application of WIM Data for Improved Modeling, Design, and Rating." Oregon Transportation Research and Education Consortium, Oregon Department of Transportation, 2011.

Moses, F. "Calibration of load factors for LRFR bridge evaluation." NCHRP Report no. 454, Washington, D.C., Transportation Research Board, 2001.

Moses, F. and Ghosn, M. "Instrumentation for Weighing Trucks-In-Motion for Highway Bridge Loads." Final Repol1, FHWAfOH-83-001 to Ohio DOT, Case Western Reserve University, August, 1983.

Nocedal, Jorge, and Stephen J. Wright. "Numerical optimization 2nd." (2006).

Nowak, A.S. "Calibration of LRFD Bridge Design Code." NCHRP 368, Washington, D.C., Transportation Research Board, 1999.

Nowak, A.S. “Calibration of LRFD Bridge Code.” Journal of Structural Engineering. Vol. 121, No. 8, pp. 1245-1251, 1995.

Nowak, A.S. “Live load model for highway bridges.” Structural Safety, Vol. 13, pp. 53-66, 1993.

Nowak, A.S., Lutomirska, M., and Sheikh Ibrahim, F.I. "The development of live load factors for long span bridges." Bridge Structures, Vol. 6, No. 1, pp. 73-79, and 2010.

O'Brien, EJ. and Caprani, c.c. "Headway modeling for traffic load assessment of short to medium span bridges." The Structural Engineer, Vol. 83, No. 16, pp. 33-36, 2005.

O'Brien, EJ. and Enright, B. "Modeling same-direction two-lane traffic for bridge loading." Structural Safety, No. 33, pp. 296-304, 2011.

O'Brien, EJ. Enright, B., and Getacllew, A. "Importance of the Tail in Truck Weight Modeling for Bridge Assessment." ASCE Journal of Bridge Engineering, Vol. 15, No.2, pp. 210-213, 2010.

O'Connor A, Jacob B, O'Brien EJ, Prat M. Report of current studies performed on normal load model of ECl Part 2. Traffic loads on bridges. Rev Francaise de Genie Civ. Vol. 5, No.4, pp. 411-33, 2001.

Olya, M. H. (2014a). Finding shortest path in a combined exponential-gamma probability distribution arc length. International Journal of Operational Research, 21(1), 25.

Olya, M. H. (2014b). Applying Dijkstra's algorithm for general shortest path problem with normal probability distribution arc length. International Journal of Operational.

Olya, M. H., & Fazlollahtabar, H. (2014). Finding Shortest Path in a Combined Exponential-Gamma-Normal Probability Distribution Arc Length. Advances in Industrial Engineering and Management, 3(4).

Olya, M. H., Fazlollahtabar, H., & Mahdavi, I. (2013). Shortest Path Problem with Gamma Probability Distribution Arc Length. International Journal of Applied Operational Research, 2(4), 55–66.

Olya, M. H., Shirazi, B., & Fazlollahtabar, H. (2013). Adapted Dynamic Program to Find Shortest Path in a Network having Normal Probability Distribution Arc Length. Advances in Industrial Engineering and Management, 2(1), 5–10.

Pelphery, J., Higgins, CH., Sivakumar, B., Groff, R.L., Hartman, B.H., Charbonneau, J.P., Rooper, J.W., and Johnson, B.V. "State-Specific LRFR Live Load Factors Using Weigh-in-Motion Data." ASCE Journal of Bridge Engineering, Vol. 13, no. 4, pp. 339-350, 2008.

Pelphrey, J. and Higgins, C. "Calibration of LRFR Live Load Factors Using Weigh-In-Motion Data, Interim Report SPR 635, June, 2006.

Probability Concepts in Engineering. Ang, H-S and Tang, W.H. John Wiley & Sons, NJ, 2007.

Qu, T., Lee, C.E. and Huang, L. "Traffic -Load Forecasting Using Weight-in-Motion Data." Center for Transportation Research Bureau of Engineering Research, the University of Texas at Austin, Report no. TX-99/987-6, 1997.

Rackwitz, R. and Fiessler, B. "Structural Reliability under Combined Random Load Sequences." Computers and Structures, Vol. 9, No. 5, pp. 484-494, 1978.

Raz, O., Buchheit, R., Shaw, M., Koopman, P., and Faloutsos, Ch. "Detecting Semantic Anomalies in Truck Weigh-In-Motion Traffic Data Using Data Mining." American Society of Civil Engineers, Journal of Computing in Civil Engineering, ISSN：0887-3801, 2004.

Rubinstein, R.Y. Simulation and the Monte Carlo Method, John Wiley & Sons, New York, 1981.

Silva M, Santos A, Figueiredo E, Santos R, Sales C, Costa JC. A novel unsupervised approach based on a genetic algorithm for structural damage detection in bridges. Engineering Applications of Artificial Intelligence. 2016 Jun 30; 52:168-80.

Sivakumar, B. “LRFR Limit States, Reliability Indices & Load Factors." Load & Resistance Factor Rating of Highway Bridge, Session 4, FHWA LRFR Seminar, HNTB Corp., 2008.

Sivakuman, B. and Ghosn, M. “Recalibration of LRFR Live Load Factors in the AASHTO Manual for Bridge Evaluation.” NCHRP Project 20-07, Task 285, 2011.

Sivakumar, B., Moses, F., Fu, G., and Ghosn, M. "Legal truck loads and AASHTO legal loads or posting." NCHRP Report 575, 2007.

Sivakumar, B., Ghosn, M., and Moses, F. "Protocols for collecting and using traffic data in bridge design." NCHRP Report 683, Washington, D.C., Transportation Research Board, 2011.

Structural Reliability Analysis and Prediction, 2nd ed. Melchers, R.E. John Wiley & Sons, NJ, 1999.

Soler, Joan, Manuel Gómez, and José Rodellar. "GoRoSo: feedforward control algorithm for irrigation canals based on sequential quadratic programming." Journal of Irrigation and Drainage Engineering 139.1 (2012): 41-54.

Tabatabai, H., Zhao, J., and Lee, C-W. "Statistical Analysis of Heavy Truck Loads Using Wisconsin Weigh-In-Motion Data." WDOT Project CFIRE 01-02, September 2009.

Traffic Monitoring Guide. FWHA-PL-Ot-021. U.S. Department of Transportation Federal Highway Administration, Office of Highway Policy Information, May 1, 2001.

Tvedt, L. “Distribution of Quadratic Forms in Normal Space--Application to Structural Reliability.” Journal of Engineering Mechanics, ASCE, Vol. 116, No. 6, pp. 1183-1197, 1990.

Van de Lindt, J. and Fu, G. "Investigation of the Adequacy of Current Bridge Design Loads in the State of Michigan." MDOT Research Report RC-1413, July 2002. Washington, D.C., Transportation Research Board, 2001.

Enevoldsen, I. and Sorensen, J. D., 1994, "Reliability-Based Optimization in Structural Engineering," Structural Safety, Vol. 15, pp. 169-196, 1994.

Tu, J., Choi, K. K., and Park, Y. H. "A New Study on Reliability Based Design Optimization," Journal of Mechanical Design, Vol. 121, No. 4, pp. 557–564, 1999.

Frangopol, D.M. "Reliability-Based Optimum Structural Design," Probabilistic Structural Mechanics Handbook, Theory and Industrial Applications, edited by Sundararajan, C. Chapman & Hall, 1995.

Rais-Rohani, M. and Xie, Q. "Probabilistic Structural Optimization under Reliability, Manufacturability, and Cost Constraints," AIAA Journal, Vol. 43, No. 4, pp. 864-873, 2005.

Kharmanda, G., Olhoff, N. "Extension of optimum safety factor method to nonlinear reliability-based design optimization." Structural and Multidisciplinary Optimization, Vol. 34, No. 5, pp. 367–380, 2007.

Aoues, Y, and Chateauneuf, A. "Benchmark study of numerical methods for reliability-based design optimization." Structural and Multidisciplinary Optimization, Vol. 41, No. pp. 277–294, 2010.

Rao, S.S. *Reliability-Based Design*, McGraw-Hill, Inc., 1992.

Qu, X. and Haftka, R. T. "Reliability-Based Design Optimization Using Probabilistic Safety Factor," Structural and Multidisciplinary Optimization, Vol. 27, No. 5, pp. 314-325, 2004.

ABSTRACT

RELIABILITY BASED DESIGN OPTIMIZATION OF LOAD AND RATING MODELS FOR BRIDGE STRUCTURES IN MICHIGAN

by

VAHID KAMJOO

August 2017

Advisor: Dr. Christopher D. Eamon

Major: Civil Engineering (Structural)

Degree: Doctor of Philosophy

The main objective of this study is to develop optimal live load models for design and rating of bridges using reliability-based design optimization (RBDO) methodology, such that target reliability levels for bridge girders subjected to Michigan traffic loads can be consistently met. Traffic data from 20 high-fidelity weigh-in-motion (WIM) sites collected over a two-year period across Michigan will be used for statistical analysis. From the filtered data, load effects are generated for a series of hypothetical bridges considering spans from 20 to 200 ft. and girder spacings from 6 to 12 ft. Simple moments and shears, for both single lane and two lane live load effects, are considered.

Based on the load effect data generated from the WIM vehicle configurations, load effects are probabilistically projected to 5 years (for rating) and 75 years (for design) to obtain estimates for the maximum load effect statistics. An extreme type I projection will be considered.

Optimal design and rating models are developed with a reliability-based optimization process using a genetic algorithm such that discrepancies in bridge structure reliability index are minimized.

AUTOBIOGRAPHICAL STATEMENT

Vahid Kamjoo has received his B.S. degree in 2007 in Civil Engineering from Semnan University, and his M.S. degree in 2010 in Civil Structural Engineering from University of Tehran. Vahid was involved with the ASCE student chapter, has participated in regional steel bridge competitions, and has worked as a Graduate Teaching and research Assistant at WSU. He is currently working as a Structural Engineer at Desai/Nasr Consulting Engineers Company.